

KATHOLIEKE UNIVERSITEIT
LEUVEN

Arenberg Doctoral School of Science, Engineering & Technology
Faculty of Engineering
Department of Electrical Engineering

HEART RATE VARIABILITY : LINEAR AND NONLINEAR ANALYSIS WITH APPLICATIONS IN HUMAN PHYSIOLOGY

Steven VANDEPUT

Dissertation presented in partial fulfillment of the requirements for the degree of Doctor in Engineering Sciences

October 2010

HEART RATE VARIABILITY : LINEAR AND NONLINEAR ANALYSIS WITH APPLICATIONS IN HUMAN PHYSIOLOGY

Steven Vandeput

Jury :
Prof. dr. ir. Y. Willems, president
Prof. dr. ir. S. Van Huffel, promotor
Prof. dr. A.E. Aubert, copromotor
Prof. dr. ir. R. Puers
Prof. dr. ir. M. Van Hulle
Prof. dr. O. Van den Bergh
Prof. dr. ir. S. Cerutti (Politecnico di Milano)

Dissertation presented in partial fulfillment of the requirements for the degree of Doctor in Engineering Sciences

October 2010

© Katholieke Universiteit Leuven – Faculty of Electrical Engineering
Kasteelpark Arenberg 10, B-3001 Leuven (Belgium)

Alle rechten voorbehouden. Niets uit deze uitgave mag worden vermenigvuldigd en/of openbaar gemaakt worden door middel van druk, fotocopie, microfilm, elektronisch of op welke andere wijze ook zonder voorafgaande schriftelijke toestemming van de uitgever.

All rights reserved. No part of the publication may be reproduced in any form by print, photoprint, microfilm or any other means without written permission from the publisher.

D/2010/7515/101
ISBN 978-94-6018-262-4

Dankwoord

In de eerste plaats zou ik mijn promotoren prof. dr. ir. Sabine Van Huffel en prof. dr. André Aubert willen bedanken. Sabine, bedankt om mij de kans te geven mijn doctoraat te behalen in jouw onderzoeksgroep. Je was altijd bereikbaar en mijn vele emails werden razendsnel beantwoord. Jouw gedrevenheid en bemoedigende woorden bij de vele pech die ik met reviewers heb gehad, waren een belangrijke steun om toch door te gaan en het doctoraat succesvol af te leggen. André, bedankt om me verder onder te dompelen in de wereld van HRV en de bijhorende fysiologie. Ik kon met mijn vragen altijd bij jou terecht. Het was ook fijn om samen met jou op conferentie te zijn: geen moment heb ik me verveeld dankzij al jouw leuke anekdotes bij een frisse pint of een lekker glas wijn.

Een belangrijk deel van het onderzoek in deze thesis werd uitgevoerd in het kader van een ESA project. Ik ben ESA en PRODEX dan ook dankbaar voor de financiële ondersteuning door middel van een doctoraatsbeurs.

Verder zou ik graag prof. dr. ir. Robert Puers, prof. dr. ir. Marc Van Hulle en prof. dr. Omer Van den Bergh willen bedanken om in mijn jury te willen zetelen. I am also very grateful to prof. dr. ir. Sergio Cerutti for organizing the nice Summerschool in Siena in 2007, for visiting his lab in Milano and for being a member of my doctoral jury. Dank ook aan prof. dr. ir. Yves Willems om deze jury voor te zitten en met wie ik een leuke tijd heb beleefd tijdens de laatstejaarsreis naar Mexico.

En dan zijn er nog de collega-onderzoekers. Frank en Bart, bedankt voor jullie kritische commentaar bij het ruimte-onderzoek. Met Martin en Eduardo had ik interessante babbels in Zaragoza en tijdens conferenties. Maar natuurlijk verdienen ook alle collega's van onze BIOMED onderzoeksgroep een bedanking voor de vele ontspannende gesprekken, de fijne middagmomenten in alma en de vele verjaardagsfeestjes. Bedankt Joachim, Wouter, Alexander, Bogdan, Maarten, Bori, Maria Isabel, Mariya, Diana, Anca, Kris, Ann-Sofie, Vanya, Jan, Ben, Jean-Baptiste, Thijs, Ivan, Vladimir en Milica. En dan is er nog mijn maatje Katrien, met wie ik een speciale band heb die veel verder gaat dan collega-zijn. Vragen, problemen of een minder moment, ik kon altijd bij jou terecht. Een oprechte merci.

Af en toe wat sporten hielp mij om goed en geconcentreerd te werken: mens sana in corpore sano. Ontspanning vond ik eerst bij de VILv voetbalploeg en daarna bij onze Hagelandse Running Club, waar ik me met de talrijke 'Bosklappers' steeds al lopend kon uitleven. Pistetraining of heuvelloop, gezelligheid stond altijd centraal. Ook de 'fietsvrienden' zorgden er regelmatig voor om eens diep te gaan en een frisse wind door de geest te laten waaien.

En dan zijn er nog mijn ouders, zus en schoonfamilie. Papa en mama, bedankt voor alle kansen die jullie mij hebben gegeven. Voor iedereen, ik apprecieer enorm jullie geduld, steun en onvoorwaardelijk geloof in mij.

Tot slot mijn gezin: Liesje, bedankt om de vele referenties te helpen ingeven, maar nog veel meer voor alle uitstekende zorgen, om me te leren relativeren en om er *gewoon* altijd voor mij te zijn. Ella, jij slaagt er telkens weer in me even het werk te doen vergeten. Je dikke knuffels zijn hartverwarmend. Zonder jullie was niets hetzelfde geweest. Ik kan me geen leven meer indenken zonder jullie en kijk uit naar de mooie toekomst samen!

Abstract

Cardiovascular diseases are a growing problem in today's society. The World Health Organization (WHO) reported that these diseases make up about 30% of total global deaths and that heart diseases have no geographic, gender or socio-economic boundaries. Therefore, detecting cardiac irregularities early-stage and a correct treatment are very important. However, this requires a good physiological understanding of the cardiovascular system.

The heart is stimulated electrically by the brain via the autonomic nervous system, where sympathetic and vagal pathways are always interacting and modulating heart rate. Continuous monitoring of the heart activity is obtained by means of an ElectroCardioGram (ECG). Studying the fluctuations of heart beat intervals over time reveals a lot of information and is called heart rate variability (HRV) analysis. A reduction of HRV has been reported in several cardiological and non-cardiological diseases. Moreover, HRV also has a prognostic value and is therefore very important in modeling the cardiac risk.

The fact that heart rate variability is a result of both linear and nonlinear fluctuations opened new perspectives as previous research was mostly restricted to linear techniques. Some situations or interventions can change the linear content of the variability, while leaving the nonlinear fluctuations intact. Also the reverse can happen: interventions, which up till now have been believed to leave cardiovascular fluctuations intact based on observations with linear methods, can just as well modify the nonlinear fluctuations. This can be important in the development of new drugs or treatments for patients. Therefore, this thesis focuses on the quantification of the nonlinear characteristics in autonomic heart rate regulation. Advanced techniques from nonlinear system dynamics and chaos theory are applied.

First, we present a new technique that can discriminate between preterm neonates with and without cardiovascular abnormalities. Further, we show in a healthy population the typical circadian (24h) profiles with several nonlinear HRV parameters as a function of age and gender. A higher nonlinear behaviour is observed during the night while nonlinear heart rate fluctuations decline with

age. The changes during the transition phases of waking up and going to sleep are described in detail. In another chapter we identify how HRV can be used to detect stress. Adaptations of the cardiovascular system in astronauts after space missions are also investigated. We prove the change in nonlinear heart rate dynamics, still present after 5 days upon return to earth and more expressed in the day period. After one month, a complete cardiovascular recovery is found. These findings are verified in a head-down bed rest (HDBR) study, simulating microgravity conditions. In addition, we show that Chinese herbal medicine restricts the influences of microgravity environment during HDBR on the cardiovascular regulation, though only partially functions as a countermeasure. Finally, we reveal that epileptic patients have a higher HR and decreased HRV compared to a normal population. Although vagal nerve stimulation reduces the epileptic activity, it affects cardiac autonomic modulation. The affected autonomic cardiac control in patients with refractory epilepsy might play an important role in arrhythmias and sudden cardiac death.

To summarize, we can say that this PhD thesis shows that nonlinear HRV techniques give additional information about autonomic cardiac control in several circumstances which cannot be obtained with standard linear analyses.

Samenvatting

Hart- en vaatziekten worden een steeds groter probleem in de huidige samenleving. In een rapport van de Wereldgezondheidsorganisatie (WGO) wordt duidelijk dat hart- en vaatziekten verantwoordelijk zijn voor 30% van het aantal doden wereldwijd en dat ze niet beperkt blijven tot één geografische ligging, geslacht of sociaal-economische toestand. Daarom is het vroegtijdig opsporen van onregelmatigheden en een correcte behandeling ervan zeer belangrijk. Dit vergt echter een goede kennis van de fysiologische werking van het cardiovasculaire systeem.

Het hart wordt elektrisch gestimuleerd vanuit de hersenen via het autonome zenuwstelsel, waarbij sympathische en vagale zenuwbanen continu interageren en zo het hartritme moduleren. De hartactiviteit kan continu in beeld gebracht worden met behulp van een ElektroCardioGram (ECG). Het opvolgen van de veranderingen in de tijd tussen opeenvolgende hartslagen levert heel wat informatie op en wordt hartritmevariabiliteit (HRV) analyse genoemd. Een gereduceerde HRV werd gevonden bij verscheidene cardiologische en niet-cardiologische ziekten. Daarenboven heeft HRV ook een grote prognostische waarde in klinische modellen die kunnen leiden tot een diagnose of risicoprofiel.

Het feit dat HRV niet alleen het gevolg is van lineaire veranderingen maar dat ook niet-lineaire schommelingen een grote bijdrage leveren, opende nieuwe perspectieven aangezien het onderzoek zich voordien hoofdzakelijk beperkte tot lineaire technieken. Sommige toestanden of interventies kunnen het lineaire deel van de variabiliteit beïnvloeden, terwijl de niet-lineaire schommelingen intact blijven. Maar het omgekeerde kan evenzeer plaatsvinden: interventies waarvan tot nu toe, gebaseerd op de lineaire technieken, verwacht werd dat ze de cardiovasculaire schommelingen ongewijzigd lieten, kunnen de niet-lineaire fluctuaties veranderen. Meer kennis hierover kan erg belangrijk zijn voor de ontwikkeling van nieuwe medicijnen en behandelingen voor patiënten. Bijgevolg focust deze doctoraatsthesis op de kwantificatie van de niet-lineaire karakteristieken in de autonome regeling van het hartritme. Hiertoe worden geavanceerde technieken afkomstig van niet-lineaire systeemdynamica en chaostheorie toegepast.

Eerst presenteren we een niet-lineaire techniek die te vroeg geboren baby's met en zonder cardiovasculaire abnormaliteiten kan onderscheiden. Verder tonen we in een gezonde populatie het typische circadiane (24u) profiel met behulp van verschillende niet-lineaire HRV maten, en dit als een functie van leeftijd en geslacht. Een sterker niet-lineair gedrag wordt waargenomen tijdens de nacht dan overdag, evenals een verminderde niet-lineariteit bij toenemende leeftijd. Ook de veranderingen tijdens de overgangsfasen zoals opstaan en gaan slapen worden beschreven. In een volgend hoofdstuk geven we aan hoe HRV kan gebruikt worden bij stressdetectie. Voorts worden aanpassingen van het cardiovasculaire systeem in astronauten na ruimtemissies bestudeerd. We bewijzen dat er veranderingen optreden in de niet-lineaire hartritme dynamica die nog aanwezig zijn 5 dagen na de landing op aarde en meer uitgesproken zijn overdag. 1 maand na de landing lijkt het cardiovasculaire systeem volledig hersteld te zijn. Deze bevindingen worden geverifieerd in een zogenaamde 'head-down bed rust' (HDBR) studie waarbij een omgeving van microgravitеit gesimuleerd wordt. We tonen hierbij ook aan dat Chinese kruidengeneeskunde de invloed van microgravitеit tijdens HDBR slechts gedeeltelijk beperkt. Uiteindelijk laten we zien dat epileptische patiënten een hoger hartritme hebben en een verlaagde hartritmevariabiliteit vergeleken met een gezonde referentiegroep. Hoewel vagale zenuwstimulatie de epileptische activiteit vermindert, beïnvloedt het wel de autonome modulatie van het hartritme. Deze veranderingen in patiënten met refractaire epilepsie kunnen een rol spelen bij eventuele latere hartritmestoornissen of een plotseling hartfalen.

Deze doctoraatsthesis laat ons bijgevolg toe te besluiten dat niet-lineaire HRV technieken bijkomende informatie leveren over autonome hartritme-controle die niet kan verkregen worden via klassieke lineaire analyses.

Nomenclature

Symbols

$a, b, \ldots$	scalars
$\mathbf{a}, \mathbf{b}, \ldots$	vectors
$\mathbf{A}, \mathbf{B}, \ldots$	matrices
$[\mathbf{a}\,\mathbf{b}]$	matrix with columns $\mathbf{a}$ and $\mathbf{b}$
$\lvert a \rvert$	absolute value of a
$\mathbf{A}^T$	transpose of the matrix $\mathbf{A}$
d	degree of model
$\in$	belongs to
Θ	Heaveside step function
κ	memory of model
λ	Lyapunov exponent
m	embedding dimension
r	Pearson correlation coefficient
$\Re$	the set of real numbers
$\sum$	sum
τ	time delay

Metrics

cm	centimeter
g	gram
h	hour
Hz	Hertz
kcal	kilocalories
kg	kilogram
m	meter
ml	milliliter
mmHg	millimeter mercury
ms	milliseconds
mV	millivolt
s	seconds
y	year

Thesis-specific symbols and abbreviations

AA	group neonates with abnormal PSG and abnormal follow-up
AN	group neonates with abnormal PSG and normal follow-up
B	Before (head-down bed rest)
Dx	x^{th} day during head-down bed rest
F	Female
$L-30$	30 days before launch
M	Male
MPT	Mental and Physical Task
MT	Mental Task
NN	group neonates with normal PSG and normal follow-up
P	P-value as outcome of statistical test
PT	Postural Task
r	tolerance level
R	Rest (phase)
$R+5$	5 days after return
$R+30$	30 days after return
Rx	x^{th} day after head-down bed rest

Abbreviations

$1/f$	1/f slope
AE	Absence of Epilepsy
AED	Anti-Epileptic Drugs
ALTE	Apparent Life Threatening Event
ANOVA	ANalysis Of VAriance
ANS	Autonomic Nervous System
ApEn	Approximate Entropy
ATRAMI	Autonomic Tone and Reflexes After Myocardial Infarction
AV	AtrioVentricular
BMI	Body Mass Index
BNP	Brain Natriuretic Peptide
BP	Blood Pressure
bpm	beats per minute
BPV	Blood Pressure Variability
BRS	BaroReflex Sensitivity
CATRC	China Astronaut Training and Research Center
CD	Correlation Dimension
CHF	Congestive Heart Failure
CHIME	Collaborative Home Infant Monitoring Evaluation
CHM	Chinese Herbal Medicine
CI	Confidence Interval
CK-MB	Creatine Kinase specific for Myocard
CNS	Central Nervous System
CO	Cardiac Output
CPAP	Continuous Positive Airway Pressure
CSF	CerebroSpinal Fluid
CWT	Continuous Wavelet Transform
DAN	Diabetic Autonomic Neuropathy
DAP	Diastolic Arterial Pressure
DFA	Detrended Fluctuation Analysis
DMN	Dorsal Motor Nucleus
ECG	ElectroCardioGram
EEG	ElectroEncephaloGram
EMG	ElectroMyoGram
EOG	Electro-OculoGram
ESA	European Space Agency
ESC	European Society of Cardiology
ESES	Electrical Status Epilepticus during Sleep
ETS	Environmental Tobacco Smoke

FD	Fractal Dimension
FFT	Fast Fourier Transform
FLE	Frontal Lobe Epilepsy
FU	Follow-Up
GA	Gestational Age
GABA	Gamma-AminoButyric Acid
HDBR	Head-Down Bed Rest
HF	High Frequency (in absolute values)
HFnu	High Frequency (in normalized units)
HR	Heart Rate
HRV	Heart Rate Variability
IP	Insular Pachygyria
IQ	Intelligence Quotient
ISS	International Space Station
LE	Lyapunov Exponent
LF	Low Frequency (in absolute values)
LFnu	Low Frequency (in normalized units)
LG	Lennox-Gastaut
LVDD	Left Ventricular Diastolic Diameter
LVDV	Left Ventricular Diastolic Volume
LVEF	Left Ventricular Ejection Fraction
MAP	Mean Arterial Pressure
ME	Myoclonic Epilepsy
MI	Myocardial Infarction
MPIP	Multicenter Post-Infarction Project
MSNA	Muscle Sympathetic Nerve Activity
MVC	Maximal Voluntary Contraction
NASPE	North American Society of Pacing and Electrophysiology
NL	Noise Limit
NLdr	Noise Limit detection rate
NN interval	Normal-to-Normal interval
non-REM	non Rapid Eye Movement
ns	non-significant
NTS	Nucleus Tractus Solitaries
OC	Output Current
OSAS	Obstructive Sleep Apnea Syndrome
PCS	Post-Conceptional Age
pNN50	number of interval differences of successive NN intervals greater than 50 ms divided by the total number of NN intervals
PNS	Peripheral Nervous System
PP	Pulse Pressure

PPA	Positive Predictive Accuracy
PRODEX	PROgramme de Développement d'EXperiences scientifiques
PSD	Power Spectral Density
PSG	Polysomnograpy
PWML	Postischemic White Matter Lesions
REM	Rapid Eye Movement
RMSSD	Root Mean Square of Successive Differences
RR	R peak to R peak
RRI	R peak to R peak Interval
RSA	Respiratory Sinus Arrhythmia
SR	Self-Rating
SAP	Systolic Arterial Pressure
SampEn	Sample Entropy
sEMG	surface ElectroMyoGram
SaO_2	Oxygen Saturation
SD	Standard Deviation
SDANN	Standard Deviation of the Averages of NN intervals in all 5 minute segments of the entire recording
SDNN	Standard Deviation of NN intervals
SDNN index	mean of the 5-minutes Standard Deviation of the NN interval calculated over the entire recording
SDSD	Standard Deviation of the Successive Differences
SDLE	Scale-Dependent Lyapunov Exponent
SPSS	Scientific Packages for Social Sciences
STAI	State-Trait Anxiety Inventory
STFT	Short-Time Fourier Transform
SUDEP	Sudden Unexpected Death in EPilepsy
SV	Stroke Volume
SWS	Slow Wave Sleep
TB	Thalamic Bleeding
TFA	Time-Frequency Analysis
TFR	Time-Frequency Representation
TLE	Temporal Lobe Epilepsy
TP	Total Power
TPR	Total Peripheral Resistance
ULF	Ultra Low Frequency (in absolute values)
VLF	Very Low Frequency (in absolute values)
VPC	Ventricular Premature Complex
XTLE	eXtra Temporal Lobe Epilepsy

Contents

Dankwoord i

Abstract iii

Samenvatting v

Nomenclature vii

Contents xiii

1 Introduction 1

1.1 Historical overview 1

1.2 Nervous system 3

1.2.1 Central nervous system 4

1.2.2 Peripheral nervous system 6

1.2.3 Transmissions in autonomic nervous system 6

1.3 Cardiovascular system 7

1.3.1 Heart 7

1.3.2 Vascular system 11

1.3.3 Baroreflex mechanism 12

1.4 Heart rate variability 13

1.4.1 Predictive value of HRV in myocardial infarction 14

1.4.2 Predictive value of HRV in diabetic neuropathy 14
1.4.3 Clinical value of HRV in other cardiological diseases 15
1.4.4 HRV in risk stratification of noncardiological disorder . . . 16
1.4.5 HRV and lifestyle 17
1.5 Aims of the thesis 19
1.6 Chapter-by-chapter overview 20
1.7 Personal contributions 23
1.8 Conclusion 25

2 Linear and nonlinear methodology 27

2.1 Peak detection and preprocessing 27
2.1.1 Pan-Tompkins algorithm 27
2.1.2 Preprocessing 28
2.2 Linear techniques 30
2.2.1 Time domain analysis 30
2.2.2 Frequency domain analysis 32
2.2.3 Time-frequency analysis 36
2.3 Nonlinear techniques 42
2.3.1 1/f slope 43
2.3.2 Fractal dimension 44
2.3.3 Detrended fluctuation analysis 48
2.3.4 Approximate entropy and sample entropy 50
2.3.5 Correlation dimension 52
2.3.6 Lyapunov exponent 55
2.3.7 Numerical noise titration 58
2.4 Physiological meaning of numerical noise titration 62
2.4.1 Introduction 62
2.4.2 Data acquisition 62

2.4.3 Data analysis 63
2.4.4 Results 63
2.4.5 Discussion 66
2.4.6 Conclusion 66
2.5 Nonlinear versus chaotic behaviour 67
2.6 Baroreflex sensitivity 69
2.7 Statistical analysis 70
2.8 Methodological remarks 71
2.8.1 Respiration and HRV 71
2.8.2 Computational complexity of nonlinear techniques 72
2.9 Conclusion 73

3 Detection of cardiovascular abnormalities in preterm neonates 75
3.1 Introduction 75
3.2 Methods 76
3.2.1 Subjects 76
3.2.2 Data collection 77
3.2.3 HRV analysis 77
3.2.4 Statistical analysis 79
3.3 Results 79
3.4 Discussion 81
3.4.1 Rhythmical fluctuations 82
3.4.2 Sleep states 83
3.4.3 Distinguishing Neonatal Groups 84
3.5 Conclusion 85

4 Circadian profile and aging in a healthy population 87
4.1 Introduction 87

4.2 Methods . . . 89
4.2.1 Study population . . . 89
4.2.2 Data acquisition . . . 89
4.2.3 Linear HRV parameters . . . 89
4.2.4 Nonlinear HRV parameters . . . 90
4.2.5 Numerical analysis . . . 90
4.2.6 Statistical analysis . . . 90
4.3 Results . . . 91
4.3.1 Day-night differences . . . 91
4.3.2 Circadian profile of nonlinear HRV . . . 91
4.3.3 Effects of aging . . . 94
4.4 Discussion . . . 98
4.4.1 Vagal autonomic control more chaotic . . . 99
4.4.2 Circadian profile of nonlinear cardiac autonomic control . . . 101
4.4.3 Aging and nonlinear cardiac autonomic control . . . 102
4.4.4 Effects of gender . . . 103
4.4.5 Limitations . . . 103
4.5 Conclusion . . . 104

5 Effect of stress on heart rate modulation 105

5.1 Introduction . . . 105
5.2 Methods . . . 107
5.2.1 Subjects . . . 107
5.2.2 Instrumentation . . . 107
5.2.3 Protocol . . . 107
5.2.4 HRV analysis . . . 108
5.2.5 Statistical analysis . . . 109
5.3 Results . . . 109

5.3.1 Performance . . . 109
5.3.2 Heart rate . . . 109
5.3.3 Heart rate variability and time-frequency analysis . . . 112
5.3.4 Self rating scores . . . 113
5.4 Discussion . . . 115
5.4.1 Influence of mental and physical state . . . 115
5.4.2 Link between physiological results and self scores . . . 117
5.4.3 Advantages and limitations . . . 117
5.5 Conclusion . . . 117

6 Impact of weightlessness in space on cardiac autonomic regulation 119

6.1 Introduction . . . 119
6.2 Methods . . . 121
6.2.1 Subjects . . . 121
6.2.2 Data collection and preprocessing . . . 121
6.2.3 HRV analysis . . . 121
6.2.4 Statistical analysis . . . 122
6.3 Results . . . 123
6.3.1 Day-night variation . . . 123
6.3.2 Linear HRV parameters . . . 124
6.3.3 Nonlinear HRV parameters . . . 124
6.3.4 Correlation coefficients . . . 124
6.4 Discussion . . . 128
6.4.1 Autonomic modulation early post-flight affected differently during day and night time: linear HRV . . . 128
6.4.2 Long-term recovery of linear HRV parameters . . . 130
6.4.3 Effect of microgravity on nonlinear dynamics of autonomic modulation . . . 131
6.4.4 Similarity between HRV parameters . . . 132

6.4.5 Limitations 132
6.5 Conclusion 133

7 Nonlinear dynamics in cardiovascular control during head-down bed rest 135

7.1 Introduction 135
7.2 Methods 137
7.2.1 Subjects and study protocol 137
7.2.2 Chinese herbal medicine 137
7.2.3 Data collection and preprocessing 137
7.2.4 HRV & BPV analysis 138
7.2.5 Statistical analysis 139
7.3 Results 139
7.3.1 Cardiac control 140
7.3.2 Blood pressure variability 142
7.3.3 Baroreflex sensitivity 146
7.4 Discussion 147
7.4.1 Effect of CHM as a countermeasure 150
7.4.2 Effect of HDBR on linear cardiovascular control 151
7.4.3 Effect of HDBR on nonlinear cardiovascular control 152
7.4.4 Comparison to spaceflight 153
7.4.5 Limitations 154
7.5 Conclusion 154

8 Cardiovascular oscillations in children with refractory epilepsy 155

8.1 Introduction: cardiac changes in epilepsy 155
8.1.1 Acute cardiac changes and epilepsy 156
8.1.2 Chronic cardiac changes and epilepsy 160
8.1.3 Summary 162

8.1.4 Study objectives . . . 163
8.2 Methods . . . 164
8.2.1 Subjects and treatment . . . 164
8.2.2 Data acquisition . . . 164
8.2.3 HRV analysis . . . 166
8.2.4 Statistical analysis . . . 166
8.3 Results . . . 166
8.4 Discussion . . . 169
8.4.1 Refractory epilepsy . . . 169
8.4.2 VNS . . . 170
8.4.3 Nonlinear HRV characteristics in epilepsy . . . 170
8.4.4 SUDEP . . . 171
8.5 Conclusion . . . 171

9 Conclusions and further research 173
9.1 General conclusions . . . 173
9.1.1 Physiological and mathematical background . . . 173
9.1.2 Goals and novelties . . . 174
9.1.3 Applications . . . 174
9.1.4 Other remarks . . . 176
9.2 Future work . . . 176

Bibliography 179

Publication list 217

Curriculum vitae 223

Chapter 1

Introduction

This chapter aims to introduce the reader in the physiology of the cardiovascular system and the usefulness of heart rate variability. First, Section 1.1 presents an historical overview from the nineteenth century knowledge to the state-of-the-art analysis nowadays. How the nervous system, comprising of the central and peripheral system, works and more specifically the role of the autonomic nervous system is briefly explained in Section 1.2. The basic physiology of the heart and the vascular system is roughly described in Section 1.3 with a focus on the electrical properties and the signals that can be measured non-invasively, such as ECG and blood pressures. Section 1.5 gives an overview of the several domains where HRV has proven its usefulness. Further, the general aims of the thesis are defined in Section 1.5 and the structure of the thesis is outlined in Section 1.6. Finally, the personal contributions are clearly mentioned in Section 1.7 and the chapter closes with some conclusions in Section 1.8.

1.1 Historical overview

Long before the invention of the electrocardiograph and the more recent emergence of modern constructs of heart rate variability (HRV), physicians recognized the potential importance of cardiac rhythms. Techniques for studying heart rate patterns were limited prior to the twentieth century. However, already for several hundred years physicians have monitored heart sounds and rhythms by auscultation and have noted beat-to-beat rhythm shifts associated with aging, illness and psychological states. The scientific investigation of beat-to-beat heart rate rhythms awaited technological advances that enables accurate and reliable quantification of the electrical activity of the heart. This technology has progressed

from the galvanometer to the kymograph, further to the inkwriting polygraph and finally to digital signal processing systems.

The galvanometer permitted in the nineteenth century the measurement of very small electrical currents by capitalizing on magnetic induction to rotate a pointer or mirror. After calibration, changes in voltage, including biopotentials generated by the heart, could be measured. Subsequently, Ludwig (1847) invented the smoked kymograph which allowed mechanical activity to be recorded. In 1894, MacKenzie developed an inkwriting polygraph and Einthoven integrated the galvanometer with photography to produce accurate and continuous tracings of the electrical activity of the heart. With the development of the electrocardiograph, it was possible to monitor normal and abnormal electrical conduction through the myocardium and to evaluate beat-to-beat changes in the heart rate pattern.

One can argue that the origins of the scientific study of heart rate variability predate the development of the electrocardiograph. The first documented observation of heart rate variability is often credited to Hales (1733), who observed a respiratory pattern in the blood pressure and pulse of a horse [150]. Ludwig (1847) was able to observe a regular quickening of pulse rate with inspiration and a slowing with expiration in a dog [215]. This may be the first report of respiratory sinus arrhythmia (RSA). Also Marey (1863) was a pioneer in the study of physiology and developed several devices for measurements as well as registrations [225]. In the second half of the nineteenth century and the first half of the twentieth century, some studies already tried to make a link between the brainstem and heart rate control. Research of heart rate variability moved initially in two directions. First, there was a trend towards understanding the physiological mechanisms mediating heart rate rhythms. Second, medical researchers identified specific relationships between heart rate variability and clinical status. Later, from the 1960's, a third trend appeared as psychophysiologists began to investigate the link between psychological processes and heart rate variability.

Both Hon and Wolf emphasized the relationship between heart rate variability and the nervous system status. Hon (1963) treated HRV as a global index of fetal distress [160] while Wolf (1967) viewed HRV as reflecting brain-vagal-heart communication which provided an important bridge between clinical research and psychophysiology [400]. Unlike physiology with its primary interest in mechanisms, or cardiology with its main focus on clinical status, psychophysiology has been driven by paradigms derived from psychology, focusing on physiological parameters that relate to psychological and behavioural states. As heart rate variability began to be recognized as an interesting and potentially important phenomenon, it was treated largely as a descriptive variable without attributing it to any specific physiological mechanism. In the 1970's, methods were oriented to process short-term tachograms with simple numerical estimates such as the difference between the shortest and the longest cardiac cycle. From the eighties on, newer distribution-based methods were developed on more solid mathematical

foundations [6]. Simultaneously, in basic research studies, it became apparent that specific patterns of heart rate variability may be related to particular physiological processes and mechanisms. Rather modern analytical methods that threat the heart beats data as a series were subsequently introduced to extract periodic components from the pattern of heart rate fluctuations. These approaches not only afforded more complete and excellent representations of the data, but also fostered further refinements of theoretical constructs. Spectral analysis [68, 323] and cross-spectral analysis [289, 40] were applied to the HRV measurements. These time series analyses offered a more powerful method for modeling periodic components of heart rate and it became increasingly clear that these procedures revealed physiological, clinical and psychophysiological significance.

Finally, these linear techniques were standardized in a report of the Task Force of the European Society of Cardiology and the North American Society of Pacing ans Electrophysiology [355]. Meanwhile, since the nineties, one already recognized that quantification and interpretation of heart rate variability not only depend on an adequate appreciation of the underlying physiological mechanisms, but also on the interactions between these mechanisms and behavioural processes. There was also evidence that nonlinear phenomena are involved in the genesis of heart rate variability. Therefore, methods of nonlinear system dynamics are expected to elicit additional information. This thesis focuses on the applicability of several nonlinear techniques to quantify heart rate variability in a more detailed way. Does the nonlinear or chaotic behaviour of cardiac control also change in case of a disturbed cardiovascular functioning (disease) or in different psychological and behavioural states?

The number of publications related to heart rate variability is still increasing. This evolution is visualized in Figure 1.1 where the number of published papers about HRV is indicated for each year since 1980. The numbers are based on information from the PubMed library, which is an online library that comprises more than 19 million citations for biomedical literature from MEDLINE, life science journals, and online books. Citations may include links to full-text content from PubMed Central and publisher websites. Only in the first five months of 2010, there were already 174 HRV publications. The black line through the points reflects the exponential increase and therefore the growing interest in HRV.

1.2 Nervous system

The nervous system is a network of cells specialized for the reception, integration and transmission of information. It comprises on one hand the central nervous system (CNS) and on the other hand sensory and motor nerve fibers that enter and leave the CNS or are completely outside the CNS (peripheral nervous system or PNS). The fundamental unit of the nervous system is the neuron, of which

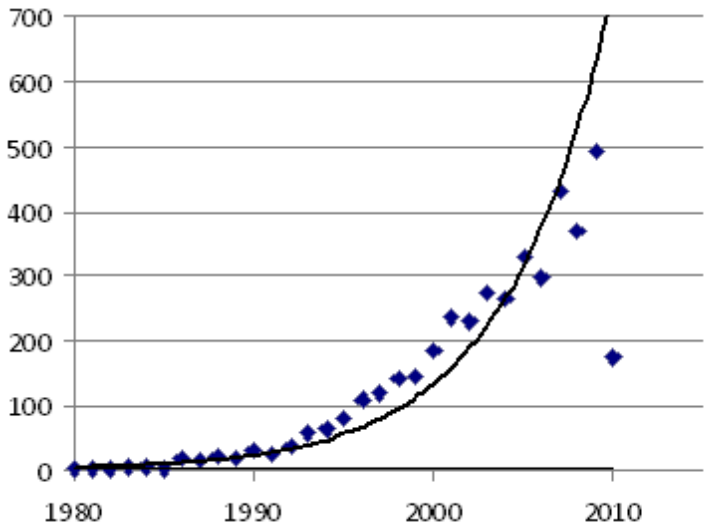


Figure 1.1: *Evolution of the number of papers about HRV in PubMed over the past 30 years. The number for 2010 is the situation on May 15, 2010. The line fitted through the points indicates the exponential increase in HRV interest.*

there are 10^{11} in the human body. Their cell bodies tend to aggregate into either compact groups, called nuclei or ganglia; or sheets, called laminae, that lie within the grey matter of the CNS or are located in specialized ganglia in the PNS. Groups of nerve fibers running in a common direction usually form a compact bundle (nerve, tract, pathway).

1.2.1 Central nervous system

The CNS comprises the brain lying within the skull and the spinal cord lying within the vertebral column. The brain (Figure 1.2) consists of the brainstem, the cerebellum, the diencephalon and the cerebrum. The brainstem, which links the spinal cord and the cerebrum, is composed of the medulla oblongata, the pons and the midbrain. The cerebellum is attached to the brainstem. The diencephalon comprises the thalamus, the subthalamus and the hypothalamus. Finally, the cerebrum consists of the right and left cerebral hemispheres, which are connected by the corpus callosum. The spinal cord has a segmental structure with dorsal and ventral roots arising on each side at more or less regular intervals.

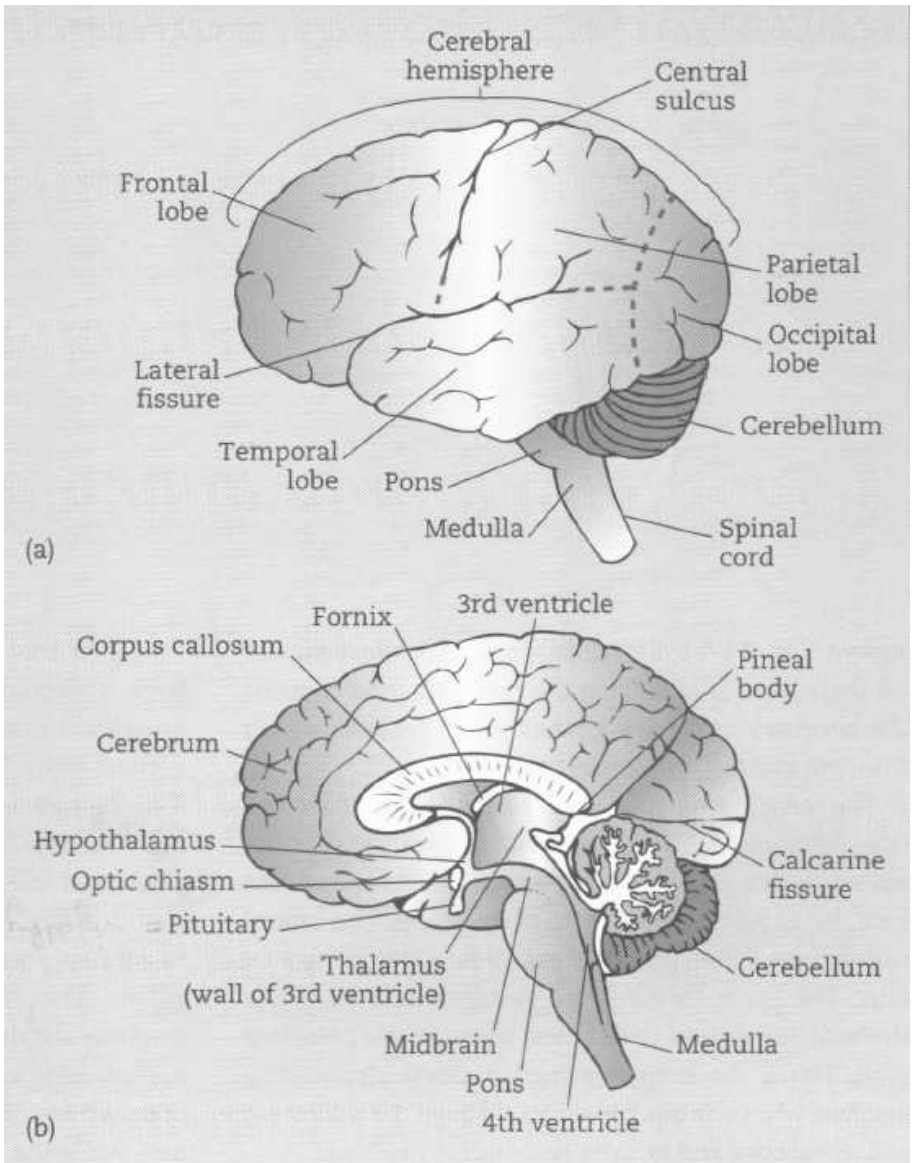


Figure 1.2: *The human brain: (a) lateral view, (b) view of midsagittal section. From [58].*

1.2.2 Peripheral nervous system

The PNS is that portion of the nervous system that lies outside the spinal cord and brain. It comprises both the somatic and the autonomic divisions. The somatic division contains all the peripheral pathways responsible for communication with the environment and the control of skeletal muscle. The autonomic nervous system (ANS) comprises all the efferent pathways from controlling centres in the brain and spinal cord to effector organs other than skeletal muscle. As heart rate variability is linked with autonomic nervous modulation, we will focus on the ANS.

The actions of the peripheral autonomic nervous system are normally involuntary and are directed to the control of individual organ function and to homeostasis. The ANS is often regarded as the 'solely motor' in function with fibres going to cardiac muscle, smooth muscles and glands. Sensory information comes from visceral and somatic afferent inputs. The peripheral autonomic nervous system is anatomically divided into the sympathetic and parasympathic system. The latter is often also called vagal system. Many tissues are innervated by both systems, having opposing effects. The network of nerves that can act independently of the CNS is called the enteric system. Both the sympathetic and parasympathic system modulates the activity of this enteric system.

1.2.3 Transmissions in autonomic nervous system

Opposing actions of the sympathetic and parasympathetic system

Many tissues have a dual autonomic innervation and therefore, stimulation of one component usually results in effects opposite to those produced by stimulation of the other. The effect of stimulating any one component may vary from tissue to tissue, being excitatory in some tissues and inhibitory in others. The parasympathetic (=vagal) effects are largely directed towards maintenance and conservation of the body function. Thus, responses to parasympathetic stimulation include slowing down of the heart, constriction of the pupils, contraction of the bladder (detrusor muscle) and increased secretion and motility in the digestive tract. In contrast, the effects of sympathetic stimulation are directed towards coping with stress and comprise the so called 'fight or flight' response described by Cannon in 1939. These changes include an increased heart rate and contractility, bronchodilation, pupillary dilation, inhibition of intestinal motility, constriction of the splanchnic vascular bed, decreased muscle fatigue and elevated blood glucose and free fatty acids. However, one can not say that the sympathetic system always acts en masse or that it is active only in stress. Most of the activity in the sympathetic nervous system is associated with normal homeostatic activity and its actions are localized (e.g. pupillary dilation and regional changes in blood flow).

The activity of tissues with dual innervation depends on the balance between parasympathetic and sympathetic discharge. Often one of the systems is dominant. For example, the diameter of the pupils and the resting heart rate are largely determined by the level of activity (tone) in their parasympathetic nerve supplies. Changes in effector activity are usually the result of reciprocal changes in both parasympathetic and sympathetic activity.

Circulating catecholamines

The activity of some autonomically innervated tissues is influenced by both noradrenaline released from nerves and by catecholamines released into the blood stream from the adrenal medullae. In humans, adrenaline comprises some 80% of the catecholamines released from the gland, the remainder being noradrenaline. The adrenaline and noradrenaline are synthesized and stored in different cells. All of the adrenaline comes from the adrenal medullae while the noradrenaline comes from the adrenal medullae and the sympathetic nerves. Low levels are maintained at rest, but during periods of stress, physical or emotional state, the rate of adrenaline release can increase about ten-fold. Adrenaline has many actions similar to noradrenaline but, because it is a more potent β_2-agonist, it has more pronounced metabolic actions. These include elevation of blood glucose and an increase in metabolic rate. Adrenaline also produces vasodilation in those vascular beds in which the β to α receptor is high, e.g. in skeletal muscle and heart muscle.

1.3 Cardiovascular system

The heart and blood vessels comprise the cardiovascular system which circulates blood around the body. This provides a transport system subserving homeostasis as it links the environment to the tissues and distributes substances (O_2 and nutrients) essential for our metabolism. A schematic overview of the cardiovascular system is given in Figure 1.3.

1.3.1 Heart

Basic characteristics

The heart, visualized in Figure 1.4, is divided into two pumps lying side by side, pumping in phase but distributing blood in series. The right side receives blood from the body and then propels it at low pressure through the vascular system of the lungs (the pulmonary circulation) while the left side receives blood from the lungs and then propels it at high pressure to all other tissues of the body, the so

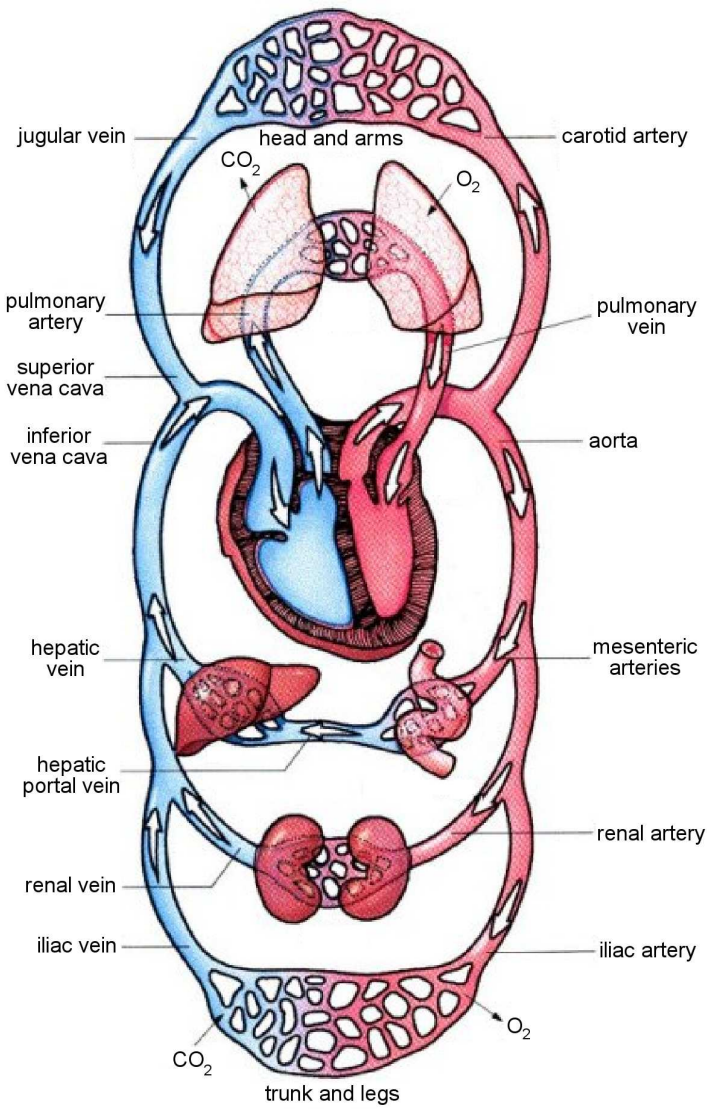


Figure 1.3: *A schematic overview of the cardiovascular system with the heart as driving force. From* `http://www.daviddarling.info/images/circulatory_system.jpg`

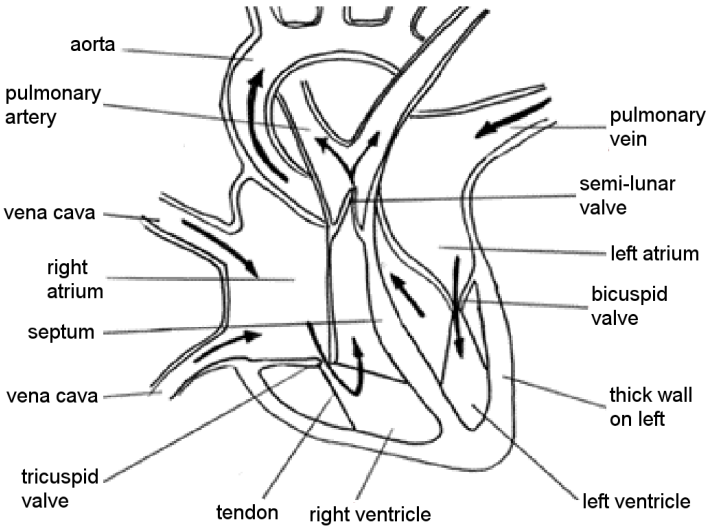


Figure 1.4: *Structure of the chambers and valves of the heart. The arrows indicate the direction of the blood flow. From* `http://www.dr-sanderson.org/images/heart.gif`

called systemic circulation. In one cycle all the output of the right part has to circulate through the lungs but, since the circulations of the different tissues are arranged in parallel, only some of the output of the left heart circulates through any one systemic tissue. Normally, there is no direct blood transfer between the two pumps.

Each side of the heart has two chambers: atrium and ventricle. The atrium receives the blood from the veins and aids its flow into the ventricle which propels it into the arteries. At the end of a contraction, the heart always contains some blood which is added to during its relaxation phase (diastole). Muscular contraction generates then pressure to expel some of that blood (systole). In other words, the pumps generate pulsatile pressure, 0 to ∼25 mmHg in the right ventricle and 0 to ∼120 mmHg in the left ventricle. When the body is at rest, diastole occupies two-thirds of the total cycle. The product of the frequency of pumping (heart rate - HR) and the volume ejected at each contraction by any one side (stroke volume - SV) is the cardiac output (CO). Typical values for a resting adult person are 60 – 70 beats per minute, 70 – 80 ml per beat and 5 – 6 liter per minute, respectively.

Electrical properties

Cardiac muscle has a myogenic rhythm, which means that it has the ability to contract rhythmically without nervous input. The action potential for each heart

beat is generated by a pacemaker in the right atrium and transmitted through the heart along specialized conducting pathways. Pacemaker cells have a resting membrane potential which slowly and spontaneously depolarizes to a threshold at which an action potential is initiated. Cardiac action potentials are typically of long duration (200 – 400 ms). There is a considerable overlap in time between the cardiac action potential and the contraction it initiates so that, in contrast to skeletal muscles, two contractions can not summate. The pacemaker firing rate, and consequently heart rate, is increased by sympathetic and decreased by parasympathetic nerve activity. The autonomic nervous system also influences conduction velocity through the heart and the duration of the cardiac action potential.

The synchronized depolarization spreading through the heart causes currents in the extracellular fluid that establishes field potentials over the whole body. These potential differences can be detected by electrodes placed on the body's surface. The signal (about Δ 1 mV) has to be amplified and the record produced is called the electrocardiogram (ECG).

The pattern of the ECG varies depending on the position of the electrodes but certain features are always present. A typical ECG of one heart beat is shown in Figure 1.5. The P wave is produced by the spread of electrical activity during atrial depolarization. The QRS complex is produced by ventrical depolarization and the T wave by ventrical repolarization. When no depolarization or repolarization is occuring, there is no potential difference in the ECG leading to the isoelectric line. Atrial repolarization does not produce any detectable wave because it occurs during the much larger QRS complex. Since ventricular repolarization is less well synchronized than ventricular depolarization, the T wave is longer in duration but smaller in amplitude than the QRS complex. Depending on the electrode position, the QRS complex may have one, two or sometimes three components. If after the P wave the first deflection from the isoelectric line is negative (by convention downwards), it is called a Q wave; if positive, it is called an R wave and if the next deflection falls below the isoelectric line, it is called an S wave. The PQ or PR interval (120 – 200 ms) is the time required for excitation to spread through the atria, atrioventricular (AV) node and bundle of His while the QS interval (60 – 100 ms) is the required time of excitation to spread through the ventricles. The duration of the ventricular and atrial action potentials is therefore given by respectively the QT (300 – 400 ms) and PS (160 – 280 ms) interval.

In this dissertation, we focus on the R peaks as the distance between two consecutive R peaks indicates the time between two successive heart beats. Based on the RR intervals, we can calculate heart rate variability.

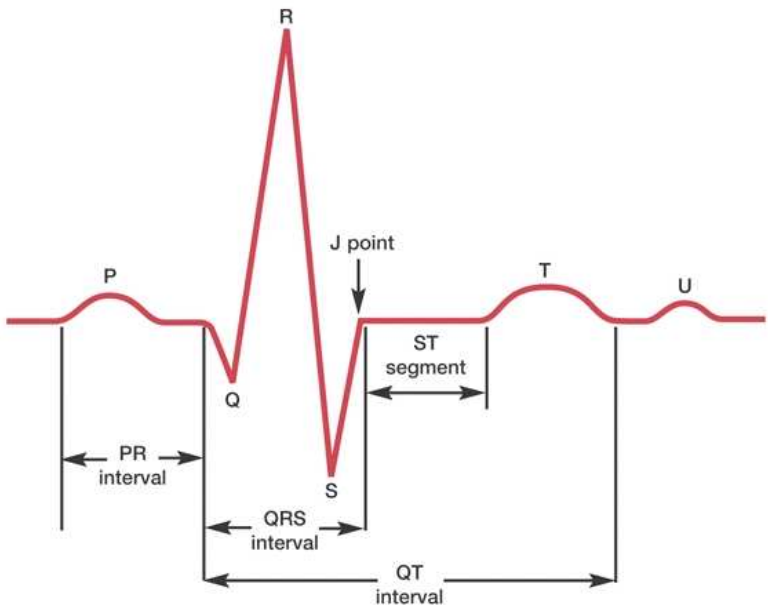


Figure 1.5: *The basic pattern of electrical activity across the heart. A typical ECG of one heart beat with P wave, QRS complex and T wave. From [15].*

1.3.2 Vascular system

The vascular system consists of a lymphatic and systemic circuit where the latter can be split in a venous and arterial part. This paragraph will be restricted to the systemic arterial circulation and its characteristics, even not discussing the systemic arterioles and systemic capillaries.

The aorta and large arteries are highly elastic and their stretching in systole and recoil in diastole converts intermittent flow of blood from the heart into a continuous pulsatile flow through the vessels. The maximum to which arterial pressure rises is called the systolic arterial pressure (SAP)(at rest the range is 100 – 140 mmHg at 20 years of age) and the minimum to which it falls is the diastolic arterial pressure (DAP)(range 50 – 90 mmHg). With increasing age, diastolic and in particular systolic pressures increase, the latter due to a loss of arterial elasticity. The difference between systolic and diastolic pressure is the pulse pressure (PP). The mean arterial pressure (MAP) is calculated by integrating the pressure against time.

The SAP and DAP are clinically often measured indirectly by a sphygmomanometer, based on the Korotkoff sounds you can hear with a stethoscope. The prime

determinants of the three parameters of arterial blood pressure (mean, systolic and diastolic) are cardiac output and total peripheral resistance (TPR). However, at a secondary level, systolic pressure is modified mainly by changes in ejection velocity and, to a lesser extent, stroke volume. Changes in total peripheral resistance and the time available for blood to leave the arteries mainly affect the diastolic pressure.

1.3.3 Baroreflex mechanism

This paragraph describes the physiological aspects of the so called baroreflex mechanism. The arterial baroreflex seeks to regulate the absolute blood pressure and ultimately to maintain circulation to the brain and other organs [344]. Baroreceptors sense systemic blood pressure indirectly by the extent of stretch of receptors in the walls of the carotid arteries and of the aorta. Changes in arterial baroreceptor afferent discharge transmitted to the central nervous system trigger reflex adjustments that buffer or oppose the changes in blood pressure: a rise in pressure elicits reflex parasympathetic activation and sympathetic inhibition, with subsequent decreases in heart rate (HR), cardiac contractility, vascular resistance, and venous return. Conversely, a decrease in arterial pressure reduces baroreceptor afferent discharge and triggers reflex increases in HR, cardiac contractility, vascular resistance, and increased venous return. Thus the baroreflex, by affecting blood pressure and HR control, provides powerful beat-to-beat negative feedback regulation of arterial blood pressure that minimizes short-term fluctuations in pressure. However, the arterial baroreflex may not be the only feedback mechanism involved in acute blood pressure control. Endogenous nitric oxide constitutes a second system, which, by acting also through a feedback mechanism, is involved in the short-term regulation of blood pressure [176]. Stimulated by the shear stress induced by increases in arterial pressure, this potent vasodilator response is rapidly effective in counteracting the initial rise in blood pressure.

An overview of the arterial baroreflex function and cardiovascular variability with all interactions and implications is given by Lanfranchi and Somers [199]. To summarize, Figure 1.6 shows schematically the most important interactions between the brains on one hand and the cardiovascular system (heart rate and blood pressure) on the other hand with the baroreflex as feedback mechanism. More detailed, the interaction betweem sympathetic and parasympathetic modulation regulates heart rate while the former is also responsible for the vasomotor tone. The combination of heart rate (HR) and stroke volume (SV) directly defines the cardiac output (CO = HR x SV), which is the total amount of blood pumped by the heart in the body in one minute. This cardiac output and the total peripheral resistance (TPR) of the vessels are the two main determinants for blood pressure (BP). Several sensors in the human body, called baroreceptors, measure this blood pressure and send the information

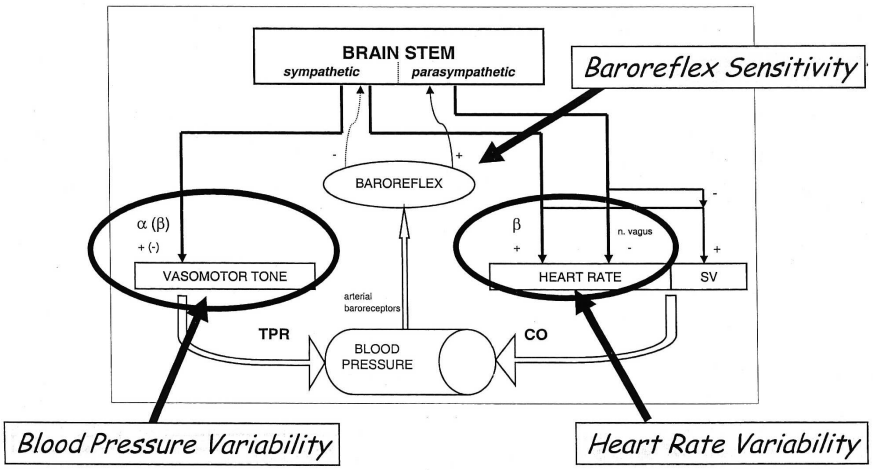


Figure 1.6: *Schematic overview of the most important interactions between the brains on one hand and the cardiovascular system (heart rate and blood pressure) on the other hand with the baroreflex as feedback mechanism. From [17].*

back to the brains . The brains process that information and use it to react, if necessary, via the autonomic modulation of heart rate and vasomotor tone.

1.4 Heart rate variability

The last two decades have witnessed the recognition of a significant relationship between the autonomic nervous system and cardiovascular mortality, including sudden cardiac death. Experimental evidence for an association between a propensity for lethal arrhythmias and signs of either increased sympathetic or reduced vagal activity has encouraged the development of quantitative markers of autonomic activity. Heart rate variability (HRV) represents one of the most promising markers. The apparently easy derivation of this measure has popularized its use. A reduction of HRV has been reported in several cardiological and non-cardiological diseases. Moreover, HRV also has a prognostic value and is therefore very important in risk stratification. This section will give an overview of the domains in which HRV already proved his usefulness and is based on several articles that have reviewed the possibilities of HRV [17, 355, 1, 349, 125].

However, a general consensus of the practical use of HRV in adult medicine has been reached only in two clinical scenarios. Depressed HRV can be used as a

predictor of risk after acute myocardial infarction (MI) and as an early warning sign of diabetic neuropathy.

1.4.1 Predictive value of HRV in myocardial infarction

A relationship between decreased HRV and mortality in post-myocardial infarction (post-MI) patients was reported by Wolf et al [399]. However, the relationship between decreased HRV and increased risk of mortality post-MI came to prominence in 1987 with the publication of the results of the Multicenter Post-Infarction Project (MPIP) [191]. Decreased HRV remained a risk factor for mortality after adjusting for other risk factors, including ejection fraction. Numerous studies have confirmed that decreased HRV in the time or frequency domain, measured shortly after MI, is associated with increased risk of mortality [48, 371, 78, 85, 106, 107, 259, 282, 293, 416, 47]. The clinical utility of HRV is improved by combining it with other traditional risk factors such as ventricular premature complexes (VPCs) [48], signal-averaged ECG [159] or left ventricular ejection fraction (LVEF) improved predictive value, with positive predictive accuracy (PPA) in the 30 – 50% range. Recent results from the ATRAMI (Autonomic Tone and Reflexes After Myocardial Infarction) study of 1284 post-MI patients showed that either reduced HRV or decreased baroreflex sensitivity (a measure of vagal tone) identified patients at elevated risk of mortality, and that decreased values of both identified a subgroup of patients at 17% risk of mortality over 2 years compared with 2% among those with well preserved indices [313].

1.4.2 Predictive value of HRV in diabetic neuropathy

As a complication of diabetes mellitus, autonomic neuropathy is characterized by early and widespread neuronal degeneration of small nerve fibres of both sympathetic and parasympathetic tracts [23]. Its clinical manifestations are ubiquitous with functional impairment and include postural hypotension, persistent tachycardia, gustatory sweating, gastroparesis, bladder atony and nocturnal diarrhoea. Once clinical manifestations of diabetic autonomic neuropathy (DAN) supervene, the estimated 5-year mortality is approximately 50%. Thus, early subclinical detection of autonomic dysfunction is important for risk stratification and subsequent management. Analyses of short-term and/or long-term HRV have proven to be useful in detecting DAN [266, 104, 222, 46, 38]. A reduction in time domain HRV parameters seems not only to carry negative prognostic value, but also to precede the clinical expression of autonomic neuropathy [188, 266, 116]. For the patient presenting with a real or suspect DAN there are three HRV methods from which to choose: (a) simple bedside RR interval methods; (b) long-term time domain measures, which are more sensitive and more reproducible than

the short-term tests; and (c) frequency domain analysis performed under short-term steady state conditions and which are useful in separating sympathetic from parasympathetic abnormalities.

Decreased HRV is a far more sensitive indicator of altered autonomic modulation than previously used standard autonomic function tests, and it can identify high-risk patients who require aggressive therapy [222].

1.4.3 Clinical value of HRV in other cardiological diseases

Cardiac transplantation

The study of HRV in the denervated donor heart of heart transplant patients provides an excellent clinical model to understand cardiovascular regulatory physiology when neural control of the heart is impaired or absent [322, 29, 31, 32]. In general, a reduced RR variance was consistently observed while the recognition of discrete spectral components was more controversial [39]. In the majority of the studies, a small respiratory-related high frequency (HF) component, considered to be independent of neural mechanisms, has been observed [39]. In a study on 120 heart and 4 heart-lung transplant recipients [295], it was shown that one third of the patients showed a very small HF component in the power spectrum. The other two thirds showed a flat spectrum, indicating the metronomic beating of the heart without any variation. Furthermore, HRV was unable to detect rejection of the donor heart.

Congestive heart failure

Congestive heart failure (CHF) is associated with profound derangements of the autonomic nervous system, which worsen with disease progression [76]. Sympathetic tone is markedly increased while parasympathetic modulation of heart rate is markedly decreased [111]. Decreased HRV is a consistent finding in CHF patients [240, 64]. Moreover, time domain indices of HRV, like SDNN, decline with increasing left ventricular dysfunction [65]. Although decreased HRV would be expected to predict mortality in CHF, results have been mixed. Some studies found no relationship between standard indices of HRV and mortality [108, 168]. Others found that HRV had remarkable predictive value, e.g. SDNN index <30 ms had a sensitivity of 75% and a specificity of 90% in predicting death in CHF [354]. Similarly, Mortara et al (51) reported that patients in whom low frequency (LF) power was nearly absent had a worse prognosis. Later, Mortara's group [241] reported that HRV did not have prognostic value in patients referred for cardiac transplantation, but among another group of patients awaiting heart

transplantation, those with SDANN <55 ms had a 20-fold relative risk of mortality compared to those with higher values[51].

Sudden cardiac death and malignant ventricular arrhythmias

A number of studies have shown that decreased parasympathetic and increased sympathetic tone lower the threshold for ventricular fibrillation and increase the prevalence of spontaneous ventricular tachycardia in ischemic animals and in humans [50, 79, 165]. It is not surprising, therefore, that patients at risk of sudden cardiac death have decreased HRV. Investigators have compared HRV in controls with that of outpatients [8], apparently healthy middle-aged adults who had Holter recordings prior to their sudden death [237], patients resuscitated from ventricular fibrillation [247], and patients who died suddenly while wearing a Holter monitor [227]. Results have consistently shown a marked decrease in HRV among sudden death patients, independent of disease status. A report of the progressive decrease in HRV in two patients with eventual sudden death within two years of the first recording offers the possibility that serial Holter monitoring can identify patients at especially high risk of sudden death [250]. When the outcome variable has included malignant arrhythmias as well as sudden death, results have been similar, with decreased HRV [85, 105, 106] and lack of circadian variation in parasympathetic indices of HRV [192] associated with higher risk.

1.4.4 HRV in risk stratification of noncardiological disorder

Essential hypertension

It has been hypothesised that in essential hypertension, an increased sympathetic and reduced vagal cardiac drive is coupled with an enhancement of vasomotor sympathetic modulation [265]. Essential hypertension was associated with impaired cardiac autonomic function [353, 336]. In a recent study, Mussalo et al showed that the severity of essential hypertension was related to the severity of impairment of cardiac autonomic control measured by time and frequency domain analysis of HRV [246].

Renal failure

Cardiac autonomic dysfunction is associated with mortality in patients with end-stage renal disease. Cashion et al [63] evaluated the value of HRV analysis in 278 patients with end-stage renal disease to identify those at high risk of sudden cardiac death. They showed that end-stage renal disease patients, particularly diabetics, had a compromised autonomic function. Although they suggest that

24-hour time domain measure of the HRV held the promise of identifying patients at increased risk of death, this study contained only 5 patients with sudden cardiac death. In patients with end-stage renal disease who underwent chronic haemodialysis, uraemia causes similar but reversible changes in HRV in non-diabetic haemodialysis patients [130].

Other applications

A number of recent studies showed that altered HRV was found in other patients populations including Parkinson disease [177], sleep apnoea [307, 394], Chagas' disease [298] etc. Altered HRV was also associated with some critical conditions such as patients with cirrhosis of the liver [296], pregnant eclampsia [407], and tetanus [142]. However, the clinical use of HRV assessment in these areas has not been systematically explored.

1.4.5 HRV and lifestyle

Gender and age

It has been proven that HRV depends on the age and sex too. HRV was higher in the physically active young and old women [89, 317]. Emese et al [249] proved that alert newborns have a lower HR variation in boys than girls. The HR variation for healthy subjects from 20 to 70 years was studied by Bonnemeir et al [57] who found that the HRV decreases with age and variation is more in women than men. Previous studies have assessed gender and age-related differences in time and frequency domain indices [294] and some nonlinear components of HRV. There also seemed to be a significant difference between day and night hours when studying HRV indices using spectral and time domain methods [294, 406].

The amount of HRV is influenced by physiologic and maturational factors. Maturation of the sympathetic and vagal divisions of the ANS results in an increase in HRV with gestational age [297] and during early postnatal life [297]. HRV decreases with age [2, 3]. This decline starts in childhood [329]. Infants have a high sympathetic activity that decreases quickly between 5 and 10 years of age [110]. The influence of provocation on HRV (i.e., standing and fixed breathing) is more pronounced at younger ages [329]. In adults, an attenuation of respiratory sinus arrhythmia with advancing age usually predominates [208, 387]. It was shown that compared to men, women are at lower risk of coronary heart disease [396].

Drugs

Heart rate variability can be significantly influenced by various groups of drugs. The influence of medication should be considered while interpreting HRV. On the other hand, HRV can be used to quantify the effects of certain drugs on the ANS.

The effects of beta-blockers and calcium channel blockers on the heart rate variability have been studied in postinfarction and hypertensive patients [37, 81, 148]. With spectral analysis, it is possible to unravel the sympathetic and parasympathetic activities of these drugs and thus explain their protective effects in cardiac diseases. In normotensive adults, the beta-adrenergic blocker atenolol appears to augment vagally mediated fast fluctuations in HR [244]. Guzzetti et al [148] studied the effect of atenolol in patients with essential hypertension. They found not only an increase in HF fluctuations, but also a decrease in the sympathetically mediated LF oscillations. This decrease in sympathetic activity was also noticed in postinfarction patients using metoprolol [37] and in patients with heart failure using acebutolol [81]. Thus, beta-blockers are able to restore the sympathetic - parasympathetic balance in cardiovascular disease. Effect of Omacor on HRV parameters in patients with recent uncomplicated MI was studied [270]. This study quantified an improvement in time domain HRV indices and can assess the safety of administering Omacor to optimally treated post-infarction patients. Eryonucu et al [101] have investigated the effects of β_2-adrenergic agonist therapy on HRV in adult asthmatic patients by using frequency domain measures of HRV. The LF and LF/HF ratio increased and TP decreased at 5, 10, 15 and 20 min after the salbutamol and the terbutaline inhalation, HF will not change significantly after the salbutamol and terbutaline inhalation.

Smoking

Studies have shown that smokers have increased sympathetic and reduced vagal activity as measured by HRV analysis. Smoking reduces the HRV. One of the mechanisms by which smoking impairs the cardiovascular function is its effect on ANS control [155, 255, 213]. Altered cardiac autonomic function, assessed by decrements in HRV, is associated with acute exposure to environmental tobacco smoke (ETS) and may be part of the pathophysiologic mechanisms linking ETS exposure and increased cardiac vulnerability [287]. Recently Zeskind and Gingras [412] have shown that cigarette exposed fetuses have lower HRV and disrupted temporal organization of autonomic regulation before effects of parturition, postnatal adaptation, and possible nicotine withdrawal contributed to differences in infant neurobehavioral function. Also, it was proved that the vagal modulation of the heart had blunted in heavy smokers, particularly during a parasympathetic maneuver. Blunted autonomic control of the heart may partly be associated with adverse event attributed to cigarette smoking [26].

Alcohol

HRV reduces with the acute ingestion of alcohol, suggesting sympathetic activation and/or parasympathetic withdrawal. Malpas et al [223] have demonstrated vagal neuropathy in men with chronic alcohol dependence using 24h HRV analysis. Ryan et al [316] have previously reported a strong positive association between average day time and night time HR, measured during 24h ambulatory BP monitoring and usual alcohol intake. It has been reported that HRV indices representing cardiac vagal nerve activity were significantly lower in acute alcoholic subjects compared to normal volunteers [223, 272, 312].

Sleep

The results from Togo and Yamamoto [361] suggest that mechanisms involving electroencephalographic desynchronization and/or conscious states of the brain are reflected in the fractal component of HRV. Compared to stages 2 and 4 non-REM sleep, the total spectrum power was significantly higher in REM sleep and its value gradually increased in the course of each REM cycle [61]. The value of the VLF component (reflects slow regulatory mechanisms, e.g., the reninangiotensin system, thermoregulation) was significantly higher in REM sleep than in stages 2 and 4 of non-REM sleep. The LF spectral component (linked mainly to the sympathetic modulation) was significantly higher in REM sleep than in stages 2 and 4 non-REM sleep. Patients with sleep apnoea tend to have a spectral peak lying between 0.01 and 0.05 cycles/beat, with the width of the peak indicating variability in the recurrence rate of the apnoea. In most of the subjects, the frequency spectrum immediately below the apnoea peak was relatively flat. The first visual analysis of the single computed spectrum from each subject led to a correct classification score of 28/30 (93%) [94]. Gates et al [127] suggested that long-lasting alternations exist in autonomic function in snoring subjects.

1.5 Aims of the thesis

The main aim of this thesis is to investigate the nonlinear dynamics in the autonomic regulation of heart rate. Heart rate variability is used here as a tool to study the cardiovascular control mechanisms exerted by the autonomic nervous system, with a focus on the nonlinear techniques. The origin of nonlinear heart rate fluctuations lies in the fractal organisation of the heart. The fractal structure of the coronary arteries and veins, the chordae tendineae and the His-Purkinje system made nonlinearity an intrinsic property of heart rate. Physiological systems can use nonlinearity to be able to respond to perturbations. Very weak changes in the initial conditions lead to wide-spread changes in the whole system. The theory on

nonlinear dynamics predicts that a variety of disease states that alter autonomic function lead to a loss of physiologic complexity and therefore to more regularity. This was illustrated extensively in paragraph .

The fact that cardiovascular variability is a result of both linear and nonlinear fluctuations opened new perspectives. Some situations or interventions can change the linear content of the variability, while leaving the nonlinear fluctuations intact. Also the reverse can happen: interventions, which up till now have been believed to leave cardiovascular fluctuations intact based on observations with linear methods, can just as well modify the nonlinear fluctuations. This can be important in the development of new drugs or treatments for patients. Yamamoto et al [403] have developed a method that allows to interpret the quantity of nonlinear fluctuations in a signal. Based on their measurements the nonlinear fluctuations comprise a very important portion of the total cardiovascular variability. For persons in supine position (awake) the nonlinear proportion was 85.5 ± 4.4 % [405]. This means that the linear analysis tools, which up till now have been considered as the standard methods only describe about 15% of the total variability. This leaves open enormous possibilities for the nonlinear analysis methods.

These nonlinear techniques are expected to provide additional information about the nonlinearity in the cardiovascular system which can not be reflected by standard HRV analysis. The goal is not that nonlinear HRV techniques would replace the linear analysis, but they have to be considered as an addition, yielding information about a specific aspect of scaling behaviour, complexity or chaos in the underlying system.

In addition to the regularly applied nonlinear methods, also the recently developed and promising numerical noise titration technique is implemented and explored further in this thesis. By applying this method on ECG and BP data of rats who underwent specific autonomic blockades, we did a first attempt to link the output with the physiology. However, this is only a small part of the thesis. The main goal is the examination whether nonlinear techniques really reveal extra information. Therefore, those nonlinear techniques are investigated in several completely different applications. An important aspect of the thesis is the simultaneous calculation of many nonlinear techniques in such an application while in literature often only one or a few of these techniques are applied at once. This enables us to check whether those nonlinear techniques give similar information or not.

1.6 Chapter-by-chapter overview

This thesis can be divided in two parts. Chapters 1 and 2 give the physiological background and all the necessary techniques to calculate heart rate variability,

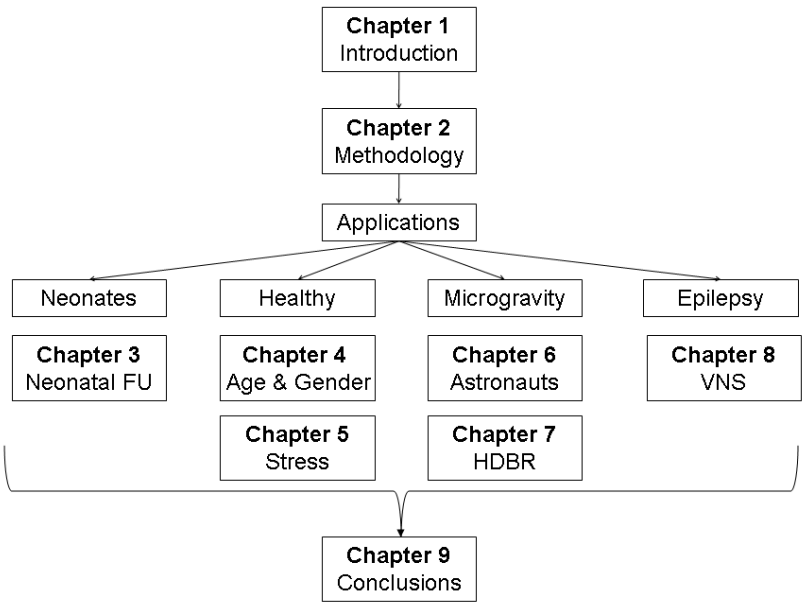


Figure 1.7: *Flowchart of the thesis chapters.*

including data acquisition, peak detection, preprocessing of RR interval time series, time and frequency domain analysis, nonlinear signal processing. A second part contains all the applications where HRV was used to extract information about linear and nonlinear cardio(vascular) regulation. The applications are rather diverse. Consequently, they show the wide possibilities of HRV, going from the beginning of human life (neonates) to all cardiovascular changes over time in healthy persons, but also from diverse conditions such as stress and microgravtiy to pathologies such as epilepsy. The structure of the thesis is summarized by means of the flowchart in Figure 1.7.

Chapter 1 introduces the physiology of the nervous system and the cardiovascular system in general. It provides the relevant background information to interprete sufficiently well the results of the applications under study in this thesis. A historical overview describes how changes in heart rate were studied in the past, how this continued over decades and how this finally evolved to the concept of heart rate variability. The wide range of application areas, still growing every year, is also discussed. Furthermore, the different goals of the thesis were addressed and a chapter-by-chapter overview was provided, including the personal contributions.

Chapter 2 provides a scientific basis for the following chapters, where the described signal processing techniques will be used in different applications. It gives an overview of the different steps from ECG signals to HRV results. In a first part, peak detection and preprocessing (filtering, normalization, ...) algorithms are explained while the second part summarizes all linear and nonlinear parameters with their advantages, drawbacks and limitations. The physiological meaning will be discussed where possible and differences between short and long term HRV will be highlighted as well as the issue on nonlinearity and chaos. Almost all these techniques can both be used for heart rate variability as well as for blood pressure variability. In a small third part, baroreflex sensitivity (BRS) parameters will briefly be mentioned as they are used in Chapter 7. Finally, a fourth section explains the test statistics used to perform statistical analysis in the following chapters.

Chapter 3 describes a first application, being the study of cardiac control in the earliest possible stage, namely when babies are born. The focus here is on the numerical noise titration method in preterm neonates with and without abnormal cardiorespiratory events, separately for REM and non-REM sleep periods. The chapter compares the distinguishing power of this new technique with the earlier used time domain measures and the detrended fluctuation analysis (DFA) parameters.

Chapter 4 makes use of a large data set of healthy persons who were monitored for 24h. The circadian profiles of the nonlinear HRV parameter are given as a function of age and gender and compared with those of the linear parameters. Especially the transition phases of waking up and going to bed has been investigated thoroughly. Further, also the changes over age categories of ten years will be discussed. We illustrate the fact that nonlinear HRV parameters are able to provide additional information about the autonomic regulation of heart rate which can not be extracted from time or frequency domain parameters. This study can be seen as a reference when we look to the autonomic cardiac control in healthy persons under special conditions (Chapter 5, 6 and 7) or to pathologic patients (Chapter 8).

Chapter 5 investigates the possibility of HRV in stress detection. The participants are again healthy persons as in Chapter 4, but now students (same age category) who underwent a stress test. This chapter uses time frequency analysis to examine the changes in sympathetic and parasympathetic modulation as a function of time. The results for several conditions (rest, physical task, mental task and combined physical and mental task) are compared with each other. The HRV results are also linked with the self-scores as output of a questionnaire.

Chapter 6 is devoted to research that has been performed within the context of the ESA-PRODEX project 'Cardiovascular autonomic control and hemodynamics: a comparison between long and short duration space missions' (ESA AO-2004-033).

This chapter examines how heart rate regulation is influenced in a microgravity environment. During a space mission, the body has to adapt due to the weightlessness condition which can lead to orthostatic intolerance when coming back on Earth. HRV techniques were applied on data from astronauts before and twice after their spaceflight. As well as in Chapter 4, nonlinear HRV will give additional insights. Moreover, long term recordings were monitored, enabling to study the adaptation proces separately during day time and at night. This in combination with the focus on nonlinear cardiac fluctuations and a relatively large dataset makes this study unique.

Chapter 7 is also related with microgravity, though in a simulated environment. The concept of head-down bed rest is used to mimick the weightlessness condition in space (Chapter 6). This chapter describes the findings of a 60 days head-down bed rest study in collaboration with the China Astronaut Training and Research Center where the study was set up. As measurements can be executed more regularly in such environment, the goal is to verify the results of real spaceflight data (Chapter 6) and to examine changes in time in more detail. Chinese herbal medicine is tested as a countermeasure. Not only HRV results will be given and discussed, but also BPV and baroreflex sensitivity.

Chapter 8 presents the sixth and last application in this thesis. No special condition in a healthy or trained population will be investigated as the previous chapters do, but one focuses on the cardiac control in a specific pathology, namely epilepsy. In a first part, a review is given about cardiac changes in epilepsy. The second part restricts to refractory epilepsy in children and how the autonomic regulation of heart rate is affected in those patients. They are all treated with vagal nerve stimulation which reduces the epileptic activity. However, the indirect effect of vagal nerve stimulation on cardiac control was unknown and is studied in the second part of this chapter.

Chapter 9 summarizes the work presented in the previous chapters and formulates the main conclusions of this thesis. Moreover, new ideas for future research will be enumerated.

1.7 Personal contributions

The work described in chapters 3 till 8 is mainly my own research. In particular, the biomedical signal processing (mainly HRV and BPV analysis) and statistical analysis was obtained by myself and based on my own ideas. The concrete contribution and collaborations with other groups will be described for every chapter separately.

Chapter 1 introduces the physiology of the nervous system and the cardiovascular

system in general. This part is common knowledge and can be found in many books about human physiology [58, 325, 364, 337] or more specifically cardiovascular physiology [236, 204, 332, 190]. The several domains where HRV proved his usefulness were already discussed in tens of review papers [355, 221, 17, 44, 349, 125, 328, 385, 1, 357]. Concerning the methodology presented in Chapter 2, this is also often described in literature. Section 2.4 presents the results of a study where I did the full analysis on data coming from the division of Experimental Cardiology at the University Hospitals Gasthuisberg (Leuven, Belgium). This work was presented and published in the 34^{th} *Annual Computers in Cardiology (CinC) conference* (Durham, NC, USA) in October 2007 [372].

Chapter 3 reports about the differences between REM and non-REM sleep on the cardiac level in preterm neonates and the ability to use a new HRV parameter to distinguish between neonates with normal and abnormal cardiorespiratory behaviour. My contribution included the implementation of this new noise titration technique, the signal processing part and the statistical analysis. The data, which was already used before in the PhD thesis of Geert Morren [238], was acquired in the neonatal division of Dr. Naulaers from the Department of Paediatrics at the University Hospitals Gasthuisberg (Leuven, Belgium). Most interpretations I made myself, in consultation with Dr. Naulaers. Preliminary results were published as an abstract in *Archives of Disease in Childhood* [375]. The complete research was later published in the international journal *Early Human Development* [376].

Chapter 4 describes an extensive study that was the sequel of studies by Ramaekers [294] and Beckers [34]. Therefore, the data was already available and preprocessed. This study was in collaboration with the group of prof. Aubert from the division of Experimental Cardiology at the University Hospitals Gasthuisberg (Leuven, Belgium), who provided the data and helped with the interpretation of the results. My contribution consisted of the complete HRV analysis, not restricting only to the linear parameters but applying the broad set of nonlinear techniques we could implement. Especially the nonlinear hour-by-hour analysis leading to clear circadian profiles as a function af age and gender was innovative. Also the complete statistical analysis was my part. A paper was submitted in revised form to the international journal *Physiological Measurement* [378].

The study of stress detection in young healthy students as presented in Chapter 5 was in close collaboration with my colleague Joachim Taelman who worked at that time within the Faculty of 'Bewegings- en revalidatiewetenschappen' (FaBeR) where the measurements took place. He was involved in the study design and data acquisition. My contribution is the analysis of the ECG data including the statistics afterwards. Taelman and I interpreted the results together. A paper about this topic has been submitted in revised form to the international journal *Journal of NeuroEngineering and Rehabilitation* [377].

Chapters 6 and 7 investigate the effect of microgravity on the cardiovascular system. Both chapters are, as Chapter 4, in collaboration with the group of prof. Aubert from the division of Experimental Cardiology at the University Hospitals Gasthuisberg (Leuven, Belgium). The data from astronauts was monitored by themself over many years of space missions while the data of head-down bed rest (HDBR) was acquired by the China Astronaut Training and Research Center with who the group of prof. Aubert has bilateral contacts. My contribution to both studies was the full HRV and BPV data analysis, statistical analysis and interpretation of the results, the latter in consultation with the team of prof. Aubert. The analysis of body weight, water intake, urine output and baroreflex sensitivity in the HDBR study (small parts in Chapter 7) was the work of Jiexin Liu as indicated clearly in the text itself. The space study has been submitted in revised form to the international journal *International Medical Journal for Experimental and Clinical Research* [379] while the HDBR study was accepted for publication in the international journal *Space Medicine and Medical Engineering* [373].

My contribution to Chapter 8, dealing with the changes in autonomic heart rate modulation in epileptic children and the consequence of vagal nerve stimulation, is limited to the linear and nonlinear HRV analysis and some statistics. The study design, measurements, data selection and most of the interpretations were the work of Katrien Jansen from the neurology division of Dr. Lagae from the Department of Paediatrics at the University Hospitals Gasthuisberg (Leuven, Belgium). This work has been submitted as a paper to the international journal *Developmental Medicine and Child Neurology* [374]. The importance of my part is reflected in my position as second author on the paper. The overview about cardiac changes in epilepsy as the first part of Chapter 8 is based on a review by Katrien Jansen published in *Seizure: European Journal of Epilepsy* [171].

1.8 Conclusion

The basic physiology of the nervous system and the cardiovascular system was introduced. This included the relation between the brains and the heart via the autonomic nervous system and the concept of heart rate variability as marker of the autonomic heart rate regulation. This relevant background information is necessary to interprete the results of the several applications described in the following chapters. The wide range of HRV application areas was discussed. Moreover, the different goals of the thesis were addressed and a chapter-by-chapter overview was provided, including the personal contributions.

Chapter 2

Linear and nonlinear methodology

Chapter 2 introduces the mathematics and techniques, necessary for a good understanding of the thesis. First the peak detection algorithm and the preprocessing methods are presented in Section 2.1. While Section 2.2 describes the linear methods in time domain, frequency domain and the time-frequency representations, Section 2.3 gives an overview of some nonlinear techniques assessing scaling behaviour, complexity and chaotic behaviour. An attempt to find a physiological meaning of the noise titration parameter is explained in Section 2.4. Section 2.5 discusses the difference between nonlinearity and chaoticity and the question whether the cardiovascular system is nonlinear and/or chaotic. Several methods to quantify baroreflex sensitivity are explained in Section 2.6. Finally, Section 2.7 reveals the test statistics used further in this thesis for the several applications. While some final remarks are given in Section 2.8, Section 2.9 summarizes the topics discussed in this chapter.

2.1 Peak detection and preprocessing

2.1.1 Pan-Tompkins algorithm

HRV analysis is based on the fluctuations in RR intervals. This means the first step in processing the ECG is to determine the R-peaks of the QRS-complexes. Pan and Tompkins [269] proposed a real-time QRS detection algorithm based on analysis of the slope, amplitude and width of the QRS complexes. The

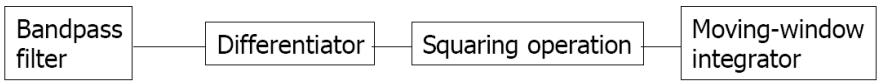


Figure 2.1: *Block diagram of the Pan-Tompkins algorithm for QRS peak detection.*

algorithm includes a series of filters and methods that perform low-pass, high-pass, derivative, squaring, integration, adaptive thresholding and search procedures as illustrated schematically in Figure 2.1. A recursive low-pass filter firstly provides an attenuation greater than 35 dB at 50 Hz to suppress power-line interference, if present. The high-pass filter has a cutoff frequency of 5 Hz and introduces a delay of 80 ms. Secondly, the derivative procedure suppresses the low frequency components of the P and T wave and provides a large gain to the high frequency components arising from the high slopes of the QRS complex. In a next step, the squaring operation makes the result positive and emphasizes large differences resulting from QRS complexes. Finally, the output of the preceding operations is smoothed through a moving window integration filter with a window width small enough to prevent merging of QRS and T waves, but large enough to yield only one peak for a single QRS complex.

2.1.2 Preprocessing

The Pan-Tompkins algorithm works well in general. Nevertheless, there will always be some mistakes, namely wrong peak detections and missed peaks as shown in Figure 2.2. Therefore, preprocessing the data is unevitable. Missed beats can be replaced via interpolation while wrong peak detections can be summed in the most optimal way, based on information of the previous beats. An example can be seen on top of Figure 2.2. Moreover, also premature supraventricular and ventricular beats need to be removed as HRV can only reliably extract information from normal sinus rhythms. To exclude these typical beats, filters are available with omission of one subsequent beat and linear interpolation of the corresponding periods. This way, type A errors (QRS detected prematurely when in fact a sinus conducted wave has not occurred) and type B errors (failing to detect an R wave that is present) could be largely avoided [178, 154]. A 20%-filter [191] was used, meaning that every RR interval that differ more than 20% from the previous one, is replaced by an interpolated value, defined via spline interpolation over the 5 previous and 5 next intervals. The assumption that underlies this correction is that the RR interval does not oscillate abruptly from the mean value and that the use of linear interpolation will introduce less high frequency noise. Secondly, a trend removal algorithm is applied that removes any trend in the signal. This has no influence on regular stationary baseline data, but it prevents artificial low frequency power. Finally, a file containing the consecutive normal-to-normal

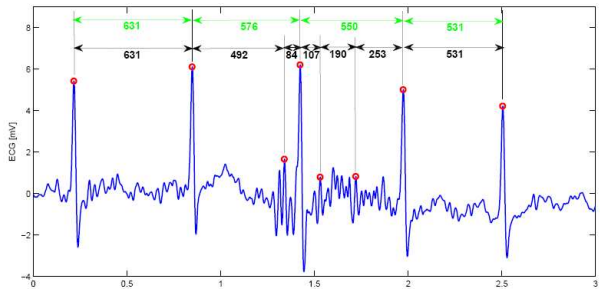


Figure 2.2: *Example of wrong peak detections by the Pan-Tompkins algorithm. The result after preprocessing is given on top and shows that the wrong intervals were concatenated correctly.*

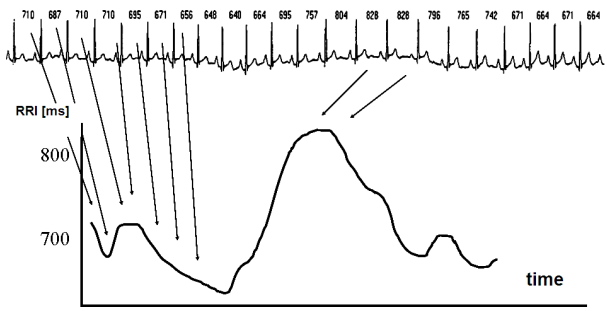


Figure 2.3: *Illustration how to derive the tachogram (RR interval time series) from the ECG signal. First, R peaks are detected (see Figure 1.5) and the time between two successive R peaks, which is called the RR interval (RRI), is calculated and expressed in milliseconds as indicated on top. Then, all these RR intervals become the samples of a new signal, called tachogram or RR interval time series shown at the bottom, where the RR intervals (ms) are plotted on the Y axis versus the time (s) at which the heart beat occurs on the X axis*

(NN) intervals is exported for later processing. Such an RR interval time series, illustrated in Figure 2.3, is called a tachogram and is the signal on which HRV techniques will be applied.

Analogously, beat-to-beat blood pressure values, resulting in a systogram, can be derived from the systolic arterial pressure (SAP) signal to calculate blood pressure variability (BPV). To summarize, a schematic overview of the preprocessing blocks as well as the ways of HRV processing is shown in Figure 2.4. More information about the linear and nonlinear processing is given in Sections 2.2 and 2.3.

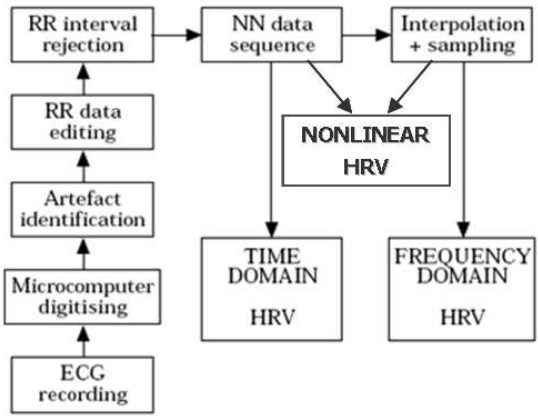


Figure 2.4: *Block diagram illustrating the different steps from ECG recording to the different HRV output parameters. Adapted from [355]*

2.2 Linear techniques

One example will be used throughout the following sections to explain more visually, if possible, what the technique does and how it can be calculated on the tachogram. The chosen example is given in Figure 2.5, being an RR interval time series extracted from an ECG signal monitored during a stress test. The tachogram has a length of 2712 seconds (45 minutes) containing 3984 heart beats. Before calculating HRV parameters, preprocessing was necessary as explained in paragraph 2.1. As indicated in the figure, some irregular or faulty RR intervals were corrected this way, changing the shortest RR interval from 256 ms to 443 ms. In other words, the impossible instantaneous heart rate of 234 bpm in such condition was corrected by the preprocessing algorithm to a maximal instantaneous heart rate of 135 bpm which was probably correct.

The linear time and frequency domain techniques for HRV were standardized in a report of the Task Force of the European Society of Cardiology and the North American Society of Pacing ans Electrophysiology [355].

2.2.1 Time domain analysis

Simple time domain variables that can be calculated include the *mean NN interval*, the *mean heart rate* and the difference between the longest and shortest NN interval.

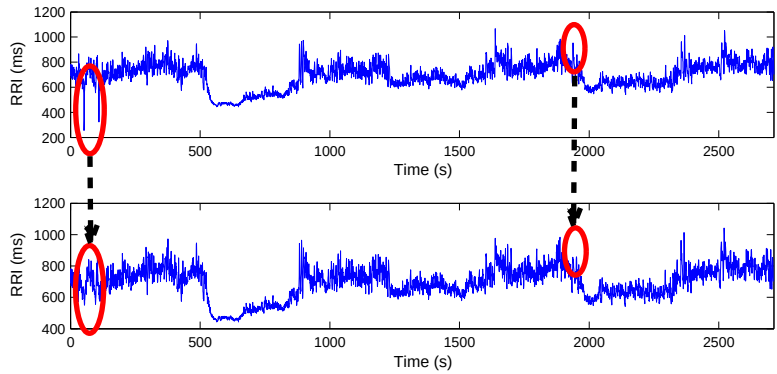


Figure 2.5: *The tachogram used as example throughout this chapter to explain more visually, if possible, what the described techniques do and how the HRV parameters can be calculated. On top, the RR interval time series is given after R peak detection while the preprocessed signal is shown at the bottom. The ellipses indicate where the signal changed after preprocessing.*

The methods may be divided into two classes, (a) those derived from direct measurements of the NN intervals, and (b) those derived from the differences between NN intervals.

The simplest variable to calculate is the standard deviation of the NN interval (*SDNN*), the square root of variance. Since variance is mathematically equal to total power of spectral analysis, SDNN reflects all the cyclic components responsible for variability in the period of recording. In many studies, SDNN is calculated over a 24h period and thus encompasses both short-term high frequency variations, as well as the lowest frequency components seen in a 24h period. As the period of monitoring decreases, SDNN estimates shorter and shorter cycle lengths. It should also be noted that the total variance of HRV increases with the length of analyzed recording [321]. Thus, on arbitrarily selected ECGs, SDNN is not a well defined statistical quantity because of its dependence on the length of recording period. Consequently, in practice, it is inappropriate to compare SDNN measures obtained from recordings of different durations. However, durations of the recordings used to determine SDNN values (and similarly other HRV measures) should be standardized. 5-minute recordings for short-term and nominal 24h for long-term recordings seem to be appropriate options.

Other commonly used statistical variables calculated from segments of the total monitoring period include *SDANN*, the standard deviation of the average NN interval calculated over short periods, usually 5 minutes, which is an estimate of the changes in heart rate due to cycles longer than 5 minutes, and the *SDNN*

index, the mean of the 5-minute standard deviation of the NN interval calculated over 24h, which measures the variability due to cycles shorter than 5 minutes.

The most commonly used measures derived from interval differences include *RMSSD*, the square root of the mean squared differences of successive NN intervals, *pNN50*, the number of interval differences of successive NN intervals greater than 50 ms divided by the total number of NN intervals and multiplied by 100 (expressed in %) and *SDSD*, the standard deviation of differences between adjacent NN intervals. All these measurements of short-term variation estimate high frequency variations in heart rate and thus are highly correlated.

For the given example, the statistical time domain parameters are: mean RR = 680.82 ms, SDNN = 106.93 ms, SDANN = 69.92 ms, SDNN index = 76.36 ms, SDSD = 29.91 ms; RMSSD = 41.74 ms and pNN50 = 17.15

2.2.2 Frequency domain analysis

Various spectral methods for the analysis of the tachogram have been applied. Power spectral density (PSD) analysis provides the basic information of how power, and therefore the variance, distributes as a function of frequency. Independent of the method employed, only an estimate of the true PSD of the signals can be obtained by proper mathematical algorithms.

Parametric versus nonparametric

Methods for the calculation of PSD may be generally classified as nonparametric and parametric. In most instances, both methods provide comparable results. The advantages of the nonparametric methods are: (a) the simplicity of the algorithm employed (Fast Fourier Transform – FFT – in most of the cases) and (b) the high processing speed, whilst the advantages of parametric methods are: (a) smoother spectral components which can be distinguished independently of preselected frequency bands, (b) easy post-processing of the spectrum with an automatic calculation of low and high frequency power components and easy identification of the central frequency of each component, and (c) an accurate estimation of PSD even on a small number of samples on which the signal is supposed to maintain stationarity. The basic disadvantage of parametric methods is the need to verify the suitability of the chosen model and its complexity (the order of the model).

In most cases, first a resampling of the RR interval time series is necessary to have equidistant time points. However, via the Lomb periodogram the spectrum can also be calculated directly from the unevenly spaced times series [**?**].

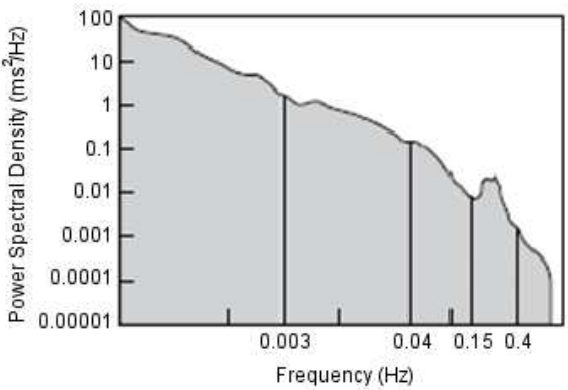


Figure 2.6: *Example of an estimate of power spectral density obtained from the entire 24h interval of a long-term Holter recording. The different frequency bands are clearly indicated: ultra-low frequency component (ULF), very low frequency component (VLF), low frequency component (LF) and high frequency component (HF). Adapted from [355].*

Short-term recordings

One has to distinguish between short-term and long-term recordings. During short-term recordings, three main spectral bands are distinguished in a spectrum: very low frequency (VLF) below 0.04 Hz, low frequency (LF) from 0.04 to 0.15 Hz, and high frequency (HF) fluctuations from 0.15 to 0.4 Hz (Figure 2.6). The distribution of the power and the central frequency of LF and HF are not fixed but may vary in relation to changes in autonomic modulations of the heart period. In each frequency band, the power is calculated as the area under the PSD curve between the corresponding lower and upper bound. The total power (TP) is defined as the power in the frequency band going from 0 Hz to 1 Hz. Calculation of VLF, LF and HF powers are usually made in *absolute values of power* (ms^2), but LF and HF may also be measured in *normalized units (n.u.)*:

$$LF(n.u.) = \frac{LF}{TP - VLF} \quad , \quad HF(n.u.) = \frac{HF}{TP - VLF} \tag{2.1}$$

The representation of LF and HF in n.u. emphasizes the controlled and balanced behaviour of the two branches of the autonomic nervous system. Moreover, normalization tends to minimize the effect on the values of LF and HF components of the changes in total power. Another measure is LF/HF, calculated as the ratio of the power in LF and HF band.

Vagal activity is the major contributor to the HF component. Disagreement exists concerning the LF component. While some studies suggest that LF, when expressed in normalized units, is a quantitative marker for sympathetic

modulations, most studies view LF as reflecting both sympathetic and vagal activity. Consequently, the LF/HF ratio is considered to mirror mainly sympathovagal balance. The physiological explanation of the VLF component is much less defined and the existence of a specific physiological process attributable to these heart period changes might even be questioned. The non-harmonic component which does not have coherent properties and which is affected by algorithms of baseline or trend removal is commonly accepted as a major constituent of VLF. Thus VLF assessed from $\leq$5 minute recordings is a dubious measure and should be avoided when interpreting the PSD of short-term ECGs.

Long-term recordings

For long-term recordings, spectral analysis may also be used to analyse the sequence of NN intervals in the entire 24h period. The result then includes an ultra-low frequency component (ULF) below 0.003 Hz, in addition to VLF (0.003 to 0.04 Hz), LF and HF components (Figure 2.6). Now, the problem of 'stationarity' comes in. A deterministic signal is said to be stationary if it can be written as a discrete sum of sinusoids :

$$x(t) = \sum_{k \in N} A_k \cos(2\pi f_k t + \Phi_k) \qquad for\ a\ real\ signal \tag{2.2}$$

$$x(t) = \sum_{k \in N} A_k \exp[j(2\pi f_k t + \Phi_k)] \qquad for\ a\ complex\ signal \tag{2.3}$$

with A_k the amplitude, f_k the frequency and Φ_k the phase of the k^{th} sinusoid. If mechanisms responsible for heart period modulations of a certain frequency remain unchanged during the whole period of recording, the corresponding frequency component of HRV may be used as a measure of these modulations. If the modulations are not stable, interpretation of the results of frequency analysis is less well defined. In particular, physiological mechanisms of heart period modulations responsible for LF and HF power components cannot be considered stationary during the 24h period [122]. Therefore, spectral analysis performed in the entire 24h period as well as spectral results obtained from shorter segments averaged over the entire 24h period (the LF and HF results of these two computations are equal) provide averages of the modulations attributable to the LF and HF components (Figure 2.6). Such averages obscure detailed information about autonomic modulation of RR intervals available in shorter recordings [122]. It should be noticed that the components of HRV provide measurements of the degree of autonomic modulations rather than of the level of autonomic tone [220] and averages of modulations do not represent an averaged level of tone.

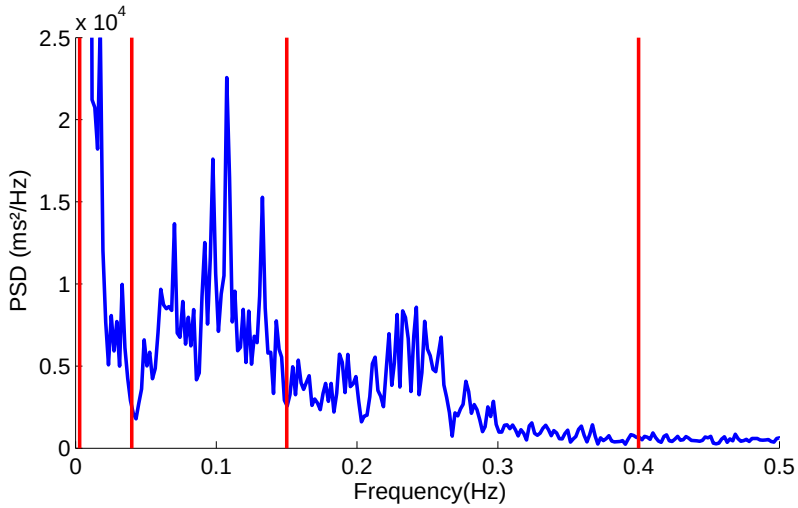


Figure 2.7: *Power spectral density (PSD) of the tachogram example given in Figure 2.5. The different frequency bands are clearly indicated by the vertical lines: ultra-low frequency component (ULF), very low frequency component (VLF), low frequency component (LF) and high frequency component (HF).*

Example

The same tachogram example as in Figure 2.5 is used. The PSD, shown in Figure 2.7, was obtained by first resampling the signal at 2 Hz and then calculating the Fast Fourier Transform (FFT) via the Welch method [388]. Internal parameters were chosen as follows: segment length of 1024 samples (here RR intervals), 50% overlap, windowing with a Hamming window and calculating 1024 FFT points. As described earlier, powers were calculated in each defined fequency band, leading to: TP = 8817 ms^2, ULF = 3214 ms^2, VLF = 1534 ms^2, LF = 848.5 ms^2, HF = 665.7 ms^2, LF/HF = 1.27, LFnu = 0.2099 and HFnu = 0.1647.

Correlation and differences between time and frequency domain measures

When analyzing stationary short-term recordings, more experience and theoretical knowledge exists on the physiological interpretation of the frequency domain measures compared to the time domain measures derived from the same recordings. However, many time and frequency domain variables measured over a long term period are strongly correlated with each other as summarized in Table 2.1. These strong correlations exist because of both mathematical and physiological relationships. In addition, the physiological interpretation of the spectral

Table 2.1: *Approximate correspondence of time domain and frequency domain methods applied to long term ECG recordings.*

time domain variable	Frequency domain correlate
SDNN	Total power
HRV triangular index	Total power
TINN	Total power
SDANN	ULF
SDNN index	Mean of 5 minute total power
RMSSD	HF
SDSD	HF
pNN50	HF

components calculated over 24 h is difficult, for the reasons mentioned before. Therefore, unless special investigations are performed which use the 24h HRV signal to extract information other than the usual frequency components (e.g. the log - log slope of spectrogram, see Section 2.3.1), the results of frequency domain analysis are equivalent to those of time domain analysis, which is easier to perform.

2.2.3 Time-frequency analysis

Because of the problem of stationarity as discussed in the previous paragraph, frequency domain HRV parameters are not reliable in case of quick changes in heart rate or its autonomic modulation. The spectrum essentially tells us which frequencies are contained in the signal, as well as their corresponding amplitudes and phases, but does not tell us at which times these frequencies occur. Luckily, there exist techniques which combine time and frequency information simultaneously, the so called time-frequency representations (TFR). An overview of TFRs is given by Auger et al [20], but we only discuss the basic short-time Fourier transform (STFT) and the more advanced continuous wavelet transform (CWT) which is used in Chapter 5. A schematic illustration of the differences between time series analysis, Fourier transform, STFT and CWT is shown in Figure 2.8 and will be explained further in the following subsections.

Short-time Fourier transform

In order to introduce time-dependency in the Fourier transform, a simple and intuitive solution consists in pre-windowing the signal $x(u)$ around a particular time t, calculating its Fourier transform, and doing that for each time instant t.

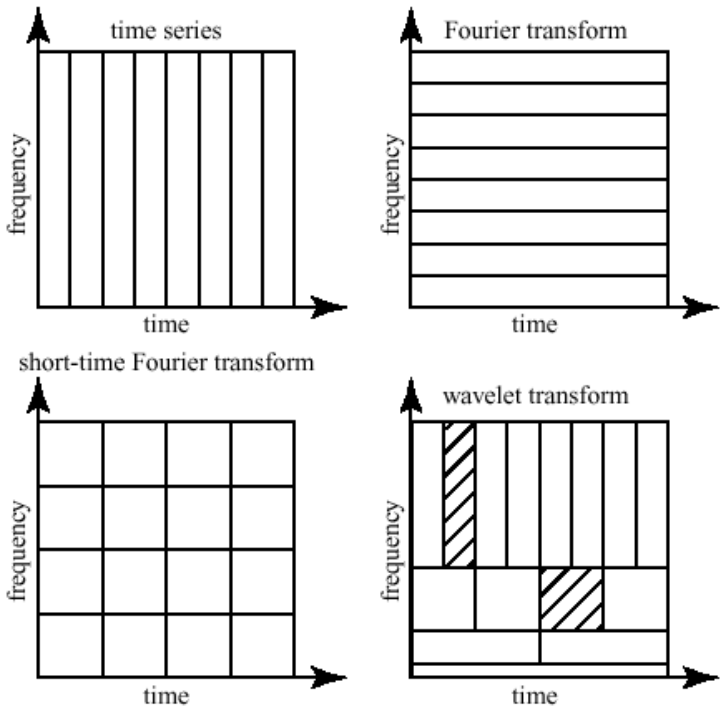


Figure 2.8: *A schematic illustration of the differences between time series analysis, Fourier transform, short-time Fourier transform and continuous wavelet transform regarding the time and frequency resolution.*

The resulting transform, called the short-time Fourier transform (STFT), is:

$$F_x(t, f; h) = \int_{-\infty}^{+\infty} x(u) \cdot h^*(u - t) \cdot e^{-j2\pi fu} \cdot du \tag{2.4}$$

where $h(t)$ is a short-time analysis window localized around $t = 0$ and $f = 0$. The STFT is als invertible, but this type of time-frequency representation has a trade-off between time and frequency resolutions. On one hand, a good time resolution requires a short window $h(t)$ while on the other hand, a good frequency resolution requires a narrow-band filter and therfore a long window $h(t)$. This limitation is a consequence of the Heisenberg-Gabor inequality.

If we consider the squared modulus of the STFT, we obtain a spectral energy density of the locally windowed signal $x(u)h^*(u-t)$:

$$S_x(t,f) = \left| \int_{-\infty}^{+\infty} x(u) \cdot h^*(u-t) \cdot e^{-j2\pi fu} \cdot du \right|^2 \tag{2.5}$$

This defines the *spectrogram*, which is a real-valued and non-negative distribution. Since the window h of the STFT is assumed of unit energy, the spectrogram satisfies the global energy distribution property :

$$E_x = \int_{-\infty}^{+\infty} \int_{-\infty}^{+\infty} S_x(t,f) \cdot dt \cdot df \tag{2.6}$$

Therefore, we can interpret the spectrogram as a measure of the energy of the signal contained in the time-frequency domain centered at the point (t,f).

Continuous wavelet transform

The idea of the continuous wavelet transform (CWT) is to project a signal x on a family of zero-mean functions (the wavelets) deduced from an elementary function (the mother wavelet) by translations and dilations:

$$T_x(t,a;\Psi) = \int_{-\infty}^{+\infty} x(s) \cdot \Psi^*_{t,a}(s) \cdot ds \tag{2.7}$$

where

$$\Psi_{t,a}(s) = |a|^{-1/2} \cdot \Psi\left(\frac{s-t}{a}\right). \tag{2.8}$$

Several types of wavelet functions exist such as the Morlet wavelet, Haar wavelet, Shannon wavelet, Daubechies wavelet, Gaussian wavelet, Meyer wavelet and Mexican hat wavelet. Some of them are illustrated in Figure 2.9.

The variable a corresponds now to a scale factor, in the sense that taking $|a| > 1$ dilates the wavelet Ψ and taking $|a| < 1$ compresses Ψ. By definition, the wavelet transform is more a time-scale than a time-frequency representation. However, for wavelets which are well localized around a non-zero frequency f_0 at scale $a = 1$, a time-frequency interpretation is possible thanks to the formal identification $f = \frac{f_0}{a}$. The basic difference between the wavelet transform and the short-time Fourier transform is as follows: when the scale factor a is changed, the duration and the bandwidth of the wavelet are both changed but its shape remains the

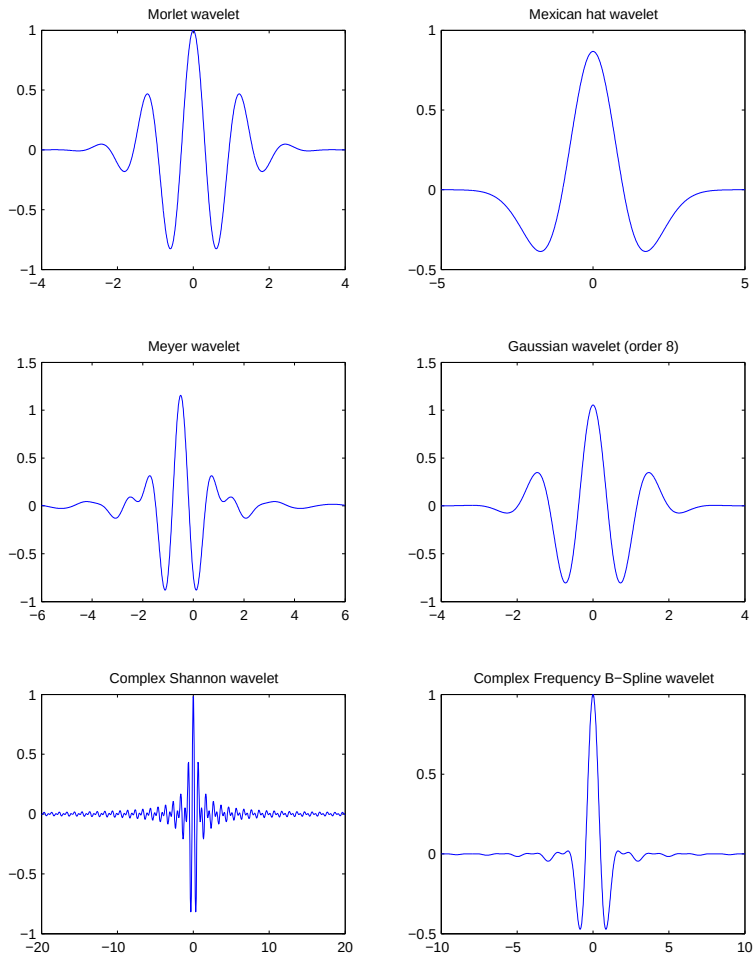


Figure 2.9: *Illustration of several types of mother wavelet functions: Morlet wavelet (top left), Mexican hat wavelet (top right), Meyer wavelet (middle left), Gaussian wavelet (middle right), complex Shannon wavelet (bottom left), complex frequency B-spline wavelet (bottom right).*

same. And in contrast to the STFT, which uses a single analysis window, the CWT uses short windows at high frequencies and long windows at low frequencies. This partially overcomes the resolution limitation of the STFT as the bandwidth B is proportional to f. The CWT can also be seen as a filter bank analysis composed of band-pass filters with constant relative bandwidth. As the STFT was inversible, the signal x can also be reconstructed from its continuous wavelet transform according to the formula:

$$x(t) = \int_{-\infty}^{+\infty} \int_{-\infty}^{+\infty} T_x(s, a; \Phi) \cdot \Psi_{s,a}(t) \cdot ds \cdot \frac{da}{a^2} \tag{2.9}$$

A similar distribution to the spectrogram can be defined in the wavelet case. Since the continuous wavelet transform behaves like an orthonormal basis decomposition, it can be shown that it preserves energy:

$$E_x = \int_{-\infty}^{+\infty} \int_{-\infty}^{+\infty} |T_x(t, a; \Psi)|^2 \cdot dt \cdot \frac{da}{a^2} \tag{2.10}$$

where E_x is the energy of x. This leads us to define the *scalogram* of x as the squared modulus of the continuous wavelet transform. It is an energy distribution of the signal in the time-scale plane, associated with the measure $dt\frac{da}{a^2}$. As for the wavelet transform, time and frequency resolutions of the scalogram are related via the Heisenberg-Gabor principle: time and frequency resolutions depend on the considered frequency.

Instantaneous frequency and power

The instantaneous frequency of a signal calculated as the derivative of the phase of its analytical signal often produces results that, in some ways, may seem paradoxical [74], and which, in any case, make their physical interpretation difficult. This drawback can be avoided by defining instantaneous frequency as the mean frequency of the spectrum at each instant, where the spectrum is obtained as a section of the time frequency distribution at this instant

$$f_s(t) = \frac{\sum_{n=1}^{N} f_n \cdot TFR_{xx}(t, f_n)}{\sum_{n=1}^{N} TFR_{xx}(t, f_n)} \tag{2.11}$$

where N is the number of samples on the frequency axis. This way, instantaneous frequencies can be calculated for each RR signal and separately in each of the

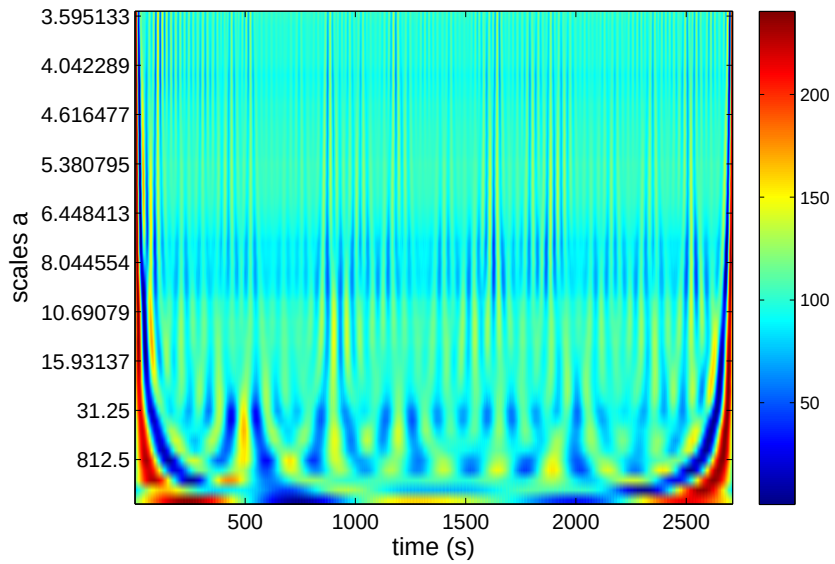


Figure 2.10: *Scalogram of the tachogram example given in Figure 2.5, obtained via the continuous wavelet transform (CWT). The frequency information is given on the vertical axis by means of scales (high scales correspond with low frequencies and vice versa) as a function of time on the horizontal axis.*

predefined frequency bands VLF, LF and HF. Analogously, in each frequency band the energy (power) can be calculated by integrating the spectogram, expressed in absolute values or normalized units.

Example

As heart rate is changing quickly in the example (Figure 2.5), a time-frequency analysis is appropriate. Figure 2.10 shows the scalogram obtained after applying the continuous wavelet transform with the Morlet wavelet and a sampling frequency of 1 Hz. After converting scales to frequencies, the frequency HRV parameters can be calculated in exact the same way as in a PSD, but now as a function of time and therefore revealing how LF or HF power or frequency change in time (Figure 2.11). These results can even be smoothed by averaging or filtering the output signal.

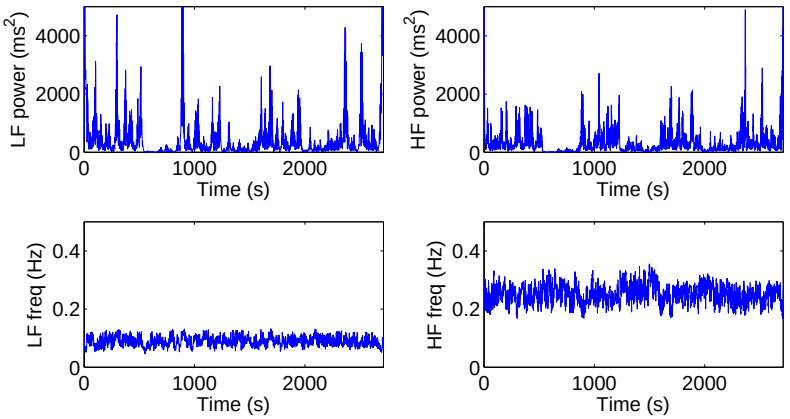


Figure 2.11: *Instantaneous LF power (top left), HF power (top right), LF frequency (bottom left) and HF frequency (bottom right) of the tachogram example given in Figure 2.5.*

2.3 Nonlinear techniques

The cardiac system is dynamic, nonlinear, and nonstationary, with performance continually fluctuating on a beat-to-beat basis as extrinsic and intrinsic stimuli simultaneously influence the state of the system [70, 411]. Due to the assumptions and conditioning requirements, linear analyses may not account for all aspects of cardiac performance, particularly the subtle interactions between the control mechanisms that regulate cardiac function [221]. Analysis techniques arising from nonlinear system dynamics theory were therefore developed to ascertain the multidimensional processes that control the cardiac system [5].

A nonlinear system is mathematically defined as a second- or higher-order power system, meaning that the independent variable in the mathematical equation contains an exponent. For example, the equation for a parabola, $y = x^2$, describes a simple nonlinear system. Whereas in a linear system the variables produce an output response, in a nonlinear system the variables contribute to the output response. Although a linear system can be decomposed into its component parts, in a nonlinear system, the parts interfere, cooperate, or compete with each other. A small change dramatically alters the nonlinear system because the initial condition of all variables along with the input stimulus influences the output response. Nonlinear system dynamics theory allows for the mathematical reconstruction of an entire system from one known variable since the reconstructed dynamics are geometrically similar to the original dynamics [179]. Chaos theory, which was popularized by Gleicks best-selling book [134], is a specialized subtheory of

nonlinear system dynamics that describes systems that are low-dimensional (3 to 5 variables), have defined boundaries, and exhibit sensitive dependence on initial conditions. This theory alerted scientists to the value of mathematical error and physiological noise when describing a systems behaviour [133]. Small differences in initial conditions (such as those due to rounding errors in numerical computation) yield widely diverging outcomes for chaotic systems, rendering long-term prediction impossible in general. This happens even though these systems are deterministic, meaning that their future behaviour is fully determined by their initial conditions, with no random elements involved. In other words, the deterministic nature of these systems does not make them predictable. This behaviour is known as deterministic chaos, or simply chaos. Also, with sinus rhythm, deterministic behaviour is exhibited during a cardiac cycle and stochastic behaviour between cardiac cycles [69, 409]. Consequently, analysis techniques based on the broader nonlinear system dynamics theory have been used to explain and account for the nonlinearity of the high-dimensional cardiac system. Numerous nonlinear analysis techniques exist.

Several commonly used nonlinear techniques will be explained now. Some recent review papers discussing nonlinear HRV are Acharya et al [1] and Voss et al [385].

2.3.1 1/f slope

Kobayashi and Musha [193] first reported the frequency dependence of the power spectrum of RR interval fluctuations. The plots had an uneven density that might overweight for data in the higher-frequency range. Therefore, a logarithmic interpolation is used, resulting in a balanced number of points for linear interpolation. The slope of the regression line of the log(power) versus log(frequency) relation $(1/f)$, usually calculated in the $10^{-4} - 10^{-2}$ Hz frequency range, corresponds to the negative scaling exponent β and provides an index for long-term scaling characteristics [321]. Figure 2.12 indicates the $(1/f)^{\beta}$ relation between PSD and frequency, reflected on a log - log scale approximately as a line. The figure is the result for the example used throughout this chapter, leading to a 1/f slope of -1.34

This broadband spectrum, characterizing mainly slow HR fluctuations indicates a fractal-like process with a long-term dependence [210]. Saul et al [321] found that β is similar to -1 in healthy young men. This linearity of the regression line and the slope of -1 in healthy persons mean that the plots of RR-interval versus time over 2 minutes $(10^{-2}Hz)$, 20 minutes $(10^{-3}Hz)$ and 3 hours $(10^{-4}Hz)$ may appear similar. This is called scale-invariance or self-similarity in fractal theory. It has been suggested that the scale invariance may be a common feature of normal physiological function. The breakdown of normal physiological functioning could

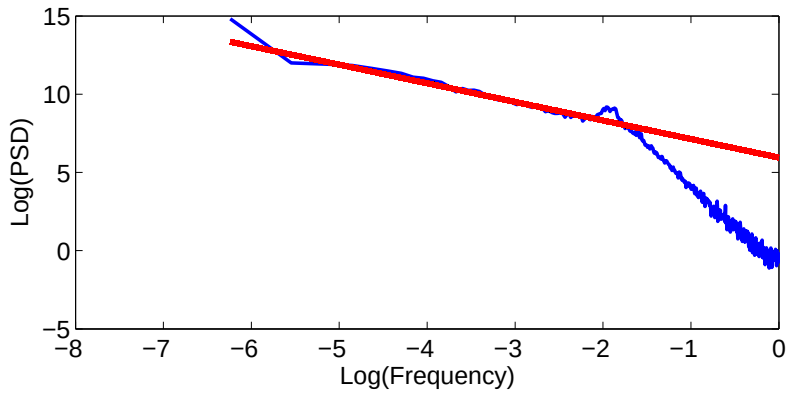


Figure 2.12: *Log(power) versus log(frequency) plot of the tachogram example given in Figure 2.5. The thick line indicates the 1/f slope or scaling exponent β and is derived as the regression line calculated in the $10^{-4} - 10^{-2}$ Hz frequency range.*

lead to either random or periodic behaviour, indicated by steeper $1/f$-slopes, which could lead to a more vulnerable state of homeostasis.

Bigger et al [49] reported an altered regression line ($\beta \approx -1.15$) in patients after MI. A disadvantage of this measure is the need for large datasets. Moreover, stationarity is not guaranteed in long datasets and artefacts and patient movement influence spectral components.

2.3.2 Fractal dimension

The term 'fractal' was first introduced by Mandelbrot [224]. A fractal is a set of points that when looked at smaller scales, resembles the whole set. An essential characteristic of a fractal is self-similarity. This means that its details at a certain scale are similar, but not necessarily identical, to those of the structure seen at larger or smaller scales. A simple mathematical example illustrating the self-similarity property is the Koch curve (Figure 2.13).

The concept of fractal dimension (FD) that refers to a noninteger or fractional dimension originates from fractal geometry. The FD emerges to provide a measure of how much space an object occupies between Euclidean dimensions. The FD of a waveform represents a powerful tool for transient detection. This feature has been used in the analysis of ECG and EEG to identify and distinguish specific states of physiological function. Several algorithms are available to determine the FD of the waveform, amongst others the algorithms proposed by Higuchi and Katz.

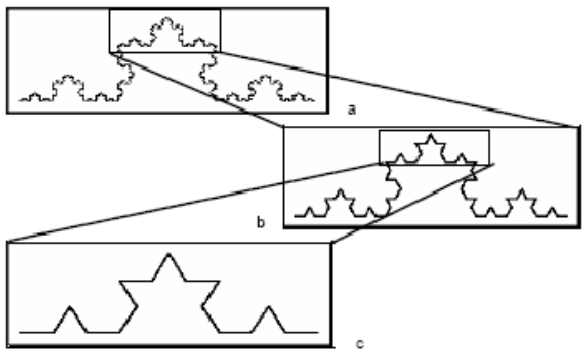


Figure 2.13: *An illustration of how fractals look like with the feature of scale independence and self-similarity: (a) the Koch curve and (b and c) details of the top of the curve.*

From a practical point of view, one often estimates the FD via the box-counting method. The higher the FD, the more irregular the signal.

Algorithm of Katz

According to the method of Katz [183] the FD of a curve can be defined as

$$D^{Katz} = \frac{\log(L)}{\log(d)} \tag{2.12}$$

where L is the total length of the curve or sum of distances between successive points, and d is the diameter estimated as the distance between the first point of the sequence and the most distal point of the sequence. Mathematically, d can be expressed as:

$$d = max(\|x(1) - x(i)\|) \qquad \forall i. \tag{2.13}$$

Considering the distance between each point of the sequence and the first, point i is the one that maximizes the distance with respect to the first point. The FD compares the actual number of units that compose a curve with the minimum number of units required to reproduce a pattern of the same spatial extent. FDs computed in this fashion depend upon the measurement units used. If the units are different, then so are the FDs. Katz approach solves this problem by creating a general unit or yardstick: the average step or average distance between successive

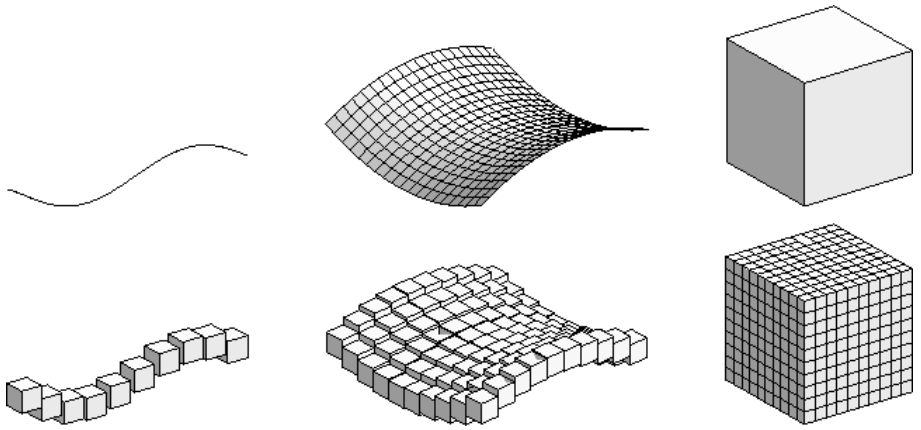


Figure 2.14: *Principle of box-counting algorithm: covering a curve, a surface, and a solid cube with cubes of diameter ϵ. Covering the unit square with little squares of side length ϵ is possible with $1/\epsilon^2$ boxes. To cover a segment of length 1, you only need $1/\epsilon$ little squares. If we think of the square and segment as sitting in space and try to cover them with little cubes ϵ on a side, we get the same answer. And if we use the little cubes to cover a 1x1x1 cube, we need exactly $1/\epsilon^3$. Note that the exponent here is the same as the dimension of the thing we are trying to cover. From* `http://www.math.sunysb.edu/~scott/Book331/Fractal_Dimension.html`

points, a. Normalizing the distances, D^{Katz} is then given by

$$FD = \frac{\log(L/a)}{\log(d/a)} \tag{2.14}$$

Box-counting method

What is the relationship between an objects length (or area or volume) and its diameter? The answer to this question leads to another way to think about dimension. Let us consider a few examples (Figure 2.14). If one tries to cover the unit square with little squares of side length ϵ, one will need $1/\epsilon^2$ boxes. To cover a segment of length 1, you only need $1/\epsilon$ little squares. If we think of the square and segment as sitting in space and try to cover them with little cubes ϵ on a side, we get the same answer. And if we use the little cubes to cover a 1x1x1 cube, we need exactly $1/\epsilon^3$. Note that the exponent here is the same as the dimension of the thing we are trying to cover. This is no coincidence, but the general rule is:

$$N_\epsilon(S) \sim 1/\epsilon^d \qquad as\, \epsilon \to 0 \tag{2.15}$$

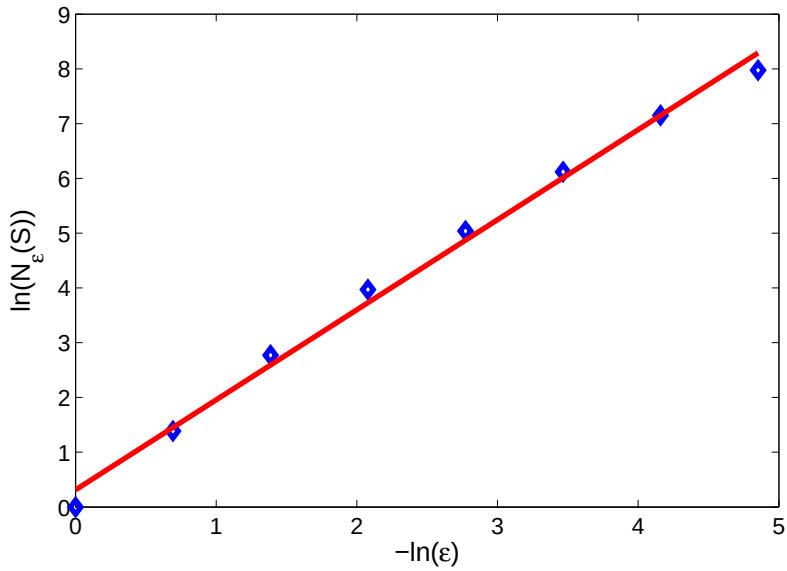


Figure 2.15: *Illustration of the box-counting method applied on the tachogram example given in Figure 2.5. First a 2D plane is built based on the dataset S, here consisting of both the RR intervals and corresponding time points. The number of boxes in that plane containing points of the dataset is counted and given by $N_\epsilon(S)$. This depends on the size of the boxes, namely ϵ. This relation is represented in a ln – ln scale by the rhombuses. The line is the best fit through these points and the slope of the line reflects the fractal dimension.*

where ϵ is the length of a box or square, S the full dataset and $N_\epsilon(S)$ the minimum number of n-dimensional boxes needed to cover S fully. d is the dimension of S. This way, the FD can be estimated via a box-counting algorithm as proposed by Barabasi and Stanley [24] as follows:

$$FD = -\lim_{\epsilon \to 0} \frac{\ln N_\epsilon(S)}{\ln \epsilon} \tag{2.16}$$

One also refers to the fractal dimension as the box-counting dimension or shortly box dimension. Given the standard RR interval time series as example (Figure 2.5), the relation between the number of boxes and the box size is shown in Figure 2.15, resulting in a FD equal to 1.6443.

2.3.3 Detrended fluctuation analysis

Detrended fluctuation analysis (DFA) is used to quantify the fractal scaling properties of short interval signals. This technique is a modification of root-mean-square analysis of random walks applied to nonstationary signals [163]. The root-mean-square fluctuation of an integrated and detrended time series is measured at different observation windows and plotted against the size of the observation window on a log - log scale. First, the RR interval time series $\mathbf{x}$ (of total length N) is integrated as follows:

$$y(k) = \sum_{i=1}^{k} [x(i) - x_{average}] \tag{2.17}$$

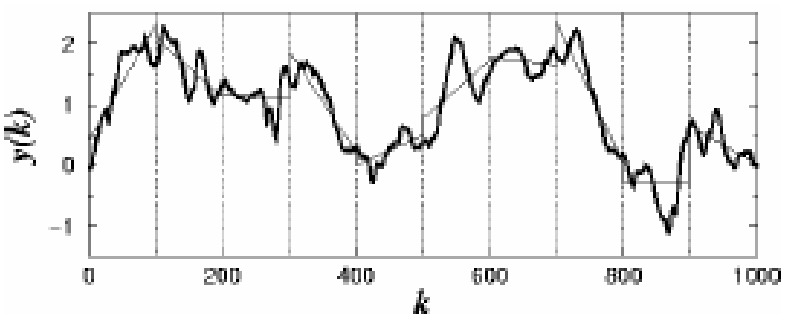
where $y(k)$ is the k^{th} value of the integrated series, $x(i)$ is the i^{th} RR interval and $x_{average}$ is the mean of the RR intervals over the entire series. Then, the integrated time series is divided into windows of equal length n. In each window of length n, a least-squares line is fitted to the data, representing the trend in that window as shown in Figure 2.16(a). The y-coordinate of the straight line segments are denoted by $y_n(k)$. Next, we detrend the integrated time series, $y_n(k)$, in each window. The root-mean-square fluctuation of this integrated and detrended series is calculated using the equation:

$$F(n) = \sqrt{\frac{1}{N} \sum_{k=1}^{N} [y(k) - y_n(k)]^2} \tag{2.18}$$

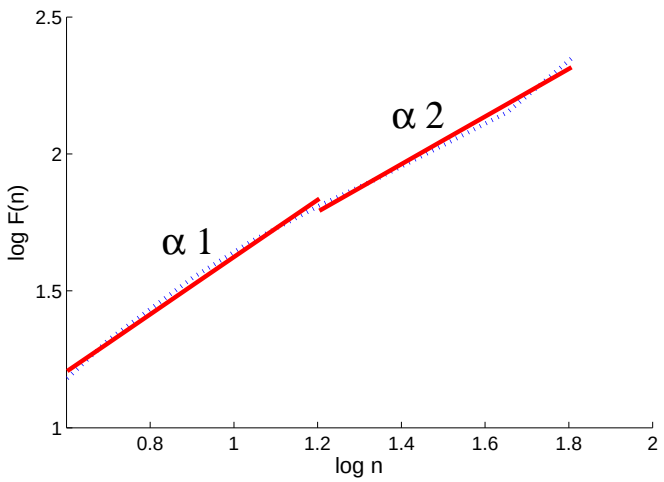
This computation is repeated over all time scales (window sizes) to obtain the relationship between $F(n)$ and the window size n (the number of points, here RR intervals, in the window of observation). Typically, $F(n)$ will increase with window size. The scaling exponent DFA α indicates the slope of this line, which relates log(fluctuation) to log(window size) as visualized in Figure 2.16(b). This method, based on a modified random walk analysis, was introduced and applied to physiological time series by Peng et al [273]. It quantifies the presence or absence of fractal correlation properties in nonstationary time series data. DFA usually involves the estimation of a short-term fractal scaling exponent α_1 over the range of $4 \leq n \leq 16$ heart beats and a long-term scaling exponent α_2 over the range of $16 \leq n \leq 64$ heart beats. Figure 2.16(b)) shows the DFA plot for the HR example, where DFA α_1 is 1.0461 and DFA α_2 is 0.8418.

Healthy subjects revealed a scaling exponent of approximately 1, indicating fractal-like behaviour. Patients with cardiovascular disease showed reduced scaling exponents, suggesting a loss of fractal-like HR dynamics ($\alpha_1 < 0.85$ [219]; $\alpha_1 < 0.75$ [163]). From many studies on test signals, one had the following α ranges:

- $0 < \alpha < 0.5$: power-law anti-correlations are present such that large values are more likely to be followed by small values and vice versa.



(a)



(b)

Figure 2.16: *The principle of detrended fluctuation analysis (DFA). (a) The integrated time series $y(k)$, calculated from the RR interval time series as given in equation (2.17), with indication of windows of size $n = 100$ (vertical dotted lines). The solid straight line segments represent the 'trend' estimated in each segment by a linear least-squares fit. The fluctuation, in this case F(100), is then calculated as the root-mean-square of the difference between the integrated time series $y(k)$ and the detrended series. When changing the window size n, other fluctuation values $F(n)$ can be obtained. From [273]. (b) The DFA plot, representing the logarithm of the fluctuation $F(n)$ versus the logarithm of the window size n, of the tachogram example given in Figure 2.5. The lines plotted on top of the dashed curve are the regression lines in two zones, of which the slopes indicate the short-term correlation α_1 and the long-term correlation α_2.*

- $\alpha = 0.5$: indicates white noise.
- $0.5 < \alpha < 1$: power-law correlations are present such that large values are more likely to be followed by large values and vice versa. The correlation is exponential.
- $\alpha = 1$: special case corresponding to $1/f$ noise.
- $\alpha > 1$: correlations exist, but cease to be of a power-law form.
- $\alpha = 1.5$: indicates Brownian noise.

The α exponent can also be viewed as an indicator of the 'roughness' of the original time series: the larger the value of α, the smoother the time series. In this context, $1/f$-noise can be interpreted as a compromise or 'trade-off' between the complete unpredictability of white noise (very rough 'landscape') and the much smoother landscape of Brownian noise.

It is important to note that DFA can only be applied reliably on time series of at least 2000 data points. DFA as such is a monofractal method, but also multifractal analysis exists [166]. This multifractal analysis describes signals that are more complex than those fully characterized by a monofractal model, but it requires many local and theoretically infinite exponents to fully characterize their scaling properties.

2.3.4 Approximate entropy and sample entropy

Entropy refers to system randomness, regularity, and predictability and allows systems to be quantified by rate of information loss or generation. Approximate Entropy (ApEn) quantifies the entropy of the system. More specifically, it measures the likelihood that runs of patterns that are close will remain close for subsequent incremental comparisons. An intuitive presentation is shown in Figure 2.17.

It was calculated according to the formula of Pincus [280]:

$$ApEn(m, r, N) = \frac{1}{N-m+1} \sum_{i=1}^{N-m+1} \log C_i^m(r) - \frac{1}{N-m} \sum_{i=1}^{N-m} \log C_i^{m+1}(r) \quad (2.19)$$

where

$$C_i^m(r) = \frac{1}{N-m+1} \sum_{j=1}^{N-m+1} \Theta(r - \|x_i - x_j\|) \quad (2.20)$$

is the correlation integral with Θ the Heavyside step function. x_i and x_j are respectively the i^{th} and j^{th} RR interval from the tachogram of length N. The

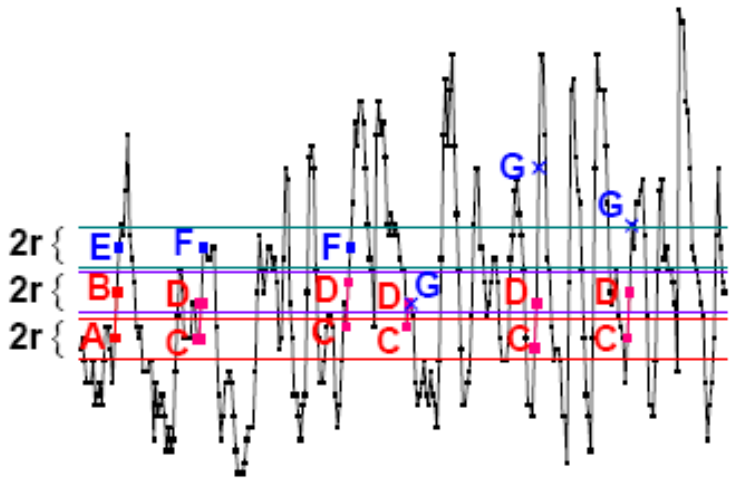


Figure 2.17: *Intuitive presentation of the principle of Approximate Entropy (ApEn) and Sample Entropy (SampEn). For a two-dimensional vector AB, the tolerance level r can be represented by horizontal red and violet lines around point A and B respectively, with width of 2r · SD. Then all vectors, say CD, whose first and second points (respectively C and D) are within the tolerance ranges of A and B (±r · SD), are counted to measure within a tolerance level r the regularity, or frequency, of patterns similarly to a given pattern of AB. In the figure, five CD vectors are close to vector AB. When increasing vector dimension from 2 to 3 (ABE), two vectors, namely CDF, remain close while the other three vectors, CDG, show emerging patterns. Thus the likelihood of remaining close is about 2/5. It is clear that such likelihood tends to 1 for regular series, and produces ApEn = 0 when taking the logarithm, while it tends to 0 for white noise and results in infinite ApEn theoretically. From [207].*

values of the input variables are chosen fixed, namely $m = 2$ and $r = 0.2$ as suggested by Goldberger et al [136] (m being the length of compared runs and r the tolerance level). High values of ApEn indicate high irregularity and complexity in time-series data.

Sample Entropy (SampEn) was developed by Richman and Moorman [299] and is very similar to the ApEn, but there is a small computational difference. In ApEn, the comparison between the template vector and the rest of the vectors also includes comparison with itself. This guarantees that probabilities $C_i^m(r)$ are never zero. Consequently, it is always possible to take a logarithm of probabilities. Because template comparisons with itself lower ApEn values, the signals are interpreted to be more regular than they actually are. These self-matches are

not included in SampEn leading to probabilities $C_i^{'m}(r)$:

$$C_i^{'m}(r) = \frac{1}{N-m+1} \sum_{j=1}^{N-m+1} \Theta(r - \|x_i - x_j\|) \qquad j \neq i \tag{2.21}$$

Finally, sample entropy is defined as:

$$SampEn(m, r, N) = -\ln[\frac{\Phi^{'m}(r)}{\Phi'^{m+1}(r)}] \tag{2.22}$$

with

$$\Phi^{'m}(r) = \frac{1}{N-m+1} \sum_{i=1}^{N-m+1} C_i^{'m}(r) \tag{2.23}$$

SampEn measures the complexity of the signal in the same manner as ApEn. However, the dependence on the parameters N (number of points) and r is different. SampEn decreases monotonically when r increases. In theory, SampEn does not depend on N where ApEn does. In analyzing time series including <200 data points, however, the confidence interval of the results is unacceptably large. For entropy measures, stationarity is required. In addition, outliers such as missed beats and artefacts may affect the entropy values.

The sample entropy of the tachogram example given in Figure 2.5 is 4.4837.

2.3.5 Correlation dimension

To describe the complexity of a system, often a transition is needed from the time domain to the so called phase space. In mathematics and physics, a phase space is a space in which all possible states of a system are represented, with each possible state of the system corresponding to one unique point in the phase space. In a phase space, every degree of freedom or parameter of the system is represented as an axis of a multidimensional space. For every possible state of the system, or allowed combination of values of the system's parameters, a point is plotted in the multidimensional space. Often this succession of plotted points is analogous to the system's state evolving over time. In the end, the phase space represents all that the system can be, and its shape can easily elucidate qualities of the system that might not be obvious otherwise. A phase space may contain many dimensions. The correlation dimension (CD) can be considered as a measure for the number of independent variables needed to define the total system, here the cardiovascular system generating the RR interval time series, in phase space [56].

Before explaining how CD is calculated from a tachogram, the terms attractor, trajectory and attractor reconstruction has to be clarified. An attractor is a set towards which a dynamical system evolves over time. That is, points that get close enough to the attractor remain close even if slightly disturbed. Geometrically, an attractor can be a point, a curve, a surface (called a manifold), or even a complicated set with a fractal structure known as a strange attractor. Describing the attractors of chaotic dynamical systems has been one of the achievements of chaos theory. A trajectory of the dynamical system in the attractor does not have to satisfy any special constraints except for remaining on the attractor. The trajectory may be periodic or chaotic or of any other type. For experimental and naturally occurring chaotic dynamical systems as the cardiovascular system is, the phase space and a mathematical description of the system are often unknown. Attractor reconstruction methods have been developed as a means to reconstruct the phase space and develop new predictive models. One or more signals from the system, here the RR interval time series reflecting heart rate, must be observed as a function of time. The time series are then used to build an approach of the observed states.

Correlation dimension analysis of HRV signals is based on the method of Grassberger and Procaccia [143]. As always, we start with a tachogram or RR interval time series $x(t)$ of data points $x_i = x(t_i)$ and $i = 1 \ldots N$ (the number of heart beats in the signal)(Figure 2.5). Next, an attractor reconstruction takes place. The reconstructed trajectory, $\mathbf{X}$, can be expressed as a matrix where each row is a phase space vector, $\mathbf{X} = (\mathbf{x_1 x_2} \ldots \mathbf{x_M})^T$. For a time series of length N, $\{x_1, x_2, \ldots, x_N\}$, each $\mathbf{x_i}$ is given by $\mathbf{x_i} = (x_i, x_{i+\tau}, x_{i+2\tau}, \ldots, x_{i+(m-1)\tau})$.

The parameters m and τ are respectively called the embedding dimension and the time delay. The time delay for the CD is the value of the first zero crossing of the normalized (mean = 0 and standard deviation = 1) autocorrelation function of the time series and the time axis. The embedding dimension is usually varied increasingly between the values 2 and 30. The distances between the reconstructed trajectories $\mathbf{x_i}$ and $\mathbf{x_j}$ ($i, j = 1 \ldots$ N and $i < j$) are calculated and the total range of these distances is divided into discrete intervals, presented by r. Based on these distances, the correlation integral $C^m(r)$, as already defined in equation (2.20), is calculated as a function of r and this for successive values of m. As for a chaotic signal the relation $C^m(r) \sim r^{CD}$ holds, CD can derived by plotting $C^m(r)$ versus r in a ln – ln scale. This is visualized in Figure 2.18(a) for different values of the embedding dimension m. Next, calculating the slope of such a curve results theoretically in the CD, but as can be seen in the figure, this slope depends on the choice of m. In fact, the slope becomes steeper as m increases but will saturate at a certain level of the embedding dimension. Therefore, the slope can be plotted as a function of this embedding dimension m which makes it possible to see from which m on the slope is saturated. As shown in Figure 2.18(b), the point on the y- and x-axis where this curve (slope versus m) saturates is called respectively the

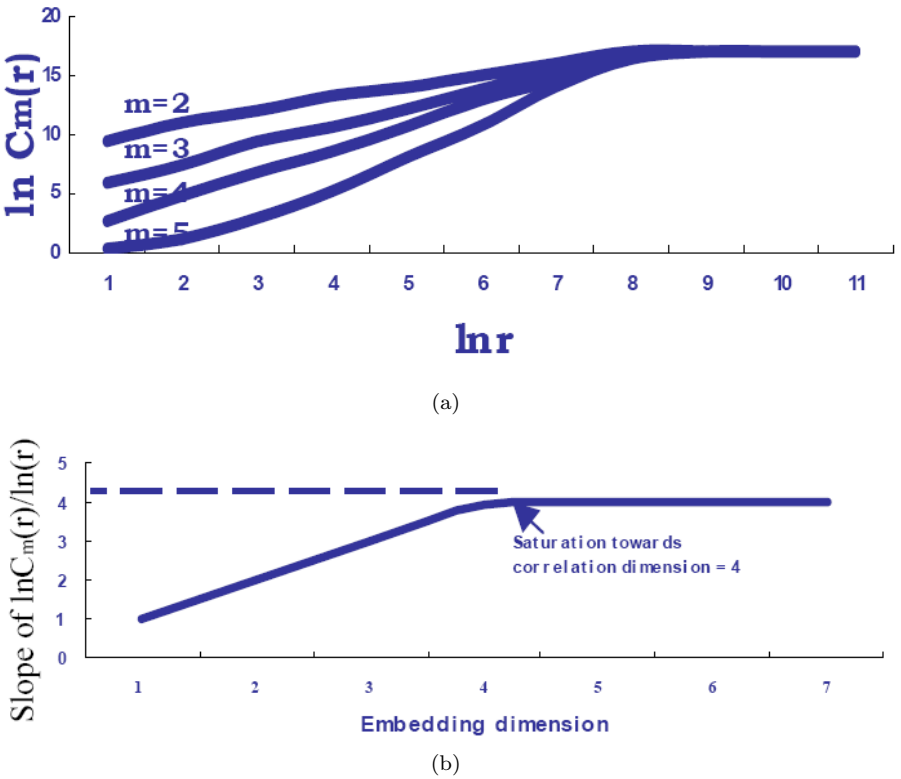


Figure 2.18: *Example of how to calculate the correlation dimension (CD). (a) Correlation integral $C^m(r)$ as function of the tolerance level r for different choices of the embedding dimension m. As $C^m(r) \sim r^{CD}$, the slope of such curve in a* ln – ln *scale results theoretically in the correlation dimension CD, but depends on m. (b) Plot of the slopes of $\ln C^m(r)/\ln(r)$ as function of m. The correlation dimension and the embedding dimension of the RR interval time series are given respectively by the point on the y- and x-axis where the curve saturates.*

correlation dimension CD and the embedding dimension of the time series.

Although the algorithm of Grassberger and Procaccia [143] is often used, it has several limitations such as the sensitivity to the length of the data, the unclear range of embedding dimensions to consider and the lack of having a confidence interval. To solve these problems, Judd [175] developed another algorithm to estimate the CD in a more robust way, which was used in this thesis. The CD of the tachogram example given in Figure 2.5 is 3.7025.

When a finite value is found for the CD of a time series, correlations are present

in the signal. To conclude whether these correlations are linear or nonlinear, a surrogate time series needs to be calculated. A significant difference between the CD of the surrogate and the original time series indicates that there are nonlinear correlations present in the signal. The significance level is calculated as: $S = [CD_{surr}$ - $CD_{data}]/SD_{surr}$. A value of S > 2 indicates that the measure reflects nonlinear correlations within the time series. In case of S > 2 the signal can be chaotic, but this is not absolutely sure unless other nonlinear parameters like e.g. Lyapunov exponents are available and positive values found. With S < 2 no significant difference is found between the two time series, the signal is not chaotic.

2.3.6 Lyapunov exponent

To discriminate between chaotic signals and periodic signals, Lyapunov exponents λ are often used. It is a measure of the rate at which the trajectories separate one from the other. The trajectories of chaotic signals in phase space follow typical patterns. Closely spaced trajectories converge and diverge exponentially, relative to each other. Quantitatively, two trajectories in phase space with initial separation δZ_0 diverge:

$$|\delta Z(t)| \approx e^{\lambda t}|\delta Z_0| \tag{2.24}$$

where λ is the Lyapunov exponent. The rate of separation can be different for different orientations of the initial separation vector. Consequently, there is a whole spectrum of Lyapunov exponents. The number of Lyapunov exponents is equal to the number of dimensions of the phase space. It is common to just refer to the largest one, the maximal Lyapunov exponent and from now on indicated as LE, because it determines the predictability of a dynamical system. The maximal Lyapunov exponent can be defined as follows:

$$LE = \lim_{t\to\infty} \frac{1}{t} \ln \frac{|\delta Z(t)|}{|\delta Z_0|} \tag{2.25}$$

A negative exponent implies that the trajectories approach a common fixed point. A zero exponent means the trajectories maintain their relative positions; in other words, they are on a stable attractor. Finally, a positive exponent implies the trajectories are on a chaotic attractor. Therefore, a positive LE is usually taken as an indication that the system is chaotic. Note that an arbitrary initial separation vector will typically contain some component in the direction associated with the LE and because of the exponential growth rate the effect of the other exponents will be obliterated over time.

Several algorithms have been proposed to calculate Lyapunov exponent [311, 398]. A large drawback of many of these algorithms is that it requires very long data series, in the order of tens of thousands of data points, depending on the system complexity (order of chaos). We used the method proposed by Rosenstein et al [311] because of its computational advantages to calculate the largest Lyapunov exponent. Moreover, it is also applicable on 'shorter' time series compared to the other Lyapunov algorithms. As already mentioned, a positive LE can be taken as a definition of chaos provided the system is known to be deterministic. Larger values of the LE indicate more complex behaviour.

Rosenstein algorithm

The first step of this approach involves reconstructing the attractor dynamics from the RR interval time series. The method of delays is used which is already described in detail when explaining the correlation dimension. After reconstructing the dynamics, the algorithm locates the nearest neighbour of each point on the trajectory. The nearest neighbour, $\mathbf{x'_j}$, is found by searching for the point that minimizes the distance to the particular reference point, $\mathbf{x_j}$. This is expressed as:

$$d_j(0) = min||\mathbf{x_j} - \mathbf{x_{j'}}|| \qquad \forall \mathbf{x_{j'}} \tag{2.26}$$

where $d_j(0)$ is the initial distance from the j^{th} point to its nearest neighbour, and $\| \; .. \; \|$ denotes the Euclidean norm. An additional constraint is imposed, namely that nearest neighbours have a temporal separation greater than the mean period of the RR interval time series. Therefore, one can consider each pair of neighbours as nearby initial conditions for different trajectories. The largest Lyapunov exponent LE is then estimated as the mean rate of separation of the nearest neighbours. More concrete, we assume that the j^{th} pair of nearest neighbours diverge approximately at a rate given by the largest Lyapunov exponent λ_1:

$$d_j(i) \approx d_j(0) e^{\lambda_1 (i \cdot \Delta t)} \tag{2.27}$$

By taking the logarithm of both sides of equation 2.27, one obtains:

$$\ln d_j(i) \approx \ln d_j(0) + \lambda_1 (i \cdot \Delta t) \tag{2.28}$$

which represents a set of approximately parallel lines (for $j = 1, 2, \ldots, M$), each with a slope roughly proportional to λ_1. This principle is visualized in Figure 2.19

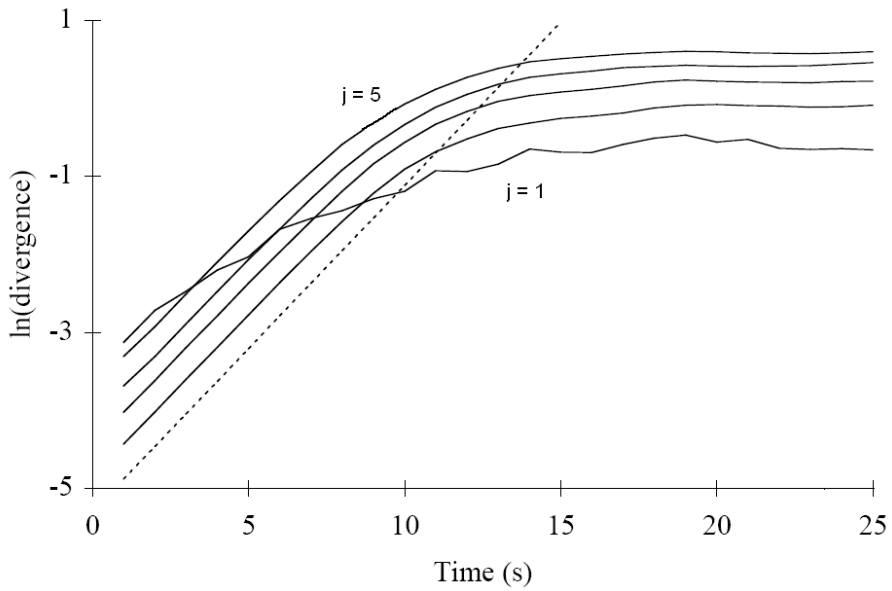


Figure 2.19: *Principle of calculating the largest Lyapunov exponent LE with the Rosenberg algorithm, applied on the tachogram example given in Figure 2.5. The natural logarithm of the divergence of the nearest neighbour to the j^{th} point in the phase space is presented as a function of time. The largest Lyapunov exponent is then calculated as the slope of the 'average' line, defined via a least-squares fit (dotted line).*

for the standard tachogram example. The largest Lyapunov exponent is now easily and accurately calculated using a least-squares fit to the 'average' line defined by:

$$y(i) = \frac{1}{\Delta t}\langle \ln d_j(i) \rangle \tag{2.29}$$

where $\langle$ .. $\rangle$ denotes the average over all values of j. This process of averaging is the key to calculating accurate values of λ_1 using smaller and noisy data sets compared to other Lyapunov algorithms. For the example tachogram, the largest Lyapunov exponent, LE, is 0.7586.

2.3.7 Numerical noise titration

Modeling

For any RR interval time series of length N; x_i, $i = 1, 2, \ldots, N$; a closed-loop version of the dynamics is proposed in which the output x_i feeds back as a delayed input. The univariate time series are analyzed by using a discrete Volterra autoregressive series of degree d and memory κ as a model to calculate the predicted time series:

$$\begin{aligned} x_i^{calc} &= a_0 + a_1 x_{i-1} + \ldots + a_\kappa x_{i-\kappa} + a_{\kappa+1} x_{i-1}^2 + \\ &\quad + a_{\kappa+2} x_{i-1} x_{i-2} + \ldots + a_M x_{i-\kappa}^d \qquad (2.30) \\ &= \sum_{m=0}^{M-1} a_m z_m(i) \qquad (2.31) \end{aligned}$$

where $M = (\kappa + d)!/(k!\, d!)$ is the total dimension. Details of the Volterra-Wiener method are described in Poon and Merril [286] and Barahona and Poon [25]. Briefly, the Volterra-Wiener algorithm produces a family of polynomial (linear and nonlinear) autoregressive models with varying memory and dynamical order, optimally fitted to predict the data. Thus, each model is parameterized by κ and d which correspond to the embedding dimension and the degree of nonlinearity of the model ($d = 1$ for linear and $d > 1$ for a nonlinear model). The coefficients a_m are recursively estimated from equation (2.31) by using the Korenberg algorithm [194].

Nonlinear detection (NLD)

The goodness of fit of a model (linear vs. nonlinear) is measured by the normalized residual sum of squared errors:

$$\varepsilon(\kappa, d)^2 = \frac{\sum_{i=1}^{N} (x_i^{calc}(\kappa, d) - x_i)^2}{\sum_{i=1}^{N} (x_i - \mu_x)} \qquad (2.32)$$

with

$$\mu_x = \frac{1}{N} \sum_{i=1}^{N} x_i. \qquad (2.33)$$

$\varepsilon(\kappa, d)^2$ represents a normalized variance of the error residuals. The best linear and nonlinear models are chosen according to the Akaike information-theoretic

criterion [4] which minimizes:

$$C(r) = \log \varepsilon(r) + \frac{r}{N} \tag{2.34}$$

where $r \in [1, M]$ is the number of polynomial terms of the truncated Volterra expansion from a certain pair (κ, d). For each data series, the best linear model is obtained by searching for κ^{linear} which minimizes $C(r)$ with $d = 1$. Analogously, varying $\kappa^{nonlinear}$ and $d > 1$ leads to the best nonlinear model. The presence of nonlinear determinism is now indicated if $d_{opt} > 1$.

Now we will explain how it can be examined whether the optimal degree d_{opt} is larger than 1. Likewise, the best linear and nonlinear models for surrogate randomized data sets are obtained [186, 181]. From each time series, a surrogate data set can be derived by randomly generating data points with the same autocorrelation and power spectrum as the original time series. Therefore, for a given time series, the generated corresponding surrogate data is not unique. Finally, this results in four competing models with error standard deviations $\varepsilon^{linear}_{original}$, $\varepsilon^{nonlinear}_{original}$, $\varepsilon^{linear}_{surrogate}$ and $\varepsilon^{nonlinear}_{surrogate}$. Further corroboration is obtained with the following objective statistical criteria: for models with Gaussian residuals, a standard F-test will serve to reject, with a certain level of confidence, the hypothesis that nonlinear models are no better than linear models as one-step-ahead predictors. This Gaussian assumption was verified throughout the analysis by using a χ^2-test with a 99% cut-off. Alternatively to the F-test, the results are confirmed by using the nonparametric Mann-Whitney rank-sum statistic, which does not depend on the Gaussian assumption [186]. Taking into account this scheme, the relevance of nonlinear predictors is established when the best nonlinear model from the original data is significantly more predictive than the best linear model from the real data series as well as the best linear and nonlinear models obtained from the surrogate series, in other words $\varepsilon^{nonlinear}_{original}$ ¡ $\varepsilon^{linear}_{original}$, $\varepsilon^{linear}_{surrogate}$, $\varepsilon^{nonlinear}_{surrogate}$ in the statistical sense.

To understand the nonlinear detection part completely, it is important to remark that surrogate data are generated by preserving only the linear autocorrelation function of the original data series. The nonlinear autocorrelations are randomized and therefore adding nonlinear terms does not increase the prediction power. Consequently, surrogate data are always best approximated by a linear model: $\varepsilon^{linear}_{surrogate} \approx \varepsilon^{nonlinear}_{surrogate}$. Consequently, and in contrast with other methods, surrogate data play only a confirmative role in this nonlinear detection procedure.

Numerical noise titration

The NLD is used to measure the chaotic dynamics inherent in the RR series by means of numerical noise titration as follows:

1. Given a time series y_n, the NLD is applied to detect nonlinear determinism. If linear, then there is insufficient evidence for chaos.

2. If nonlinear, it may be chaotic or non-chaotic. To discriminate these possibilities, a small (<1% of signal power) amount of random white noise is added to the data and then NLD is applied again to the noise corrupted data. If linear, the noise limit (NL) of the data is zero and the signal is non-chaotic.

3. If nonlinearity is detected, the level of added noise is increased and again NLD is applied.

4. The above step is repeated until nonlinearity can no longer be detected when the noise is too high (low signal-to-noise ratio). The maximum noise level (i.e. NL) that can be added to the data just before nonlinearity can no longer be detected, is directly related to the Lyapunov exponent (LE) [285].

Decision tool

According to this numerical titration scheme, NL > 0 indicates the presence of chaos, and the value of NL gives an estimate of relative chaotic intensity. Conversely, if NL $= 0$, then the time series may be non-chaotic or the chaotic component is already neutralized by the background noise. Therefore, the condition NL > 0 provides a simple sufficient test for chaos.

Analysis and output parameters

After resampling the RR interval time series, the numerical noise titration is applied using a 300-second window and sliding the window every 30 seconds [91]. A resampling frequency of 2 Hz was chosen to cover well natural heart rhythm and this choice is in correspondance with the suggestion by Singh et al for resampling before calculating the power spectral density [343]. The choice for the window length and the overlap was based on Deng et al [91] who used these values when calculating numerical noise titration in a pediatric obstructive sleep apnea study. Moreover, we did an internal study (not published) to investigate the influence of these choices (sampling frequency, window length and overlapping period) on the noise titration output and concluded that this was an appropriate choice taking into account a good time resolution and accuracy.

Only in case of the study of rats, described in Section 2.4, other values for these internal parameters are chosen. The reason is that rats have a heart rate which is approximately five times higher than human heart rate. Therefore, a resampling frequency of 10 Hz was chosen as well as windows of 60 seconds and sliding them

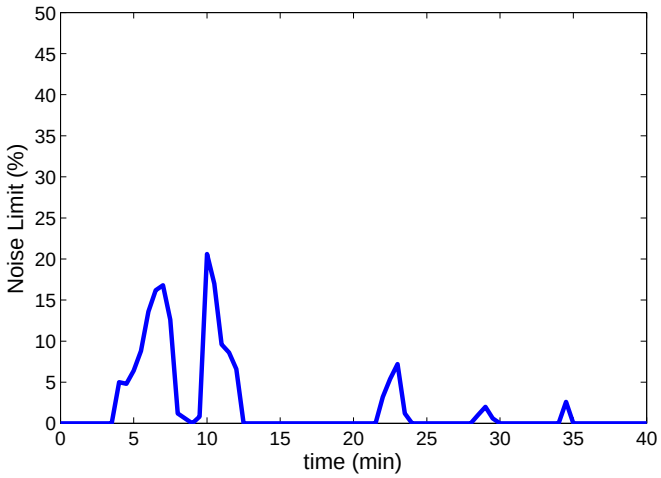


Figure 2.20: *Output of the noise titration technique applied on the tachogram example given in Figure 2.5. The noise limit (NL), representing the relative amount of chaos, is given as a function of time.*

every 5 seconds. Consequently, windows contained more or less the same number of samples as in a 5-minute window of human RR intervals.

Two noise titration measures to assess the changes in chaos level can be extracted. The detection rate (NLdr) is defined as the percentage of all time segments in which nonlinearity is detected. This measure gauges the mean cardiac chaos level. NLmean was calculated as the average of all NL's excluding the segments with NL = 0. It estimates the chaos level directly and can be used as a highly time-resolved measure.

Example

Figure 2.20 shows the result of the noise titration technique for the standard example used throughout the chapter. Contrarily to most other nonlinear techniques, noise titration has the advantage that is applicable on short and noisy signals and therefore a time series of NL values can be derived from a given RR interval time series. This is visualized in Figure 2.20. The mean noise limit is 7.1833 and the detection rate is 29.63%.

2.4 Physiological meaning of numerical noise titration

2.4.1 Introduction

The nonlinear control of heart rate (HR) and blood pressure (BP) makes it physiologically easier to adapt faster and more subtly to changes in physiological needs. Nonlinear methods are typically designed to assess the quality, scaling and correlation properties, rather than to assess the magnitude of variability like conventional HRV methods do. Furthermore, it has been shown that ANS control underlies the nonlinearity and possible chaos of normal HRV [138].

Due to the increased use of nonlinear system dynamics in clinical studies, it is very important to understand the physiological mechanisms underlying the generation of these fluctuations. Changes in nonlinear behaviour were already found in several pathologies, but the exact physiological mechanisms that cause this nonlinear behaviour need to be investigated further. We hypothesize here that nonlinear cardiovascular fluctuations are generated by the autonomic nervous system. Suppressing the activity of one branch of the autonomic nervous system using pharmacological blockades should alter the nonlinear characteristics of HR and BP fluctuations in order to compensate for the disturbance of the equilibrated system. Using different types of autonomic blocking agents in rats allows the examination of the involvement of the sympathetic and vagal nervous system in the generation of nonlinear cardiovascular fluctuations.

In the present study, the influence of different pharmacological interventions was investigated in rats on chaotic signatures by applying the numerical noise titration algorithm to RR interval (RRI) and BP time series. The aim is to examine the influence of several autonomic blocking agents on nonlinear HRV and BPV indices, and more specifically to detect and quantify changes in deterministic chaos of HRV and BPV in response to changes in autonomic control.

2.4.2 Data acquisition

13 male Wistar rats were conditioned in a Plexiglas triangular restrainer for at least 2 weeks before the actual experiment. On the day of the experiment, 3 precordial electrocardiogram electrodes were inserted subcutaneously under short halothane anaesthesia and with artificial ventilation. After termination of anaesthesia, rats were placed in the plexiglas restrainer in a quiet room with dimmed lights and were allowed to recover for several hours (minimum 2 hours). This was sufficiently long to exclude the effect of anaesthesia. After checking blood gases to exclude

respiratory acidosis and obtaining values within the normal range, the recordings were performed.

Blockade of α- and β-adrenoceptors was achieved using the intravenous administration, over 1 minute, of phentolamine or propanolol respectively, while atropine sulphate was used for the cholinergic blockade. Recordings were made up to 30 minutes after the intravenous administration of the antagonist(s). Of the group of 13 rats, 4 received α-adrenoceptor blockade, 5 received β-adrenoceptor blockade and 4 received cholinergic blockade without cross-over.

Recordings of at least 20 minutes after autonomic blockade were sufficiently long to calculate nonlinear indices because of the high HR in rats. Each recording contained at least 7000 RR intervals. The sampling rate was 1000 Hz per channel. The RR intervals and systolic BP values were calculated [30] and, after visual inspection, exported for further analysis. More details concerning the way the rats were conditioned and the signals were measured, are described in [34].

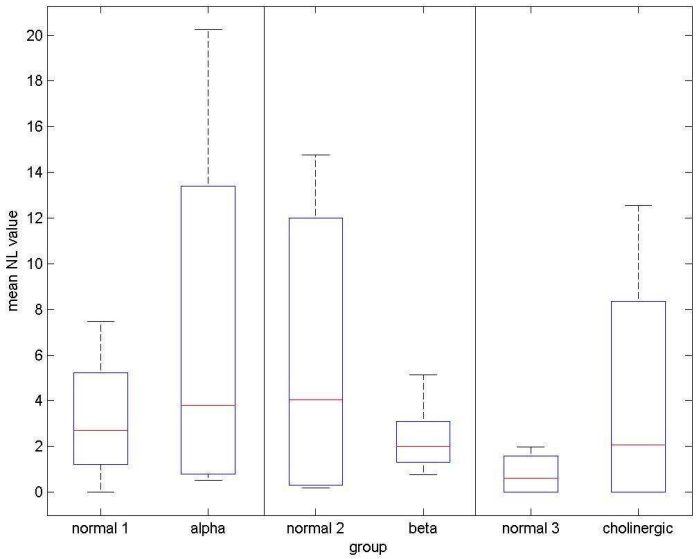
2.4.3 Data analysis

Numerical noise titration was applied on the resampled (10 Hz) RRI and BP time series using a 60-second window and sliding the window every 5 seconds. Statistical comparison between means within groups, before and after intravenous pharmacological blockade, was analyzed by Wilcoxon signed rank tests. Differences between groups were analyzed in general by the Kruskal-Wallis test with post-hoc analysis afterwards.

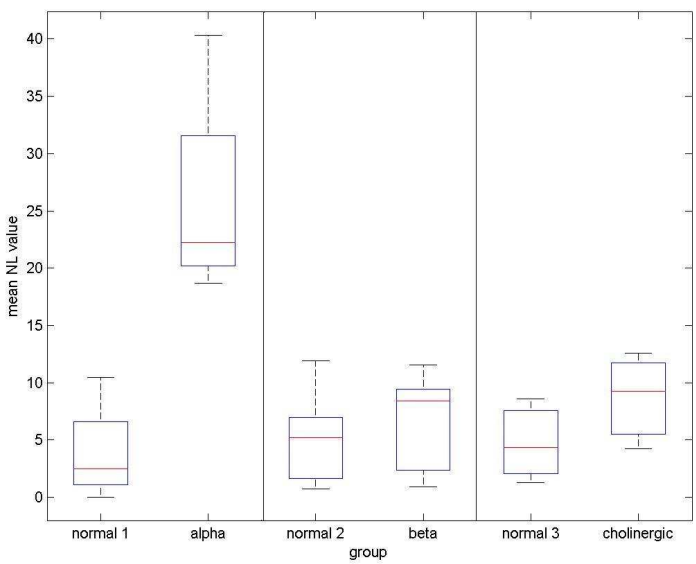
2.4.4 Results

The mean NL value was calculated for each rat under each condition. Within each group, this mean NL under a specific pharmacological blockade was compared pairwise with that of the corresponding normal control group. The results for the different groups are plotted by means of boxplots in Figure 2.21 and the p-values of the statistical analysis are shown in Table 2.2.

Next, we compared the same measure between the different groups. Figure 2.22 indicates that an α-adrenoceptor blockade leads to a higher mean NL, in particular in case of BP. The Kruskal-Wallis test gives $p = 0.8625$ for HRV and $p = 0.0096$ for BPV. Table 2.3 shows for the BP signal the original p-values between 2 groups, confirming the discriminating character to distinguish the α-adrenoceptor blockade group from any other group. Even after correction for multiple testing, statistical significance remains.

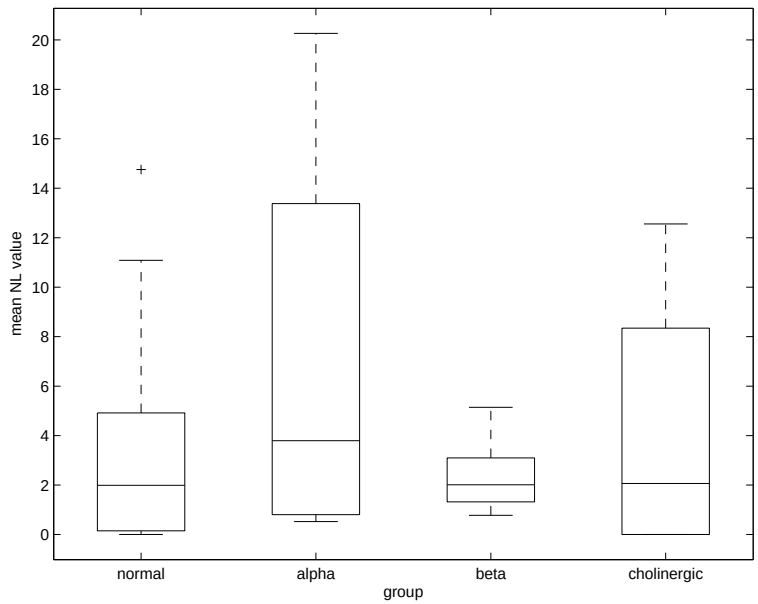


(a)

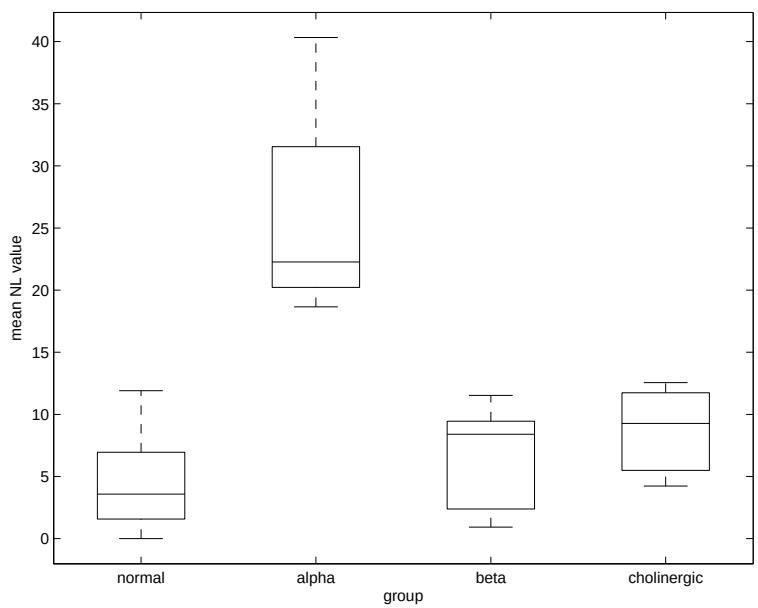


(b)

Figure 2.21: *Boxplots to compare pairwise different groups of pharmacological blockade with their corresponding normal control group for (a) HRV and (b) BPV.*



(a)



(b)

Figure 2.22: *Boxplots to compare between different groups for (a) HRV and (b) BPV.*

Table 2.2: *p-values of pairwise comparison of mean NL between normal condition and pharmacological blockade for HR and BP.*

groups	HR	BP
α -blockade vs. normal	0.3209	**0.0051**
β -blockade vs. normal	0.2775	0.5714
cholinergic blockade vs. normal	0.3882	0.4774

Table 2.3: *Original p-values of comparison between different groups for BPV.*

P	normal	α	β	cholinergic
normal	1	**0.019**	0.387	0.210
α		1	**0.022**	**0.032**
β			1	0.517
cholinergic				1

2.4.5 Discussion

The present results support, partially, the hypothesis that disturbing the autonomic nervous system induces changes in the nonlinear modulation of HR and BP, but in a complicated way. In rats, the α-adrenoceptor pathways seem to have an important contribution in the generation and control of nonlinear HR and especially BP fluctuations, while β-adrenoceptor and cholinergic interventions have a negligible contribution to the nonlinear dynamical control. Such finding is in correspondance with a previous study of Beckers et al [33].

A critical remark can be made concerning some limitations of the study. Only a limited number of rats could be used for the present study for ethical reasons. Moreover, a pharmacological blockade drives the cardiovascular system out of the normal physiological range.

2.4.6 Conclusion

An important contribution of this work is our finding that the numerical noise titration technique seems very sensitive to changes in vasomotion control. This might help to understand the physiological origin of nonlinear blood pressure control.

2.5 Nonlinear versus chaotic behaviour

When assessing cardiac function, differentiation between parasympathetic and sympathetic activity may never be possible due to the ubiquitous nature of the autonomic nervous system. Instead, one may need to consider the modulation of sympathetic-parasympathetic interactions and the influence this autonomic modulation has on the multilevel control mechanisms (feedback loops). In other words, how well do the sympathetic and parasympathetic nervous systems modulate each other, such that the control mechanisms can operate within the neurocardiac milieu and maintain homeostasis? Pathology may result when the control mechanisms cannot operate optimally due to loss of neurocardiac modulation when one autonomic division dominates the other, such as in heart failure. Neurocardiac regulation may be nonlinear in structure due to the multilevel nature of the interactions between the autonomic nervous system and the various control mechanisms. Therefore, nonlinear techniques may offer advantages over linear techniques in identifying and quantifying the modulation of interactions among neurocardiac control mechanisms.

Nonlinear techniques have the advantage over linear techniques in providing better repeatability and reliability across measurements (small random error). Therefore, nonlinear indices may be more suitable for diagnostic purposes, as well as for assessing individual treatment effects [218, 348]. Nowadays, the meaning of the indices used for nonlinear system dynamics is not as clear as those derived from time or frequency domain methods. Moreover, spectral analysis is also superior in visualizing the results. Future research will need to focus on determining clear physiological interpretations for all indices. For the noise titration technique, we did a first attempt by using pharmacological blockades in rats as shown in Section 2.4. Concerning other nonlinear HRV parameters, some physiological relations are already given by Beckers et al [34, 33] and Aubert et al [19].

Specifics of the biological systems require modifications of standard nonlinear sytem dynamics algorithms. The main problems of the nonlinear analysis, when applying it to biological signals can be summarized as follows:

- high level of random noise in the biological data. Consequently, the applied nonlinear systen dynamics methods should be robust to the noise influence.
- short experimental data sets due to the low frequencies of the biological signals. Short realizations cause large error bars in the estimation of the nonlinear or chaos parameters.
- nonstationarity of the biological systems, i.e., ECG, EEG have different modulations influenced by a various external factors with different characteristic times.

- spatially extended character of the system.

It is also important to remark that chaos theory and nonlinear system dynamics theory are frequently used as interchangeable terms despite their technically different meanings.

The numerical noise titration technique is claimed by Poon et al [285] to detect deterministic chaos in a better way than for the Lyapunov exponent. Apparently chaotic HRV seen in sinus rhythm can be produced by stochastic modulation of the sinoatrial node. Therefore, the identification of HRV data as chaotic in case of a positive noise limit requires both caution and a quantitative, predictive mechanistic model that is fully deterministic [413]. There is currently no available technique to readily distinguish spontaneous or induced deterministic chaos from noise-induced chaos or noise annihilation of deterministic chaos in nonautonomous nonlinear dynamic systems. As long as the chaotic characteristics of a time series can be reliably quantified, the precise mathematical classification of the chaos (spontaneous or induced, deterministic or stochastic) or nonchaos is unimportant [283, 284]. Even then, there is some controversy whether heart rate is chaotic or not.

Interesting conclusions emerged from a special session in a recent issue of the *Chaos* journal, edited by L. Glass, in which the topic was 'Introduction to controversial topics in nonlinear science: Is the normal heart rate chaotic?' [132]. Also Cerutti et al [66] reported about the new issues in the cardiovascular system as one of the four most promising research areas in biomedical signal processing nowadays. Some [285] argue that heart rate modulation is a chaotic system while other claim that normal heart beat series are nonchaotic, nonlinear and multifractal, based on results of the parametric and semiparametric estimation of the long memory parameter (long-range dependence) [22]. Freitas et al [119] showed that there is no efficient tool to provide a conclusive answer to the question 'is the normal heart rate chaotic?' at least until a global model is obtained. Nevertheless, they concluded there is a high probability for a nonlinear underlying process whose deterministic nature is still questioned.

The concept of the cardiovascular system as a multifractal system was also raised by other research groups. Hu et al [161] employed a new multiscale complexity measure, the scale-dependent Lyapunov exponent (SDLE), to characterize HRV. SDLE has been shown to readily characterize major models of complex time series including deterministic chaos, noisy chaos, stochastic oscillations, random $1/f$ processes, random Levy processes, and complex time series with multiple scaling behaviours. SDLE was used to characterize the relative importance of nonlinear, chaotic, and stochastic dynamics in HRV of healthy, congestive heart failure, and atrial fibrillation subjects. They found that while HRV data of several groups were mostly stochastic, the stochasticity was different among the groups. A study of Sassi et al [319] also supported the use of multifractal series to model HRV. They

marked additionally that the regulatory action of the autonomous nervous system might play a role in the observed multifractality.

According to Wessel et al [390], the question whether these time series are chaotic or not cannot be answered satisfactorily without investigating the underlying mechanisms leading to them. Giving an example of the dominant influence of respiration on heart beat dynamics, they showed that observed fluctuations can be mostly explained by respiratory modulations of heart rate and blood pressure (coefficient of determination: 96%). Therefore, they recommended reformulating the following initial question: 'Is the normal heart rate chaotic?' rather into: 'Is the normal heart rate chaotic due to respiration?'

2.6 Baroreflex sensitivity

One index of baroreflex 'health' is the degree of change in heart rate or sympathetic traffic for a given unit change in blood pressure [277]. This may be quantified as the response of the cardiovascular system to the application of an external stimulus, mechanical or pharmacological, in standardized laboratory conditions.

An alternative in vivo approach evaluates spontaneous baroreflex modulation of heart rate in a daily life setting by identifying sequences of consecutive beats in which progressive increases in systolic blood pressure (SBP) are followed by a progressive lengthening in pulse interval (or vice versa) [45]. The slope of the regression line between SBP and pulse intervals within these sequences is taken as the magnitude of the reflex gain.

In the sequence method, BRS is evaluated exactly in the same way as in the slope method, but instead of concentrating on a singular pressure rise or fall period the calculation is performed several times along the SAP and RRI signals. In this case the pressure rise and fall is not activated using external means. Instead, naturally occurring fluctuations of these signals are utilized. There are certain conditions which much be fulfilled before we can accept a sequence for BRS calculations. Firstly, in the sequence to be used both SAP and RRI signals must be rising or falling monotonically in the same direction for at least three beats. Normally one is using RRI signal values, which have been moved forward by one beat in order to compensate for the assumed adjustment delay. Secondly each consecutive change of SAP and RRI values must exceed a certain limit. This condition acts as a kind of filter, which removes random noise related changes. The value of the limits critically effects how many acceptable sequences can be found and they must be selected case by case.

A third method to assess baroreflex function is provided by cross-spectral analysis of short segments of SBP and RR intervals. This approach relies on the assumption

that a certain frequency band of HR variability, between 0.04 and 0.35 Hz [55], is modulated by the baroreflex. This construct is based on the coherent relationship between SBP and RR intervals, each of which oscillate at the same frequency in the power spectrum [267]. Baroreflex sensitivity is expressed by the gain of the transfer function relating changes in blood pressure to coherent changes in RR or MSNA [266, 304].

All these methods for computing baroreflex gain assume linearity of the relationship between changes in blood pressure and RR intervals. Simple mathematical models indicate that there is a strong linear coupling between arterial blood pressure and RR interval. However, there is emerging evidence that the RR interval responses to blood pressure may be modulated in accordance with nonlinear system dynamics [301].

In this thesis, BRS is only calculated in the study about head-down bed rest, described in Chapter 7 and the measures to describe BRS are limited to the BRS slope and the number of BRS estimates according to the sequence method.

2.7 Statistical analysis

Statistical analysis is often performed with Matlab R2006b or R2008a (The MathWorks Inc., Natick, MA, USA). In Chapter 4 and Chapter 6, parts of the statistics are obtained with SPSS Windows version 11.5 and 16.0 respectively (Scientific Packages for social Sciences, Chicago, IL, USA) (Scientific Packages for Social Sciences, Chicago, IL, USA).

Differences between two behavioural states or between day and night are analyzed pairwise by the nonparametric Wilcoxon signed rank tests. Those tests are robust with respect to outliers, which are present in this study, because they deal with the order and not with the absolute values. The nonparametric Mann-Whitney U test examines the gender differences or in general the difference between two populations.

In case of more than two groups or conditions that have to be compared with each other, the previously mentioned tests are not valid anymore. If there is only a within subject variable (phase), the nonparametric Friedman test is obtained adjusted for possible between subject effects to test whether the within subject variable affects the HRV parameters. Post hoc Tukey contrasts are used afterwards in order to explore further differences between two phases, taking into account multiple testing. If there are two dependent variables (time and condition), a 2-way ANOVA analysis is performed on all parameters resulting in one general p-value for each variable. A third p-value is given for the interaction term in the model to assess significant differences between groups across time. To compare,

for each parameter, pairwise the different time moments with a baseline value, a post hoc analysis was obtained again taking into account the multiple testing problem.

In Chapter 6, results of different parameters relating to the same aspect of autonomic heart rate modulation, are combined in one group via the Repeated Measures Multivariate ANOVA. Therefore, all values are transferred to z-scores, obtained by subtracting the mean value and dividing by the standard deviation over all signals. This test statistic offers a solid testing method to determine whether the weightlessness had a significant influence on a certain group of parameters and therefore on a specific part of the ANS. The p value was obtained by the Wilks' Lambda test statistic.

To test associations, i.e. between nonlinear HRV parameters and age, a two-tailed Pearson correlation coefficient r is calculated.

In all test statistics, $p < 0.05$ was considered statistically significant.

2.8 Methodological remarks

2.8.1 Respiration and HRV

The role of respiration in the genesis of heart rate variability (HRV) has been the subject matter of many experimental and modeling studies. Effects of parameters such as respiratory frequency, tidal volume, expiration/inspiration time ratio and respiratory dead space have been studied [42, 43, 291, 367].

In general, there is consensus on the idea that respiration is the main contributor to the generation of the HF peak of HRV PSD. On the other hand, there is a debate on the possible role of respiration in the genesis of the low frequency (LF) peak which is usually centered around 0.1 Hz. LF oscillations in arterial pressure, with a period of about 10 s for human, are called Mayer waves. Mayer waves may exhibit themselves as short damped oscillations as well as in a sustained form. The hypothesis that arterial pressure Mayer waves result from rhythmic, sympathetic vasomotor activity and generate RR interval oscillations at the same frequency through the baroreflex has been widely accepted until recently [75]. Another possible mechanism to explain the LF oscillations is the baroreflex feedback theory. This baroreflex feedback theory may offer an explanation for the possible role of respiration in the LF band. Average respiratory frequency in a normal resting person is in the HF band. However, it is known that respiration is not perfectly periodic and even a resting person experiences irregular breathing due to several factors. Therefore, the influence of respiration on blood pressure and HRV would not be expected to be only in the HF band but also at other frequencies to be

observed in the power spectrum of a recorded respiratory signal, e.g. respiratory volume. Since the baroreflex feedback system has its maximum gain at its natural frequency [382], e.g. at about 0.1 Hz, the effect of respiration will be more profound if it has frequency components in the LF band.

In fact, Bernardi et al [43] have claimed that in the absence of simultaneous analysis of respiration, the changes in the LF/HF ratio should not be taken as a clear evidence of changes in sympathovagal balance. In order to incorporate respiration into the interpretation of HRV PSD, one must look closely into the mechanisms of interaction between respiration and the heart rate control system. Despite many past studies, the precise physiological mechanisms of LF and HF components of HRV and their relation to respiration are still being debated [43, 367].

Respiration-induced heart rate variation in the respiratory frequency range is called respiratory sinus arrhythmia (RSA). The relationship of respiratory rate and depth to RSA has been a topic of substantial discussion, e.g. Denver et al [92], Grossman and Taylor [146] and Ritz and Dahme [303]. Of particular concern, some have advocated that measures of RSA be 'corrected' or 'unconfounded' from respiratory effects [146, 302]. Respiratory phase and duration (rate), though, essentially defines RSA.

Wessel et al [390] gave an example of cardiorespiratory modeling which demonstrates that the complex behaviour of the heart rate is mainly caused by the respiration which influences the coupling of heart rate and blood pressure. They suggested therefore that the complex heart rate fluctuation resulted from a modulation by breathing and that this complex respiratory behaviour can be explained by the regulation of ventilation.

2.8.2 Computational complexity of nonlinear techniques

While linear techniques are very easy to implement and can be calculated very quickly, nonlinear techniques are more complex. A few lines of code are not anymore sufficient to implement these techniques as they often consist of several steps with more complicated computations. Moreover, sometimes these steps have to be repeated iteratively until a certain condition is obtained or they have to be executed for a full range of internal parameters to see which the optimal choices are. As a consequence, the execution time of such nonlinear techniques is longer, in the order of seconds or minutes to analyse one signal, while this is limited to some milliseconds for time and frequency domain measures. Obviously, the length of a signal plays an important role. The computational complexity is even different between the described nonlinear techniques. While techniques such as detrended fluctuation analysis or entropies are rather fast, techniques searching for chaotic signatures require a much heavier computational workload.

Whether the computational complexity, and therefore the execution time, is a limitation or not, depends on the application. If you want to include the nonlinear HRV parameters in a clinical model for diagnostic purposes, time is not a key factor. A computer can calculate the values after the complete recording. Two recent studies showed that it is worth to calculate those more complex nonlinear parameters as they have the advantage over linear techniques in providing better repeatability and reliability across measurements (small random error), making them consequently more suitable for diagnostic purposes, as well as for assessing individual treatment effects [218, 348]. In case of real-time applications, nonlinear techniques are probably not directly usable. Not only the too long execution time to perform nonlinear analysis instantaneously will be a problem, but these more advanced techniques also require longer data sets before they can be applied reliably.

2.9 Conclusion

We introduced the mathematics and techniques, necessary for a good understanding of the methodology used in this thesis. After the peak detection algorithm and the preprocessing methods, the linear methods in time domain, frequency domain and the time-frequency representations were represented. Also an overview of some nonlinear techniques assessing scaling behaviour, complexity and chaotic behaviour was given. An attempt to find a physiological meaning of the noise titration parameter was explained in Section 2.4. Further, the difference between nonlinearity and chaoticity and the question whether the cardiovascular system is nonlinear and/or chaotic was discussed. Several methods to quantify baroreflex sensitivity, reflecting the interaction between heart rate and blood pressure, were explained as well as the test statistics used further in this thesis.

Chapter 3

Detection of cardiovascular abnormalities in preterm neonates

Chapter 3 presents a first application. Preterm neonates need to be monitored by polysomnographies (PSG) to identify risk infants who need cardiorespiratory home monitoring. Here, the goal was to examine whether a new nonlinear HRV technique, called numerical noise titration and quantifying chaos, can be used to get similar information, but only based on the ECG signal. Also differences between REM and non-REM sleep were studied. The chapter starts with an introduction (Section 3.1), after which the data and the analysis techniques are given in Section 3.2. Section 3.3 presents all results. Rhythmical fluctuations which are typically present in neonatal RR interval time series are discussed in Section 3.4. Additionally, differences between sleep states and between babies with a normal and abnormal cardiorespiratory behaviour are also interpreted in this section. The chapter ends with the main conclusions (Section 3.5).

3.1 Introduction

Polysomnography (PSG) is the continuous recording of physiological parameters such as heart rate (HR), respiration and peripheral oxygen saturation (SaO_2). An apparent life threatening event (ALTE) is defined as an episode that is frightening to the observer and is characterized by some combinations of apnea (central or occasionally obstructive), color change (usually cyanotic or pallid),

marked change in muscle tone, choking or gagging [395]. In preterm neonates, usually with a heart rate between 120 and 160 beats per minute (bpm), and infants having experienced ALTE, more subsequent life threatening events are found when the polysomnography is abnormal [88, 80]. Polysomnographies can thus be used to identify risk infants who need cardiorespiratory home monitoring (ECG, respiration and possibly SaO_2). In the University Hospitals of Leuven, the criteria for an abnormal polysomnography are threefold, central or obstructive apnea for more than 15 seconds combined with a bradycardia below 60 bpm or oxygen saturation below 80%, or a bradycardia below 50 bpm for at least 4 seconds. The home monitoring is also evaluated in cases of bradycardia below 50 bpm for at least 4 seconds as criterion for abnormal follow-up (FU) [88]. Children with an abnormal polysomnography were systematically followed up with a cardiorespiratory home monitor with memory, so that new events at home could be documented. According to the results of the polysomnographies and follow-up, infants can thus be divided in 3 groups: NN (normal PSG and normal FU), AN (abnormal PSG and normal FU) and AA (abnormal PSG and abnormal FU). For each infant, periods of non-REM sleep and REM sleep can be indicated.

We hypothesize here that the deficiencies in the autonomic nervous system that cause the abnormal cardiorespiratory events are reflected in the heart rate, not only in abnormal bradycardia but also in more subtle changes. Analogously, we expect different cardiovascular fluctuations in different sleep states of neonates. Fetal heart rate variability (HRV) was already studied in test animals and several relations were found with sleep and other biological rhythms [87]. HRV will differ during non-REM compared to REM [93], therefore these periods may be characterized by nonlinear HRV parameters. Thus an automatic distinction between non-REM sleep and REM sleep in neonates may be within reach.

The present study investigates whether REM sleep and non-REM sleep periods can be distinguished in general and in particular in the different aforementioned groups (NN, AN, AA) using the Noise Limit (NL) value of the numerical noise titration technique, calculated within periods free from abnormal bradycardia. This could well improve the rating of REM and non-REM sleep in future.

3.2 Methods

3.2.1 Subjects

For the present study, polysomnographies of preterm neonates recorded in the University Hospitals Gasthuisberg (Leuven) between 2000 and 2003 were available. An abnormal PSG was recorded in 39 preterm infants, 15 of whom experienced further abnormal events during the follow-up. Some were excluded because of too

many artefacts, mainly due to movement. Moreover, maturation is an important determinant of heart rate requiring age-matched AN and AA groups. Therefore, 10 subjects were selected in each group. Also ten age-matched infants were retained from the NN group. The mean post-conceptional age (PCA) at the time of the PSG was 36.4 weeks for the NN preterms, 36.3 weeks for the AN preterms and 36.4 weeks for the AA preterms. The mean gestational age (GA) at birth was 32.3 weeks, 31.9 weeks and 32.3 weeks respectively for the NN, AN and AA preterms. Other anthropomorphic details about the study population are given in Table 3.1.

The experiment protocol was approved in advance by the local ethical committee of the University Hospitals Gasthuisberg. The parents of the neonates provided written informed consent before participating. The study complies with the Declaration of Helsinki.

3.2.2 Data collection

The physiological parameters measured during the polysomnographies included electrocardiogram (ECG), thoracic and abdominal respiratory movements, nasal flow (thermistor), SaO_2, chin electromyogram (EMG) and electro-oculogram (EOG). As we were not interested in a detailed sleep scoring, but only in well defined periods of REM and non-REM sleep, EEG was not needed and a non-standard method could be used. Periods of REM sleep were defined by the irregular breathing pattern (irregular rapid respirations), movement, tonically inhibited muscle tone on the EMG and single rapid eye movements on the EOG. Non-REM sleep was defined by slow-wave activity on the EOG, slow and regular respirations and normal muscle tone on the EMG. To prevent contamination of the study results, heart rate (variability) was excluded as a criterion to categorize sleep periods. Only well defined periods of REM and non-REM were selected. All polysomnographies were rated independently by one single investigator (HD) who was not involved in the HRV analysis [109, 54, 358]. After sampling all signals at 100 Hz, the RR intervals (RRI) were derived from the ECG signal. The R peaks were detected by an automatic peak detection algorithm based on the second derivative of the digitized ECG signal. To avoid errors due to faulty peak detection, all RR interval series were inspected for false and missed peaks, and corrected if necessary. The mean duration of the ECG recordings was more than 8 hours (504.35 ± 161.24 minutes), yielding on average 75000 RRI per patient.

3.2.3 HRV analysis

Four standard time-domain HRV parameters were calculated as recommended by the Task Force [355]: SDNN, RMSSD, TI and SDANN. Also the numerical noise titration is applied in this study. For each RR interval series, both short term

Table 3.1: *Anthropomorphic details of the study population with median and 95% confidence interval (CI) for all different parameters in each group. Statistical analysis by ANOVA test did not show any significant difference between the groups.*

	AA		AN		NN	
	median	95% CI	median	95% CI	median	95% CI
Apgar score 1 minute	7.00	6.14 – 8.86	8.00	3.55 – 8.00	8.00	1.00 – 9.00
Apgar score 5 minutes	8.00	7.14 – 9.00	8.00	3.55 – 8.86	9.00	7.48 – 9.00
Days of ventilation	0.00	0.00 – 1.00	0.00	0.00 – 4.31	0.00	0.00 – 0.00
Days of CPAP	0.00	0.00 – 10.00	1.00	0.00 – 11.03	0.00	0.00 – 4.63
Birth weight [g]	2240	1374 – 2566	2100	1285 – 2331	2083	1462 – 2607
Postnatal age at registration [days]	21.00	14.00 – 61.86	28.00	20.69 – 48.90	29.50	9.28 – 63.63
Postmenstrual age at birth [weeks]	34.00	28.55 – 34.86	32.00	30.00 – 34.00	33.00	29.95 – 35.00
Postmenstrual age at registration [weeks]	37.00	36.00 – 37.00	36.00	36.00 – 37.00	37.00	36.00 – 39.05

CPAP = continuous positive airway pressure

and long term variability was assessed. For the short term HRV, all non-REM sleep and REM sleep periods were analyzed separately. For the long term HRV, the complete recordings were analysed. The HRV measures calculated on the complete RR interval series are referred to as 'global' HRV measures. SDNN and RMSSD were calculated both globally and on the separate sleep states. TI and SDANN were only calculated for the complete RR interval series because they can not be estimated accurately on short segments. Regarding the numerical noise titration algorithm, the technique was applied on the resampled (2 Hz) RR interval time series using a 300-second window and sliding the window every 30 seconds. Resampling the RR interval time series to a fixed sampling frequency is important because the algorithm requires equidistant samples. A sampling frequency of 2 Hz is chosen because this corresponds well to the natural neonatal heart rhythm, usually between 120 and 160 beats per minute. Other resampling frequencies were tried out to study their influence, but a higher resampling frequency resulted in loss of information due to interpolation.

3.2.4 Statistical analysis

Statistical analysis was performed with Matlab R2006b. Differences between behavioural states as non-REM and REM sleep periods were analyzed pairwise by the nonparametric Wilcoxon signed rank tests. Those tests are robust with respect to outliers, which are present in this study, because they deal with the order and not with the absolute values. Comparing the three groups to each other was done by the nonparametric Man Whitney U test. $P < 0.05$ was considered statistically significant.

3.3 Results

For the standard time-domain HRV parameters, the mean $\pm$ standard deviation values for each group of subjects are shown in Table 3.2. No differences between groups are observed, neither in the complete recording, nor in non-REM or REM segments.

A typical result of applying the numerical noise titration technique to a RR interval time series is shown in Figure 3.1. On top, the 2 Hz resampled RR interval time series of a preterm infant is shown while the periods of non-REM and REM sleep are indicated in the middle frame by -1 and $+1$ respectively. The NL signal, containing one NL value for each window of 5 minutes, slid every 30 seconds, is plotted in the bottom frame. It also illustrates that NL values can strongly fluctuate in time, even within the same subject and the same conditions, e.g. sleep state. Therefore, we calculated the mean NL value for each subject. Other

Table 3.2: *Standard time-domain HRV parameters, calculated on the complete RR interval series and on all non-REM sleep and REM sleep segments. The mean values ± standard deviations for each group of subjects are shown. No significant differences between groups were found.*

		AA	AN	NN
Complete	RRI $[ms]$	405 ± 21	401 ± 22	396 ± 15
	SDNN $[ms]$	41.4 ± 9.5	42.4 ± 9.9	43.6 ± 8.7
	RMSSD $[ms]$	10.3 ± 2.4	10.1 ± 3.2	10.8 ± 3.9
	TI	9.1 ± 2.6	8.7 ± 2.3	9.7 ± 2.2
	SDANN $[ms]$	27.0 ± 8.2	26.0 ± 4.8	29.5 ± 6.8
Non-REM	RRI $[ms]$	432 ± 32	426 ± 44	431 ± 25
	SDNN $[ms]$	12.2 ± 4.9	10.7 ± 5.4	9.9 ± 3.8
	RMSSD $[ms]$	7.2 ± 2.6	5.9 ± 3.0	6.8 ± 3.9
REM	RRI $[ms]$	408 ± 25	407 ± 33	412 ± 18
	SDNN $[ms]$	26.7 ± 5.8	27.1 ± 11.3	25.6 ± 9.5
	RMSSD $[ms]$	8.0 ± 1.6	7.7 ± 2.4	8.3 ± 3.5

Table 3.3: *Results of numerical noise titration calculated on the complete RR interval series and on all non-REM sleep and REM sleep segments. The mean values ± standard deviations for each group of subjects are shown.*

NLmean	NN	AN	AA
Complete RR series	12.62 ± 8.07	15.12 ± 5.87	17.40 ± 11.80
REM segments	12.84 ± 7.25	14.64 ± 8.12	14.17 ± 13.17
Non-REM segments	4.38 ± 2.77	1.67 ± 1.29 *	1.39 ± 1.81 **

* $P < 0.05$ by Man Whitney U test compared to NN group
** $P < 0.01$ by Man Whitney U test compared to NN group

measures such as median NL and 3 proportionality measures, were calculated too, but since they all give similar results, those measures will not be outlined here. The NL values (mean ± standard deviation) are given in Table 3.3 for all groups and each behavioural state. Differences between groups were only visible during the non-REM segments. In these quiet periods, both AN and AA subjects have significantly lower NL values compared to NN subjects.

During periods of non-REM sleep, the NL values are in general much lower, as could already be observed in Figure 3.1. The boxplots in Figure 3.2 confirm this finding. In each group, non-REM seems to be different from REM and from the

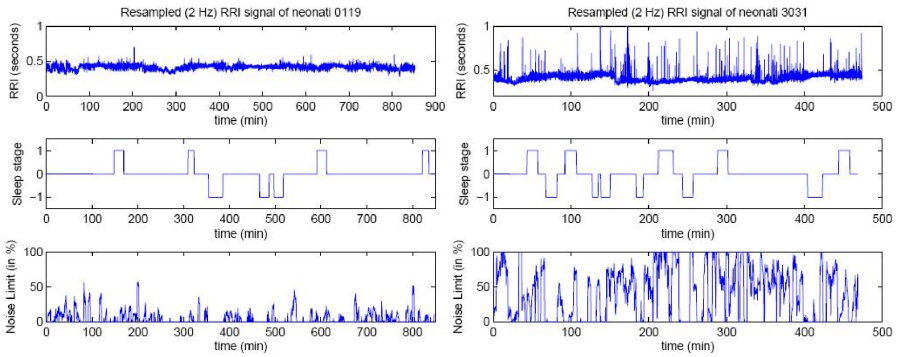


Figure 3.1: *Typical result of applying the numerical noise titration technique to a RR interval time series coming from a subject of NN group (left) and AA group (right). On top, the 2 Hz resampled RR interval time series is given, while the periods of non-REM and REM sleep are indicated in the middle by respectively* -1 *and* $+1$*. The NL signal, containing one noise limit value for each window of 5 minutes, slid every 30 seconds, is plotted in the bottom frame, where the vertical lines indicate the boundaries of the non-REM periods.*

Table 3.4: *P-values of the differences in mean NL in the three different groups between behavioural states. The Wilcoxon signed rank test for matched samples was used to assess the statistical significance.* $P < 0.05$ *was considered statistically significant and is printed in bold.*

P-value	NN	AN	AA	All
Complete vs. non-REM	**0.002**	**0.002**	**0.002**	**1.73 E-6**
Complete vs. REM	0.131	0.695	**0.049**	**0.017**
Non-REM vs. REM	**0.006**	**0.002**	**0.002**	**2.35 E-6**

total recording period. The p-values in Table 3.4 show that these differences are statistically significant, independently whether PSG and follow-up were normal or abnormal. When looking to the complete population of 30 neonates, even REM periods could be discriminated from the complete recording period.

3.4 Discussion

Measuring heart rate variability is a useful method to understand the state of the autonomic nervous system (ANS). The normal variability is due to the autonomic

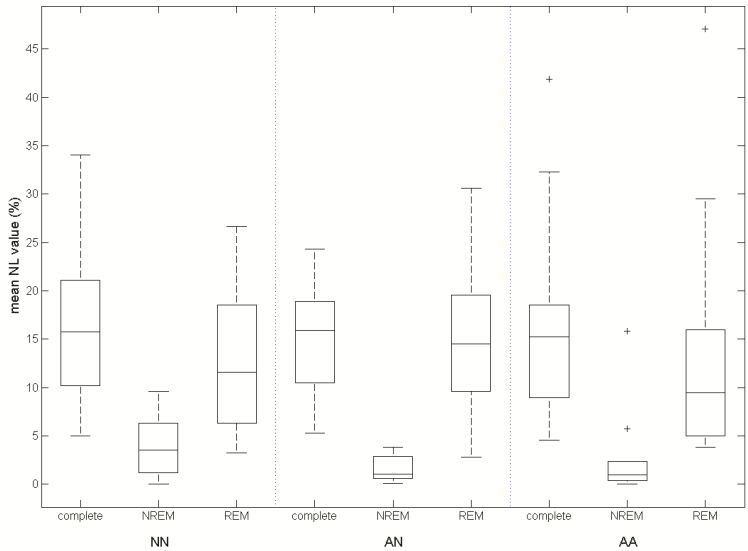


Figure 3.2: *Boxplots to compare pairwise in each group different behavioural states with the mean NL value as measure.*

neural regulation of the heart and the circulatory system. In premature infants the ANS is still immature and this is reflected in the higher incidence of severe bradycardias and acute life threatening events in this group are most probably a reflection of this immaturity [1].

3.4.1 Rhythmical fluctuations

A typical neonatal RR interval series was shown in Figure 3.1. A closer look at the data reveals several rhythmical fluctuations. Respiratory sinus arrhythmia (RSA) is a periodic fluctuation in heart rate associated with respiration [271]. Since the respiration rate in neonates, typically between 40 and 80 breaths per minute, is sometimes larger than half the heart rate, usually between 120 and 160 beats per minute, RSA cannot always be observed in neonates as limited by the Nyquist theorem. Respiratory events such as sighs [99], respiratory pauses (apneas) [86] or periodic breathing also influence the heart rate. Furthermore, slower rhythmical fluctuations with a period around 30 heart beats (10 seconds) can be observed in most RR interval series, Although this 10s-rhythm has been described in many other studies, its origin remains uncertain. It is believed to be related to the Mayer waves observed in blood pressure and is attributed to baroreceptor reflex

[271]. Some other phenomena such as non-nutritive sucking cause similar rhythms in the RR interval series [239]. In addition to RSA and the 10s-rhythm, in some RR interval time series slower rhythmical fluctuations due to thermoregulation [169] or body movements are observed.

Another specific heart rate pattern, which is also found in full term neonates and sometimes even in adults, is the observation of spikes. There are two types of spikes: short HR decelerations and spikes due to cardiac arrhythmias such as premature beats which affect only one or two RR intervals. Faulty peak detection, e.g. missed RR peaks or false detections, causes similar effects as certain cardiac arrhythmias. However, such spikes are not present in our RR interval series, as all faulty peak detections or premature ventricular contractions (PVC) were manually corrected based on the ECG recording.

3.4.2 Sleep states

The behavioural state has an important effect on heart rate. Heart rate is lower during non-REM sleep than during REM sleep or wakefulness [271, 182]. The duration of the non-REM periods depends in general on age. For our recordings it was mostly between 10 and 30 minutes, which corresponds to approximately 2000 to 4000 RR intervals. In each ECG signal, multiple periods of non-REM and REM could be determined with a mean total duration of 53.74 ± 26.76 minutes and 62.08 ± 14.00 minutes respectively.

The present results support the idea that different sleep states have, already from birth on, different cardiovascular fluctuations. The mean heart rate and SDNN values in this study are comparable to the values reported in literature for healthy preterm infants with similar age (PCA, GA) [182, 98, 67, 141]. Regarding the other standard time-domain HRV measures, to our knowledge, no comparable data is available in literature. Compared to normal full-term neonates with postnatal age of less than 72 hours, all standard time-domain parameters are smaller [232]. This finding agrees with results from studies on the maturation of the cardiac control in neonates [182, 98]. Heart rate, SDNN and RMSSD are significantly smaller in non-REM than in REM, a finding which was also observed in other studies [182, 141, 14, 97].

The numerical noise titration technique showed that periods of non-REM sleep have lower noise limit values and can be distinguished significantly from periods of REM sleep and from the total recording period. The RR interval series during non-REM sleep is less chaotic and in many cases NL is 0, which means that that signal part can be modelled sufficiently well in a linear way. The presence of abnormal events does not influence this finding. Moreover, if we do not consider each group separately, but all subjects together, a stronger difference between the

sleep states is found and even REM periods become statistically significant from the total recording.

The use of a nonlinear HRV parameter is a new aspect in the domain of sleep study of preterm neonates. During the last years, a large dataset of 190 sleep scored infants is collected and analyzed in the CHIME (Collaborative Home Infant Monitoring Evaluation) study with as main goal the development of a reliable decision system to determine sleep and wake based only on the electrocardiogram (ECG) of infants via HRV parameters [206, 205]. Although HRV is investigated many times in different ways the last decades, the numerical noise titration technique is a very interesting and useful technique to distinguish sleep states from each other. Because the numerical noise titration technique only emerged recently, it has not yet been widely applied. In Zapanta et al [410] and Deng et al [91], the technique has been applied for studying obstructive sleep apnea syndrome (OSAS) in children. Those studies concluded that it can be used to identify normal subjects from OSAS patients and that heart rate exhibits higher chaotic intensity in REM compared to non-REM sleep. However the latter was also investigated in this study, we have to emphasize that children and preterm neonates are two completely different population groups because their sleep patterns differ enormously [14, 198, 211, 229].

3.4.3 Distinguishing Neonatal Groups

Not only differences between sleep states were examined, but also a comparison between groups was done. While the standard time domain measures could not discriminate between NN, AN and AA, neither in the complete recording, nor in non-REM or REM periods, the nonlinear NL parameter succeeded. It proves that nonlinear measures can give extra information because they reflect other aspects of heart rate variability [29, 1]. Here, that other aspect reveals how chaotic the tachogram is. The more chaos in the signal, the less predictable it is and different studies showed a loss of heart rate variability in pathologic situations such as central hypoventilation or sudden infant death syndrome [97] and sepsis or urinary tract infection [145]. For this reason, NL is significantly higher for NN subjects compared to AN or AA subjects, at least during non-REM segments. Therefore, this study suggests that analyzing non-REM periods might be maybe sufficient to indicate whether a polysomnography was normal or abnormal, just based on the tachogram and without need of a full PSG. However, this link between the level of maturity of the cardiorespiratory system and the lack of chaos during non-REM periods requires more data reflecting different gestational ages. NL is lower in the AA than the AN group, although not statistically significant, maybe due to the limited number of neonates in each group. From a practical point of view, it should be very interesting if AN and AA neonates can be discriminated because

this will help deciding whether a baby needs a follow-up by home monitoring or not.

A similar study in preterm newborns was done by Morren [238] by making use of detrended fluctuation analysis (DFA). This well accepted classical technique computes nonlinear HRV parameters providing information about the scaling behaviour of the underlying system. That study did not show any significant difference between the groups when considering the complete night recording, nor in active sleep periods. Only the long term correlation coefficient 2 in a quiet sleep period showed significantly higher values for the AA group compared to NN and AN. Therefore, DFA might be useful to discriminate between AN and AA as aimed in this study. A drawback of that study was the limitation that not all periods of active and quiet sleep in the PSG were analyzed, but only the first ones so that the results can not be generalized.

3.5 Conclusion

In this study, the heart rate variability (HRV) of preterm infants during polysomnography was analyzed. In addition to standard time-domain HRV parameters, a nonlinear technique, called numerical noise titration, was used to quantify more dynamical aspects of the heart rate variability. The methodology for calculating these HRV parameters was adapted to deal with the specific characteristics of neonatal heart rate data and the relatively low ECG sampling rate (100 Hz). Regarding the numerical noise titration technique, periods of non-REM sleep have strongly significantly lower noise limit values, which means that the RR interval series is less chaotic during non-REM sleep. This provides further insights in the mechanisms causing periods of non-REM or REM sleep.

While the standard time domain measures could not discriminate between NN, AN and AA, neither in the complete recording, nor in non-REM or REM periods, the nonlinear NL parameter succeeded.

Chapter 4

Circadian profile and aging in a healthy population

While chapter 2 provided an overview of different HRV quantification approaches, this chapter studies the effect of gender and age on all these HRV parameters with a focus on the nonlinear ones. In addition, the circadian 24h profile is shown. The chapter starts with an introduction (Section 4.1), followed by a description of the study population, the data acquisition, the applied HRV parameters and the numerical and statistical analysis which is given in Section 4.2. Section 4.3 summarizes the results of the day-night differences, the ciradian profile and the effect of aging. The interpretation of the results as well as the limitations of the study will be discussed in Section 4.4. The main conclusions are mentioned in Section 4.5.

4.1 Introduction

Cardiovascular structures and functions change with age, increasing the risk of developing cardiovascular disease [264]. Even during day and night periods, the autonomic cardiovascular modulation is different. Epidemiologic studies highlighted the existence of a circadian profile in the onset of adverse cardiovascular (such as acute myocardial infarction, sudden death, ventricular arrhythmia) and cerebrovascular (such as ischemic and hemorrhagic stroke) events, which occur most frequently in the morning hours [245, 392]. Although the exact mechanisms underlying this circadian profile of adverse vascular events are still unknown, the sympathetic nervous system is believed to be primarily responsible for the increase in disease onset in the morning [10].

How the autonomic nervous system (ANS) exactly modulates the heart rate remains an open question. Heart rate variability (HRV) can be used to quantify several aspects of the autonomic heart rate modulation [6]. Standard time and frequency domain methods of HRV are well described by the Task Force of the European Society of Cardiology and the North American Society of Pacing and Electrophysiology [355], but they fail to show the dynamic properties of the fluctuations. Therefore, nonlinear methods are typically designed to assess the quality, scaling and correlation properties, rather than to assess the magnitude of variability like standard HRV methods do. However, in agreement with Lefebvre et al [201] and Yamamoto and Hughson [404], it seems likely that the cardiovascular system follows some nonlinear fluctuations which need to be explored further. Indeed, an important feature of a healthy cardiovascular system is adaptation, which can be defined as the capacity to respond to unpredictable stimuli. Consequently, a nonlinear behaviour would offer greater flexibility than a linear behaviour. The use of nonlinear techniques will probably give additional information related to the dynamical changes in cardiovascular control. While the day-night difference as well as the influence of gender and age on the autonomic modulation of heart rate have often been studied, most studies were limited to the standard HRV parameters. Ramaekers et al [294] already reported a significant difference between day and night standard HRV, reflecting a higher vagal modulation during the night while Beckers et al [34] described a tendency for higher nonlinearity during night time. Schwartz et al [330] found a decreasing autonomic modulation with advancing age, which already starts in childhood. With respect to gender, global autonomic activity was higher in men compared to women [82, 164, 406] while vagal modulation was similar in both sexes. Consequently, one speculates that the male population has an overall higher sympathetic drive, which is related to a higher susceptibility to fatal arrhythmia and the development of coronary artery disease [331]. According to our knowledge, hour-by-hour HRV analysis of Holter recordings was only studied by Bonnemeier et al [57] and moreover restricted to time domain HRV parameters.

In this study, not only linear but also a large set of nonlinear techniques are applied to quantify scaling behaviour and complexity. In particular, we focus on the recently developed numerical noise titration technique [285], which provides a highly sensitive test for deterministic chaos and a relative measure for tracking chaos of a noise-contaminated signal in short data segments, for example 5 minutes of data. The main goal of this study is to examine the nonlinear system dynamics in autonomic heart rate control according to gender, age and day-night periods. Therefore, the study includes a large number of healthy subjects between adolescence and old age. We hypothesize that the chaotic behaviour, given by the numerical noise titration, is higher during night than by day and that it decreases with increasing age. In addition, hour-by-hour analysis is obtained for all nonlinear HRV parameters, enabling to investigate the circadian profile more in detail instead of only day-night variations.

4.2 Methods

4.2.1 Study population

This study used the same dataset as in two previous studies [294, 34], but now with a focus on many nonlinear HRV techniques and their circadian profile. 276 healthy subjects (135 women and 141 men) were recruted from two centres of occupational medicine (Medi Leuven and IDEWE, Leuven, Belgium) and from a group of volunteers of the Christelijke Mutualiteiten (health insurance institution, Leuven, Belgium). All participants were between 18 and 71 years of age, with at least 40 participants per 10 years age category. A detailed medical history was obtained from each participant. Subjects with diabetes, hypertension, cardiovascular, neurological or psychiatric diseases were excluded. Smoking behaviour, height, weight and education level were registered. All subjects gave informed consent to the protocol approved by the local Ethical Committee. The study complies with the Declaration of Helsinki.

4.2.2 Data acquisition

Twenty-four hour ECG recordings were obtained using Holter monitoring (ELA Medical, sampling frequency 200 Hz). Only recorders with time tracking were used. Data acquisition and treatment has been fully explained in [18]. Data were reviewed and edited by the technicians using standard Holter analysis procedures. All analyses were reviewed in detail by an expert cardiologist. Correct manual annotation was made and premature supraventricular and ventricular beats, missed beats and pauses were filtered, with omission of one subsequent beat and linear interpolation of the corresponding periods. Special attention was paid to ensuring that only N-N beats with uniformly detected onsets were included in the initial tachogram. This way, type A errors (QRS detected prematurely when in fact a sinus conducted wave has not occurred) and B type errors (failing to detect an R wave that is present) could be largely avoided [178, 154]. A 20%-filter [191] was used, meaning that every RR interval that differ more than 20% from the previous one, is replaced by an interpolated value, defined via spline interpolation over the 5 previous and 5 next intervals. Finally, a file containing the consecutive RR intervals, called tachogram, was exported for later processing. The 24h recordings were split into day time (8 – 21h) and night time (23 – 6h).

4.2.3 Linear HRV parameters

All standard HRV parameters are calculated in agreement with the standards of measurement proposed by the Task Force of the European Society of Cardiology

and the North American Society of Pacing and Electrophysiology [355]. As time domain measures, we calculated mean RR, SDNN, SDANN, rMSSD and pNN50. After resampling the tachogram at 2 Hz [343] power spectral density was computed by using fast Fourier transformation on 256s tachgrams with 50% overlap and multiplication by a Hanning window. As frequency domain measures, we calculated low frequency power (LF and LFnu), high frequency power (HF and HFnu) and the ratio LF/HF.

4.2.4 Nonlinear HRV parameters

Nonlinear HRV parameters do not describe the amount of modulation as such, but are able to describe the scaling and complexity properties of the signal. Often used parameters which study the scaling of the system are $1/f$ slope, fractal dimension (FD) and detrended fluctuation analysis (DFA α_1 & α_2) while the complexity is addressed via the correlation dimension (CD) and approximate entropy (ApEn). Also a chaotic signature is calculated by means of the Lyapunov exponent (LE) and the numerical noise titration parameter (NL).

4.2.5 Numerical analysis

After resampling the RR interval time series to 2 Hz, the numerical noise titration was applied using a 300-second window and sliding the window every 30 seconds [91]. We used two noise titration measures to assess the changes in chaos level. The detection rate (NLdr) is defined as the percentage of all time segments in which nonlinearity is detected. This measure gauges the mean cardiac chaos level. NLmean was calculated as the average of all NL's excluding the segments with NL = 0. It estimates the chaos level directly and can be used as a highly time-resolved measure. All described HRV parameters were calculated during day time (8 – 21h) and night time (23 – 6h) as well as for each hour of the day.

4.2.6 Statistical analysis

Statistical analysis was performed with SPSS Windows version 11.5 (Scientific Packages for Social Sciences, Chicago, IL, USA). Variations between day and night were analysed pairwise by the nonparametric Wilcoxon Signed Rank test while the nonparametric Mann-Whitney U test examined the gender differences. To test the association between the different nonlinear HRV parameters and age, a two-tailed Pearson correlation coefficient was calculated. $P < 0.05$ was considered statistically significant.

4.3 Results

4.3.1 Day-night differences

All values, expressed as mean ± standard deviation, for the linear as well as nonlinear indices are listed in Table 4.1, separately for day and night. For every HRV parameter, it is indicated whether the day-night difference is statistically significant or not. As expected during the night, heart rate was significantly lower (higher mean RR interval). A day-night variation was not only present in all linear but even in all nonlinear HRV parameters, although one has to remark that day and night period have a different recording length which can slightly affect some nonlinear HRV parameters.

Concerning the time and frequency domain indices, parameters related to vagal modulation (pNN50, rMSSD and HF power) were higher at night. Low frequency power exhibited higher absolute values during the night, but a higher relative contribution during the day. These variations were present in both men and women and in all age categories. The relatively small differences in SDNN, SDANN and LF power, however, did not always reach statistical significance in these smaller groups. Those day-night changes in vagal modulation were linked to the day-night changes in basal heart rate (correlation between differences in day-night heart rate and day-night high frequency power $r = -0.45$, $P < 0.001$).

With respect to the nonlinear HRV indices, significant day-night variation was visible in both male and female population for $1/f$ slope, FD, DFA α_1, DFA α_2, ApEn and LE. The value of CD increased slightly during the night, but not significantly for women. Regarding the outcome of the noise titration technique, all results with or without gender or day-night distinction are given in Table 4.2. The day-night difference was significant in men and women. Both NLmean and NLdr were significantly higher during the night period. With respect to the gender difference, one can remark a lower NLmean and NLdr value for women than men as well during day as night. However, the higher NLmean in men compared to women is almost statistically significant during night while the higher NLdr in male compared to female population is clearly expressed during day time.

4.3.2 Circadian profile of nonlinear HRV

More subtle changes during the transitions between day and night are reflected for all HRV parameters by quantifying each of the 24 hours. Mean and standard error for each hour are plotted, separately for men and women, for time domain HRV (Figure 4.1), frequency domain HRV (Figure 4.2) and nonlinear HRV parameters (Figure 4.3).

Table 4.1: *HRV parameters, expressed in mean ± standard deviation, over complete population during day and night. Significance of day-night difference was obtained by the nonparametric Wilcoxon Signed Rank test.*

	Day	Night	Significance
Time domain HRV			
mean RR [ms]	724.2 ± 89.7	920.5 ± 125.9	***
SDNN [ms]	104.3 ± 33.1	110.6 ± 40.1	*
SDANN [ms]	82.9 ± 31.3	74.9 ± 33.8	***
rMSSD [ms]	31.5 ± 16.6	48.9 ± 29.9	***
pNN50 [%]	7.4 ± 7.3	17.5 ± 15.5	***
Frequency domain HRV			
LF [ms^2]	817 ± 572	1086 ± 983	***
LFnu [%]	82.8 ± 8.7	74.8 ± 11.9	***
HF [ms^2]	187 ± 246	433 ± 626	***
HFnu [%]	17.2 ± 8.7	25.5 ± 11.9	***
TP [ms^2]	2010 ± 1424	2846 ± 2319	***
LF/HF []	6.5 ± 3.5	4.0 ± 2.7	***
Nonlinear HRV			
$1/f$ slope	-1.19 ± 0.18	-1.12 ± 0.21	***
FD	1.28 ± 0.09	1.22 ± 0.10	***
DFA α_1	1.49 ± 0.14	1.42 ± 0.15	***
DFA α_2	1.04 ± 0.11	1.14 ± 0.11	***
CD	4.08 ± 0.76	4.41 ± 1.27	*
ApEn	0.77 ± 0.17	0.86 ± 0.19	***
LE	0.26 ± 0.07	0.29 ± 0.09	***

* $P < 0.05$, ** $P < 0.01$, *** $P < 0.001$

In general, an evolution over 24 hours can be observed for all indices, except LE. Concerning the standard HRV parameters in time and frequency domain, these diurnal variations can be seen in the male and female population. Sometimes there is a smooth transition from night to day, spread over several hours while in other cases (in particular SDNN), a strong change can be observed between two consecutive hours in the morning.

Heart rate starts already increasing extremely from 5 a.m., becoming stable from 8 a.m. on and again decreasing monotonously after 7 p.m. reaching the lowest peak at 4 a.m. The values of FD and DFA α_1 increase just before and during waking up, are almost constant afterwards and start to decrease slightly from late afternoon on. While DFA α_1 increases in the morming hours till 10 a.m., DFA α_2 reflects exactly the opposite profile. $1/f$ and CD show an abrupt fall just before

Table 4.2: *Difference in chaotic behaviour parameters, expressed in mean ± standard deviation, according to gender and day or night period. Significance of day-night variation was obtained by the nonparametric Wilcoxon Signed Rank test while the nonparametric Mann-Whitney U test was used to examine gender differences.*

	Day	Night	24h
NLmean [%]			
Men	19.20 ± 10.66	21.43 ± 8.37 **	19.96 ± 8.76
Women	17.88 ± 9.34	19.93 ± 7.80 **	18.60 ± 7.79
All	18.57 ± 10.06	20.72 ± 8.13 ***	19.32 ± 8.32
P (gender)	*0.3560*	*0.0519*	*0.2159*
NLdr [%]			
Men	53.07 ± 19.43	60.35 ± 14.09 ***	55.85 ± 17.28
Women	48.21 ± 19.56	57.64 ± 19.83 ***	51.94 ± 18.21
All	50.77 ± 19.61	59.06 ± 19.46 ***	53.99 ± 17.80
P (gender)	*0.0725*	*0.2897*	*0.1236*

* $P < 0.05$, ** $P < 0.01$, *** $P < 0.001$ indicating day-night differences
P (gender) indicates the p-value for gender differences

and during awakening, similar to heart rate, and a big jump in the late evening. LE did not show a clear 24h profile; however a transient dip was observed in the morning hours. When looking in particular to the noise titration parameters (Figure 4.4), deterministic chaos seems to increase monotonously in the evening, reaching a maximum early in the morning (4 – 5 a.m.), followed by a decrease and sharp fall around 8 a.m.

The circadian evolution over 24 hours is often similar in both male and female population. At every moment of the day, heart rate was on average higher in women than men. These hour-by-hour results also confirm that the nonlinear HRV parameters are in general higher in women than men, except for the chaotic parameters.This holds for each of the 24 hours in case of ApEn. While CD shows the gender difference especially at night, DFA α_2 has it particularly by day. DFA α_1, as usually acting oppositely, is higher in men than women, although only during night. FD is almost every time moment higher in women compared to men, but between 5 and 8 a.m., the increase is steeper for men than women. $1/f$ shows higher absolute values for women than men in general, but not consistently for each hour. No clear gender difference can be found in the LE. Opposite to most scaling and complexity parameters, the noise titration parameters were clearly higher in the male than female population. For NLmean, this holds for all hours while for NLdr, the gender difference was present by day, but nearly disappeared at night.

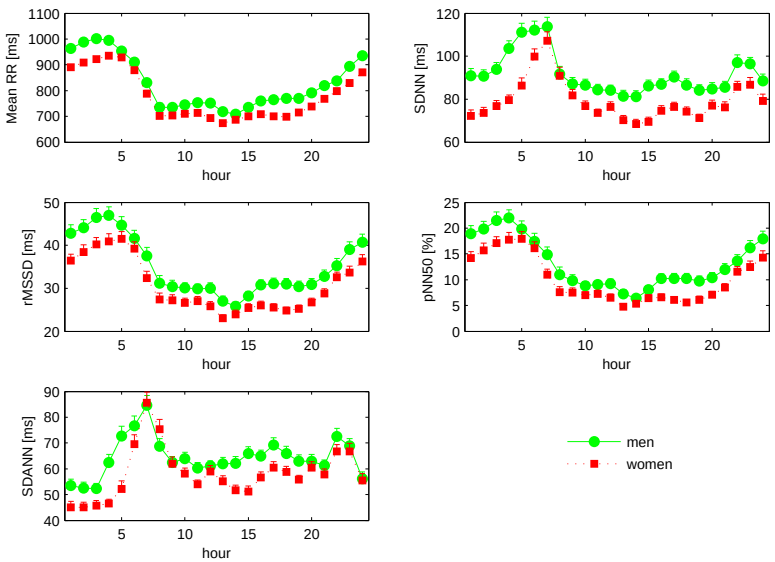


Figure 4.1: *Gender differences in circadian variation, expressed by mean and standard error, for the time domain HRV parameters mean RR, SDNN, rMSSD, pNN50 and SDANN. The results for men and women are indicated respectively via green circles and red squares.*

4.3.3 Effects of aging

Concerning the influence of age, all nonlinear indices, except NLmean, were significantly correlated with age. Table 4.3 gives the Pearson correlation coefficients r for the different nonlinear HRV parameters, separately for day and night and for women and men. Especially during the day, the correlation with age was very clear and it was also more pronounced in the female population. During night time, this relation disappeared in some parameters. Only DFA α_2 increased with increasing age, while all other described nonlinear HRV parameters were negatively correlated with age. The strongest relation with age could be found for FD (r between -0.45 and -0.70, $P < 0.001$). In addition, we also examined the influence of age on the full circadian profile. Figures 4.5, 4.6 and 4.7 show respectively for time domain, frequency domain and nonlinear HRV parameters the hour-by-hour results separately for each age category of 10 years. Here, the HR pattern shifted to a higher heart rate with increasing age till the age of 50 years. This increase is most pronounced during the sleeping hours and seems to disappear between 9 a.m. and 2 p.m. Age categories higher than 50 years show a

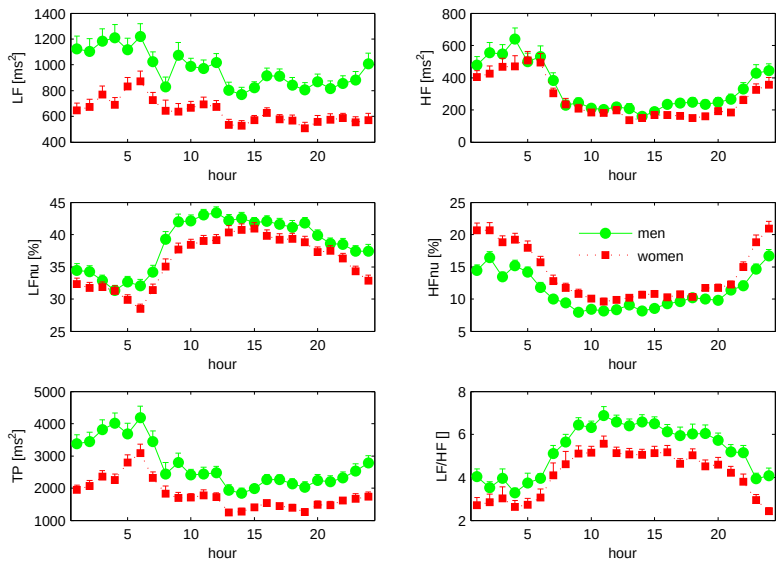


Figure 4.2: *Gender differences in circadian variation, expressed by mean and standard error, for the frequency domain HRV parameters LF, HF, LFnu, HFnu, TP and LF/HF. The results for men and women are indicated respectively via green circles and red squares.*

decreasing heart rate during day and night time. The $1/f$ slope profile only starts to decrease (become more negative) from the age of 50 years on, particularly during the forenoon. The most unmistakable and consistent age influence is observed in FD. A clear decrease of FD with increasing age can be noticed over all 24 hours. While DFA α_1 increases till the age of 50 years and decreases afterwards, DFA α_2 remains approximately the same till the age of 50 and starts then to increase. In both DFA parameters, the described tendencies are most expressed by day. CD, ApEn, LE and NLdr decreases with aging. While this decrease is for ApEn and LE more pronounced from the age of 50 years on, NLdr decreases especially before 50 years of age, still decreasing afterwards though not monotonously for each hour. Concerning NLmean, changes due to age are slightly different for day and night periods. At night, NLmean decreases till the age of 50 years, becoming more or less stable afterwards. By day, NLmean also decreases with increasing age, but only up to 40 years of age and increasing drastically in the higher age categories. Finally, one can observe that day-night differences are more expressed in the lowest age categories while they often (HR, FD, NLmean) disappear in higher age categories.

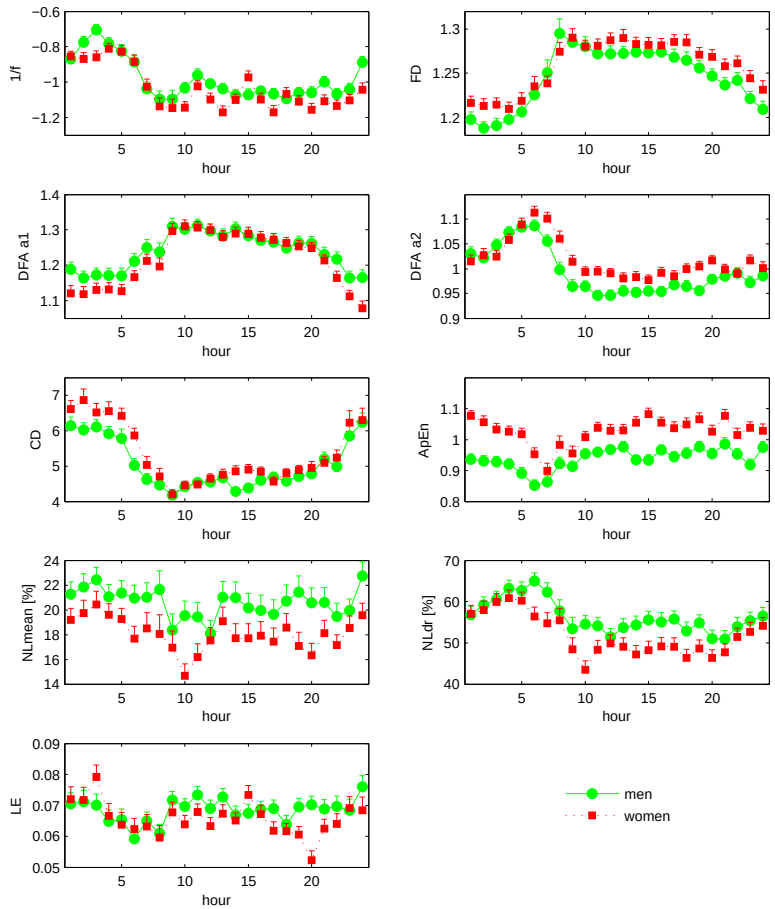


Figure 4.3: *Gender differences in circadian variation, expressed by mean and standard error, for the nonlinear HRV parameters $1/f$, FD, DFA α_1, DFA α_2, CD, ApEn, NLmean, NLdr and LE. The results for men and women are indicated respectively via green circles and red squares.*

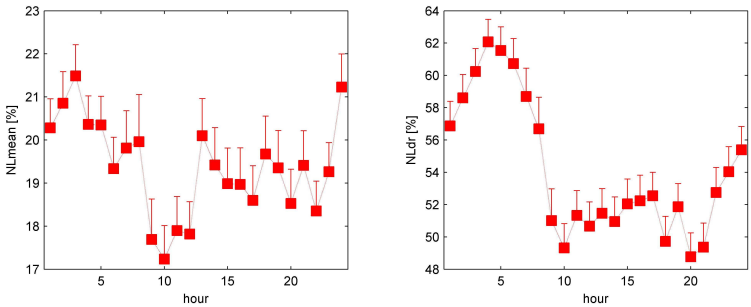


Figure 4.4: *Circadian evolution, expressed by mean and standard error, of the chaotic HRV parameters NLmean (left) and NLdr (right) over the complete study population, ignoring gender and age variations.*

Table 4.3: *Pearson correlation coefficients r between nonlinear HRV parameters and age, separately for day and night and for women and men.*

	Day				Night			
	Men		Women		Men		Women	
$1/f$	-0.241	**	-0.375	**	0.034	ns	-0.273	**
FD	-0.672	**	-0.699	**	-0.450	**	-0.531	**
DFA α_1	-0.144	ns	-0.296	**	0.115	ns	0.056	ns
DFA α_2	0.433	**	0.600	**	0.517	**	0.420	**
CD	-0.313	**	-0.511	**	-0.198	*	-0.131	ns
ApEn	-0.271	**	-0.455	**	-0.236	**	-0.354	**
LE	-0.273	**	-0.314	**	-0.067	ns	0.049	ns
NLmean	0.134	ns	0.078	ns	0.046	ns	0.110	ns
NLdr	-0.297	**	-0.319	**	-0.301	**	-0.260	**

* $P < 0.05$, ** $P < 0.01$, ns = non-significant

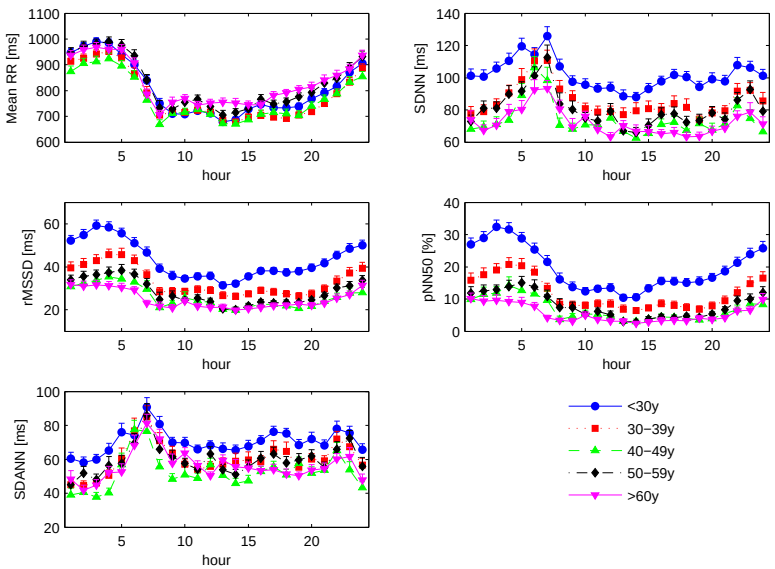


Figure 4.5: *Influence of age on circadian variation, expressed by mean and standard error, for the time domain HRV parameters mean RR, SDNN, rMSSD, pNN50 and SDANN. The results for the age categories* $< 30y$, $30 - 39y$, $40 - 49y$, $50 - 59y$ *and* $> 60y$ *are indicated respectively via blue circles, red squares, green upper triangles, black rhombuses and magenta lower triangles.*

4.4 Discussion

Heart rate variability is considered a parameter of autonomic cardiovascular control. In this study, the most commonly used nonlinear HRV parameters ($1/f$ slope, FD, DFA, CD, ApEn and LE) were examined in a population of 276 healthy subjects between 18 and 71 years of age. In addition, the recently developed method of numerical noise titration was applied leading to the new chaotic HRV parameters NLmean and NLdr. Nowadays, this technique has only been applied a few times and always to study relative differences between patient groups [410, 91, 402]. Many previous studies have tried to assess day-night variations or gender- and age-related differences in HRV parameters, although most of these studies have major limitations: small groups, fixed age category, unequal amount of male and female subjects, short duration recordings and use of only a few parameters. All these shortcomings were taken into account in this study. In addition, via hour-by-hour analysis, we presented for each nonlinear HRV parameter the clear circadian profile as a function of age or gender.

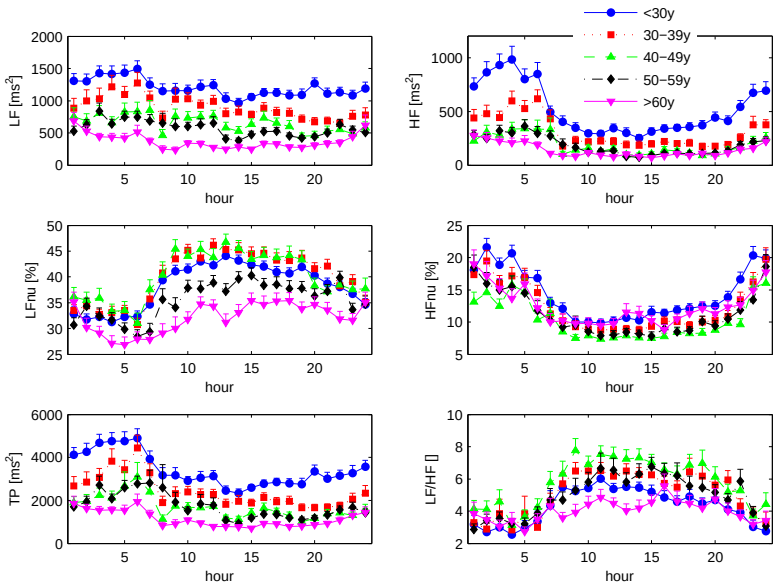


Figure 4.6: *Influence of age on circadian variation, expressed by mean and standard error, for the frequency domain HRV parameters LF, HF, LFnu, HFnu, TP and LF/HF. The results for the age categories* $< 30y$, $30 - 39y$, $40 - 49y$, $50 - 59y$ *and* $> 60y$ *are indicated respectively via blue circles, red squares, green upper triangles, black rhombuses and magenta lower triangles.*

4.4.1 Vagal autonomic control more chaotic

Concerning the day-night variation, Ramaekers et al [294] already reported a significant difference between day and night standard HRV, reflecting a higher vagal modulation. There was a tendency for higher nonlinearity during night time as already described by Beckers et al [34]. LE, CD, DFA α_2 and ApEn increased while the $1/f$ slope came closer to real $1/f$ behaviour. Only FD and DFA α_1 decreased. This was the case in both the male and female population. Our hypothesis that RR interval time series at night are more chaotic compared to those at day time was confirmed. Consequently, in healthy persons the autonomic heart rate modulation is more chaotic during sleep than awake and heart rate is less predictable during night than by day. This is probably due to the gravitational load during day time with more sympathetic influences on heart rate control. Therefore, we suggest that vagal modulation is more chaotic than sympathetic modulation. LE, which is a similar measure to quantify chaos, was believed to be uncorrelated to autonomic modulation [149] and is therefore in conflict with our hypothesis.

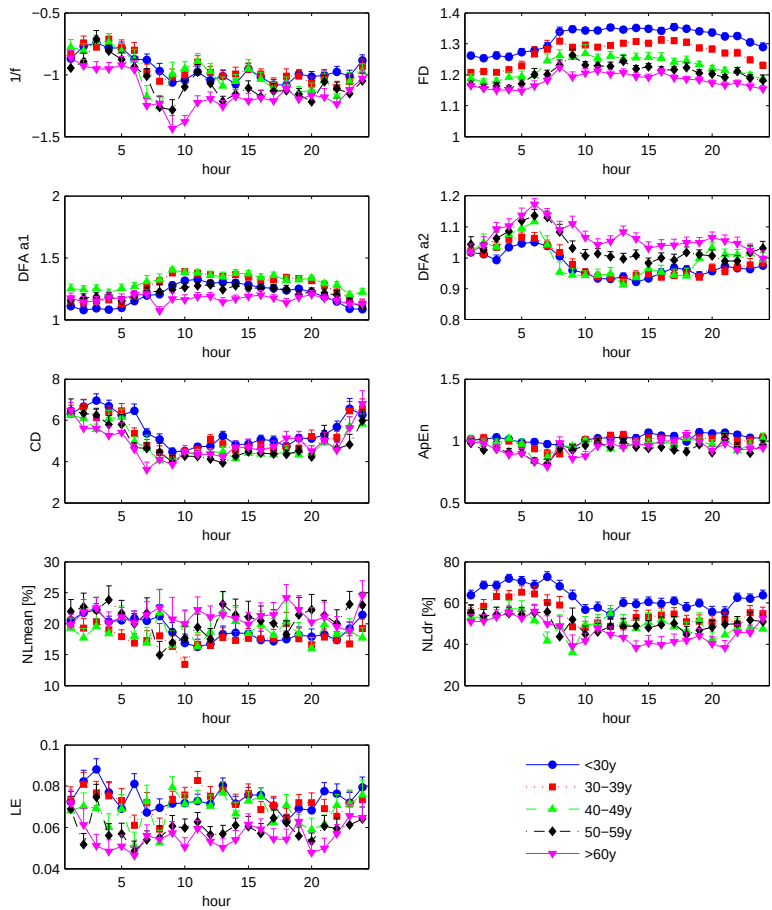


Figure 4.7: *Influence of age on circadian variation, expressed by mean and standard error, for the nonlinear HRV parameters* $1/f$*, FD, DFA* α_1*, DFA* α_2*, CD, ApEn, NLmean, NLdr and LE. The results for the age categories* $< 30y$*,* $30 - 39y$*,* $40 - 49y$*,* $50 - 59y$ *and* $> 60y$ *are indicated respectively via blue circles, red squares, green upper triangles, black rhombuses and magenta lower triangles.*

But Poon and Barahona [285] noted that numerical noise titration is a better alternative for the Lyapunov exponent (LE) which fails to specifically distinguish chaos from noise. LE can not detect chaos reliably unless the data series are excessively long and virtually free of noise. However, these two requirements are difficult, mostly even impossible, to fulfill for most empirical data. Nevertheless, according to Beckers et al [34], the majority of the nonlinear HRV parameters, and in particular ApEn, DFA α_1 and FD, showed a clear relation with indices representing vagal modulation. Our hypothesis that vagal modulation is more chaotic than sympathetic modulation fits in that context.

4.4.2 Circadian profile of nonlinear cardiac autonomic control

It is generally acknowledged that there is a unique circadian distribution of cardiovascular events with a striking preponderance in the morning hours [243, 368, 306]. A possible link to physiological rhythms with a similar diurnal variation is therefore inevitable. According to our knowledge, only Bonnemeier et al [57] studied hour-by-hour HRV analysis of Holter recordings in healthy subjects as a function of age and gender, although restricted to only time domain HRV parameters. Our study is an extension and complementary to the previous study as we performed an analysis with nonlinear HRV parameters, giving the benefit of examining the daily profile more in detail instead of only day-night variations. The potentially important information in the morning and evening periods was already noted by Kozak et al [195] and proposed in our previous study [34]. The circadian heart rate profile as described by Bonnemeier et al [57], was completely confirmed in our study.

Mean RRI increased continuously during sleep time with a peak around 4 - 5 a.m. followed by a steep decrease till baseline level around awakening. The lowest RRI's, so the highest heart rates, are observed short after noon. The circadian profiles of rMSSD and pNN50, both reflecting parasympathetic control and short term HRV, showed exactly the same characteristic pattern as mean RRI, supporting the idea that heart rate is mainly defined by parasympathetic modulation. Estimates of long term HRV such as SDANN or of total HRV such as SDNN and total power (TP) peaked around the hour of awakening.

Nonlinear cardiac characteristics showed a clear circadian profile, often even more pronounced than for the time domain HRV parameters [57]. Especially the transition phases from day to night and night to day are very valuable and instructive. The DFA α_2 pattern over 24h showed a high similarity with the vagal-associated parameters pNN50 and rMSSD in the study of Bonnemeier et al [57]. However, heart rate starts to increase earlier in the morning than the onset of the reduction in vagal-associated parameters, probably because the time right before waking, as well as REM sleep, is known as a time of higher sympathetic

activity. This is exactly what can be seen in the nonlinear parameters $1/f$, CD and NLdr, which showed a remarkably similar circadian profile as mean RR, although the decrease always lasted till 10 a.m. while heart rate became stable at 8 a.m. FD and DFA α_1 revealed the opposite pattern of mean RR, but the transition phase in the evening starts earlier than the change in heart rate. These are all indications that (1) heart rate is modulated nonlinearly, (2) more subtle changes in the cardiovascular system occur before or after a change in heart rate and (3) each of the nonlinear HRV parameters represent a slightly other aspect of scaling, complexity or chaotic behaviour. Since adverse cardiovascular events occur very often in the morning hours [10] and most nonlinear HRV parameters change then, studying the nonlinear cardiovascular dynamics will probably give more insight. During that transition phase from sleep to wake condition, the autonomic modulation changes drastically and it seems that among other measures, also the noise titration parameter is able to reflect this. The absence of a reduction in the dynamic behaviour of the cardiovascular control during the morning hours might be a possible indication for adverse cardiovascular events. Therefore, future diagnostic studies can incorporate the nonlinear HRV parameters to improve their prognostic model. Moreover, Maestri et al [218] proved that nonlinear parameters are more suitable for diagnostic purposes as they enable the cardiovascular system to respond more quickly to changing conditions.

4.4.3 Aging and nonlinear cardiac autonomic control

A strong correlation with age was detected in most nonlinear indices. Increasing age was associated with decreasing nonlinear behaviour as hypothesized: decrease in FD, CD, ApEn, LE, NL and a steeper $1/f$ slope. These findings are in accordance with some previous studies [3, 180, 279, 135] and can be related to the general concept of decreasing autonomic modulation with advancing age, which already start in childhood [330]. Increasing age might result in an increased inability of the cardiac system to respond adequately to changing conditions. For those nonlinear indices, the age dependency was especially prominent during day time and also more pronounced in the female population. An inverse association between linear HRV parameters and age was already in several studies [408, 350, 370, 197]. However linear indices were stronger related with age in men than in women [294, 57], nonlinear HRV parameters showed a stronger correlation with age in the female population compared to the male population. A more thorough analysis per age category of 10 years showed that often age tendencies changed when passing the age of 50 years. While for heart rate and DFA α_1, an increase with advancing age turned over in a decrease, other parameters only started to decrease ($1/f$) or increase (DFA α_2) from the age category of 50-59 years or the tendency became from then on more expressed (CD, ApEn, LE). This finding corresponds to results described by Ramaekers et al [294] where also in linear indices the decline stabilized around the age of 40 years. Moreover,

our results can be linked most likely with a much higher chance on cardiovascular diseases after the age of 50 years, especially in women [140]. A recent study of Stein et al [347] in older people (> 65 years) found that declines in traditional frequency domain measures slow at age of 70 years whereas nonlinear HRV parameters decline continuously throughout advancing age.

4.4.4 Effects of gender

Women live longer and develop cardiovascular illness at a later age than man [396], giving rise to the hypothesis of a more chaotic and less predictable heart rate signal in women [317]. However, evidence of higher heart rate fluctuations in the female population was not found which is in correspondence with Pikkujamsa et al [278]. On the contrary, global autonomic activity was higher in men compared to women while vagal modulation was similar in both sexes [82, 164, 406]. While those studies suggest a higher sympathetic tone in male subjects and the absence of gender differences in vagal modulation, Bonnemeier et al [57] attributed the gender difference to a higher nocturnal vagal modulation in younger healthy male subjects and noted less pronounced gender differences with increasing age. Beckers et al [34] showed only gender related differences in approximate entropy, short range detrended fluctuation analysis and the Lyapunov exponent, which is partly confirmed by our hour-by-hour analysis. Although ApEn and NLmean had the same circadian evolution for men and women, both parameters had a higher gender difference compared to other nonlinear parameters. This study also rejects the hypothesis of a more chaotic and less predictable autonomic heart rate modulation in women as the mean chaos level (NLdr) was lower in women than men. Nevertheless many scaling behaviour or complexity parameters showed higher values for women than men, again confirming the added value of chaotic HRV parameters with respect to the other nonlinear HRV parameters.

4.4.5 Limitations

Despite the attempt to create a similar recording environment, physical activity by day or sleep stages (REM vs. non-REM) at night via polysomnographies were not measured. This may hamper the interpretation of our results since both affect heart rate variability [84, 139]. REM sleep which takes up about 25% of the night and a lot of the time right before waking, is a time of higher sympathetic activity and relatively unstable heart rates while non-REM, especially earlier in the night, is a time of very stable heart rate patterns with a great deal of correlated behaviour. Also preprocessing the data can have an impact on some nonlinear parameters as the 20% filter can filter out good sinus beats or fail to capture true supraventricular ectopic beats. Nevertheless, this filtering was recommended by Kleiger et al [191] and is nowadays generally accepted. Further, a sampling frequency of 200 Hz is

rather low and nowadays one of the restrictions for use of Holter equipments in HRV research.

4.5 Conclusion

This study showed the typical circadian profiles for several nonlinear HRV parameters as a function of age and gender. Not only parameters providing information about the scaling behaviour or the complexity of the autonomic heart rate modulation are included, but also the chaotic behaviour was quantified by means of the recently developed numerical noise titration technique. This method can be applied on short noisy time series, which can be a big advantage in clinical environment in the future. A higher nonlinear behaviour was observed during the night while nonlinear heart rate fluctuations decline with age. A clear circadian profile could be found for almost every parameter, showing in particular which changes occur during the transition phases of waking up and going to sleep. The results support the involvement of the autonomic nervous system in the generation of nonlinear and complex heart rate dynamics.

Chapter 5

Effect of stress on heart rate modulation

Whereas in the previous chapter, HRV was applied on a large healthy population to study effects of age, gender and the circadian profile, now the influence of stress, physical as well as mental stress, on the autonomic heart rate modulation will be presented in chapter 5. Section 5.1 introduces the problem of stress in daily life and the need to detect stress easily. The instrumentation and study design are explained in Section 5.2. This section also describes how time-frequency analysis can be used to study fast changes in time. The results of the stress test and the corresponding changes in HRV are given in Section 5.3 and discussed in Section 5.4. The link between the physiological output and the self scores, based on a questionnaire, will also be reported. Finally, Section 5.5 summarizes the conclusions.

5.1 Introduction

Since the nineties, markers of stress and other psychosocial factors have been associated with coronary disease [226]. In contrast with other lifestyle risk factors, no consensus about stress exists with respect to either definition or measurement. Inevitably, stress is subjective and it can encompass several aspects, from external stressors such as adverse life events, financial problems or job stress to potential reactions such as depression, vital exhaustion, sleeping difficulties or anxiety [216, 174, 231, 292]. Several studies have shown a link between the level of work stress and disease [189, 389]. Stress, here defined as a mismatch between perceived demands and perceived capacities to meet those demands [115], is a psychophysiological phenomenon that changes the physiological

balance of amongst others the autonomic nervous system (ANS) [288, 383]. The ANS is divided into a sympathetic and parasympathetic or vagal branch. Both components operate simultaneously and balance each other dynamically in normal conditions. When a person is exposed to a stressor, the sympathetic system becomes more activated, resulting in the secretion of the hormones epinephrine and norepinephrine into the blood [292]. This hormonal secretion causes a change in some physiological signals, e.g. an increased heart rate (HR) and breathing rate. This reaction is called the fight or flight reaction since Walter Cannon's work on the fight-or-flight response in the 1930s [356]. When the stressor disappears, the vagal system takes over to decrease among others sweating, heart rate and breathing rate.

Heart rate variability (HRV) refers to alternations in heart beat time-intervals and provides quantitative markers of autonomic regulation [6, 355]. Moreover, it is a simple and powerful noninvasive methodology having enormous practical advantages with a minimum of technical constraints, which makes it useful in many applications. Therefore, HRV has been used to examine the responses to mental and physical demands on the ANS. Expressed physical tasks strongly influence HRV indices related to ANS as shown for static handgrip at 25% of maximal voluntary contraction (MVC) [268], bicycle exercise [274] or static leg extension at 30% MVC [139]. Mental stress in laboratory experiments (cognitive demands, mental arithmetic) has been associated with decreased HRV, indicating a disturbed ANS [248, 345, 234, 126, 158]. Many studies only focus on either physical or mental load, but only a few consider both.

The goal of this study was to evaluate the effect of physical and mental stress on HRV parameters of autonomic activity separately. More specifically, the discrimination between mental load and physical activity, in literature known to be methodologically difficult [318], is studied. Additionally, the effect of the combined physical and mental demand was examined. However the relative contribution of mental and physical stress on HRV is still not completely clear, we hypothesized a bigger change of the HRV parameters, and therefore autonomic modulation of heart rate, in the combined task compared to a single task. While almost all previous studies were either interested in the relation between HRV and a questionnaire based stress level or the influence of imposed demands on HRV, this study also investigated the time evolution. Time-frequency analysis, as applied here, was rarely used in literature, although it enables to study trends within the same condition or transitions between several phases. After describing the data and the HRV methods, results are given for every HRV parameter separately. We then discuss these results by focusing on the differences in HRV characteristics during rest, mental load, physical load and the combination of the latter two.

5.2 Methods

5.2.1 Subjects

28 participants were monitored, 15 men and 13 women with 22 $\pm$ 1.96 (mean $\pm$ standard deviation) years of age and a body mass index of 22.2 $\pm$ 0.43 kg/m^2. The study population consisted of students and young people working at the Katholieke Universiteit Leuven. No exclusion criteria were used. Before the experiment, information about neck or shoulder complaints, cardiovascular problems and whether subjects were right- or left handed was noted. The experiment was approved by the Ethics Committees of the Department of Psychology and of the Faculty of Medical Sciences. Each subject provided written informed consent before participating. The study complies with the Declaration of Helsinki.

5.2.2 Instrumentation

Upon arrival, the test subjects were prepared for the measurements. The hair on the left chest was removed if appropriate and the skin was cleaned. Electrodes (Ag-AgCl, 10 mm diameter, Nikomed, Denmark) were placed on the body to measure simultaneously the electrocardiogram (ECG) and surface electromyography (sEMG) of the M. Trapezius. ECG (sampling frequency: 1000 Hz) was obtained by two electrodes placed around the heart and a reference electrode on the sternum. sEMG was monitored for purposes which are beyond the scope of this paper. The data were registered with EMG preamplifiers from Mega Electronics Ltd (Finland). These analog signals were amplified and low pass filtered (450Hz). The Daqbook 2005 (IoTech, Ohio, USA) was used to digitize the signals at a frequency of 1000 Hz with 16-bit resolution before storage on a personal computer.

5.2.3 Protocol

In a laboratory environment, the subjects were instructed to perform five tasks according to the following protocol made in collaboration with researchers from the Psychology Department at Katholieke Universiteit Leuven. A first task implied sitting at ease with the hands in the laps. During this rest period (R), a series of relaxing photos was shown on the computer screen. A second task was a postural task (PT) in which the subjects performed a shoulder abduction of 45°with stretched arms during 6 minutes. This prolonged static posture was intended to induce muscle fatigue in the shoulder girdle, which we also investigated via measuring muscle activity (EMG). Nevertheless, these results will be described in another study. A third task consisted of a mental stressor (MT).

The subjects were sitting with their hands in their laps and performed a complex and challenging mental task, part 1 of the home version of the MENSA test (http://www.mensa.be). Time to complete the test was limited to 10 minutes and subjects were not informed about the expired time, causing an extra stressor. The combination of a mental and postural task formed the fourth condition (MPT). Here, the subjects performed a shoulder abduction of 45°with stretched arms and had to solve part 2 of the MENSA test. Time to complete the MENSA test was again limited to 10 minutes. Finally, after each of the described tasks a self rating (SR) took place. The subjects were asked to rate their feelings at that moment on the short version of the Spielberger State-Trait Anxiety Inventory (STAI) [90]. This provided subject perceptions of their stress or anxiety levels at the instant of rating. The scale comprises 6 terms rated on a scale of 1 to 4: 3 of negative affect (tense, nervous, worried) and 3 of positive affect (calm, content, relaxed).

Tasks 2, 3 and 4 are called the active conditions (PT, MT and MPT). Each active condition was followed by a rest condition and the sequence of these active conditions was fully randomized amongst the participants. While the PT condition had a fixed duration of 6 minutes, MT and MPT were of variable length depending on the speed the subjects solved the IQ questions with a maximum of 10 minutes. The participants were instructed to give the answers of the IQ test orally to the experimenter. Apart from this, the participants were asked not to move and to speak. All tasks were performed with the subject in a sitting position facing the screen to ensure similar effects across tasks on HRV.

5.2.4 HRV analysis

After deriving the tachogram from the ECG signal, the data was checked manually for missing and ectopic beats and extra ventricular beats were replaced by a 20%-filter. Linear HRV parameters were obtained in agreement with the standards of measurement, proposed by the Task Force of the European Society of Cardiology and the North American Society of Pacing and Electrophysiology [355]. Mean, SDNN, RMSSD and pNN50 were calculated in the time domain. After resampling the tachogram at 2 Hz, the power spectral density (PSD) was computed by using fast Fourier transformation. In the frequency domain, LF, HF, Lfnu, HFnu and LF/HF were calculated.

As some HRV parameters, such as SDNN, depend on the recording length, a comparison between conditions can only be done by calculating each HRV parameter on segments of 2 minutes, which is the duration of the shortest condition in the dataset. We considered in addition to the first 2 also the last 2 minutes, making it possible to examine a potential evolution in time. The HRV parameters of all rest periods are averaged. Additionally, to overcome the possible non-stationarity and to describe the changes in HRV spectra during transients, time-

frequency analysis (TFA) is used by applying continuous wavelet transformation (CWT). The Morlet wavelet is used as the literature showed that this is an appropriate function to study HRV [196]. TFA enables to track LF and HF parameters reliably over time: the power as well as the instantaneous frequency [72] in each frequency band. All algorithms were implemented in-house using Matlab R2008a (The MathWorks Inc., Natick, MA, USA).

5.2.5 Statistical analysis

Statistical analysis was executed using the nonparametric Friedman test adjusted for possible between subject effects to test whether the different phases (R, PT, MT and MPT) affected the HRV parameters. Post hoc Tukey contrasts were used in order to explore further differences between two phases, taking into account multiple testing. How the parameters changed over time between the beginning and end of each phase was analysed pairwise by the nonparametric Wilcoxon Signed Rank test. $P < 0.05$ was considered statistically significant.

5.3 Results

5.3.1 Performance

The mean score (SD) of the mensa test was 75 (12.6)% for the questions during MPT and 63 (17.5)% during MT, resulting in a mean score of 69 (12.7)%. The better results during MPT could be caused by easier questions than during MT as the order of questions was not randomised. Moreover, a time effect was observed. Most participants scored better on their second part of the mensa test (12/14 for the subjects that started with MT and 8/14 for the group that started with MPT).

5.3.2 Heart rate

A typical tachogram with indication of the different conditions is illustrated in Figure 5.1. During a first visual inspection of the signal, a clear transition between the different conditions can be noticed. Phase had a significant (begin: $F = 41.19$, $p < 0.0001$; end: $F = 59.4$, $p < 0.0001$) effect on mean RR of which the boxplot is shown in Figure 5.2. Contrast analysis revealed a significantly higher mean RR in R than in the active conditions MT, PT or MPT (all $p < 0.001$) as could be expected from Figure 5.1. In the beginning of each phase, heart rate was highest during MPT ($p < 0.01$ vs. PT and $p < 0.05$ vs. MT) followed by MT ($p = 0.24$ vs. PT) and PT. The latter had the highest heart rate during the last 2 minutes of the experimental conditions.

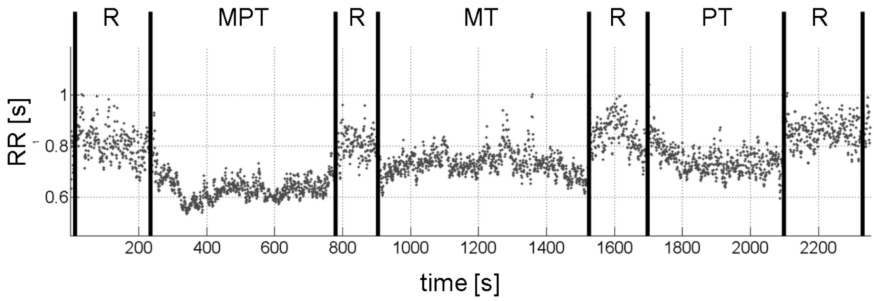


Figure 5.1: *Typical tachogram of a subject with indication of the different experimental conditions.*

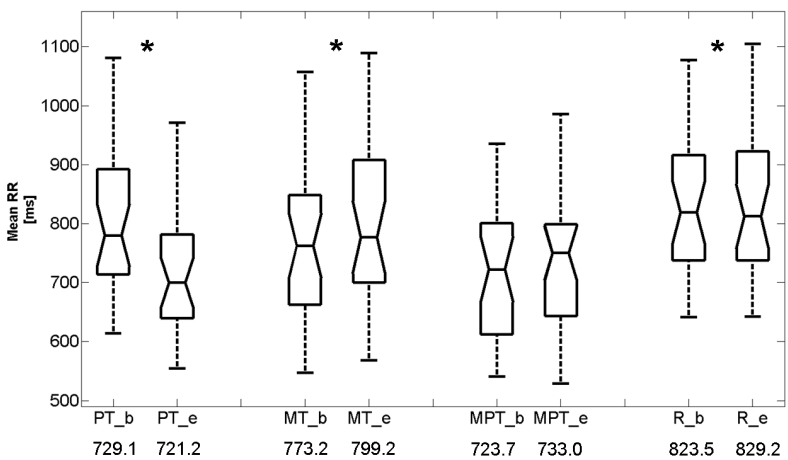


Figure 5.2: *Boxplots of mean RR intervals for the different conditions, where b indicates the first 2 minutes and e the last 2 minutes of the specific condition. Statistical differences ($p < 0.05$) between both time periods are shown by *. Below the figure, the mean values are given.*

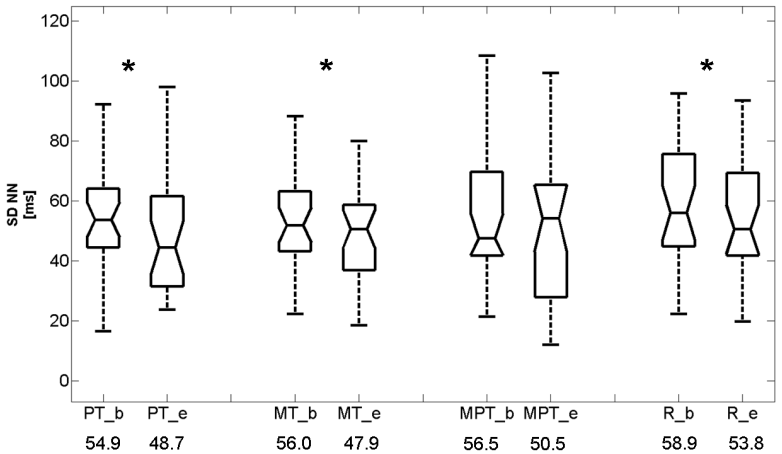


Figure 5.3: *Boxplots of SDNN (total heart rate variability) for the different conditions, where b indicates the first 2 minutes and e the last 2 minutes of the specific condition. Statistical differences ($p < 0.05$) between both time periods are shown by *. Below the figure, the mean values are given.*

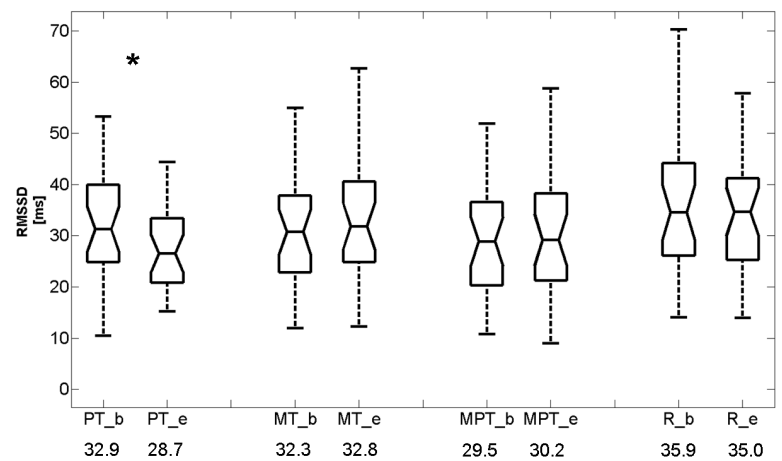


Figure 5.4: *Boxplots of RMSSD (vagal autonomic modulation) for the different conditions, where b indicates the first 2 minutes and e the last 2 minutes of the specific condition. Statistical differences ($p < 0.05$) between both time periods are shown by *. Below the figure, the mean values are given.*

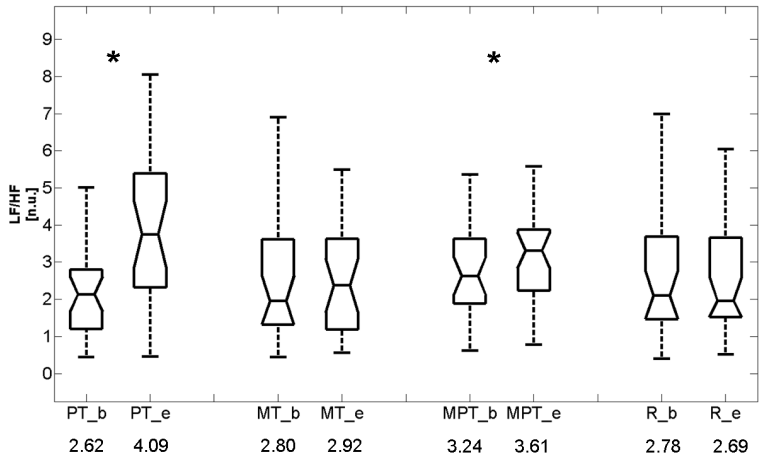


Figure 5.5: *Boxplots of LF/HF (sympathovagal balance) for the different conditions, where b indicates the first 2 minutes and e the last 2 minutes of the specific condition. Statistical differences ($p < 0.05$) between both time periods are shown by *. Below the figure, the mean values are given.*

5.3.3 Heart rate variability and time-frequency analysis

Results on HRV showed that phase also had a significant effect on SDNN (begin: $F = 3.39$, $p = 0.34$; end: $F = 8.79$, $p < 0.05$), rMSSD (begin: $F = 19.41$, $p < 0.0001$; end: $F = 24.09$, $p < 0.0001$), pNN50 (begin: $F = 16.18$, $p < 0.001$; end: $F = 15.62$, $p < 0.01$), LF (begin: $F = 16.63$, $p < 0.001$; end: $F = 6.56$, $p = 0.08$), HF (begin: $F = 32.79$, $p < 0.0001$; end: $F = 20.19$, $p < 0.01$), LFnu (begin: $F = 4.16$, $p = 0.24$; end: $F = 19.33$, $p < 0.001$), HFnu (begin: $F = 6.81$, $p = 0.08$; end: $F = 27.3$, $p < 0.0001$) and LF/HF (begin: $F = 9.5$, $p < 0.05$; end: $F = 19.97$, $p < 0.001$). SDNN, providing information about the total variability of heart rate control and shown in Figure 5.3, was higher during rest, although this difference was only significant ($p = 0.01$) compared to the mental task during the last 2 minutes.

Figure 5.4 presents the results for rMSSD, which reflects vagal modulation of ANS as pNN50 and HF do according to the literature. These three parameters showed similar evolutions as expected. The differences are quasi identical to mean RR, namely significantly higher in R compared to PT, MT and MPT. In addition, those parameters were significantly lower in MPT than MT, both in the beginning ($p < 0.05$) and at the end ($p < 0.05$) of the period. Even here, the results for PT changed over time, being the highest of all active conditions the first minutes and becoming the lowest at the end. A typical time evolution of HF power is shown

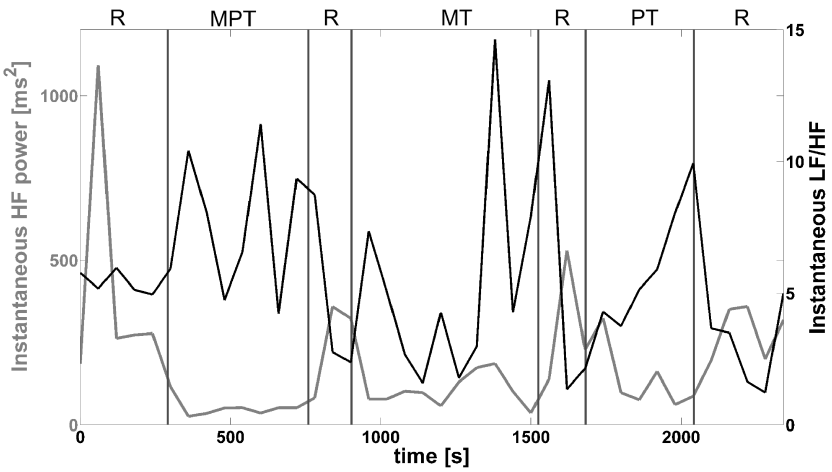


Figure 5.6: *Typical evolution of instantaneous HF power (grey line) and LF/HF ratio (black line) over time with indication of the different conditions.*

in Figure 5.6 via TFA, visualizing all described changes between and within the phases.

LF/HF and LFnu, both characterizing the sympathovagal balance and depicted in Figure 5.5, had a big increase during MPT. During the first 2 minutes, this increase was only significant compared to PT ($p < 0.05$). When considering the last 2 minutes, this significance in sympathovagal balance between MPT and PT disappeared, but LF/HF and LFnu became significantly higher in MPT than during MT ($p < 0.01$) and R ($p < 0.05$). Again, the parameters changed completely within the PT condition, from the lowest one to the highest one. This can also be seen in Figure 5.6 where the LF/HF ratio trend is plotted over time.

Figure 5.7 shows the instantaneous frequencies as a time series, reflecting a nearly constant main frequency of 0.08 Hz in the LF band while it fluctuates between 0.23 and 0.26 Hz in the HF band. Especially during MT, an increased HF frequency is observed.

5.3.4 Self rating scores

Table 5.1 shows the scores on subjective experiences (tensed, nervous, worried, calm, happy and relaxed). For three subjective experiences (tensed, happy and relaxed), the test subject gave significantly different scores during rest compared to the active phases. They reported to be more happy, less tensed and more relaxed during the rest period compared to the MT, PT and MPT (not significant for

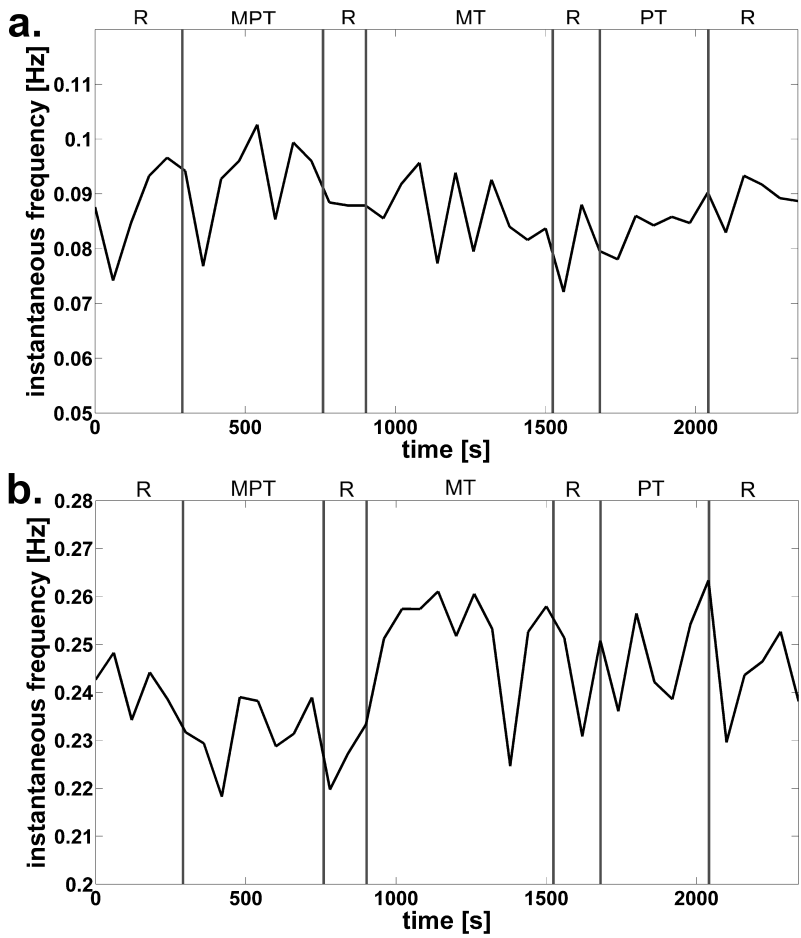


Figure 5.7: *Typical evolution of instantaneous frequency in (a) LF and (b) HF band over time with indication of the different conditions.*

Table 5.1: *Mean (SD) for scores on subjective experiences during the different conditions (R, PT, MT, MPT) in the protocol. Scales ranged from 1 to 4 (1 = not and 4 = extremely) ($n = 28$)*

Variable	R	MT	PT	MPT
Tensed	1.66 (0.56)	2.14 (0.65) ⋆	2.79 (0.74) ⋆,◇	2.54 (0.79) ⋆
Nervous	1.52 (0.44)	1.64 (0.73)	1.68 (0.82)	1.79 (0.69)
Worried	1.23 (0.55)	1.46 (0.74)	1.39 (0.69)	1.36 (0.73)
Calm	3.16 (0.61)	2.50 (0.75)	2.21 (0.79)	2.25 (0.75)
Happy	2.88 (0.50)	2.46 (0.79) ⋆	2.25 (0.89) ⋆	2.57 (0.74)
Relaxed	2.95 (0.61)	2.36 (0.62) ⋆	1.79 (0.92) ⋆	1.68 (0.77) ⋆

⋆ Significant difference with R ($P < 0.05$)
◇ Significant difference with MT ($P < 0.05$)

happy) phase. The subjects also revealed to feel significantly more tensed during PT compared to MT.

5.4 Discussion

5.4.1 Influence of mental and physical state

HRV parameters were calculated in several conditions: rest, physical task, mental task and a combination of both tasks. For almost all described measures, the active conditions can be distinguished from the rest condition, meaning that heart rate variability is sensitive to any change in mental or physical state. The combination of a physical and a mental task was expected to result in a higher load compared to one of both tasks separately. Our hypothesis was confirmed by a significantly higher heart rate and a significantly lower vagal modulation (rMSSD, pNN50, HF). The effect of the physical task (increased HR, decreased vagal modulation) is superposed to the cardiovascular effect of the single mental load. This suggests an additional effect when multiple tasks are combined. A similar observation was found for the sympathovagal balance (LF/HF, LFnu), being on average higher during MPT than PT or MT, showing a constant sympathetic dominance due to the combination of both tasks. Nevertheless, this finding is opposite to what Garde et al [126] found. That study reported that the addition of mental demands to a physical computer task does not elicit any further effect on HRV parameters related to autonomic modulation. Therefore, they suggested that the physical demands have a major influence on the observed ANS changes whereas the influence of the mental load is insignificant while our study, with a heavier physical task, rejects

their hypothesis. A mental load as such influences autonomic cardiac modulation, even in combination with a simultaneous physical task.

Mental stress decreased HF power of heartbeat interval time series as already mentioned in Zhong et al [415] and Hjortskov et al [158]. The shift towards a slightly higher instantaneous HF frequency during MT can probably be related to a higher respiration frequency as the main peak in the HF band is normally caused by respiration [352, 290]. An increased respiration frequency during a 1h low-grade mental stress task in healthy subjects was already found in Nilsen et al [256]. Also Vlemincx et al [384] reported an increased breathing rate during mental stress, although Bernardi et al [42] observed oppositely a slowing respiration frequency.

The results for the condition with the physical task only vary in time with values between those of rest and mental load in the beginning, but exceeding those of the combined task in the last 2 minutes. This indicates the fatiguing process of the body during the physical performance. In particular, the LF/HF ratio is increasing monotonously during PT (Figure 5.6), indicating the fast increase in sympathetic dominance caused by the heavy physical task. Evolutions in time were also observed within other conditions. Mean RR interval increased significantly within rest phase ($p = 0.02$) and during mental load ($p = 0.01$), indicating a decreasing HR, respectively because people are recuperating after a mental or physical load and because they become more familiar with the mental task [184]. In both cases, we hypothesize that this HR decrease was caused by the relaxation process. Concerning the HR in the combined task, the opposite effect of the mental (lower HR in time) and physical (higher HR in time) task counteracts, leading to a small decrease. This observation suggests the hypothesis that the familiarization to the mental stressor has a bigger impact on heart rate control than the exhaustion by the physical task. With respect to the sympathovagal balance, there is a decrease during rest, but an increase during both phases with mental load ($p = 0.05$) showing that the vagal pathways of ANS became relatively a bit more active in rest while the sympathetic modulation gained importance in case of mental stress.

Seong et al [334] reported a steep increase in LF/HF in the beginning and at the end of a mental task, which can also be observed here (Figure 5.6). Another recent study [187] found that HRV patterns showed significantly decreased variances in highly stressed subjects, indicating somewhat disturbed ANS rhythms under the influence of stress. Consequently, sympathetic predominance and vagal withdrawal might represent the autonomic counterpart of the complex psychophysiological changes underlying the increase in cardiovascular risk associated with stress [214, 257].

5.4.2 Link between physiological results and self scores

As the subjects were less happy, more tensed and less relaxed during the active conditions compared to rest, the different active tasks brought the participants into another emotional state. The fact that the subjects revealed to feel more tensed during PT compared to MT is probably due to the interpretation of tension as physical tension. MT and MPT being not significantly different with respect to the tension level confirmed this idea. Because of the mental distraction, the perception of tension due to the physical task is reduced. Despite the marked difference in several HRV parameters between the active conditions, this was not visible in the self rating scores. Therefore, even if subjects do not indicate a difference in stress level, often there are changes in physiology which can be observed via amongst others heart rate variability.

5.4.3 Advantages and limitations

ECG, and consequently the tachogram, can be monitored easily and cheaply. In addition, calculating HRV parameters is at low computational cost making the findings of this study useful in daily life. However, two limitations of the study have to be noticed. First, not all conditions are equal in length causing problems in calculating one value for each HRV parameter in each condition. Concerning the frequency domain parameters, this was solved by applying time-frequency analysis leading to a more detailed study how those parameters change over time. Second, respiration was not monitored although the effect of breathing can be considered minimal. As the mental stimuli did not disappear at fixed interval, synchronization could be prevented. Therefore, new measurements are being recorded solving both remarks. In the new study, respiration will be monitored to include breathing information and its inherent influence on HRV. Moreover, the heavy 45°shoulder abduction as physical task will be replaced by a clicking task with a computer mouse to focus more on job stress in an office environment.

5.5 Conclusion

This study showed clearly that heart rate variability (HRV) is a very useful and inexpensive tool to detect mental and physical stress. We were able to distinguish between rest, physical and mental load by combining different HRV characteristics. The addition of a mental load to a physical task did elicit any further effect on HRV parameters related to autonomic cardiac modulation.

Chapter 6

Impact of weightlessness in space on cardiac autonomic regulation

All HRV parameters in a healthy population were considered in Chapter 4 with a focus on the nonlinear ones and their day-night variations, gender differences and changes over age categories. In this chapter, the same techniques are used, but applied on data of astronauts before and after a space mission. Some background information and the goal to examine the effect of weightlessness on the cardiac regulation mechanism is described in Section 6.1. The data set and signal analysis is presented in Section 6.2. Section 6.3 describes the results. How the HRV parameters changed early post-flight and whether a recovery took place is dicussed in Section 6.4. Finally, the main conclusions are summarized in Section 6.5.

6.1 Introduction

In astronauts, the human cardiovascular control system is disturbed by microgravity. The transition from weightlessness in space to normal gravity on Earth causes post-flight a decrease in blood and stroke volume and a cardiac and vascular remodelling to maintain blood pressure (Figure 6.1). The overall result of these physiological adaptations is a reduction in cardiac output and vasoconstrictor reserve, the two main contributors to orthostatic intolerance after spaceflight [121]. Although many astronauts are not suffering after spaceflight, their heart rate (HR) and autonomic nervous system (ANS) are not completely recovered the first days

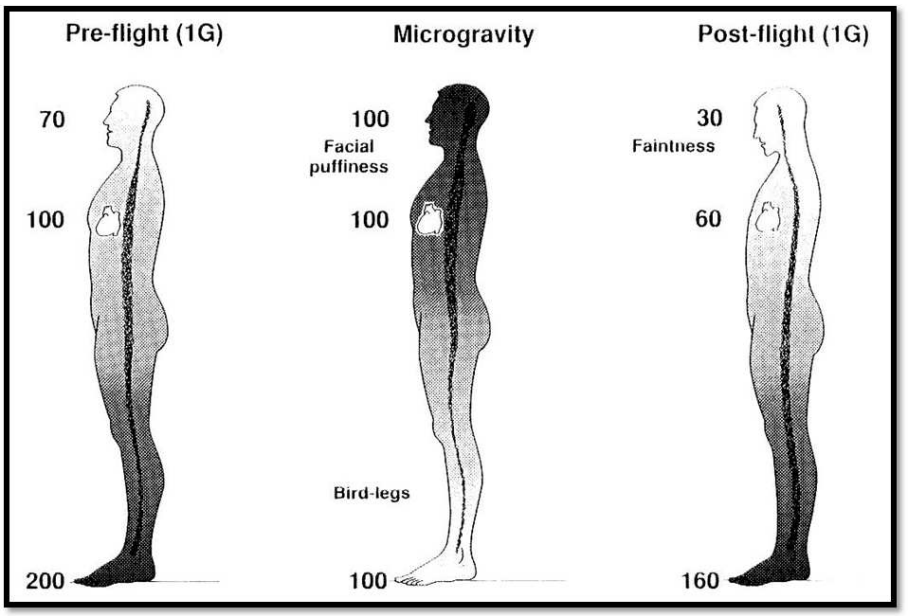


Figure 6.1: *Expected distributions of tissue fluid (shading) and mean arterial pressure (numerical values in mmHg) at head, heart and feet during preflight standing posture on Earth (left), microgravity (middle) and postflight on Earth (right). During microgravity, all gravitational blood pressure gradients disappear. From [152].*

after returning, lasting between 5 days [36] and 25 days [380] according to the literature. The ANS affects heart rate by a continuous interaction between the sympathetic and parasympathetic branch.

Post-flight changes in HR and HRV have been frequently studied by linear parameters. Often, a sympathetic dominance after spaceflight is reported due to a reduced vagal modulation [36, 21]. To the best of our knowledge, nonlinear analysis was only applied in two previous studies, both using approximate entropy as measure [35, 136]. No significant change after spaceflight was found compared to pre-flight. Nevertheless, we expect that changes in autonomic heart rate control are not only reflected in linear HRV parameters, but also in the more subtle nonlinear parameters. In particular, we hypothesize a reduction of the nonlinear parameter values shortly after spaceflight, increasing afterwards towards the pre-flight values. The goal of this study is to investigate how all parts of the autonomic nervous system are influenced when astronauts return on Earth after spaceflight and how it recovers afterwards. We specifically focus on the change in cardiovascular dynamics induced by microgravity by applying many nonlinear HRV parameters. Additionally, day and night periods are examined separately.

6.2 Methods

6.2.1 Subjects

8 male astronauts (age: 43.2 ± 4.4 years, length: 1.79 ± 0.04 m, mass: 76.0 ± 12.4 kg, BMI: 23.7 ± 3.7 kg/m^2) who went to the International Space Station (ISS) participated in the study. Five were in space for a long term mission of 6 months while the other 3 were in space for 10 days during the Odissea-, Cervantes- and Delta missions. Each astronaut was measured at three different time moments, namely pre-flight (L-30), early post-flight (R+5) and late post-flight (R+30). No fixed time schedule was imposed to the astronauts due to several obligations before launch and after landing.

The experiment protocol was approved in advance by the local ethical committee and the ESA Medical Board. Each subject provided written informed consent before participating. The study complies with the Declaration of Helsinki.

6.2.2 Data collection and preprocessing

Twenty-four hour ECG recordings were obtained using Holter monitoring (ELA Medical, LCC Plymouth, MN, USA) with a sample rate of 200Hz on a PC based platform. Although the measurements were done over 24h, 2 blocks of 2 hours (one for day and one for night) were selected manually to meet the following criteria: (1) no baseline trends, (2) no measurement discontinuities, (3) no movement artefacts and finally (4) stationary and high quality ECG signal with clear R peaks. As no activity log was available, this selection based on visual inspection of RR interval trends, was used to exclude periods of physical exercise or other stressful conditions which might affect our results. Equal data length for day and night period as well as for all astronauts was guaranteed this way to extract consistent and reliable HRV parameters. Each heart beat was automatically annotated by the SyneTec software delivered with the Holter system: N = normal, A = artifact, C = calibration and V = premature ventricular beats. For each recording, a file containing the consecutive RR intervals with corresponding annotations was exported and checked manually. Extra ventricular beats were replaced by a 20%-filter, meaning that every RR interval that differ more than 20% of the previous one, is replaced by an interpolated value with weighted interpolation methods.

6.2.3 HRV analysis

All standard HRV parameters are calculated in agreement with the standards of measurement proposed by the Task Force of the European Society of Cardiology

and the North American Society of Pacing and Electrophysiology [355]. As time domain measures, we calculated mean RR, SDNN, SDANN, RMSSD and pNN50. After resampling the tachogram at 4 Hz [343] with the use of a cubic spline approximation [18], power spectra were obtained by using the Welch method. The direct current component was removed by subtracting the mean value of the data set. A sliding Hamming window of 1024 points (corresponding to 256 s) with 50% overlap was used. As frequency domain measures, TP, LF, HF, LFnu, HFnu and LF/HF were calculated.

Because nonlinear HRV techniques have not been standardized as much as the linear ones [355], most commonly used nonlinear parameters were computed. Often used parameters which study the scaling of the system are $1/f$ slope, fractal dimension (FD) and detrended fluctuation analysis (DFA α_1 & α_2). In order to address the complexity of the signals, sample entropy (SampEn), correlation dimension (CD) and maximal Lyapunov exponents (LE) are calculated.

6.2.4 Statistical analysis

Statistical analysis was performed with SPSS Windows version 16.0 (Scientific Packages for social Sciences, Chicago, IL, USA). Advice about the correct test statistics was given by the Biostatistical and Statistical Bioinformatics Centre in Leuven. To compare, for each HRV parameter, between the different time moments, the nonparametric Friedman test was obtained with a multiple comparison afterwards. The nonparametric Wilcoxon Signed Rank test was used to investigate the day-night differences. The two-tailed Pearson Correlation Coefficient r was calculated to examine the similarity between the HRV parameters.

Results of different parameters relating to the same aspect of autonomic heart rate modulation, are combined in one group via the Repeated Measures Multivariate ANOVA. Therefore, all values are transferred to z-scores, obtained by subtracting the mean value and dividing by the standard deviation over all signals. In particular, TP and SDNN are grouped to describe the total variability in general while RMSSD, pNN50 and HF on one hand and LF/HF and LF (n.u.) on the other hand represent respectively vagal modulation and sympathovagal balance. With respect to the nonlinear HRV parameters, the model assessing the scaling behaviour of the ANS consists of $1/f$ slope, FD and DFA α_1 & α_2, while SampEn, CD and LE are grouped to reflect the cardiac complexity. This test statistic offers a solid testing method to determine whether the weightlessness had a significant influence on a certain group of parameters and therefore on a specific part of the ANS. The P value was obtained by the Wilks' Lambda test statistic.

In general, $P < 0.05$ was considered statistically significant.

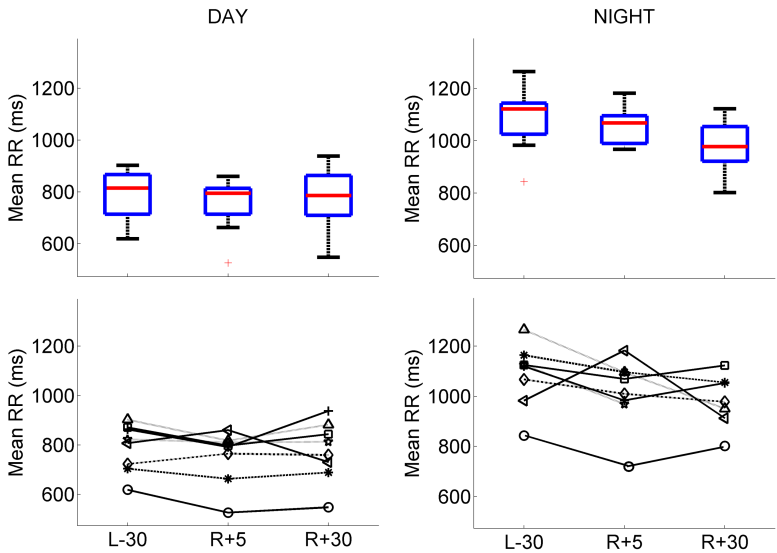


Figure 6.2: *Mean RRI at pre-flight (L-30), early post- (R+5) and late post- (R+30) flight during day (left) and night periods (right), over all subjects via boxplots (top) and individually (bottom).*

6.3 Results

An overview of the results averaged over all astronauts, expressed in mean ± standard deviation, is given in Table 6.1. As no remarkable difference was found between astronauts from short and long term space missions, no distinction is made. More detailed information about the mean RR intervals is shown in Figure 6.2, indicating the time evolution for the complete study population as well as on an individual level.

6.3.1 Day-night variation

As expected, heart rate was significantly higher during daytime than at night (Table 6.1 & Figure 6.2). The differences between day and night were reproduced for most parameters, with significantly higher values during the night for all time domain measures. Also TP and LF increased significantly during the night as well as HF due to the respiratory sinus arrhythmia (RSA), while LF/HF decreased. All nonlinear parameters, except for DFA α_1 and FD, showed different values

between day and night recordings; however, these differences were statistically not significant at each measurement moment.

6.3.2 Linear HRV parameters

Although heart rate was no longer affected at R+5 (Figure 6.2), many linear HRV parameters showed statistically significant changes 5 days after spaceflight compared to pre-flight. During day time, SDNN, RMSSD, pNN50, TP and LF were significantly decreased early post-flight compared to the pre-flight values while at night this was only valid for RMSSD and pNN50 and additionally for HF, LF/HF, LF (n.u.) and HF (n.u.) (Table 6.1). Figure 6.3 shows the time evolution for several linear HRV parameters, averaged over the complete population and clustered in groups based on its physiological meaning. Note that the distribution of z-scores on the Y-axis was set over a fixed range which enables the reader to see more reliably the time evolution and the day-night variations. All parameters belonging to the same group indicated a similar evolution. Microgravity caused a fall in the total variability (TP, SDNN) although only significant during day ($p = 0.007$). While indices of vagal modulation decreased significantly (day: $p = 0.004$, night: $p = 0.011$) at early post-flight, the sympathovagal balance decreased slightly during daytime ($p = 0.328$), but increased strongly ($p = 0.010$) at night 5 days after returning to Earth. All these effects seemed to have disappeared 30 days after return (R+30).

6.3.3 Nonlinear HRV parameters

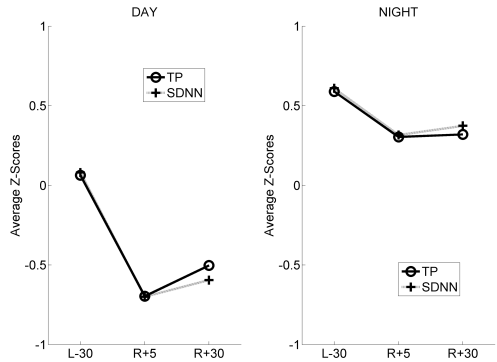
The results of the nonlinear parameters were less consistent compared to the linear ones. During daytime, there was only a statistically significant decrease from pre- (L-30) to early post-flight (R+5) for FD ($p = 0.036$), SampEn ($p = 0.012$) and LE ($p = 0.013$) and a significant increase of CD ($p = 0.025$). For night recordings a statistically significant increase in DFA α_1 ($p = 0.028$) was noted as well as a nearly significant decrease of SampEn ($p = 0.063$) and LE ($p = 0.091$). At R+30, none of these parameters were still significantly different from the corresponding one at L-30. The nonlinear parameters were also grouped in either scaling behaviour or complexity measures as shown in Figure 6.4 by means of z-scores. In general, the nonlinear parameters did not show a clear alignment or time evolution.

6.3.4 Correlation coefficients

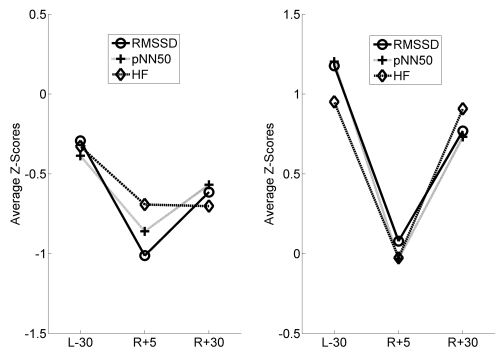
Finally, the similarity between the different HRV parameters was studied. A lot of significantly large r values were found, but here, only the most significant results

Table 6.1: *Overview of all linear and nonlinear HRV parameters, expressed in mean ± standard deviation, at pre flight (L–30), early post flight (R+5) and late post flight (R+30), both for day and night time separately. Statistical analysis between day and night is obtained by the nonparametric Wilcoxon Signed Rank test while the Friedman test followed by a multiple comparison was used to examine the changes from pre to post flight (*). $P < 0.05$ was considered statistically significant and indicated in bold.*

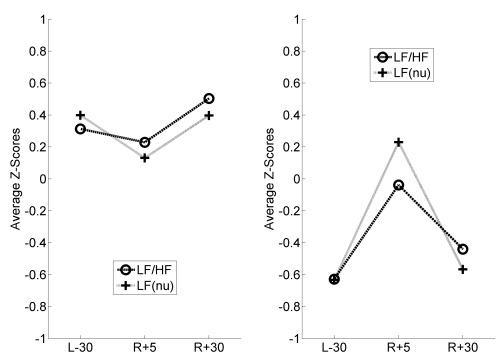
	L − 30			R + 5			R + 30		
	Day	Night	P	Day	Night	P	Day	Night	P
Mean RR [ms]	789.4 ± 98.0	1086.4 ± 126.5	**0.012**	754.1 ± 108.2	1057.6 ± 75.7	**0.011**	775.7 ± 122.7	981.9 ± 106.7 *	**0.012**
SDNN [ms]	83.0 ± 20.3	94.5 ± 13.6	0.161	66.1 ± 18.1 *	88.1 ± 23.5	**0.025**	68.3 ± 26.1	89.3 ± 14.2	**0.036**
SDANN [ms]	46.6 ± 12.6	38.9 ± 10.9	0.327	37.9 ± 9.6	35.9 ± 13.7	0.401	39.4 ± 23.6	37.8 ± 12.0	0.797
RMSSD [ms]	33.5 ± 7.0	50.7 ± 6.7	**0.017**	25.1 ± 6.4 *	37.8 ± 9.3 *	**0.012**	29.7 ± 5.2	45.9 ± 11.4	**0.012**
pNN50 [%]	10.1 ± 5.7	25.8 ± 6.3	**0.010**	5.4 ± 4.5 *	13.6 ± 8.5 *	**0.012**	8.3 ± 5.0	21.1 ± 10.8	**0.010**
TP [ms^2]	5987 ± 2700	7493 ± 2045	0.208	3806 ± 2202 *	6673 ± 3335	**0.017**	4359 ± 3529	6720 ± 1794	**0.036**
VLF [ms^2]	2390 ± 1171	3895 ± 1170	**0.025**	1566 ± 956 *	3792 ± 2423	**0.017**	1651 ± 1185	3334 ± 804	**0.012**
LF [ms^2]	1501 ± 992	1747± 940	0.484	912 ± 795 *	1436 ± 579	**0.017**	1142 ± 766	1598 ± 682	**0.017**
HF [ms^2]	304.9 ± 161.9	666.5 ± 157.7	**0.012**	202.2 ± 128.2	390.3 ± 203.5 *	**0.011**	199.3 ± 70.3	654.4 ± 430.3	**0.012**
LFnu [%]	80.8 ± 7.3	69.8 ± 9.7	**0.036**	77.9 ± 11.8	79.0 ± 5.8 *	0.889	80.8 ± 10.5	70.5 ± 13.8	**0.012**
HFnu [%]	19.2 ± 7.3	30.2 ± 9.7	**0.036**	22.1 ± 11.8	21.0 ± 5.8 *	0.889	19.2 ± 10.5	29.5 ± 13.8	**0.012**
LF/HF	5.0 ± 2.5	2.7 ± 1.4	**0.036**	4.8 ± 2.9	4.1 ± 1.7 *	0.575	5.5 ± 3.1	3.2 ± 2.0	**0.010**
$1/f$	-0.779 ± 0.359	-1.590 ± 0.317	**0.010**	-0.859 ± 0.391	-1.567 ± 0.424	**0.012**	-0.762 ± 0.274	-1.338 ± 0.413	**0.017**
DFA α_1	1.376 ± 0.218	1.249 ± 0.139	0.093	1.382 ± 0.222	1.393 ± 0.056 *	0.889	1.347 ± 0.324	1.264 ± 0.199	0.161
DFA α_2	0.963 ± 0.083	1.041 ± 0.152	0.176	0.961 ± 0.128	1.087 ± 0.158	0.093	0.932 ± 0.028	1.060 ± 0.072	**0.017**
FD	1.769 ± 0.065	1.753 ± 0.028	0.161	1.716 ±0.050 *	1.741 ± 0.058	0.068	1.734 ± 0.036	1.749 ± 0.034	0.484
CD	2.745 ± 0.212	2.666 ± 0.084	0.401	2.915 ± 0.200 *	2.712 ± 0.092	**0.012**	2.914 ± 0.341	2.685 ± 0.279	**0.025**
SampEn	2.887 ± 0.256	3.387 ± 0.136	**0.012**	2.546 ± 0.249 *	3.049 ± 0.295	**0.011**	2.827 ± 0.157	3.178 ± 0.203	**0.017**
LE	0.449 ± 0.133	0.584 ± 0.124	**0.036**	0.338 ± 0.157 *	0.400 ± 0.143	0.208	0.383 ± 0.113	0.576 ± 0.311	0.123



(a)

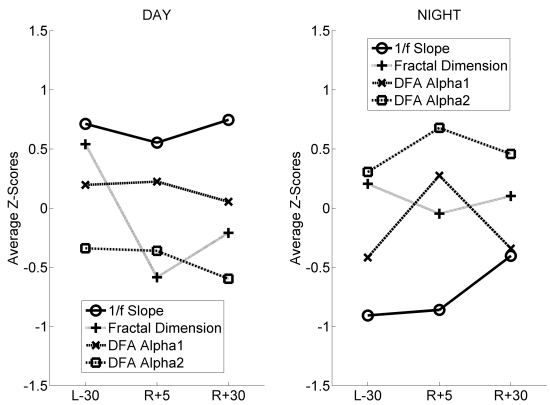


(b)

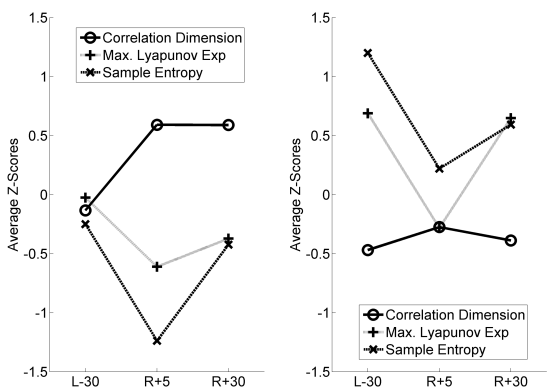


(c)

Figure 6.3: *Average z-scores over pre- (L-30), early post- (R+5) and late post- (R+30) flight for the individual HRV parameters related to (a) total variability, (b) vagal modulation and (c) sympathovagal balance during day (left) and night periods (right). Abbreviations: see Methods*



(a)



(b)

Figure 6.4: *Average z-scores over pre- (L-30), early post- (R+5) and late post- (R+30) flight for the individual HRV parameters related to (a) scaling behaviour and (b) complexity during day (left) and night periods (right). Abbreviations: see Methods*

($r > 0.5$ and $p < 0.001$) are summarized in Table 6.2 for further consideration. The parameters which are known to express vagal modulation, namely HF, pNN50 and RMSSD, were strongly correlated ($0.973 > r > 0.893$) but also LE and SampEn seemed to join this group ($0.973 > r > 0.718$). Sympathovagal balance parameters LF/HF and LF(n.u.) were clearly related with each other ($r = 0.887$) and both with DFA α_1 as well ($r = 0.781$ & 0.881). These findings were also visible in the corresponding figures. For the nonlinear parameters, correlations between CD and LE, SampEn and $1/f$ and between DFA α_2 and $1/f$ were found with correlation coefficients r of respectively -0.503, -0.512 and -0.774. The strong correlations (r > 0.981) between TP and SDNN on one hand and between LF(n.u.) and HF(n.u.) on the other hand were expected, due to their mathematical connection.

6.4 Discussion

In this study, the autonomic modulation of heart rate was examined in 8 astronauts before and after spaceflight. While most studies in the past used short time measurements of 5 or 10 minutes, here 24h Holter recordings were monitored. Firstly, this enabled us to study the ANS changes due to microgravity separately during day and night period which is very important as the cardiovascular system is controlled differently by the ANS in both periods [222, 346]. The results showed clearly that the regulation of heart rate was still influenced after 5 days of recovery, however not in a similar way for day and night time. Secondly, nonlinear HRV methods were applied. Significant changes were found early post-flight compared to pre-flight, indicating that also the nonlinear characteristics of cardiac modulation were influenced by microgravity.

6.4.1 Autonomic modulation early post-flight affected differently during day and night time: linear HRV

The heart rate only increased slightly at early post-flight compared to preflight. Probably, heart rate was much higher the first days after landing [380, 131], but the tachycardia response mostly disappeared at R+5. Although heart rate seemed already restored 5 days after returning on Earth, we still observed significant changes in heart rate modulation. During day time, vagal modulation (RMSSD, pNN50, HF) dropped significantly while the sympathovagal balance (LF/HF, LFnu) did not change compared to preflight, which means that also sympathetic modulation dropped as much as vagal modulation did. A decrease in sympathetic modulation can also be observed via a significant fall in LF power early post-flight compared to the pre-flight condition. This reduced activity of the sympathetic pathways is at odds with many studies describing the sympathetic dominance after spaceflight. The haemodynamic instable situation during day time can be

Table 6.2: *Overview of the strongest Pearson correlation coefficients r between all described HRV parameters. Only correlations $r > 0.5$ with significance $p < 0.001$ are given.*

	$1 > \|r\| > 0.9$	$0.9 > \|r\| > 0.75$	$0.75 > \|r\| > 0.5$
Mean RR			SDNN, RMSSD, VLF, HF, $1/f$, CD, SampEn
SDNN	TP, VLF	LF, CD	Mean RR, SDANN, RMSSD, pNN50, HF, SampEn, LE
SDANN			SDNN, TP, LF
RMSSD	pNN50, HF	SampEn, LE	Mean RR, SDNN, TP, VLF, LF, CD
pNN50	RMSSD	HF, SampEn, LE	SDNN, TP, VLF, LFnu, HFnu
TP	SDNN, VLF	LF	SDANN, RMSSD, pNN50, HF, CD, SampEn, LE
VLF	SDNN, TP		Mean RR, RMSSD, pNN50, LF, HF, DFA α_2, CD, SampEn
LF		SDNN, TP	SDANN, RMSSD, VLF, FD, CD, LE
HF	RMSSD	pNN50, LE	Mean RR, SDNN, TP, VLF, LFnu, HFnu, CD, SampEn
LFnu	HFnu	LF/HF, DFA α_1	pNN50, HF
HFnu	LFnu	LF/HF, DFA α_1	pNN50, HF
LF/HF		LFnu, HFnu, DFA α_1	$1/f$
$1/f$		DFA 2, SampEn	Mean RR, LF/HF
DFA α_1		LF/HF, LFnu, HFnu	
DFA α_2		$1/f$	VLF
FD			LF
CD		SDNN	Mean RR, RMSSD, TP, VLF, LF, HF, LE
SampEn		RMSSD, pNN50	Mean RR, SDNN, TP, VLF, HF, $1/f$
LE		RMSSD, pNN50, HF	SDNN, TP, LF, CD

a possible explanation. Even by manually selecting the data, external influences still occurred as well as changing postures, being inherent in Holter recording. Early post-flight, the day schedule was very tight, possibly leading to mental stress which can influence the measurements. During night time, we found early post-flight an excessive decrease in vagal modulation, but instead of an approximately equal sympathovagal balance as noted during day, at night there is a significant increase in LF/HF and LFnu compared to pre-flight. This means that sympathetic modulation of heart rate became relatively more important at R+5 when sleeping at night. Norsk et al [258] suggested that the sympathetic dominance after spaceflight might result from a decreased stroke volume and cardiac output due to gravity on Earth. Beckers et al [36] observed changes in heart rate modulation and baroreflex sensitivity (BRS) early postflight and linked them with a postural reduction in pulse pressure (PP). This suggests thoracic hypovolemia early post-flight, requiring an increased heart rate and sympathetic drive to maintain orthostatic blood pressure. According to our results, the findings of these previous studies are confirmed, but only during night. Moreover, the significant day-night variation in LF/HF, LFnu and HFnu pre-flight was disappeared early post-flight, being again present late post-flight. None of those studies used 24h monitoring, although in the best case, astronauts were measured for 10' in supine and standing position, causing only a profound effect on HRV after spaceflight in the standing position [36]. Nevertheless, our study showed as well during day (∼standing) as during night (∼supine) time significant changes in cardiac control.

6.4.2 Long-term recovery of linear HRV parameters

Although symptoms of reduced orthostatic tolerance disappear rather quickly after return from microgravity conditions, the cardiovascular control system might recover much slower. Despite the unknown duration of recovery, most studies have only performed a follow-up of maximum 1 week [83, 342] while just a few studies did measurements up to 18 days. Recently we showed already that 25 days of recovery after short duration space flight is sufficient to restore vagal-cardiac outflow to pre-flight conditions [380]. Here, at R+30, none of the described HRV parameters was still significantly different from the pre-flight values. There seems to be an almost complete recovery. Especially at night, the strong differences in vagal modulation and sympathovagal balance early post-flight compared to pre-flight, were totally annulled late post-flight. During day time, vagal modulation restored clearly, however not completely to the initial pre-flight values. It may indicate that the vagal recovery still persists, even one month after return on Earth. Although a recent study [2] showed no significant differences at all in cardiovascular control in supine position and even a restored vagal modulation in standing position 4 days after returning, this study proved that the autonomic recovery in astronauts lasts much longer. This slow (mostly vagal) recovery after return to Earth was

also found by others after short [120] and long [21, 77] term space missions. This recovery period seems not to be related strongly by the duration of the spaceflight as no remarkable differences could be found between astronauts from short and long term space missions.

6.4.3 Effect of microgravity on nonlinear dynamics of autonomic modulation

The influence of microgravity on nonlinear heart rate dynamics in astronauts was investigated for the first time in 1994 by Goldberger et al [136], using approximate entropy as complexity measure and $1/f$ slope as spectral scaling measure. Both parameters did not change over time, concluding that HR dynamics appear remarkably stable during long-term spaceflight. Afterwards, to the best of our knowledge, only one study [35] applied nonlinear HRV techniques (again approximate entropy).

This study applied a series of nonlinear techniques, reflecting scaling behavior and complexity of the underlying autonomic nervous system. Instead of approximate entropy, sample entropy (SampEn) is used as it is not sensitive to the data length [299]. We found both during day and night time a strong decrease in SampEn at early post-flight compared to pre-flight condition (Fig. 6.4(b)), although only statistically significant during day. At both time moments, 1 out of 8 astronauts showed an opposite reaction (increase) causing the restricted significance. Contrarily, Beckers et al [35] only found a very soft decrease in ApEn at R+1 in standing (0.78 to 0.76) and supine (0.98 to 0.90) position, but certainly not statistically significant. Here, also other nonlinear parameters showed a significant change after 5 days of recovery compared to pre-flight, proving that also the nonlinear HR dynamics are affected by microgravity in space. Particularly the complexity measures (SampEn, CD and LE) changed drastically early post-flight, which were more pronounced during the day than the night. While SampEn and LE were significantly decreased, CD increased. Concerning the scaling behavior measures, they did not show any consistent alignment and were in general rather stable over time, except for a significant drop in FD at day time and a significant rise of DFA α_1 at night. We suggest that nonlinear HRV parameters, and in particular the complexity measures, are more sensitive during day than night time. All nonlinear parameters that were statistically significantly different after 5 days of recovery evolved afterwards towards the pre-flight values, except CD. One month after retuning to Earth, the nonlinear dynamics of heart rate control was restored, acting again as in normal conditions. Consequently, our hypothesis was mainly confirmed by the nonlinear results.

Nonlinear HRV parameters give additional information about the nonlinear dynamics in the cardiovascular system which can not be reflected by standard HRV

analysis. It is important to note that nonlinear HRV techniques will not replace linear analysis, but have to be considered as a completion, yielding information about a specific aspect of scaling behavior or complexity. Therefore, clustering the nonlinear parameters in groups is probably not the best choice, but we have to interpret them all separately. Nonlinear techniques have the advantage over linear techniques in providing better repeatability and reliability across measurements (small random error) [218]. Therefore, nonlinear indices may be more suitable for diagnostic purposes, as well as for assessing individual treatment effects. Nowadays, the meaning of the indices used for nonlinear system dynamics is not as clear as those derived from time or frequency domain methods. Moreover, spectral analysis is also superior in visualizing the results. Future research will need to focus on determining clear physiological interpretations for all indices. Some physiological relations are already given by Beckers et al [34] and Aubert et al [19].

6.4.4 Similarity between HRV parameters

LE and SampEn were highly correlated with vagal modulation while DFA α_1 was clearly related with sympathovagal balance, confirming the findings in previous studies by Beckers et al [34] and Tulppo et al [369]. In addition, it indicates that especially vagal modulation has not only a linear but also nonlinear behaviour. A previous study [41] showed that VLF contributed importantly to the nonlinear behaviour of autonomic heart rate control which is confirmed partly in our study via the correlations with DFA α_2, CD and SampEn.

6.4.5 Limitations

The number of subjects available in spaceflight experiments is very limited, especially in the post-Columbia accident era with less manned space missions. However, having data of 8 astronauts with completed measurements at three time moments is more than most similar previous studies [36, 380, 136, 131, 258, 77], resulting in more reliable conclusions on group level. Although we have imposed standardization of experimental procedures between the different space missions, we cannot control differences in workload between these missions, nor the quantity and quality of sleep. Personal exercise tasks, fluid intake and nutrition before, during and after space flight could not be controlled. As no Holter data were available at R+1, we could not make any statement about the cardiovascular adaptation immediately after spaceflight. Therefore, we restrict our results and conclusions to the time period from 5 till 30 days after returning to Earth.

6.5 Conclusion

The influence of microgravity on cardiovascular control was confirmed in this study, however no remarkable difference was found between astronauts from short and long duration spaceflights. While the vagal modulation decreased significantly during day and night at early post-flight, the sympathovagal balance decreased slightly during day time, but increased strongly at night. Therefore, our results confirmed the sympathetic dominance early post-flight, but only at night. This study also proved the change in nonlinear heart rate dynamics, still present after 5 days upon return to Earth and more expressed in the day period. Therefore, nonlinear HRV seems to be more sensitive during day than night time. Those nonlinear HRV parameters will not replace linear analysis, but have to be considered as a completion, yielding extra information about a specific aspect of scaling behaviour or complexity of the underlying cardiovascular system. After one month, a complete cardiovascular recovery was found.

Chapter 7

Nonlinear dynamics in cardiovascular control during head-down bed rest

Whereas in the previous chapter HRV was applied on data of astronauts, Chapter 7 examines the effect of microgravity on the global cardiovascular system in a head-down bed rest study. Section 7.1 introduces the use of HDBR as a simulated microgravity environment and explains the traditional Chinsese medicine. The study design, data collection and processing, including the statistical analysis, are presented in Section 7.2. The results of cardiac control, blood pressure variability and baroreflex sensitivity are described in Section 7.3 and discussed in Section 7.4. Not only the effect of HDBR on linear and nonlinear cardiovascular control is reflected, but also the role of Chinese herbal medicine as a countermeasure. The most important findings are repeated shortly in Section 7.5.

7.1 Introduction

During space missions, the lack of gravitational stress is associated with an adaptation in cardiovascular structure and neurohumoral control circuits [16, 29, 152, 339, 392, 414]. Because of many limitations related to real human spaceflight such as high cost, limited access, small number of subjects and limited crew time, head-down bed rest (HDBR) is often applied as an alternative to investigate physiological adaptations to microgravity.

During the first hours of HDBR, a shift in body fluids from the lower to the upper part results in an increased thoracic plasma volume [129, 144]. After a few days, a decrease in plasma volume may occur to restore the central blood volume to the initial level [53, 173, 341]. Arterial baroreflex function is chronically unchallenged during HDBR, which may result in decreased baroreflex sensitivity (BRS). Many studies hypothesized that this decreased BRS is caused by deconditioning of the autonomic nervous system (ANS) [341, 162, 366, 304]. However, the exact mechanisms are still poorly understood. How the ANS is deconditioned or influenced by microgravity remains an open question. As the ANS modulates directly the heart rate and indirectly also blood pressure, heart rate variability (HRV) and blood pressure variability (BPV) analysis can be used to study the autonomic modulation mechanism under microgravity conditions. Most studies reported a decrease in total HRV and in high frequency power (HF) reflecting parasympathetic influence at rest. However, no univocity exists when this decrease takes place. While the majority of those studies used linear techniques, only a few studied the nonlinear dynamics of this physiological system [162, 136, 114, 35].

Traditional Chinese medicine has been developed based on theories formulated through millennia of observation and practical experience [185]. It considers that the processes within the human body are interrelated, more specifically in balance (Yin and Yang) and in constant interaction with the environment. From this point of view, diseases are due to an imbalance. One of the most important treatments of traditional Chinese medicine is the application of Chinese herbs which will be coined Chinese herbal medicine (CHM). As a form of non-invasive therapeutic intervention, herbal medicines may contain some biochemical agents and might avoid the toxicity of some chemically composed drugs. The main goal of this study was to investigate how the autonomic modulation mechanism changed during HDBR. Most studies in the past were limited to the linear parameters or even to the pure hemodynamic signals. However, in agreement with Lefebvre et al [201] and Yamamoto & Hughson [404], it seems likely that the cardiovascular system follows some nonlinear pattern which need to be explored further. Therefore, we not only applied linear but also a large set of nonlinear techniques. Parallel investigations of HRV and BPV could provide a better understanding of how nonlinear cardiovascular regulation is adapted during HDBR. We hypothesize that HDBR would decrease some nonlinear HRV and BPV characteristics. As a previous animal microgravity simulation study showed the possibility of CHM as a countermeasure [235], we tested additionally the hypothesis that CHM will improve orthostatic function after HDBR.

7.2 Methods

7.2.1 Subjects and study protocol

In this study, 14 male Chinese healthy volunteers (age: 30 ± 4 y; height: 170 ± 4 cm; weight: 61 ± 4 kg) were enrolled for 60 days head-down bed rest. The subjects were randomly allocated to a control group (n = 7) and a CHM group (n = 7). Subjects in the control group received a placebo, consisting of amylum, saccharine and pigment, during HDBR, while subjects in the CHM group were given Chinese herbal medicine (Tai Kong Yang Xin Prescription) during HDBR. All subjects spent 90 days in the Bed Rest Study Lab in the China Astronaut Training and Research Center (CATRC): 15 days pre test period, 60 days −6 degrees head-down bed rest period and 15 days recovery period. All subjects were in excellent health, without any history of chronic or recent acute illness. None of them participated in regular athletics. On the first day of bed rest, after showering and breakfast, the subjects moved from standing upright to head-down position. During the bed rest the subjects were allowed once a day to use the bathroom for defecation only (about 5 minutes). During their free time subjects could watch TV, listen to music or read books or newspapers. Dietary intake was: 2600 – 2800 kcal/day of which 90 – 100 g/day protein, 85 – 95 g/day fat and 390 – 430 g/day carbohydrate. Medication, smoking, alcohol and caffeine-containing drinks were not allowed during the whole study. The experiment protocol was approved in advance by the Medical Committee of CATRC. Each subject provided written informed consent before participating. The study complies with the Declaration of Helsinki.

7.2.2 Chinese herbal medicine

Tai Kong Yang Xin Prescription, a Chinese herb formulae composed of about 10 Chinese herbs was used in this study as a countermeasure to reduced orthostatic tolerance. The main parts of Tai Kong Yang Xin Prescription are Radix Ginseng (containing saponins), C.A. May and Angelica Sinensis (Oliv.) Diels. It was provided as pills of 6 g and given 3 times a day orally. The formula prescription (patent pending) was developed and provided by CARTC for astronaut use and microgravity simulation study.

7.2.3 Data collection and preprocessing

Data collection was performed before (day −10), during (day 2, 7, 21, 41, 56) and after (day $R + 6$, $R + 12$) bed rest. Recording took place in the morning before 1 p.m. in a temperature-controlled room at 24°C. Subjects were monitored for 10

minutes while resting quietly in the supine position with comfortable uncontrolled respiration. Non-invasive beat-to-beat blood pressure was measured with an infrared finger photoplethysmograph (Finometer Blood Pressure Monitor, TNO-TPD Biomedical Instrumentation, Amsterdam, the Netherlands), using a brachial return to flow-calibration in the supine position before each measurement. The measured signal was analog-to-digital converted at 200 Hz, and stored on a hard-disk for off-line analysis. Systolic and diastolic arterial pressures (SAP and DAP) were derived from the arterial pressure waveform. Mean arterial pressure (MAP) was the true integral of the arterial pressure wave over one beat divided by the corresponding beat interval. Pulse pressure (PP) was defined as the difference between systolic and diastolic pressure. RR interval time series (RRI) were computed from ECG recordings and expressed in ms. Before analyzing the signals, pre processing the data was necessary. Extra ventricular beats were replaced by a 20%-filter, meaning that every RR interval that differs more than 20% of the previous one, is replaced by an interpolated value, defined via spline interpolation over the 5 previous and 5 next intervals. Finally, all data were checked manually.

7.2.4 HRV & BPV analysis

All standard HRV parameters are calculated in agreement with the standards of measurement proposed by the Task Force of the European Society of Cardiology and the North American Society of Pacing and Electrophysiology [355]. As time domain measures, we calculated mean RR, SDNN, RMSSD and pNN50. After resampling the tachogram at 2 Hz [343] with the use of cubic spline approximation [18], power spectra were obtained by using the Welch method. The direct current component was removed by subtracting the mean value of the data set. A sliding Hamming window of 1024 points with 50% overlap was used. The three classical frequency bands were defined: a very low frequency (VLF) band from 0 to 0.04 Hz, a low frequency (LF) band from 0.04 to 0.15 Hz and a high frequency (HF) band from 0.15 to 0.40 Hz, in which the power was expressed in absolute values and in normalized units. Total power was calculated between 0 and 1 Hz. Moreover, a low-to-high frequency power ratio is calculated to reflect the sympathovagal balance. With respect to BPV, the same linear parameters were calculated, except pNN50 was replaced by pNN5, indicating the percentage of BP values that differ more than 5 mmHg from the previous one.

During the 10 minutes baseline recording time-domain analysis of spontaneous baroreflex sensitivity (BRS) was performed using the cross-correlation method [391]. The SAP and RRI time series were resampled at 1 Hz. In a 10-second window, the correlation and regression slope between SAP and RRI were computed. Delays of 0- to 5-second increments in RRI were computed, and the delay with the highest positive coefficient of correlation was selected (Tau). The slope between SAP and RRI was recorded as a BRS estimate if the correlation

was significant at P = 0.01. The number of significant BRS estimates was also calculated and expressed per minute.

Nonlinear parameters do not describe the amount of modulation as such, but are able to describe the scaling and complexity properties of the signal. Often used parameters which study the scaling of the system are $1/f$ slope, fractal dimension (FD) and detrended fluctuation analysis (DFA α_1 & α_2) while the complexity is addressed via sample entropy (SampEn). Also a chaotic signature is calculated by means of the recently developed numerical noise titration technique [286, 285]. All the nonlinear techniques were applied in exactly the same way for RRI and BP time series.

7.2.5 Statistical analysis

Statistical analysis was performed with Matlab R2008a (The MathWorks Inc., Natick, MA, USA). To investigate the evolution over time and the difference between both groups, a 2-way ANOVA analysis was performed on all HRV and BPV parameters with the time sessions (before, during and after bed rest) as within subject factor and the experimental conditions (control group vs. CHM group) as between subject factor. A third p-value is given for the interaction term in the model to assess significant differences between groups across experimental conditions. To compare, for each HRV and BPV parameter, pairwise the different time moments with the baseline value, a post hoc analysis was obtained taking into account the multiple testing problem. Similarly, the nonparametric Mann-Whitney U test was used to evaluate group differences at each time moment. P-values < 0.05 were considered statistically significant.

7.3 Results

All subjects completed the whole study. Baseline characteristics in the two groups are shown in Table 7.1. No significant differences were observed between groups for age, weight, height and BMI, as well as for the hemodynamic data or baroreflex sensitivity parameters. As recently published in a previous study by a co-worker [209], also for body weight and water intake, no change over time throughout the HDBR study was observed in both groups. In contrast to water intake, a significant increase in urine output was observed from day 30 – 45 of HDBR in both experimental groups.

Table 7.1: *Baseline characteristics in CHM and control group, expressed in mean ± standard deviation.*

	Control (n=7)	CHM (n=7)	Significance
Age [y]	30 ± 3	30 ± 6	ns
Weight [kg]	61 ± 3	61 ± 6	ns
Height [cm]	171 ± 3	168 ± 4	ns
BMI [kg/m^2]	21 ± 1	21 ± 2	ns
Hemodynamic data			
HR [bpm]	72 ± 12	70 ± 13	ns
SAP [mmHg]	109 ± 7	116 ± 5	ns
DAP [mmHg]	61 ± 4	67 ± 7	ns
MAP [mmHg]	77 ± 4	82 ± 6	ns
PP [mmHg]	48 ± 5	46 ± 4	ns
Resp. freq. [min^{-1}]	17 ± 3	15 ± 4	ns
Baroreflex sensitivity (BRS)			
Slope [ms/mmHg]	17 ± 11	16 ± 13	ns
Tau [s]	1.6 ± 0.6	1.5 ± 0.7	ns
No. estimates [min^{-1}])	11 ± 3	12 ± 5	ns

BMI (Body Mass Index) = Weight/Height^2 ; HR = heart rate; SAP = systolic arterial pressure; DAP = diastolic arterial pressure; MAP = mean arterial pressure; PP = pulse pressure; Tau = optimal time delay with the highest positive coefficient of correlation; ns = non-significant

7.3.1 Cardiac control

Mean and standard error at each measurement time before, during and after HDBR are plotted, separately for the control and CHM group, for time domain HRV (Figure 7.1), frequency domain HRV (Figure 7.2) and nonlinear HRV parameters (Figure 7.3). The output of the 2-way ANOVA test statistic revealed that, for all parameters, the effect of the within subject factor time and the between subject factor group was not additive, meaning that there is no interaction between time and group. Therefore, the result of the F-test for each factor is correct and can be interpreted now. The p-values for the within subject factor time and the between subject factor group are listed in Table 7.2 for all parameters.

The between subject factor group (control vs. CHM) was statistically significant for mean RR, DFA α_2 and $1/f$. In general (over all time sessions), heart rate and $1/f$ slope were higher in the control group compared to CHM subjects while DFA α_2 showed lower values. Looking to each time moment, especially on day 2 of bed

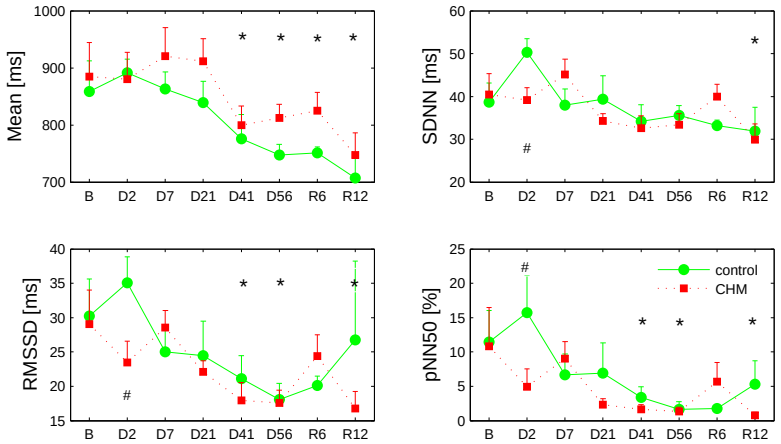


Figure 7.1: *Evolution of the time domain HRV characteristics mean RR, SDNN, rMSSD and pNN50 before (B), during (D) and after (R) head-down bed rest, separately for the CHM (red squares) and the control (green circles) group. Mean and standard error are given. Dx, Rx = the x^{th} day during and after bed rest respectively. * $P < 0.05$ compared to before bed rest; # $P < 0.05$ between groups.*

rest CHM subjects had completely different values for SDNN, RMSSD and pNN50 compared to the control group (see # in figure). Opposite to an increase of these HRV parameters in the control subjects shortly after starting bed rest compared to baseline, the CHM subjects showed decreasing values.

With respect to the change in time (over all 14 participants, see Table 7.3 for all results), the within subject factor was statistically significant for mean RR, SDNN, pNN50, TP, LF and SampEn. Mean RR remained approximately the same till day 21 of HDBR, but dropped significantly from day 41 of HDBR. Even after HDBR, no change to the initial baseline values could be observed. This increased heart rate is more expressed in the control group compared to the CHM group. SDNN and TP (total cardiac variability), LF (mainly sympathetic modulation) and SampEn reflect all the same time evolution, namely an increase at day 2 of HDBR followed by a gradual decrease till day 56 of HDBR. 6 days after HDBR, those parameters increased, although still not reaching the baseline level. However, we can not talk of a recovery since they decreased again at day 12 after HDBR. Vagal modulation (RMSSD, pNN50 and HF, although less pronounced) did not change the first days of HDBR, but declined monotonously from day 7 of HDBR till the end of HDBR, becoming significantly lower than the corresponding baseline value from day 41 of HDBR on. After HDBR, a slow increase started, but even after 12 days, the values were still significantly lower than before HDBR. DFA α_1, reflecting

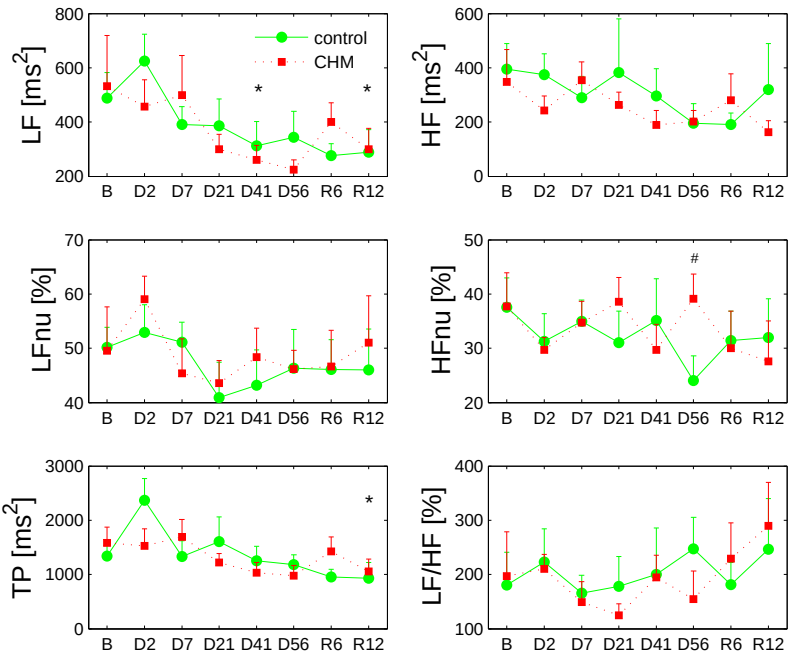


Figure 7.2: *Evolution of the frequency domain HRV characteristics LF power, HF power, LFnu, HFnu, total power (TP) and LF/HF before (B), during (D) and after (R) head-down bed rest, separately for the CHM (red squares) and the control (green circles) group. Mean and standard error are given. Dx, Rx = the x^{th} day during and after bed rest respectively. * $P < 0.05$ compared to before bed rest; # $P < 0.05$ between groups.*

short term correlation, was significantly higher at day 2 of HDBR compared to baseline and remained that high until even 12 days after HDBR. Finally, NLmean and NLdr, both giving information about chaotic behaviour of HR modulation, were drastically lower during HDBR compared to the period before HDBR. While NLmean increased quickly after HDBR to the initial values, NLdr remained low.

7.3.2 Blood pressure variability

Mean and standard error at each measurement time before, during and after HDBR are plotted, separately for the control and CHM group, for time domain BPV (Figure 7.4), frequency domain BPV (Figure 7.5) and nonlinear BPV parameters (Figure 7.6). Analogously to the HRV results above, no interaction

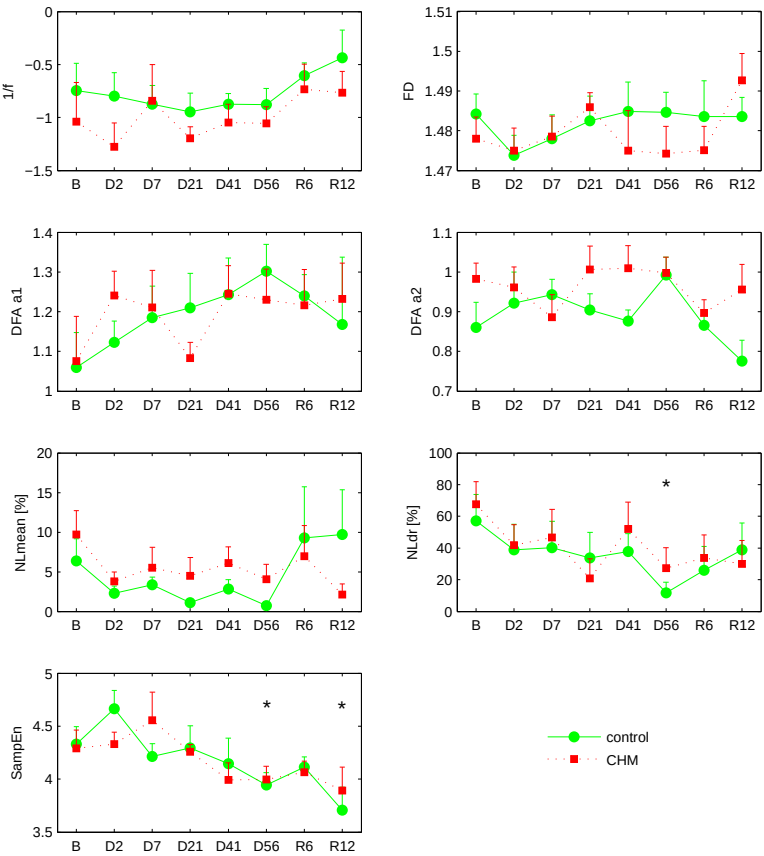


Figure 7.3: *Evolution of the nonlinear HRV characteristics* $1/f$*, FD, DFA* α_1*, DFA* α_2*, NLmean, NLdr and SampEn before (B), during (D) and after (R) head-down bed rest, separately for the CHM (red squares) and the control (green circles) group. Mean and standard error are given. Dx, Rx = the* x^{th} *day during and after bed rest respectively. * P < 0.05 compared to before bed rest; # P < 0.05 between groups.*

Table 7.2: *P-values of 2-way ANOVA applied on all HRV and BPV parameters. $P < 0.05$ was considered statistically significant and is indicated in bold.*

	HRV		BPV	
	Within subj. factor	Between subj. factor	Within subj. factor	Between subj. factor
Mean	**<0.0001**	**0.0247**	**0.0014**	0.6564
SDNN	**0.0060**	0.6699	0.9509	**0.0046**
RMSSD	0.0610	0.2325	0.9854	0.3851
pNN50/5	**0.0082**	0.1837	0.8821	0.0536
LF	**0.0247**	0.7122	0.4607	0.3829
HF	0.6207	0.2928	0.4608	0.3855
LFnu	0.5283	0.5937	0.1638	0.1767
HFnu	0.8438	0.6558	0.9336	**0.0031**
TP	**0.0209**	0.6972	0.4499	0.3539
LF/HF	0.6367	0.7603	0.7228	**<0.0001**
DFA α_1	0.4283	0.9878	0.9194	**<0.0001**
DFA α_2	0.2433	**0.0071**	0.7314	0.2944
$1/f$	0.3136	**0.0425**	0.9255	0.1008
FD	0.5622	0.4155	0.5583	0.9801
SampEn	**0.0013**	0.9701	0.9560	0.2278
NLmean	0.2952	0.5400	0.7141	0.2720
NLdr	0.1454	0.5499	0.7144	0.2361

between the within subject factor time and the between subject factor group was found. Again, the result of the F-test for each factor can be interpreted now and the corresponding p-values are also listed in Table 7.2.

The between subject factor group (control vs. CHM) was statistically significant for SDNN, HFnu, LF/HF and DFA α_1. pNN5 and $1/f$ had a nearly significant factor group. In general (over all time sessions), all these parameters, except HFnu, were higher in the control group compared to the CHM subjects. Some group differences were also found on a specific time moment.

Concerning the change in time (over all 14 participants), the within subject factor was only statistically significant for mean SAP. Systolic arterial pressure was decreasing when HDBR started (baseline: 112 ± 7 mmHg, day 2 of HDBR: 102 ± 9 mmHg; p = 0.02), reaching a minimum on day 7 of HDBR (99 ± 7 mmHg; p = 1.2 E-4 compared to baseline). From day 21 on, SAP was slightly increasing being not anymore significantly lower than baseline level at the end (day 56 of HDBR: 108 ± 14 mmHg; p = 0.17 compared to baseline). After HDBR, SAP first decreased (day 6 after HDBR: 100 ± 5 mmHg; p = 8.5 E-4 compared to baseline)

Table 7.3: *Time evolution of HR and all HRV parameters, expressed by mean ± standard deviation over all 14 subjects. B = before head-down bed rest; Dx, Rx = the x^{th} day respectively during and after head-down bed rest.*

	B	D2	D7	D21	D41	D56	R6	R12
Mean RR [ms]	872 ± 144	886 ± 94	892 ± 109	875 ± 105	788 ± 98 *	780 ± 64 *	788 ± 72 *	727 ± 96 *
SDNN [ms]	39.6 ± 11.9	44.7 ± 9.8	31.5 ± 10.1	36.8 ± 10.7	33.4 ± 8.7	34.5 ± 6.1	36.5 ± 6.7	30.9 ± 12.2 *
RMSSD [ms]	29.6 ± 13.2	29.2 ± 10.6	26.8 ± 8.4	23.3 ± 9.6	19.5 ± 7.8 *	17.8 ± 5.4 *	22.2 ± 6.5	21.7 ± 21.8 *
pNN50 [%]	11.1 ± 13.1	10.3 ± 12.1	7.9 ± 7.2	4.6 ± 8.5	2.5 ± 3.1 *	1.5 ± 2.4 *	3.7 ± 5.5 *	3.0 ± 6.6 *
LF [ms^2]	510 ± 376	541 ± 265	445 ± 293	343 ± 208	287 ± 188 *	284 ± 195	338 ± 162	294 ± 204 *
HF [ms^2]	372 ± 274	308 ± 182	322 ± 189	323 ± 372	243 ± 210	199 ± 149	235 ± 197	241 ± 325
LFnu [%]	49.9 ± 16.1	56.0 ± 12.4	48.3 ± 13.7	42.3 ± 13.9	45.8 ± 15.4	46.2 ± 14.3	46.4 ± 15.5	48.5 ± 20.7
HFnu [%]	37.6 ± 14.8	30.5 ± 10.1	34.8 ± 10.0	34.8 ± 13.7	32.4 ± 16.4	31.6 ± 14.1	30.7 ± 15.7	29.8 ± 18.7
TP [ms^2]	1463 ± 685	1947 ± 1013	1512 ± 798	1414 ± 894	1142 ± 600	1077 ± 488	1190 ± 591	993 ± 666 *
LF/HF [%]	189 ± 183	216 ± 120	158 ± 90	151 ± 110	198 ± 170	201 ± 148	205 ± 142	268 ± 222
DFA α_1	1.07 ± 0.26	1.18 ± 0.16	1.20 ± 0.22	1.15 ± 0.18	1.24 ± 0.21	1.27 ± 0.19	1.23 ± 0.19	1.20 ± 0.35
DFA α_2	0.92 ± 0.15	0.94 ± 0.17	0.91 ± 0.13	0.96 ± 0.14	0.94 ± 0.13	1.00 ± 0.11	0.88 ± 0.08	0.87 ± 0.18
$1/f$	-0.89 ± 0.82	-1.04 ± 0.62	-0.86 ± 0.69	-1.07 ± 0.39	-0.96 ± 0.37	-0.97 ± 0.40	-0.67 ± 0.48	-0.60 ± 0.62
FD	1.48 ± 0.01	1.47 ± 0.01	1.48 ± 0.01	1.48 ± 0.01	1.48 ± 0.02	1.48 ± 0.02	1.48 ± 0.02	1.49 ± 0.02
SampEn	4.31 ± 0.43	4.50 ± 0.41	4.39 ± 0.55	4.28 ± 0.40	4.07 ± 0.53	3.97 ± 0.31 *	4.09 ± 0.25	3.80 ± 0.56 *
NLmean [%]	8.03 ± 7.60	3.03 ± 2.79	4.43 ± 5.10	2.81 ± 4.56	4.46 ± 4.60	2.39 ± 3.86	8.10 ± 13.63	5.92 ± 11.17
NLdr	0.62 ± 0.40	0.40 ± 0.37	0.44 ± 0.44	0.27 ± 0.37	0.45 ± 0.37	0.19 ± 0.27	0.30 ± 0.38	0.34 ± 0.41

* $P < 0.05$ compared to baseline level, calculated via post hoc analysis taking into account the multiple testing problem

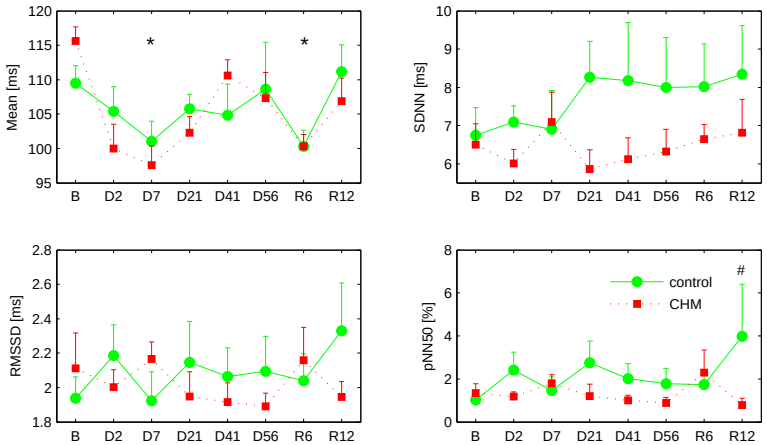


Figure 7.4: *Evolution of the time domain BPV characteristics mean RR, SDNN, rMSSD and pNN50 before (B), during (D) and after (R) head-down bed rest, separately for the CHM (red squares) and the control (green circles) group. Mean and standard error are given. Dx, Rx = the x^{th} day during and after bed rest respectively. * $P < 0.05$ compared to before bed rest; # $P < 0.05$ between groups.*

after which it increased again to the baseline level (baseline: 112 ± 7 mmHg, day 6 after HDBR: 110 ± 9 mmHg; p = 0.72). In contrast to many HRV parameters, BPV parameters did not show a clear time evolution, but fluctuated more or less around the values before HDBR.

7.3.3 Baroreflex sensitivity

These results are obtained by Jiexin Liu and taken from his paper [209]. The results before, during and after HDBR can be seen in Figure 7.7. BRS decreased during HDBR (BRS: from 16.3 ± 11.2 ms/mmHg before HDBR to 9.3 ± 2.9 ms/mmHg at day 56 of HDBR, p = 0.021) and remained suppressed until 12 days of recovery. The number of significant baroreflex estimates per minute decreased at the second day of HDBR (from 11.7 ± 4.3 min^{-1} before HDBR to 9.0 ± 2.4 min^{-1} at day 2, p = 0.014) and then gradually recovered to baseline after 56 days of HDBR.

Figure 7.8 shows the distributions of optimal time delays (Tau: 0 – 5 seconds) in the cardiac baroreflex mechanism (time delay of RRI response to systolic blood pressure change) before during and after HDBR. A shift of Tau towards higher values was observed after 56 days of HDBR in the two groups (p < 0.001 compared

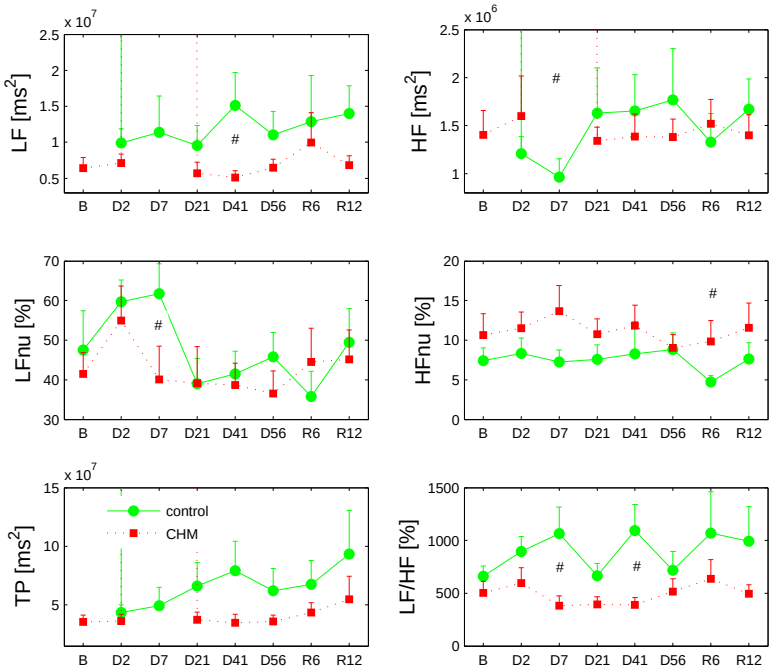


Figure 7.5: *Evolution of the frequency domain BPV characteristics LF power, HF power, LFnu, HFnu, total power (TP) and LF/HF before (B), during (D) and after (R) head-down bed rest, separately for the CHM (red squares) and the control (green circles) group. Mean and standard error are given. Dx, Rx = the x^{th} day during and after bed rest respectively. * $P < 0.05$ compared to before bed rest; # $P < 0.05$ between groups.*

to baseline). In the control group, the increased time delay persisted until day 12 of recovery; however, in the CHM group, a partial recovery occurred from day 56 of HDBR to day 12 of recovery (p = 0.04).

7.4 Discussion

In this study, heart rate and blood pressure modulation was examined in 14 Chinese healthy men before, during and after head-down bed rest. We also tested the hypothesis that Chinese Herbal Medicine acts as a countermeasure. Our main findings are twofold. Firstly, administering Chinese herbs during HDBR did not really change the time evolution of any HRV or BPV parameter, limiting

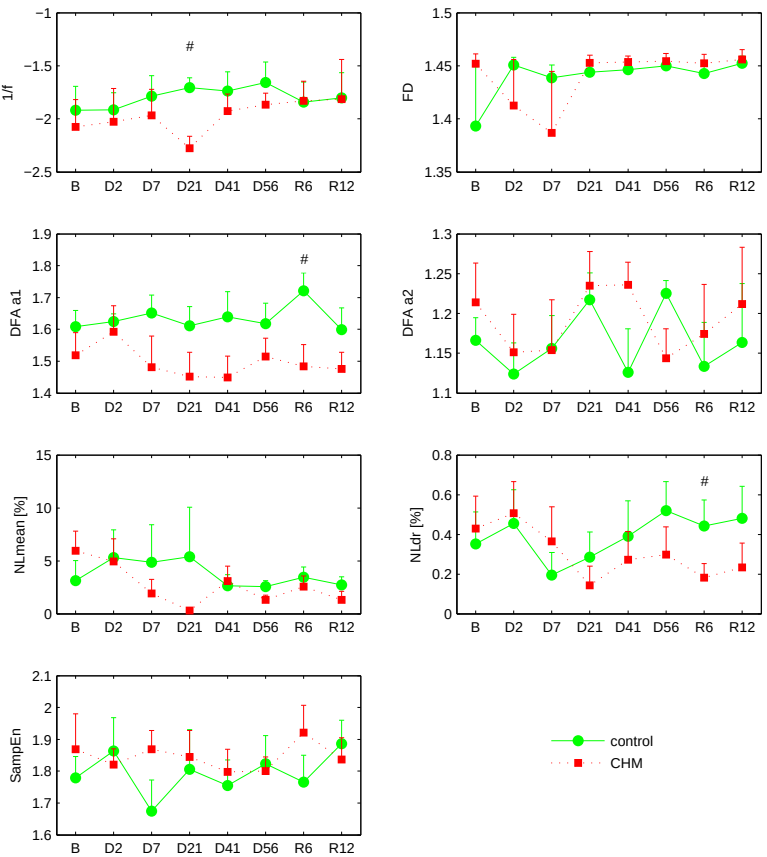


Figure 7.6: *Evolution of the nonlinear BPV characteristics* $1/f$*, FD, DFA* α_1*, DFA* α_2*, NLmean, NLdr and SampEn before (B), during (D) and after (R) head-down bed rest, separately for the CHM (red squares) and the control (green circles) group. Mean and standard error are given. Dx, Rx = the* x^{th} *day during and after bed rest respectively. * P < 0.05 compared to before bed rest; # P < 0.05 between groups.*

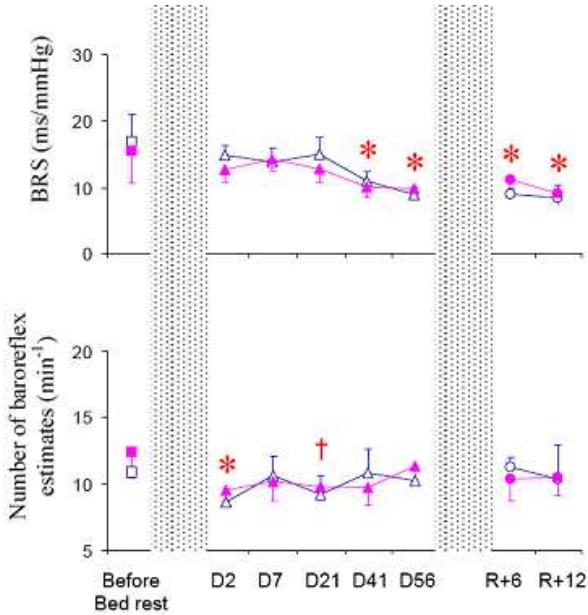


Figure 7.7: *Baroreflex sensitivity (BRS) and number of baroreflex couplings in the control (blue) and CHM group (magenta). Dx, R+x = the x^{th} day during and after bed rest respectively. * $P < 0.05$ compared to before bed rest; † $p < 0.10$ compared to before bed rest. From [209].*

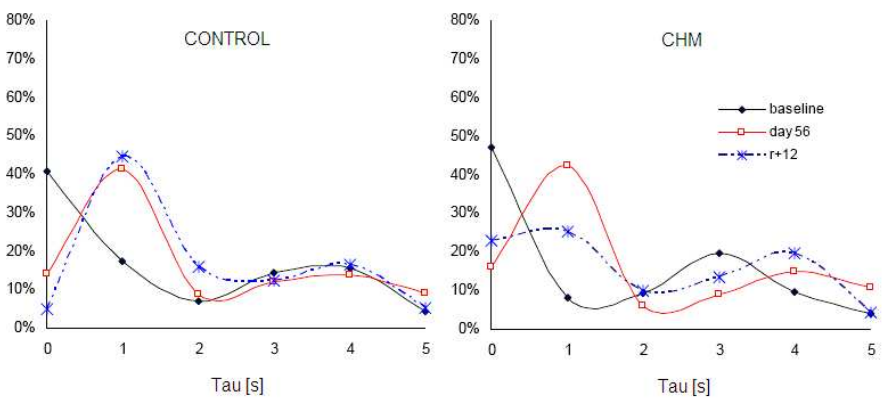


Figure 7.8: *Distribution of optimal time delay Tau (s) of each baroreflex estimation before bed rest (black solid line with diamonds), at the end of bed rest (red solid line with squares) and at 12^{th} day during recovery (blue dotted line with asterix). From [209].*

its function as a countermeasure. However, it influenced some of the parameters statistically compared to the control group. Secondly, significant changes were found over time as a consequence of head-down bed rest, simulating microgravity conditions as during spaceflight missions. Especially cardiac modulation was affected, often still present after HDBR, while blood pressure was not influenced a lot. Furthermore, while most studies in the past only used linear measures, this study showed that also nonlinear dynamics of cardiovascular control were altered during HDBR. Another advantage of this study are the many measuring times during HDBR, especially in the beginning (day 2 and day 7), enabling to investigate more in detail when changes occur. As explained earlier, the evolution of weight, water intake and urine output during HDBR has already been discussed in our previous study [209].

7.4.1 Effect of CHM as a countermeasure

Traditional Chinese Medicine considers the processes of the human body to be interrelated and in balance (Yin and Yang), as well as in constant interaction with the environment. Living harmoniously can be translated into Western Medicine as a homeostatic balance and optimal food intake, based on the holistic (systemic) approach considering the body as an interconnected system. From this point of view, CHM claims the diminished orthostatic tolerance after spaceflight is due to the extra consumption of Qi (a concept in Chinese culture, often defined as vitality or spiritual energy), the imbalance between Qi and blood, and the damage of the heart and kidney. Mi et al [235] showed that after 28 days of tail suspension, Tai Kong Yang Xin Prescription increased left ventricular diastolic diameter (LVDD), left ventricular diastolic volume (LVDV) and stroke volume (SV) in rats. Hence, they suggested that Tai Kong Yang Xin Prescription may protect heart pump function in rats after simulated microgravity.

The results of our study do not support that CHM fully counteracts the deconditioning of the cardiovascular control system during prolonged HDBR because no significant interaction terms were observed between the factors time and group. This means that the effect of CHM did not change the time evolution differently from the control group. However, CHM has an effect on the cardiovascular system in a positive way since it decreased heart rate (higher mean RR) compared to the control group. Consequently, the increase in HR during HDBR is reduced by CHM and therefore remains closer to the baseline level than in the control subjects. The same reasoning holds for SDNN, pNN5, LF/HF and DFA α_1 on the blood pressure data. These findings suggest that CHM restricts the influences of a simulated microgravity environment on the cardiovascular regulation, though not completely eliminates them. CHM also influenced nonlinear characteristics of heart rate and blood pressure control. The increase in DFA α_2

towards 1 and the decrease of $1/f$ slope towards -1 are typically indications for scaling behaviour in HR modulation.

Liu et al [209] did not find an effect of CHM in the hemodynamic parameters, except for the optimal time delay in the cardiac baroreflex mechanism. Their findings suggested that the influence of CHM in the setting of bed rest deconditioning is limited to a partial recovery of the distribution in cardiac baroreflex optimal time delay toward lower values after 12 days of recovery. However the exact mechanism underlying this partial recovery remained uncertain, they proposed the following speculations. Firstly, dynamic baroreflex control of HR acts through the 'fast' (vagal) pathways and 'slow' (sympathetic) pathways. A zero second time delay can therefore be expected for vagal control of heart rate, while increasing time lags result from combined effects of vagal and sympathetic influences on baroreflex regulation of cardiac cycle length [55]. Hence, the increase in tau at day 56 of HDBR was interpreted as a shift towards more sympathetic influence on cardiac modulation, also supported by other findings, i.e. higher HR, higher MAP, higher LF power of SAP and lower BRS. Alternatively, the faster recovery in tau after 12 days might be an indication of a faster recovery in sympathovagal balance. This however was not supported by other neural indices of cardiovascular regulation, rendering the tau distribution a more sensitive index of sympathovagal RRI modulation. They also gave an alternative explanation for the larger tau values at day 56 of HDBR, namely an increased time interval for processing afferent baroreceptor signals within the central nervous system. In this respect, Gulli et al [147] documented an increased baroreflex lag in syncopal patients with poor orthostatic tolerance. The reduction in RRI-to-SAP lag may then lead to instability and inadequate blood pressure control. In their study, tau was observed to be partially recovered in the CHM group only (not in the control group) after 12 days recovery. Consequently, Chinese herbal medicine may play a certain role in the response time of the central nervous system during recovery from HDBR deconditioning.

7.4.2 Effect of HDBR on linear cardiovascular control

This study found no remarkable change in HR during the first 3 weeks of HDBR. From day 41 of HDBR on, HR became significantly higher. Other studies reported no change or an increase depending on the bed rest duration. Goldberger et al [136] showed no HR change in 8 healthy women during a 13-day HDBR. While Sigaudo et al [340] described an increased HR from day 6 of HDBR, Fortrat et al [114] reported an increase from day 22, both in a 42-day HDBR. Two long term (90-day and 120-day) HDBR studies found a progressively increasing resting HR, significant in the second half of the study [338] [ESA/CNES/NASDA clinical report]. Therefore, HR seems only to be affected by HDBR provided the duration is sufficiently long (>20 days) and remained high even after more than 12 days

of recovery. This phenomenon is probably related to the hemodynamic changes in the second phase of HDBR, in which plasma volume is reduced and central blood volume has been restored to the baseline level. The significant increase in urine output after day 30-45 of HDBR, reported in Liu et al [209], confirms this. Fortney et al [113] described that the reactivity of autonomic nerves in long-term bed rest was unstable in their central and peripheral regulation. A decreased total cardiac variability (SDNN) during HDBR was also reported by Fortrat et al [114]. Many studies already found a decreased vagal modulation and therefore a more sympathetic dominance at the end of HDBR, as also valid for this study. Thanks to the frequently measured times, we remarked that vagal modulation (pNN50, RMSSD, HF) was not decreasing the first week of HDBR, resulting in a stable sympathovagal balance, but started declining slightly afterwards. According to the literature, this decrease in total HRV and parasympathetic indices is evident in chronic adaptation to HDBR after 2 weeks [167], 4 weeks [162] and 6 weeks [366]. Another 42-day HDBR study resulted in strongly reduced vagal influences from the first till the last day of HDBR and with no significant changes in sympathetic influences [340].

The specific evolution of SAP during HDBR, namely a gradual decrease during the first week of HDBR, followed by a slight increase to baseline level, was not reported elsewhere. Another study found first an increase in SAP, decreasing again after 15 days of HDBR approximately to the initial value [340]. Shiraishi et al [338] stated that systolic blood pressure did not show significant differences at any time moment during 120-day HDBR, though described a tendency to attenuate in the second half period. A reduced SAP might be related to a damaged adaptability of the body to the external environment, possibly causing cardiovascular deconditioning.

7.4.3 Effect of HDBR on nonlinear cardiovascular control

This study focused more on the nonlinear HRV and BPV characteristics being not investigated often, though expected to give extra information [201, 404]. The actions and continuous interactions of sympathetic and parasympathetic control mechanisms are nonlinear [137, 300] and therefore limiting the applicability of techniques based solely on linear models such as spectral analysis. Consequently, measures of scaling behaviour, chaotic behaviour and complexity, derived from the analysis of dynamical systems, offer potentially useful new approaches for quantifying those specific features. The reason why we hypothesize reduced nonlinearity during HDBR is that when physiological systems become less complex, they are less adaptable and less able to cope with the demands of changing status.

Goldberger et al [136] did a first preliminary study using approximate entropy

(ApEn) during 13-days HDBR in healthy young women, observing only a decrease in HRV ApEn at peak levels of applied lower body negative pressure. Probably, the duration of bed rest was not long enough to induce changes in resting nonlinear fluctations. Hughson et al [162] have shown changes in HRV fractal noise during 28-days HDBR. Here, HRV SampEn [299], a better version of ApEn, decreased during HDBR as well as the parameters related to chaotic behaviour. This confirms our hypothesis. Another indication was the increased HRV DFA α_1, in literature known to act opposite to the other nonlinear techniques (higher in pathologic patients compared to healthy persons). The technique of fractal dimension, on HRV as well as BPV, seemed not to be influenced by HDBR conditions. As fractal dimension and detrended fluctuation analysis were not used in such studies before, no comparison is possible. Finally, $1/f$ slope, another fractal parameter, showed different changes as described in literature. For HRV, the values were a bit lower, although far from statistically significant, during HDBR and higher after HDBR compared to the period before, while Fortrat et al [114] reported a significant decrease during as well as after HDBR, taken into account the opposite definition of $1/f$ slope. Also for BPV $1/f$, no consensus exists in literature. While we found a small increase during HDBR, followed by a small decrease after HDBR towards the baseline level, showing a possible indication of recovery, other studies described the opposite evolution [114] or only a significant decrease after HDBR compared to the period before [338].

The changes in nonlinear characteristics of HRV and BPV seem to be independent in amplitude and behaviour, despite the links between heart rate and blood pressure. However, this is in correspondence with the observation of Butler et al [62] that HRV and BPV fractal components are independent. Several studies described a link between HRV fractal alteration during HDBR and the baroreflex, mainly vagally mediated [162, 340, 96, 52]. As baroreflex sensitivity quickly recovers after HDBR [96] and nonlinear HRV and BPV parameters are either still influenced after HDBR or show another trend, a change in baroreflex cannot fully explain the change in cardiovascular dynamics. Other factors seem to be involved such as vagal modulation for nonlinear HRV which we mentioned earlier. Regarding nonlinear BPV, peripheral resistance of the vessels probably plays an important role since it changes during HDBR [52].

7.4.4 Comparison to spaceflight

HDBR has proven its usefulness as a simulation model in the past 20 years, not only for the physiological study on the ground, but also for developing countermeasures to be used during spaceflight [365]. The effects of HDBR are very similar to what happens after spaceflight as well, i.e. postural tachycardia with a variable degree of orthostatic intolerance. The higher heart rate, decreased total heart rate variability (SDNN) and increased sympathovagal balance after HDBR are in line

with the results early post-flight [21, 36, 258]. While during HDBR, a progressive increase in both HR and MAP [209] was demonstrated, HR and MAP have been reported to be well maintained during prolonged exposure to microgravity in space [21, 381]. A reasonable interpretation of these differences could be that, as a ground-based simulation model, HDBR does not eliminate the influence of gravity. In spaceflight studies, nonlinear cardiovascular dynamics are investigated even less often than with respect to HDBR studies [35]. To the best of our knowledge, we are the only ones who recently applied several nonlinear HRV techniques to 24h Holter recordings before and after spaceflight (see Chapter 6). Similarly to HDBR, nonlinear HRV parameters showed significant changes 5 days upon return to Earth compared to pre-flight. The decreased complexity (SampEn) and chaotic behaviour, here quantified by the numerical noise titration technique instead of the less robust Lyapunov exponent in the spaceflight study, was also found early post-flight. Only the fractal dimension did not change during and after HDBR while it was significantly lower early post-flight compared to pre-flight. More research will be necessary to verify or explain this inconsistency.

7.4.5 Limitations

The number of subjects available in HDBR studies is very limited. Although standardization of experimental procedures was imposed, there will always be some differences compared to other HDBR studies. The length of the HDBR is another important factor. Also the fact that all participants were Chinese men has to be taken into account as there are some indications that autonomic cardiovascular control is different between European astronauts and Chinese taikonauts. No women were included which can be seen as another limitation.

7.5 Conclusion

The influence of head-down bed rest on autonomic cardiovascular control was confirmed in this study. In particular, we proved a change in nonlinear heart rate and blood pressure dynamics during HDBR, often still present after a week of recovery. Those nonlinear HRV and BPV parameters will not replace linear analysis, but provide complementary information, yielding extra information about scaling behaviour, chaotic behaviour or complexity. Chinese herbal medicine (Tai Kong Yang Xin Prescription) seems to restrict the influences of microgravity environment during HDBR on the cardiovascular regulation, though only partially functions as a countermeasure.

Chapter 8

Cardiovascular oscillations in children with refractory epilepsy

This chapter first aims to present a review about the many cardiac changes related to epilepsy. Section 8.1 describes the acute and chronic changes of the cardiac system in epileptic patients in general. Also the study objectives are outlined at the end. The treatment with vagal nerve stimulation and the data acquisition and analysis afterwards are given in Section 8.2. Section 8.3 reports the results of the study which are extensively dicussed in Section 8.4. To conclude, Section 8.5 contains the main findings.

8.1 Introduction: cardiac changes in epilepsy

In recent years, it became clear that epilepsy and seizures can have a profound effect on cardiac function. Subtle cardiac rhythm changes in the pre-ictal and ictal period are potential biomarkers and can be used in algorithms to anticipate and detect seizures. The phenomenon of sudden unexpected death in epilepsy (SUDEP) is closely linked to ictal cardiac changes.

This overview of cardiac changes in epilepsy is based on the work of Katrien Jansen (Department of Pediatrics, University Hospitals Gasthuisberg, Leuven), with who I collaborated. It describes the most frequent autonomic cardiac changes occuring during seizures and in epilepsy. Emphasis will be put on the recent insights into the links between different seizure types and cardiac changes. In

general, the autonomic nervous system is fundamental for maintaining homeostasis in the body through regulation of heart rate, respiration, micturition, digestion and reproduction. The output from the autonomic nervous system is determined by a balance of medullary reflexes and influences of the cerebral cortex. The medulla integrates information from the respiratory, cardiovagal and vasomotor reflex centers where a distinction can be made between parasympathetic and sympathetic reflex centers.

8.1.1 Acute cardiac changes and epilepsy

Changes in cardiac function in epilepsy imply an activation of the central autonomic network. In patients with seizures, epileptic discharges are thought to propagate to the central autonomic network and change or disturb normal autonomic control of vital cardiac functions. This activation of the central autonomic nervous system is thought to be responsible for the peri-ictal autonomic cardiac symptoms observed in epilepsy patients. The importance of these autonomic features in the pathophysiology of epilepsy and its complications has become more clear in the last years [393, 172, 112, 28]. Due to the hemispheric specific organisation of the central autonomic nervous system, autonomic symptoms in epileptic seizures can provide lateralizing and localizing information. In return, better recognition of clinical autonomic signs in epilepsy can provide more information on the organisation of the central autonomic nervous system.

Tachycardia

Ictal tachycardia has been reported in up to 100% of seizures. Tachycardia can precede, coincide or follow ictal discharges [230, 203, 128]. As tachycardia may also precede the clinical and EEG onset of the seizure it is not always considered secondary to the clonic phase. The time lag between tachycardia and seizure onset varies between 0.7 – 49.3 seconds. A possible mechanism is the propagation of epileptic discharges to the right insular cortex [262]. A predominance for tachycardia in right sided temporal seizures can be expected and is in some [203, 228] but not all [324, 100] studies confirmed, suggesting influence of other factors to explain the tachycardia. Ictal onset tachycardia seems more prominent in temporal lobe epilepsy (TLE) as compared with extratemporal seizures (XTLE) [117, 123], supporting the hypothesis that involvement of insular cortex is a key part of ictal tachycardia. The duration of the tachycardia is also longer in patients with mesial temporal lobe epilepsy compared to XTLE. It is possible that epileptic discharges propagate towards the insular cortex more easily and for a longer duration in TLE as compared to XTLE.

Tachycardia and development of tachyarrhythmia during seizures is one of the possible causes of sudden unexplained death in epilepsy patients (SUDEP). Tachycardia leading to malignant ventricular tachycardia and ventricular fibrillation has been illustrated to be the cause of near SUDEP in a patient with TLE [102].

Bradycardia and asystole

Bradycardia and bradyarrhythmia are much less frequent and take place in seizures of various origin. A severe slowing of the heart rate leading to asystole and syncope is referred to as the ictal bradycardia syndrome [60]. Factors predisposing patients to ictal brady-arrhythmia remain difficult to define. The pathophysiology of bradyarrhythmia is probably mediated through a complex cortical network. Cortical stimulation of the left insular cortex and amygdalae have been noted to elicit bradycardia [156, 263]. The left hemisphere appears to be the more common site of origin, again supporting the hypothesis of hemispheric specific organisation of cortical cardiac control [360, 305]. An atrio-ventricular block was noted in 1 patient during cortical stimulation of the left temporal basal area [9]. These results suggest a higher risk of bradyarrythmia in epileptic seizures with seizure spreading to the left insular cortex and amygdalae. The onset zone of epileptic discharges in patients with ictal bradycardia is most frequent temporal and less frontal, supporting the hypothesis of an insular influence. Ictal bradycardia up to ictal asystole has been reported in patients with refractory partial seizures and could be another important link with SUDEP [314].

Conduction disorders

Conduction disorders seem to be common during seizures in intractable epilepsy. Nei et al [253] could demonstrate the presence of arrhythmias or conduction disorders in seizures, particularly if these are prolonged or generalized. They include atrial fibrillation, supraventricular tachycardia and atrial and ventricular premature depolarisation. ECG changes, including T-wave inversion and ST-depression, were more frequent and potentially more dangerous in patients with generalized seizures [261].

Sudden unexpected death in epilepsy

It is well known that people with epilepsy have an increased risk for sudden unexpected death or SUDEP. SUDEP is defined as the sudden unexpected non-traumatic and non-drowning death of patients with epilepsy with or without evidence of a seizure, excluding documented status epilepticus, and in whom post-mortem examination does not reveal a structural or toxicological cause for death

[363]. Opeskin and Berkovic [260] looked at demographics and risk factors among epilepsy patients. Their profile of patients at risk for SUDEP are young persons with epilepsy. They are most likely to die during sleep and seizure-related. They found no correlation with seizure frequency or particular epilepsy or number of anti-epileptic drugs (AED). They did not find a difference in duration of epilepsy between SUDEP and control groups. However, previous studies have shown that SUDEP patients have earlier onset, longer duration of epilepsy and more frequent seizures. There is evidence for an increase of cardiac autonomic stimulation in patients with SUDEP, more pronounced in epileptic seizures during sleep [252], compatible with the demographic findings.

The exact mechanism of SUDEP remains an open question but is probably multifactorial. An interaction between the central and peripheral autonomic nervous system and cardiopulmonary system is assumed. There are three mechanisms already known to contribute to the pathogenesis of SUDEP [202, 251, 200]:

- ictal arrhythmias including ictal asytole and the lock-step phenomenon
- neurogenic pulmonary oedema
- ictal respiratory suppression

The first possible mechanism underlying SUDEP are seizure related cardiac arrhythmias with bradycardia and ictal asystole as explained above. Both a sudden increase of vagal tone or the effect of postganglionic epileptic discharges on the heart as described below can be considered as an explanation for the disturbed cardiac rhythm in epileptic seizures. Schuele reported a series of 10 patients with focal epilepsy and ictal asystole, 8 with TLE and 2 with XTLE [327, 326]. The loss of consciousness was observed during video-electroencephalographic observation and occurred late during the clinical event. Loss of postural tone was preceded by 8 seconds of asystole. In these patients activation leading to ictal asystole is most likely mediated through an increased vagal tone. The pattern of ictal asystole and the slowing EEG pattern of cerebral hypoperfusion closely resembled the pattern seen in vasovagal asystole. The underlying mechanism is most likely similar in both conditions and assumes involvement of medullary reflex centers responsible for the increase of vagal tone. In the two patients with XTLE, asystole could have been triggered by hypoxia due to prolonged tonic muscle contraction and respiratory arrest. Another important neurophysiological phenomenon was described by Hilz et al [157]. Seizure induced activation of the central autonomic nervous system can cause a direct effect on postganglionic discharges on the heart. This results in a synchronisation of cardiac autonomic discharges with epileptogenic activity, called the lock-step phenomenon and induces a lethal brady-arrythmia or asystole.

Secondary neurogenic pulmonary edema is known as a rare life-threatening complication of central nervous system injuries and epilepsy. Experimental studies have postulated severe sympathetic discharge as the base of neurogenic pulmonary edema. The cerebral sites regarded as trigger zones of the sympathetic discharge are found in the posterior part of the hypothalamus and in the ventral and dorsal medulla, comprising the medial reticulated nucleus, dorsal motor vagus nucleus and solitary tract [27]. The sympathetic discharge causes systemic and pulmonary vasoconstriction, resulting in increase in pulmonary capillary hydrostatic pressure and shift of fluid into the alveoli and interstitium [333].

A third possible mechanism in SUDEP is central respiratory depression as a result of epileptic discharges. Apnoe is a rare clinical feature of seizures, but laryngeal spasm and apnoe have been reported as isolated epileptic features or in complex partial seizures [73]. The focal seizures associated with apnoe seem to originate mostly from the temporal lobe [386]. This observation together with the results of invasive EEG monitoring in adults points to involvement of the limbic system in seizures complicated by respiratory depression [254].

Syncope

The difference between syncope due to cardiac arrhythmia and seizures in patients with established epilepsy remains clinically challenging. In patients with epilepsy a distinction has to be made between a cardiovascular or epileptic cause of loss of consciousness and syncope. As we mentioned earlier, patients with epileptic seizures can develop various cardiovascular problems, arrhythmias, ictal bradycardia and prolonged asystole leading to ictal syncope as a result of cerebral hypoperfusion. But the sudden loss of tone in patients with ictal asystole may be the result of ictal activation of specific areas in the brain leading to loss of consciousness. Rapid spread of ictal epileptic discharges with involvement of the pontine reticular formation can lead to loss of consciousness and a clinical syncope [59].

Cardiac ischemia

As earlier mentioned, excessive autonomic stimulation may result in cardiac arrhythmias. But repetitive autonomic stimulation can also lead to structural damage to the heart. This increases the susceptibility to cardiac arrhythmias or ischemia. Myocardial fibrosis has already been found in patients with SUDEP [254]. Patients with uncomplicated seizures do not seem to have postictal troponin elevation, but signs of ischemia on ECG and elevated cardiac enzymes in epileptic patients suggest secondary cardiac damage [401, 359]. Alehan et al could show presence of elevated brain natriuretic peptide (BNP) and myocard specific creatine

kinase (CK-MB) in patients with seizures, the first evidence of subtle cardiac dysfunction in epilepsy patients [7].

8.1.2 Chronic cardiac changes and epilepsy

Heart rate variability was found to be lower in patients with chronic refractory epilepsy, possibly resulting from parasympathetic or vagal reduction. This can make patients more susceptible to tachycardia and fibrillation and possibly SUDEP [362, 153]. Impaired baroreflex function was observed in a study of Dutsch et al [95] in patients with temporal lobe epilepsy. The impaired function can be another sign of autonomic instability in these epileptic patients and a contributing factor in cardiac arrhythmias. Serious heart rate oscillations in the postictal phase were noted in a few patients [230]. Although they occur in a minority of patients, they could be a potential risk factor for SUDEP.

Anti-epileptic drugs

Heart rate variability seems to be different in treated patients compared to untreated. It is possible that treatment of seizures prevents detrimental effects on autonomic cardiac control. Hallioglu et al [151] found a significant difference in children treated with valproic acid, oxcarbazepine or phenobarbital and children without treatment. In the treated group better HRV was found. These results indicate that patients without anti-epileptic drug treatment have suppressed parasympathetic activity . But treatment can also have a negative effect on HRV. A suppressive effect of carbamazepine on both parasympathetic and sympathetic cardiac function was found in newly diagnosed epileptic patients [275]. Lossius et al [212] looked at autonomic parameters after discontinuation of monotherapy, they found an increase of both parasympathetic and sympathetic functions, demonstrated by spectral analysis of HRV.

Chronic and refractory epilepsy

Patients with longlasting and multiple seizures seem to be prone to chronic dysfunction of autonomic cardiac control. In patients with newly diagnosed (median time 27 months) and untreated epilepsy, no difference was found in heart rate variability [276]. Mukherjee et al [242] studied a cohort of well controlled and a cohort of refractory patients and could show with a series of autonomic tests that higher vasomotor tone, higher sympathetic tone, lower parasympathetic tone and reactivity was found in the group of refractory epilepsy patients. The observed dysautonomia could be a predisposing factor to SUDEP. Chroni et al [71] could demonstrate altered cardiovagal control in patients with chronic epilepsy. They

used simple neurophysiologic tests of the autonomic nervous system, Valsalva, Tilt-test, RR interval in normal and deep breathing and sural nerve conductance to show a chronic effect of epilepsy on the autonomous nervous system. Sathyaprabha et al [320] used heart rate and blood pressure measurements in rest, after Valsalva and postural change. Autonomic dysfunction was found in 56.3% of the patients with chronic refractory epilepsy, compared to a control group. In their study the dysfunction of the autonomic system was more severe if the epilepsy was longer lasting.

Ansakorpi et al [13, 12] looked at refractory TLE patients to demonstrate interictal autonomic dysfunction in response to certain stimuli. He used newer analysis methods to demonstrate altered complexity of heart rate in refractory epilepsy patients. Ronkainen et al [308] found loss of HRV and suppressed circadian dynamics in TLE, as well in controlled as in refractory patients. In children with refractory epilepsy, the same arguments for a chronic autonomic dysfunction are found. Heart rate abnormalities were noted in children and adolescents with complex partial seizures. The abnormalities were much more frequent compared to adults and occurred in 98% of the complex partial seizures. Heart rate variability also seems to be lower in children with chronic refractory epilepsy, possibly resulting from parasympathetic or vagal reduction. This can make patients more susceptible to tachycardia and fibrillation [153].

Vagal nerve stimulation

The vagal nerve consists for 80% of afferent and 20% of efferent fibers. Vagal efferents originate in the nucleus ambiguus and dorsal motor nucleus (DMN) of the vagus. Cell bodies in the nucleus ambiguus send special visceral efferent fibers to the striated muscle fibers of palate, pharynx, larynx and esophagus. Cell bodies in the dorsal motor nucleus send general efferents to the heart, lungs and gastro-intestinal tract. Afferent fibers originate in the end organs: heart, lungs and gastro-intestinal tract. As shown in Figure 8.1, these cells project axons to the nucleus tractus solitaries (NTS), which then projects further to hypothalamus, amygdale, dorsal raphe and thalamus. Vagal nerve stimulation produces evoked potentials recorded from the cerebral cortex, the hippocampus, the thalamus, and the cerebellum (Figure 1.2). Most of the cardiovagal fibers run through the right vagus nerve and therefore stimulation of the left vagus in the treatment of epilepsy is preferred to avoid potential detrimental effects on heart rhythm [315]. Figure 8.2 visualizes how the vagus nerve is stimulated artificially. Via surgery, a pulse generator is implanted under the chest which is connected with some electrodes by a thin and flexible wire. These electrodes at the level of the neck can then stimulate the vagus nerve. Those structures in turn synapse throughout the cerebral cortex and seem to have an overall inhibitory effect. This was supported by the study of Ben-Menachem et al [233], who showed an increase of gamma-aminobutyric acid

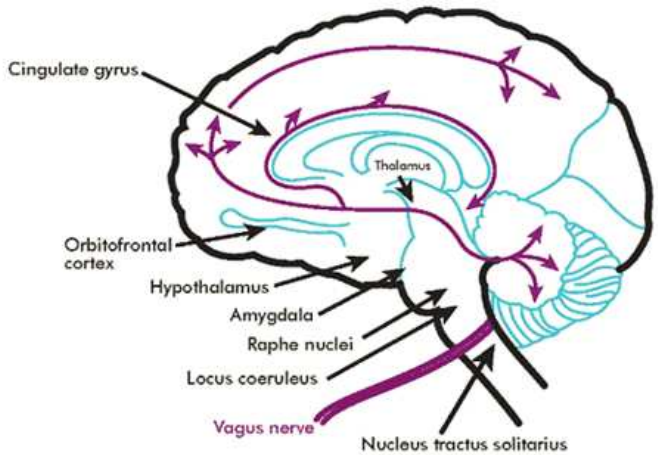


Figure 8.1: *Cells originating in several organs project axons via the vagus nerve to the nucleus tractus solitaries, which then projects further to hypothalamus, amygdale, dorsal raphe and thalamus. From* `http://www.vnstherapy.com/images/pathway_brain.gif`

(GABA) in the cerebrospinal fluid (CSF) in patients with VNS and a decrease of the excitatory aspartate.

Up to now, stimulation of the vagal nerve with VNS was thought to have no effect on cardiac action. In contrast, Frei and Osorio [118] showed that left vagal nerve stimulation has complex effects on instantaneous heart rate and heart rate variability with large interindividual variability. They found different cardiac chronotropic effects, either bradycardia or tachycardia, immediately followed by bradycardia during stimulation. HRV was found to be increased or decreased. The recent work of Stemper et al [351] showed that VNS influences both sympathetic and parasympathetic cardiac regulation. The variability of the observed responses in patients treated with VNS illustrates the interplay of divers afferent information and central influences.

8.1.3 Summary

There is growing evidence for the importance of the involvement of the central autonomic nervous system in epilepsy patients. Short term alteration of cardiac functions in patients with seizures is caused by involvement of the central autonomic control centers in seizure activity. Due to a hemispheric specific localization of these control centers, the effect can give information on lateralization of the seizure. The cardiac changes in epilepsy play also an important

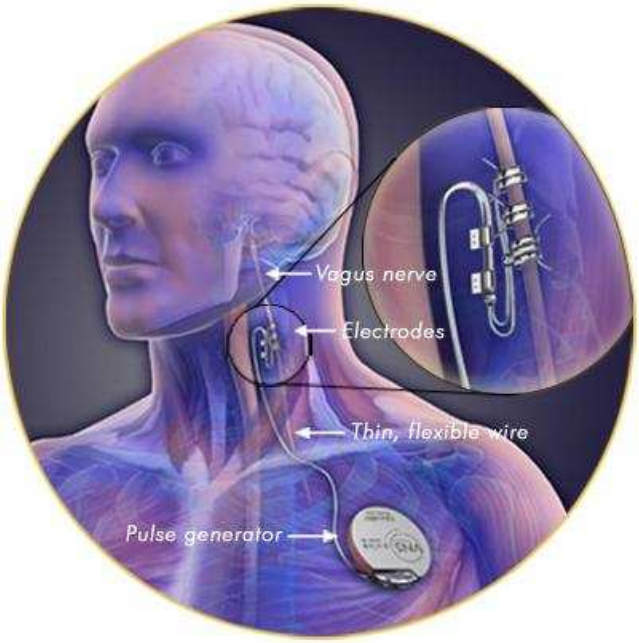


Figure 8.2: *The principle of vagal nerve stimulation from a practical point of view. From* `http://corleyz.com/wp-content/uploads/vns_implant.jpg`

role in the pathophysiology of SUDEP. In patients with longlasting epilepsy and multiple seizures, there are arguments for a chronic dysfunction of the autonomic nervous system. Early recognition and possible prevention of these short and long term effects can prove to be of vital importance in the future.

8.1.4 Study objectives

In patients with refractory epilepsy, vagus nerve stimulation (VNS) is an alternative therapeutic option of which the working mechanism is still incompletely understood. In normal subjects, there is a relative vagal predominance during sleep compared to wakefulness and this vagal component of heart rate modulation reaches a maximum in synchronized or slow wave sleep [61] while in early sleep stages there is still a relatively high influence of the sympathetic branch on heart rate variability. Reduced HRV is a marker of dysfunction of the autonomic nervous system and can be considered a risk factor in chronic diseases. Various diseases including epilepsy are now known to be accompanied by a loss of autonomic functionality and reduced HRV [71]. Only recently, diminished heart rate variability has been associated with high risk arrhythmias and sudden

unexpected death in epilepsy patients [362]. Therefore, this study tries to evaluate the autonomic nervous system in children with refractory epilepsy by using HRV with a focus on the nonlinear cardiac dynamics. A second goal is to examine the influence of vagus nerve stimulation on the ANS function in those patients with refractory epilepsy.

8.2 Methods

8.2.1 Subjects and treatment

17 children (13 male, 3 – 16 years of age) were selected from the epilepsy clinic of the University Hospitals Leuven and the Epilepsy Centre Pulderbos in Belgium. They suffered all from refractory epilepsy. 8 were diagnosed with Lennox-Gastaut epilepsy, 3 with myoclonic epilepsy, 2 with electrical status epilepticus during sleep (ESES), 2 frontal lobe epilepsy, 1 absence epilepsy and 1 temporal lobe epilepsy. All were treated with implantation of a vagus nerve stimulator (model Neurocybernetic prosthesis; Cyberonics, Pulse Generator, Houston, TX, USA). Output current was between 0.75 and 2.25 mA, stimulation frequency 30Hz, pulse width 500 ms, on time 30 seconds, off time 5 minutes. Back ground medication was kept as stable as possible. The mean time between the baseline registration and implantation of VNS was 7.5 months (range 1 – 48 months), mean time between registration after implantation was 11 months (range 1 – 39 months). The mean duration of epilepsy was 6.4 years (range 1 – 14 years). Patient characteristics are shown in Table 8.1. 17 age- and sex-matched subjects in a control group were referred to the epilepsy clinic for staring or learning problems and had normal EEG findings.

The experiment protocol was approved in advance by the local ethical committee of the University Hospitals Gasthuisberg. The parents of the children provided written informed consent before participating. The study complies with the Declaration of Helsinki.

8.2.2 Data acquisition

24 hour EEG and ECG data were obtained before and after implantation of the VNS. Sleep data were used to evaluate the normal shifts in autonomic balance during sleep and to exclude differences due to mental and physical state during daytime. 50 minute epochs of ECG were extracted from stage 2 sleep and slow wave sleep (SWS) in the first sleep cycle to exclude circadian and endocrine influences. Sleep stage was determined by an expert based on visual analysis of the EEG and

Table 8.1: *Characteristics of the study population.*

No.	Age [y]	Sex	Type	AED at time of implementation	AED after implementation	Imaging	OC [mA]
1	16.5	M	LG	lamotrigine, levetiracetam, sodiumvalproate	lamotrigine, sodiumvalproate, clobazam	N	2.25
2	6.6	M	ESES	topiramate	topiramate, clobazam, sodiumvalproate	TB	0.75
3	8.7	M	ESES	sodiumvalproate, lamotrigine	sodiumvalproate, lamotrigine	TB	1.50
4	5.7	M	LG	sodiumvalproate, lamotrigine, levetiracetam	sodiumvalproate, lamotrigine, clobazam	IP	1.25
5	7.5	M	LG	topiramate, lamotrigine, clonazepam	topiramate, lamotrigine, clonazepam	N	1.50
6	4.8	M	FLE	levetiracetam, carbamazepine	carbamazepine	N	1.25
7	4.3	F	LG	sodiumvalproate, lamotrigine, clonazepam	sodiumvalproate, lamotrigine, clonazepam	N	1.50
8	4.0	M	MA	sodiumvalproate, lamotrigine, nitrazepam	sodiumvalproate, levetiracetam, clonazepam	N	1.50
9	4.0	M	LG	sodiumvalproate, gabapentin	sodiumvalproate, gabapentin	N	1.50
10	6.6	M	FLE	sodiumvalproate, lamotrigine	sodiumvalproate, lamotrigine	N	1.00
11	3.0	M	ME	sodiumvalproate, levetiracetam, clonazepam	sodiumvalproate, levetiracetam, clonazepam	N	0.75
12	6.8	F	ME	sodiumvalproate, levetiracetam, clonazepam, ethosuximide	topiramate, clobazam, sodiumvalproate	N	2.25
13	8.7	F	LG	levetiracetam, clobazam, sodiumvalproate	levetiracetam, clobazam, sodiumvalproate	N	1.00
14	13.2	M	LG	phenytoin, carbamazepine, sodiumvalproate	phenytoin, carbamazepine, clobazam, phenobarbital	N	1.00
15	12.5	F	AE	sodiumvalproate, lamotrigine clobazam	lamotrigine, ethosuximide		0.75
16	11.9	M	TLE	sodiumvalproate, lamotrigine	sodiumvalproate, clonazepam	PWML	1.25
17	4.3	M	LG	sodiumvalproate, clonazepam	sodiumvalproate, topiramate, clobazam	N	1.50

Sex: M = male, F = female
Epilepsy type: LG = Lennox-Gastaut, ESES = electrical status epilepticus during sleep, FLE = frontal lobe epilepsy, MA = myoclonic astatic, ME = myoclonic epilepsy, AE = absence epilepsy, TLE = temporal lobe epilepsy
Imaging: N = normal, TB = thalamic bleeding, IP = insular pachygyria, PWML = Postischemic white matter lesions
OC = output current

spectral analysis by BrainRT (OSG Belgium). RR intervals were calculated by the BrainRT software.

8.2.3 HRV analysis

All standard HRV parameters are calculated in agreement with the standards of measurement proposed by the Task Force of the European Society of Cardiology and the North American Society of Pacing and Electrophysiology [355]. As time domain measures, we calculated mean RR, SDNN, RMSSD and pNN50. After resampling the tachogram at 2 Hz [343] with the use of cubic spline approximation [18], power spectra were obtained by using the Welch method. The direct current component was removed by subtracting the mean value of the data set. A sliding Hamming window of 1024 points with 50% overlap was used. Three frequency bands were defined (VLF, LF and HF) of which the spectral power was expressed in absolute values (in ms^2) and in normalized units (n.u.) which represent the relative value of each power component in proportion to the total power minus the VLF component. This representation emphasizes the controlled and balanced behavior of the two branches of the autonomic nervous system and additionally, it minimizes the influence of changes in total power. Moreover, a low-to-high frequency power ratio is calculated to reflect the sympathovagal balance.

In addition to the standard HRV parameters, also nonlinear techniques were applied. Detrended fluctuation analysis (DFA) [273] indicates the scaling behaviour of the ANS system while sample entropy (SampEn) [299] describes the complexity and numerical noise titration (NLdr) [285] measures the chaotic characteristics of heart rate regulation.

8.2.4 Statistical analysis

Statistical analysis was executed in Matlab R2008a (The Mathworks Inc. Natick, MA, USA). How the VNS influenced the autonomic heart rate modulation of the epileptic patients was analyzed pairwise by the nonparametric Wilcoxon signed rank test. Differences between epileptic patients and the control group were obtained via the nonparametric Wilcoxon rank sum test. $P < 0.05$ was considered statistically significant.

8.3 Results

The results for the time domain HRV parameters are given in Table 8.2. No significant differences were found, except for heart rate. Heart rate is significantly

Table 8.2: *Time domain HRV results, presented as mean ± standard deviation, in children with refractory epilepsy before and after implantation of vagus nerve stimulation (VNS) and in an age- and sex-matched control group during stage 2 sleep and slow wave sleep (SWS).*

	Sleep	Refractory epileptic children		Control subjects
		Before VNS	After VNS	
Mean RR	stage 2	716.99 ± 89.45 *	715.08 ± 95.43 *	837.32 ± 136.53
	SWS	719.66 ± 107.41 *	723.78 ± 84.20 *	814.64 ± 129.57
SDNN	stage 2	90.46 ± 46.63	78.88 ± 35.69	98.05 ± 28.31
	SWS	83.76 ± 35.55	84.55 ± 49.40	75.38 ± 27.87
SDANN	stage 2	28.31 ± 20.13	23.92 ± 18.20	29.86 ± 14.61
	SWS	26.46 ± 15.76	25.51 ± 18.05	19.00 ± 11.69
RMSSD	stage 2	98.76 ± 62.99	77.13 ± 39.86	92.19 ± 43.82
	SWS	90.07 ± 47.66	82.15 ± 59.86	84.87 ± 50.44
pNN50	stage 2	33.36 ± 21.98	27.42 ± 22.54	38.31 ± 22.45
	SWS	33.22 ± 24.18	28.04 ± 23.52	39.90 ± 24.02

* $P < 0.05$ compared to control subjects, calculated via the nonparametric Wilcoxon rank sum test

higher in epileptic patients compared to the control group, both in stage 2 sleep ($p = 0.0089$) as during SWS ($p = 0.0421$). However, VNS does not alter the higher heart rate in refractory epilepsy children directly.

Frequency domain HRV results are visualized in Figure 8.3. LF and HF power are different in patients with refractory epilepsy compared to healthy subjects. During stage 2 sleep, LFnu in patients with refractory epilepsy is lower than control level before VNS therapy, but increases towards controls after implementation of VNS. HFnu is increased in refractory epilepsy before VNS compared to controls, but decreases after VNS towards the control level. During slow wave sleep, there is an increase of LFnu and decrease of HFnu in patients with refractory epilepsy before VNS therapy compared to control subjects. After implementation of VNS these changes observed in patients with epilepsy become more prominent and statistically significant. (LFnu in epilepsy patients after VNS treatment versus controls: $p = 0.007$; HFnu in epilepsy patients after VNS treatment versus controls: $p = 0.009$). In the control group, the sympathovagal balance (LF/HF) shifts more towards sympathetic predominance in stage 2 sleep compared to SWS. In contrast, in epileptic patients LF/HF was higher during SWS than stage 2 sleep and this was even more pronounced after VNS. LF/HF is therefore statistically significantly higher during SWS in epilepsy patients after VNS treatment than in the control group ($p = 0.007$).

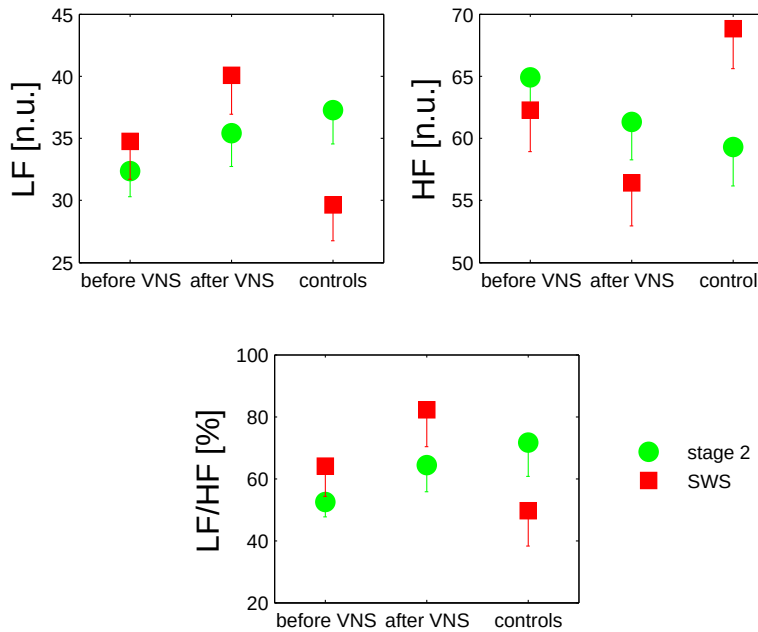


Figure 8.3: *Frequency domain HRV results, presented as mean and standard error, in children with refractory epilepsy before and after implantation of vagus nerve stimulation (VNS) and in an age- and sex-matched control group during stage 2 sleep (green circles) and slow wave sleep (SWS) (red squares).*

Also nonlinear cardiac regulation is affected by epilepsy as can be seen in Figure 8.4. Both DFA parameters increased after VNS. In stage 2 sleep, this increase is towards the corresponding values in the control group while during SWS, this increase was significant (DFA α_1: $p = 0.0148$; DFA α_2: $p = 0.0217$) and opposite to the much lower DFA values in the control subjects. Cardiovascular complexity (SampEn) does not differ at all between both sleep stages. SampEn is lower, though not significantly (stage 2 sleep: $p = 0.3179$; SWS: $p = 0.3892$), in epileptic patients compared to normal population and it even decreases further due to VNS, in SWS as well as in stage 2 sleep. The mean chaos level (NLdr) was significantly higher in epileptic patients before VNS compared to the control group (stage 2 sleep: $p = 0.0458$; SWS: $p = 0.0661$), but VNS caused a slight decrease.

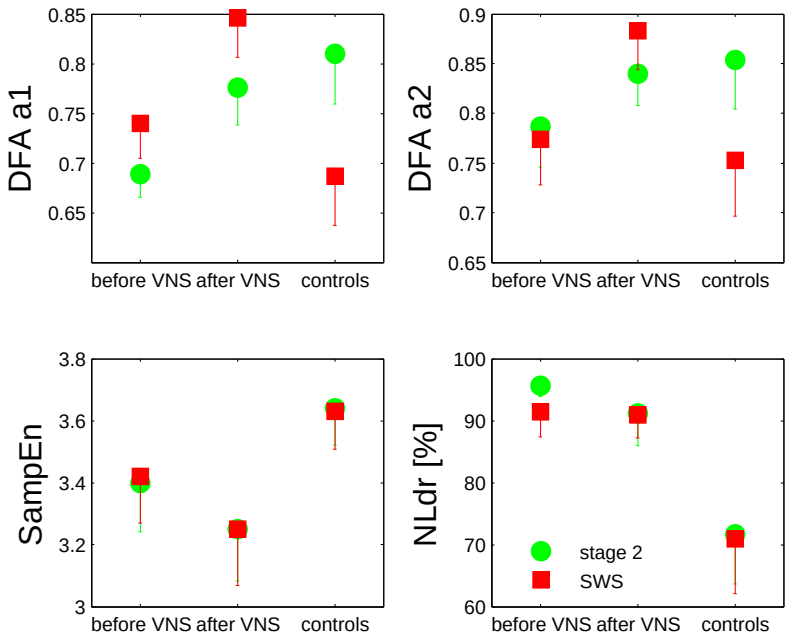


Figure 8.4: *Nonlinear HRV results, presented as mean and standard error, in children with refractory epilepsy before and after implantation of vagus nerve stimulation (VNS) and in an age- and sex-matched control group during stage 2 sleep (green circles) and slow wave sleep (SWS) (red squares).*

8.4 Discussion

8.4.1 Refractory epilepsy

The significantly higher heart rate in patients with refractory epilepsy compared to a control group, both in stage 2 and in slow wave sleep, was a first indication for a change in autonomic modulation, in particular sympathetic dominance, in patients with longlasting epilepsy. Vagal influences become more important during sleep with a maximum in synchronized sleep [61], which is confirmed in our control subjects. The fact that epileptic children show a higher sympathetic tone in SWS than stage 2 sleep leads to the hypothesis that changes in control centers, which regulate the peripheral ANS in the brain [28, 59], due to epilepsy are responsible for the more prominent sympathetic activity. The vagal reduction observed in our patients with refractory epilepsy has been previously reported in adults with

refractory epilepsy and children with complex partial seizures [71, 362, 103]. In lesional epilepsy it is possible that parts of the central autonomic regulation centers are disrupted, while in patients with longlasting epilepsy and multiple drugs, an effect of chronic administration of medication remains a possibility. Another hypothesis is that the almost continuous epileptic discharges itself in patients with epileptic encephalopathy disturb the normal function of the autonomic nervous system. Moreover, changes in HF and LF power bands between both sleep stages were smaller in patients with refractory epilepsy compared to the control subjects. This could be considered a marker of impaired modulation capacity in patients with severe epilepsy.

8.4.2 VNS

In previous reports on VNS in refractory epilepsy, non-consistent results were found. Some studies found no difference in cardiac parameters in epilepsy patients after implantation of VNS, but often only short fragments were used for analysis [309, 335]. Stemper et al [351] found an increase of both LF and HF power of the RR intervals during 60 seconds on phase. Finally, Galli et al [124] noted a reduction in vagal tone, marked by a reduction in HF power, after long term vagal nerve stimulation mainly during sleep, which is confirmed by our results. The mechanism of action in VNS is still not completely understood. VNS is noted to increase the extracellular concentrations of norepinephrine in cortex and hippocampus [310]. This increase in plasma catecholamines could be the explanation for the additional increase in sympathetic activity in HRV characteristics in patients with VNS compared to controls. However, VNS also increased the difference between stage 2 sleep and slow wave sleep, as well for LFnu as for HFnu and consequently also for LF/HF. This can be interpreted as a partial recovery of the impaired modulation capacity in patients with severe epilepsy.

8.4.3 Nonlinear HRV characteristics in epilepsy

With respect to nonlinear HRV, to the best of our knowledge, only a research group within the Department of Neurology at the University of Oulu (Finland) applied nonlinear HRV on epilepsy patients. Our results for both DFA parameters are very similar to LH/HF. The higher DFA α_1 and α_2 and lower entropy in patients with refractory epilepsy was also found by Ansakorpi [12] but then restricted to temporal lobe epilepsy in adults. It is important to note that nonlinear HRV techniques will not replace linear analysis, but have to be considered as a completion. Nonlinear techniques have the advantage over linear techniques in providing better repeatability and reliability across measurements (small random error). Therefore, nonlinear indices may be more suitable for diagnostic purposes, as well as for assessing individual treatment effects [218]. Nowadays, the meaning

of the indices used for nonlinear system dynamics is not as clear as those derived from time or frequency domain methods.

8.4.4 SUDEP

HRV is clearly impaired in patients with refractory epilepsy and became, for some HRV parameters, even more impaired after VNS implementation, e.g. further reduction of cardiac complexity. The clinical relevance of these changes remains an open question. This impairment in cardiac autonomic control might be of relevance in relation to the risk of sudden unexpected death in patients with chronic refractory epilepsy (SUDEP). One of the possible mechanisms underlying SUDEP are seizure related cardiac arrhythmias: either tachyarrhythmias leading to ventricular fibrillation or bradycardia most likely due to a sudden increase in vagal tone. Despite this negative VNS side effect, Annegers et al [11] found an even lower incidence after 2 years of follow-up in patients with refractory epilepsy treated with VNS. Therefore, we have to suggest that the positive cardiac effect of VNS, namely a (partial) recovery of the impaired modulation capacity, is more important than the negative side effects (increased sympatetic dominance causing a higher chance for severe tachyarrhythmias, decreased nonlinear cardiac dynamics). This improved modulation after VNS implementation might be a protective factor against SUDEP.

8.5 Conclusion

Epileptic patients showed a higher HR and decreased HRV compared to a normal population. Although VNS reduced the epileptic activity, it affected cardiac autonomic modulation as it increased the sympathetic dominance and also changed some nonlinear HRV characteristics. The affected autonomic cardiac control in patients with refractory epilepsy probably plays an important role in arrhythmias and sudden cardiac death.

Chapter 9

Conclusions and further research

In this final chapter, findings and conclusions of the presented work are summarized in Section 9.1 and suggestions for future research directions are given in Section 9.2.

9.1 General conclusions

9.1.1 Physiological and mathematical background

First we introduced the basic physiology of the nervous system and the cardiovascular system in general. The relation between the brains and the heart via the autonomic nervous system and the concept of heart rate variability as marker of the autonomic heart rate regulation were clarified. Also the methodology was discussed extensively, starting with peak detection and preprocessing algorithms to all linear and advanced nonlinear techniques. If possible, the physiological meaning of these HRV parameters was given with their advantages, drawbacks and limitations. Especially the issue whether a normal heart rate is nonlinear and/or chaotic was addressed in detail.

9.1.2 Goals and novelties

The main goal of this thesis was to investigate the nonlinear system dynamics in the autonomic regulation of heart rate. Heart rate variability was used here as a tool to study the autonomic nervous system with a focus on the nonlinear techniques. We investigated whether they provide additional information about the nonlinearity in the cardiovascular system which can not be reflected by standard HRV analysis. Therefore, several completely different data sets were used on which those techniques were applied. An important aspect of the thesis was the combination of many nonlinear techniques in the same study, enabling comparisons, while in literature often only one or a few of these techniques were studied at once. In addition to the already used nonlinear methods, we also implemented a recently developed and promising technique, called numerical noise titration, and explored it further.

9.1.3 Applications

Physiological meaning of numerical noise titration

By applying the method of numerical noise titration on data of rats with specific autonomic blockades, we did a first attempt to link the output of the method with its possible physiological meaning. The results supported, partially, the hypothesis that disturbing the autonomic nervous system induces changes in the nonlinear modulation of HR and BP, but in a complicated way. In rats, the α-adrenoceptor pathways seem to have an important contribution in the generation and control of nonlinear HR and especially BP fluctuations, while β-adrenoceptor and cholinergic interventions have a negligible contribution to the nonlinear dynamical control. An important contribution of this work was the finding that the numerical noise titration technique seems very sensitive to changes in vasomotion control. This might help to understand the physiological origin of nonlinear blood pressure control.

Detection of cardiovascular abnormalities in preterm neonates

In this study, HRV of preterm infants was analyzed based on polysomnographies. In addition to standard time domain HRV parameters, the nonlinear numerical noise titration was used to quantify more dynamical aspects of HRV. We adapted the methodology for calculating these HRV parameters to deal with the specific characteristics of neonatal heart rate data and the relatively low ECG sampling rate (100 Hz). Periods of non-REM sleep have strongly significantly lower noise limit values, which means that the RR interval series is less chaotic during non-

REM sleep. This provides further insights in the mechanisms causing periods of non-REM or REM sleep. While the standard time domain measures or DFA could not discriminate between the groups NN, AN and AA, neither in the complete recording, nor in non-REM or REM periods, the nonlinear NL parameter succeeded.

Circadian profile and aging in a healthy population

We showed the typical circadian profiles for several nonlinear HRV parameters as a function of age and gender. Not only parameters providing information about the scaling behaviour or the complexity of the autonomic heart rate modulation were included, but also the chaotic behaviour was quantified by means of the numerical noise titration technique. A higher nonlinear behaviour was observed during the night while nonlinear heart rate fluctuations decline with age. A clear circadian profile could be found for almost every parameter, showing in particular which changes occur during the transition phases of waking up and going to sleep. The results supported the involvement of the autonomic nervous system in the generation of nonlinear and complex heart rate dynamics.

Effect of stress

In the study about stress, HRV was very useful to detect mental and physical stress. We were able to distinguish between rest, physical and mental load by combining different HRV characteristics. The addition of a mental load to a physical task did elicit any further effect on HRV parameters related to autonomic cardiac modulation. The fact that quantifying HRV is easy and inexpensive makes it a promising tool to use in daily life environment in near future.

Impact of weightlessness in space

We confirmed the influence of microgravity on cardiovascular control, but — contrarily to what was thought in literature — no remarkable difference was found between astronauts from short and long duration spaceflights. While the vagal modulation decreased significantly during day and night at early post-flight, the sympathovagal balance decreased slightly during day time, but increased strongly at night. Therefore, our results confirmed the sympathetic dominance early post-flight, but only at night. This study also proved the change in nonlinear heart rate dynamics, still present after 5 days upon return to Earth and more expressed in the day period. Therefore, nonlinear HRV seems to be more sensitive during day than night time. After one month, a complete cardiovascular recovery was found.

Nonlinear dynamics in cardiovascular control during head-down bed rest

As microgravity in space affected autonomic cardiovascular control, head-down bed rest (HDBR) also did which was expected as this is used to simulate microgravity on Earth. In particular, we proved a change in nonlinear heart rate and blood pressure dynamics during HDBR, often still present after a week of recovery. Moreover, we tested the role of Chinese herbal medicine (Tai Kong Yang Xin Prescription) and it seemed to restrict the influences of microgravity environment during HDBR on the cardiovascular regulation, though only partially functions as a countermeasure.

Children with refractory epilepsy

Epileptic patients showed a higher HR and decreased HRV compared to a normal population. Although vagal nerve stimulation (VNS) reduced the epileptic activity, it affected cardiac autonomic modulation as it increased the sympathetic dominance and also changed some nonlinear HRV characteristics. The affected autonomic cardiac control in patients with refractory epilepsy probably plays an important role in arrhythmias and sudden cardiac death.

9.1.4 Other remarks

As clearly mentioned in the text and demostrated multiple times,those nonlinear HRV parameters will not replace linear analysis, but have to be considered as a complement, yielding extra information about a specific aspect of scaling behaviour or complexity of the underlying cardiovascular system. Nonlinear system dynamics provide additional and independent information about physiological as well as pathophysiological cardiovascular regulation. Therefore, it also might provide a valuable addition to current patient monitoring systems.

9.2 Future work

Updating the Task Force

Some nonlinear techniques were very briefly mentioned in the Task Force [355], but since the nineties and especially the last decade, new techniques were developed and improved a lot. The strong increase in calculation power of computers nowadays and in near future makes nonlinear analysis within reach everywhere. However, the wide variety of ways to calculate one specific nonlinear HRV

parameter hinders comparison between studies. Therefore, standardization is required in an updated version of the Task Force.

Physiological meaning of nonlinear techniques

The main disadvantage of nonlinear HRV techniques is without any doubt the lack of a physiological meaning. The mechanisms by which the nonlinear fluctuations are produced need to be further explored. Using more selective drugs or peptides will help to elucidate the pathways involved. Also, several other interventions can be performed to modify the cardiovascular autonomic modulation (instead of pharmacological interventions) such as paced breathing, stress tests, Valsalva manoeuvre, etc. As long as there is no physiological explanation, it will be very hard to convince medical doctors of the usefulness of these nonlinear parameters. In addition, attention has to be paid to make the software user friendly for the medical doctors as they are the main end-users. This is not an easy task because of the strong mathematical background of these methods.

Risk stratification and prognostic value

It has been proven that nonlinear methods add prognostic information to the clinical model, statistically independent from linear measurements in risk stratification of among others congestive heart failure (CHF) patients [217]. Therefore, the quantification of nonlinear properties of HRV provides new powerful tools in cardiovascular diagnosis. There is a variety of potential indices from nonlinear system dynamics theory that seem promising, but have yet to be validated in further clinical trials [218]. Further research is necessary to define which nonlinear parameters have the best discriminating character and for which (cardiovascular) pathology.

Common dynamics and coupling between interacting physiological systems

Combining information from heterogeneous signals is one of the general trends in biomedical signal processing. Nonlinear HRV methods can also be combined with additional cardiovascular signals, such as blood pressure and respiration. The analysis of interactions, couplings and synchronizations is also a powerful tool for research in cardiovascular regulation. It is commonly known that respiration affects HRV (e.g. HF band in spectrum), but how to take this effect ino account remains an open question. Studying the coupling between cardiac and respiratory activity was tried by means of bispectral analysis [170, 397]. The bispectrum was also used to analyze the coupling between blood pressure and HRV in heart

transplant patients [281]. Nevertheless, much more research is needed to quantify these interactions, couplings and common dynamics.

Multicenter studies

With the growing interest in the field of cardiovascular variability, both in linear and nonlinear analysis methods, it can be expected that more multicenter studies will be set-up to explore this interesting field of neurocardiology.

Bibliography

[1] U.R. Acharya, K.P. Joseph, N. Kannathal, C.M Lim, and J.S. Suri. Heart rate variability: a review. *Medical and Biological Engineering and Computing*, 44(12):1031–1051, 2006.

[2] U.R. Acharya, N. Kannathal, and S.M. Krishnan. Comprehensive analysis of cardiac health using heart rate signals. *Physiological Measurement*, 25:1139–1151, 2004.

[3] U.R. Acharya, N. Kannathal, O.W. Seng, L.Y. Ping, and T. Chua. Heart rate analysis in normal subjects of various age groups. *BioMedical Engineering OnLine*, 3(1):24, 2004.

[4] H. Akaike. A new look at the statistical model identification. *IEEE Transactions on Automatic Control*, 19:716–723, 2003.

[5] M. Akay. *Nonlinear Biomedical Signal Processing Vol. II: Dynamic Analysis and Modeling*. Wiley-IEEE Press, NY, USA, 2000.

[6] S. Akselrod, D. Gordon, F.A. Ubel, D.C. Shannon, A.C. Berger, and C.J. Cohen. Power spectrum analysis of heart rate fluctuation: a quantitative probe of beat-to-beat cardiovascular control. *Science*, 213:220–222, 1981.

[7] F. Alehan, I. Erol, T. Cemil, N. Bayraktar, E. Ogüs, and K. Tokel. Elevated CK-MB mass and plasma brain-type natriuretic peptide concentrations following convulsive seizures in children and adolescents: Possible evidence of subtle cardiac dysfunction. *Epilepsia*, 50(4):775–760, 2009.

[8] A. Algra, J.G. Tijssen, J.R. Roelandt, J. Pool, and J. Lubsen. Heart rate variability from 24-hour electrocardiography and the 2-year risk for sudden death. *Circulation*, 88(1):180–185, 1993.

[9] D.M. Altenmüller, M. Zehender, and A. Schulze-Bonhage. High grade atrioventricular block triggered by spontaneous and stimulation induced epileptic activity in the left temporal lobe. *Epilepsia*, 45:1640–1644, 2004.

[10] A. Amici, P. Cicconetti, C. Sagrafoli, A. Baratta, P. Passador, T. Pecci, G. Tassan, W. Verrusio, V. Marigliano, and M. Cacciafesta. Exaggerated morning blood pressure surge and cardiovascular events. A 5-year longitudinal study in normotensive and well-controlled hypertensive elderly. *Archives of Gerontology and Geriatrics*, 49(2):105–109, 2009.

[11] J.F. Annegers, S.P. Coan, W.A. Hauser, and J. Leestma. Epilepsy, vagal nerve stimulation by the ncp system, all-cause mortality, and sudden, unexpected, unexplained death. *Epilepsia*, 41:549–553, 2000.

[12] H. Ansakorpi, J.T. Korpelainen, H.V. Huikuri, U. Tolonen, V.V. Myllylä, and J.I. Isojärvi. Heart rate dynamics in refractory and well controlled temporal lobe epilepsy. *Journal of Neurology, Neurosurgery and Psychiatry*, 72(1):26–30, 2002.

[13] H. Ansakorpi, J.T. Korpelainen, K. Suominen, U. Tolonen, V.V. Myllylä, and J.I. Isojärvi. Interictal cardiovascular autonomic responses in patients with temporal lobe epilepsy. *Epilepsia*, 41(1):42–47, 2000.

[14] R. Ariagno, M. Mirmiran, M. Adams, A. Saporito, A. Dubin, and R. Baldwin. Effect of position on sleep, heart rate variability, and QT interval in preterm infants at 1 and 3 months' corrected age. *Pediatrics*, 111:622–625, 2006.

[15] E.A. Ashley and J. Niebauer. *Cardiology Explained*. Remedica, London, England, 2004.

[16] A.E. Aubert, F. Beckers, and B. Verheyden. Cardiovascular function and basics of physiology in microgravity. *Acta Cardiologica*, 60:129–151, 2005.

[17] A.E. Aubert and D. Ramaekers. Neurocardiology: the benefits of irregularity. The basics of methodology, physiology and current clinical applications. *Acta Cardiologica*, 54(3):107–120, 1999.

[18] A.E. Aubert, D. Ramaekers, F. Beckers, R. Breem, C. Denef, F. Van de Werf, and H. Ector. The analysis of heart rate variability in unrestrained rats. Assessment of methods and results. *Computer Methods and Programs in Biomedicine*, 60:197–213, 1999.

[19] A.E. Aubert, S. Vandeput, F. Beckers, J. Liu, B. Verheyden, and S. Van Huffel. Complexity of cardiovascular regulation in small animals. *Philosophical Transactions of the Royal Society of London. Series A: Mathematical and Physical Sciences*, 367:1239–1250, 2009.

[20] F. Auger, P. Flandrin, P. Gonçalvès, and O. Lemoine. Time-Frequency Toolbox. *CNRS France-Rice University*, 1996.

[21] R.M. Baevsky, V.M. Baranov, I.I. Funtova, A. Diedrich, A.V. Pashenko, A.G. Chernikova, J. Drescher, J. Jordan, and J. Tank. Autonomic cardiovascular and respiratory control during prolonged spaceflights aboard the international space station. *Journal of Applied Physiology*, 103:156–161, 2007.

[22] R.T. Baillie, A.A. Cecen, and C. Erkal. Normal heartbeat series are nonchaotic, nonlinear and multifractal: new evidence from semiparametric and parametric tests. *Chaos*, 19:028503, 2009.

[23] R. Bannister and C.J. Mathias. *Autonomic failure: a textbook of clinical disorders of the autonomic nervous system*. Oxford University Press, NY, USA, 1992.

[24] A.L. Barabási and H.E. Stanley. *Fractal concepts in surface growth*. Cambridge University Press, New York, USA, 1995.

[25] M. Barahona and C.S. Poon. Detection of nonlinear dynamics in short, noisy data. *Nature*, 381:215–217, 1996.

[26] I. Barutcu, A.M. Esen, D. Kaya, M. Turkmen, O. Karakaya, M. Melek, O.B. Esen, and Y. Basaran. Cigarette smoking and heart rate variability: dynamic influence of parasympathetic and sympathetic maneuvers. *Annals of Noninvasive Electrocardiology*, 10(3):324–329, 2005.

[27] A. Baumann, G. Audibert, J. McDonnell, and P.M. Mertes. Neurogenic pulmonary edema. *Acta Anaesthesiologica Scandinavica*, 51:447–455, 2007.

[28] C. Baumgartner, S. Lurger, and F. Leutmezer. Autonomic symptoms during epileptic seizures. *Epileptic Disorders : International Epilepsy Journal with Videotape*, 3:103–116, 2001.

[29] F. Beckers. *Linear and non-linear dynamics of cardiovascular variability: validation and clinical applications*. PhD thesis, K.U.Leuven, 2002.

[30] F. Beckers, D. Ramaekers, and A.E. Aubert. Acts: Automated calculation of tachograms and systograms. *Programs in Biomedical Research*, 4:160–165, 1999.

[31] F. Beckers, D. Ramaekers, J. van Cleemput, W. Droogne, J. Vanhaecke, F. Van de Werf, and A.E. Aubert. Association between restoration of autonomic modulation in the native sinus node and haemodynamic improvement after cardiac transplantation. *Transplantation*, 73:1614–1620, 2002.

[32] F. Beckers, D. Ramaekers, J. van Cleemput, W. Droogne, J. Vanhaecke, F. Van de Werf, and A.E. Aubert. Different evolutions in heart rate variability after heart transplantation: 10-year follow-up. *Transplantation*, 78(10):1523–1531, 2004.

[33] F. Beckers, D. Ramaekers, B. Verheyden, B. Swynghedauw, and A.E. Aubert. Effect of autonomic blockade on nonlinear cardiovascular variability indices. *Journal of Clinical and Experimental Pharmacology*, 33(5-6):431–439, 2006.

[34] F. Beckers, B. Verheyden, and A.E. Aubert. Aging and nonlinear heart rate control in a healthy population. *American Journal of Physiology. Heart and Circulatory Physiology*, 290:2560–2570, 2006.

[35] F. Beckers, B. Verheyden, K. Couckuyt, and A.E. Aubert. Non-linear heart rate control in orthostatic tolerant cosmonauts after short-duration spaceflight. *Microgravity Science and Technology*, 19 (5-6):98–101, 2007.

[36] F. Beckers, B. Verheyden, J. Liu, and A.E. Aubert. Cardiovascular autonomic control after short-duration spaceflights. *Acta Astronautica*, 65:804–812, 2009.

[37] S. Bekheit, M. Tangella, A. El-Sakr, Q. Rasheed, W. Craelius, and N. El-Sherif. Use of heart rate spectral analysis to study the effects of calcium channel blockers on sympathetic activity after myocardial infarction. *American Heart Journal*, 119(1):79–85, 1990.

[38] F. Bellavere, I. Balzani, G. De Masi, M. Carraro, P. Carenza, C. Cobelli, and K. Thomaseth. Power spectral analysis of heart-rate variations improves assessment of diabetic cardiac autonomic neuropathy. *Diabetes*, 41(5):633–640, 1992.

[39] L. Bernardi, F. Keller, M. Sanders, P.S. Reddy, B. Griffith, F. Meno, and M.R. Pinsky. Respiratory sinus arrhythmia in the denervated human heart. *Journal of Applied Physiology*, 67(4):1447–1455, 1989.

[40] L. Bernardi, M. Rossi, and L. Ricordi. Clinical assessment of respiratory sinus arrhythmia by computerized analysis of RR interval and respiration. *Gionale Italiano di Cardiologia*, 22(4):517–529, 1992.

[41] L. Bernardi, F. Valle, M. Coco, A. Calciati, and P. Sleight. Physical activity influences heart rate variability and very-low frequency components in Holter electrocardiograms. *Cardiovascular Research*, 32:324–327, 1996.

[42] L. Bernardi, J. Wdowczyk-Szulc, C. Valenti, S. Castoldi, C. Passino, G. Spadacini G, and P. Sleight. Effects of controlled breathing, mental activity and mental stress with or without verbalization on heart rate variability. *Journal of the American College of Cardiology*, 35:1462–1469, 2000.

[43] L.C. Bernardi, A. Porta, L. Gabutti, Spicuzza, and P. Sleight. Modulatory effects of respiration. *Autonomic Neuroscience: Basic & Clinical*, 90:47–56, 2001.

[44] G.G. Berntson, J.T.Jr. Bigger, D.L. Eckberg, P. Grossman, P.G. Kaufmann, M. Malik, H.N. Nagaraja, S.W. Porges, J.P. Saul, P.H. Stone, and M.W. Van Der Molen. Heart rate variability: origins, methods, and interpretive caveats. *Psychophysiology*, 34(6):623–648, 1997.

[45] G. Bertinieri, M. Di Rienzo, A. Cavalazzi, A.U. Ferrari, A. Pedotti, and G. Mancia. A new approach to analysis of the arterial baroreflex. *Journal of Hypertension. Supplement: Official Journal of the International Society of Hypertension*, 3:79–81, 1985.

[46] A. Bianchi, B. Bontempi, S. Cerutti, P. Gianoglio, G. Comi, and M.G. Natali Sora. Spectral analysis of heart rate variability signal and respiration in diabetic subjects. *Medical and Biological Engineering and Computing*, 28(3):205–211, 1990.

[47] J.T.Jr. Bigger, J.L. Fleiss, L.M. Rolnitzky, and R.C. Steinman. Frequency domain measures of heart period variability to assess risk late after myocardial infarction. *Journal of the American College of Cardiology*, 21(3):729736, 1993.

[48] J.T.Jr. Bigger, J.L. Fleiss, R.C. Steinman, L.M. Rolnitzky, R.E. Kleiger, and J.N. Rottman. Frequency domain measures of heart period variability and mortality after myocardial infarction. *Circulation*, 85(1):164–171, 1992.

[49] J.T.Jr. Bigger, R.C. Steinman, L.M. Rolnitzky, J.L. Fleiss, P. Albrecht, and R.J. Cohen. Power law behavior of RR-interval variability in healthy middle-aged persons, patients with recent acute myocardial infarction, and patients with heart transplants. *Circulation*, 93(12):2142–2151, 1996.

[50] G.E. Billman and R.S. Hoskins. Time-series analysis of heart rate variability during submaximal exercise. Evidence for reduced cardiac vagal tone in animals susceptible to ventricular fibrillation. *Circulation*, 80(1):146–157, 1989.

[51] T. Binder, B. Frey, G. Porenta, G. Heinz, M. Wutte, G. Kreiner, H. Gössinger, H. Schmidinger, R. Packer, and H. Weber. Prognostic value of heart rate variability in patients awaiting cardiac transplantation. *Pacing and Clinical Electrophysiology*, 15(11):2215–2220, 2006.

[52] C.A. Blamick, D.J. Goldwater, and V.A. Convertino. Leg vascular responsiveness during acute orthostasis following simulated weightlessness. *Aviation, Space, and Environmental Medicine*, 59:40–43, 1988.

[53] S. Blanc, S. Normand, P. Ritz, C. Pachiaudi, L. Vico, C. Gharib, and G. Gauquelin-Koch. Energy and water metabolism, body composition, and hormonal changes induced by 42 days of enforced inactivity and simulated weightlessness. *The Journal of Clinical Endocrinology and Metabolism*, 83:4289–4297, 1998.

[54] K.E. Bloch. Polysomnography: a systematic review. *Technology and Health Care : Official Journal of the European Society for Engineering and Medicine*, 5:285–305, 1997.

[55] R.W. De Boer, J.M. Karemaker, and J. Strackee. Hemodynamic fluctuations and baroreflex sensitivity in humans: a beat-to-beat model. *American Journal of Physiology*, 253(3):680–689, 1987.

[56] C. Bogaert, F. Beckers, D. Ramaekers, and A.E. Aubert. Analysis of heart rate variability with correlation dimension method in a normal population and in heart transplant patients. *Autonomic Neuroscience : Basic & Clinical*, 90:142–147, 2001.

[57] H. Bonnemeier, U.K.H. Wiegand, A. Brandes, N. Kluge, H.A. Katus, G. Richardt, and J. Potratz. Circadian profile of cardiac autonomic nervous modulation in healthy subjects: differing effects of aging and gender on heart rate variability. *Journal of Cardiovascular Electrophysiology*, 14:791–799, 2003.

[58] J.J. Bray, P.A. Crag, A.D.C. Macknight, and R.G. Mills. *Lecture notes on human physiology.* Wiley-Blackwell, 4^{th} edition, 1999.

[59] J.W. Britton and E.E. Bennaroch. Seizures and syncope, anatomic basis and diagnostic considerations. *Clinical Autonomic Research: Official Journal of the Clinical Autonomic Research Society*, 16:18–20, 2006.

[60] J.W. Britton, G.R. Ghearing, E.E. Benarroch, and G.D. Cascino. The ictal bradycardia syndrome: localization and lateralization. *Epilepsia*, 47:737–744, 2006.

[61] P. Bušek, J. Vaòková, J. Opavská, J. Salinger, and S. Nevšímalová. Spectral analysis of heart rate variability in sleep. *Physiological Research*, 54:369–376, 2005.

[62] G.C. Butler, Y. Yamamoto, and R.L. Hughson. Fractal nature of short-term systolic bp and hr variability during lower body negative pressure. *The American Journal of Physiology*, 267:26–33, 1994.

[63] A.K. Cashion, P.A. Cowan, E.J. Milstead, A.O. Gaber, and D.K. Hathaway. Heart rate variability, mortality, and exercise in patients with end-stage renal disease. *Progress in Transplantation*, 10(1):10–16, 2000.

[64] G. Casolo, E. Balli, T. Taddei, J. Amuhasi, and C. Gori. Decreased spontaneous heart rate variability in congestive heart failure. *The American Journal of Cardiology*, 64(18):1162–1167, 1989.

[65] G.C. Casolo, P. Stroder, A. Sulla, A. Chelucci, A. Freni, and M. Zerauschek. Heart rate variability and functional severity of congestive heart failure secondary to coronary artery disease. *European Heart Journal*, 16(3):360–367, 1995.

[66] S. Cerutti. In the spotlight: Biomedical Signal Processing. A well established discipline or a paradigm to promising integrated visions? *IEEE Reviews in Biomedical Engineering*, 2:9–11, 2009.

[67] U. Chatow, S. Davidson, B. Reichman, and S. Akselrod. Development and maturation of the autonomic nervous system in premature and full-term infants using spectral analysis of heart rate fluctuations. *Pediatric Research*, 37:294–302, 1995.

[68] G.F. Chess, R.M. Tam, and F.R. Calaresu. Influence of cardiac neural inputs on rhythmic variations of heart period in the cat. *American Journal of Physiology*, 228(3):775–780, 1975.

[69] S. Chillemi, M. Barbi, A. Di Garbo, R. Balocchi, C. Michelassi, C. Carpeggiani, and M. Emdin. Detection of nonlinearity in the healthy heart rhythm. *Methods of Information in Medicine*, 36(4-5):278–281, 1997.

[70] D.J. Christini, K.M. Stein, S.M. Markowitz, S. Mittal, D.J. Slotwiner, M.A. Scheiner, S. Iwai, and B.B. Lerman. Nonlinear-dynamical arrhythmia control in humans. *Proceedings of the National Academy of Sciences of the United States of America*, 98(10):5827–5832, 2001.

[71] E. Chroni, V. Sirrou, E. Trachani, G.C. Sakellaropoulos, and P. Polychronopoulos. Interictal alterations of cardiovagal function in chronic epilepsy. *Epilepsy Research*, 83:117–123, 2008.

[72] F. Clariá, M. Vallverdu, R. Baranowski, L. Chojnowska, and P. Caminal. Heart rate variability analysis based on time-frequency representation and entropies in hypertrophic cardiomyopathy patients. *Physiological Measurement*, 29:401–416, 2008.

[73] H.A. Cohen, H. Ashkenazi, A. Barzilai, and E. Lahat. Acute nocturnal laryngospasm in children: a possible epileptic phenomenon. *Journal of Child Neurology*, 15(3):202–204, 2000.

[74] L. Cohen. *Time-frequency analysis*. Prentice Hall Signal Processing Series. Prentice Hall, Englewood Cliffs, NJ, USA, 1995.

[75] M.A. Cohen and J.A. Taylor. Short-term cardiovascular oscillations in men: measuring and modelling the physiologies. *Journal of Physiology*, 542:669–683, 2002.

[76] J.N. Cohn. Abnormalities of peripheral sympathetic nervous system control in congestive heart failure. *Circulation*, 82(Suppl 2):I59–I67, 1990.

[77] W.H. Cooke, J. Iv, A.A. Crossman, J.F. Fox, T.A. Kuusela, K. Tahvanainen, L.B. Moon, J. Drescher, F.J. Baisch, T. Mano, B.D. Levine, C.G. Blomqvist, and D.L. Eckberg. Nine months in space: effects on human autonomic cardiovascular regulation. *Journal of Applied Physiology*, 89:1039–1045, 2000.

[78] X. Copie, K. Hnatkova, A. Staunton, L. Fei, A.J. Camm, and M. Malik. Predictive power of increased heart rate versus depressed left ventricular ejection fraction and heart rate variability for risk stratification after myocardial infarction: Results of a two-year follow-up study. *Journal of the American College of Cardiology*, 27(2):270–276, 1996.

[79] P.B. Corr, K.A. Yamada, and F.X. Witkowski. Mechanisms controlling cardiac autonomic function and their relation to arrhythmogenesis. In H.A. Fozzard, E. Haber, R.B. Jenning, and A.M. Katz, editors, *The heart and cardiovascular system*, page 1343. Raven, New York, USA, 2^{nd} edition, 1986.

[80] A. Cote. Home and hospital monitoring for alte. *Paediatric Respiratory Reviews*, 7(suppl 1):199–201, 2006.

[81] P. Coumel, J.S. Hermida, B. Wennerblom, A. Leenhardt, P. Maison-Blanche, and B. Cauchemez. Heart rate variability in left ventricular hypertrophy and heart failure, and the effects of beta-blockade: A non-spectral analysis of heart rate variability in the frequency domain and in the time domain. *European Heart Journal*, 12(3):412–422, 1991.

[82] M.J. Cowan, K. Pike, and R.L. Burr. Effects of gender and age on heart rate variability in healthy individuals and in persons after sudden cardiac arrest. *Journal of Electrocardiology*, 27(suppl):1–9, 1994.

[83] J.F. Cox, K. Tahvanainen, T. Kuusela, B.D. Levine, W.H. Cooke, T. Mano, S. Iwase, M. Saito, Y. Sugiyama, A.C Ertl, I. Biaggioni, A. Diedrich, R.M. Robertson, J.H. Zuckerman, L.D. Lane, C.A. Ray, R.J. White, J.A. Pawelczyk, J.C. Buckey, F.J. Baisch, C.G. Bomqvist, D. Robertson, and D.L. Eckberg. Influence of microgravity on astronauts' sympathetic and vagal responses to valsalva's manoeuvre. *The Journal of Physiology*, 538:309–320, 2002.

[84] V. Crasset, S. Mezzetti, M. Antoine, P. Linkowski, J.P. Degaute, and F. van de Borne. Effects of aging and cardiac denervation on heart rate variability during sleep. *Circulation*, 103:84–88, 2001.

[85] T.R. Cripps, M. Malik, T.G. Farrell, and A.J. Camm. Prognostic value of reduced heart rate variability after myocardial infarction: clinical evaluation of a new analysis method. *British Medical Journal*, 65(1):14–19, 1991.

[86] L. Curzi-Dascalova, E. Christova, P. Peirano, B. Singh, and C.G.G. Vicente. Relationship between respiratory pauses and heart rate during sleep in normal premature and full-term newborns. *Journal of Developmental Physiology*, 11:323–330, 1989.

[87] K.J. Dalton, G.S. Dawes, and J.E. Patrick. Diurnal, respiratory and other rhythms of fetal heart rate in lambs. *American Journal of Obstetrics and Gynecology*, 127:14–24, 1977.

[88] H. Daniëls, G. Naulaers, F. Deroost, and H. Devlieger. Polysomnography and home documented monitoring of cardiorespiratory pattern. *Archives of Disease in Childhood*, 81:434–436, 1999.

[89] K.P. Davy, C.A. Desouza, P.P. Jones, and D.R. Seals. Elevated heart rate variability in physically active young and older adult women. *Clinical Science*, 94(6):579–584, 1998.

[90] P.B. Defares, H.M. van der Ploeg, and C.D. Spielberg. Een Nederlandstalige bewerking van Spielberger State-Trait Anxiety Inventory: de zelf-beoordelingsvragenlijst. *De psycholoog*, 15:460–467, 1980.

[91] Z.D. Deng, C.S. Poon, N.M. Arzeno, and E.S. Katz. Heart rate variability in pediatric obstructive sleep apnea. In *Proceedings of the* 28^{th} *Annual International Conference of the IEEE Engineering in Medicine and Biology Society (EMBS)*, volume 28, pages 3565–3568, New York, NY, USA, 2006.

[92] J.W. Denver, S.F. Reed, and S.W. Porges. Methodological issues in the quantification of respiratory sinus arrhythmia. *Journal of Mathematical Biology*, 74:286–294, 2007.

[93] O.M. Doyle, I. Korotchikova, G. Lightbody, W. Marnane, D. Kerins, and G.B. Boylan. Heart rate variability during sleep in healthy term newborns in the early postnatal period. *Physiological Measurement*, 30:847–860, 2009.

[94] M. Drinnan, J. Allen, P. Langley, and A. Murray. Detection of sleep apnoea from frequency analysis of heart rate variability. In *Proceedings of the* 27^{th} *Annual Computers in Cardiology (CinC*, pages 259–262, Cambridge, MA, USA, 2000.

[95] M. Dütsch, M. Hilz, and O. Devinsky. Impaired baroreflex function in temporal lobe epilepsy. *Journal of Neurology*, 253:1300–1308, 2006.

[96] D.L. Eckberg and J.M. Fritsch. Influence of ten-day head-down bed rest on human carotid baroreceptor-cardiac reflex function. *Acta Physiologica Scandinavica*, 144(S604):69–76, 1992.

[97] A. Edner, M. Katz-Salamon, H. Lagercrantz, M. Ericson, and J. Milerad. Heart rate variability in infants with apparent life-threatening events. *Acta Paediatrica*, 89:1329–1329, 2000.

[98] M. Eiselt, L. Curzi-Dascalova, J. Clairambault, F. Kauffmann, C. Medigue, and P. Peirano. Heart rate variability in low-risk prematurely born infants reaching normal term: a comparison with full-term newborns. *Early Human Development*, 32:183–195, 1980.

[99] M. Eiselt, L. Curzi-Dascalova, C. Leffler, and E. Christova. Sigh-related heart rate changes during sleep in premature and full-term newborns. *Neuropediatrics*, 23:286–291, 1992.

[100] M.A. Epstein, M.R. Sperling, and M.J. O'Connor. Cardiac rhythm during temporal lobe seizures. *Neurology*, 42(1):50–53, 1992.

[101] B. Eryonucu, K. Uzun, N. Guler, and M. Bilge. Comparison of the acute effects of salbutamol and terbutaline on heart rate variability in adult asthmatic patients. *European Respiratory Journal*, 17(5):863–867, 2001.

[102] P.S. Espinoza, J.W. Lee, U.B. Tedrow, E.B. Bromfield, and B.A. Dworetzky. Sudden unexpected near death in epilepsy: malignant arrhythmia from a partial seizure. *Neurology*, 72(19):1702–1703, 2009.

[103] H. Evrengül, H. Tanriverdi, D. Dursunoglu, A. Kaftan, O. Kuru, U. Unlu, and M. Kilic. Time and frequency domain analyses of heart rate variability in patients with epilepsy. *Epilepsy Research*, 63:131–139, 2005.

[104] D.J. Ewing, J.M. Neilson, C.M. Shapiro, J.A. Stewart, and W. Reid. Twenty four hour heart rate variability: effects of posture, sleep, and time of day in healthy controls and comparison with bedside tests of autonomic function in diabetic patients. *British Medical Journal*, 65(5):239–244, 1991.

[105] T.S. Faber, A. Staunton, K. Hnatkova, A.J. Camm, and M. Malik. Step wise Strategy of Using Short-and Long-Term Heart Rate Variability for Risk Stratification After Myocardial Infarction. *Pacing and Clinical Electrophysiology*, 19(11):1845–1851, 2006.

[106] T.G. Farrell, Y. Bashir, T. Cripps, M. Malik, J. Poloniecki, E.D. Bennett, D.E. Ward, and A.J. Camm. Risk stratification for arrhythmic events in postinfarction patients based on heart rate variability, ambulatory electrocardiographic variables and the signal-averaged electrocardiogram. *Journal of the American College of Cardiology*, 18(3):687–697, 1991.

[107] L. Fei, X. Copie, M. Malik, and A.J. Camm. Short-and long-term assessment of heart rate variability for risk stratification after acute myocardial infarction. *The American Journal of Cardiology*, 77(9):681–684, 1996.

[108] L. Fei, P.J. Keeling, J.S. Gill, Y. Bashir, D.J. Statters, J. Poloniecki, W.J. McKenna, and A.J. Camm. Heart rate variability and its relation to ventricular arrhythmias in congestive heart failure. *British Medical Journal*, 71(4):322–328, 1994.

[109] R. Ferber and M. Kryger. *Principles and practice of sleep medicine in the child*. W.B. Saunders, Philadelphia, USA, 1995.

[110] J.P. Finley, S.T. Nugent, and W. Hellenbrand. Heart-rate variability in children. Spectral analysis of developmental changes between 5 and 24 years. *Canadian Journal of Physiology and Pharmacology*, 65(10):2048–2052, 1987.

[111] J.S. Floras. Clinical aspects of sympathetic activation and parasympathetic withdrawal in heart failure. *Journal of the American College of Cardiology*, 22(4 Suppl A):72A–84A, 1993.

[112] A. Fogarasi, J. Janszky, and I. Tuxhorn. Autonomic symptoms during childhood partial epileptic seizures. *Epilepsia*, 47:584–588, 2006.

[113] S.M. Fortney, V.S. Schneider, and J.E. Greenleaf. The physiology of bed rest. In M.J. Fregly and C.M. Blatteis, editors, *Handbook of Physiology Vol. II*, pages 889–942. Oxford University Press, NY, USA, 1996.

[114] J.O. Fortrat, D. Sigaudo, R.L. Hughson, A. Maillet, Y. Yamamoto, and C. Gharib. Effect of prolonged head-down bed rest in complex cardiovascular dynamics. *Autonomic Neuroscience : Basic & Clinical*, 86:192–201, 2001.

[115] M. Frankenhaeuser, U. Lundberg, H. Augustson, S. Nilsson, H. Hedman, and K. Wahlstrøm. In *Work, stress, job satisfaction*, pages 1–20. Resta Grafiska, 1989.

[116] R. Freeman, J.P. Saul, M.S. Roberts, R.D. Berger, C. Broadbridge, and R.J. Cohen. Spectral analysis of heart rate in diabetic autonomic neuropathy: a comparison with standard tests of autonomic function. *Archives of Neurology*, 48(2):185–190, 1991.

[117] R. Freeman and S.C. Schachter. Autonomic epilepsy. *Seminars in Neurology*, 15:158–166, 1995.

[118] M.G. Frei and I. Osorio. Left vagus nerve stimulation with the neurocybernetic prosthesis has complex effects on heart rate and on its variability in humans. *Epilepsia*, 42:1007–1016, 2001.

[119] U. Freitas, E. Roulin, J.F. Muir, and C. Letellier. Identifying chaos from heart rate: the right task? *Chaos*, 19:02805, 2009.

[120] J.M. Fritsch, J.B. Charles, B.S. Bennett, M.M. Jones, and D.L. Eckberg. Short-duration spaceflight impairs human carotid baroreceptor-cardiac reflex responses. *Journal of Applied Physiology*, 73:664–671, 1992.

[121] Q. Fu, S. Witkowski, and B.D. Levine. Vasoconstrictor reserve and sympathetic neural control of orthostasis. *Circulation*, 110:2931–2937, 2004.

[122] R. Furlan, S. Guzzetti, W. Crivellaro, S. Dassi, M. Tinelli, G. Baselli, S. Cerutti, F. Lombardi, M. Pagani, and A. Malliani. Continuous 24-hour assessment of the neural regulation of systemic arterial pressure and RR variabilities in ambulant subjects. *Circulation*, 81(2):537–547, 1990.

[123] C.A. Galimberti, E. Marchioni, F. Barzizza, R. Manni, I. Sartori, and A. Tartara. Partial epileptic seizures of different origin variably affect cardiac rhythm. *Epilepsia*, 37:742–747, 1997.

[124] R. Galli, U. Limbruno, C. Pizzanelli, F.S. Giorgi, L. Lutzemberger, G. Strata, L. Pataleo, M. Mariani, A. Iudice, and L. Murri. Analysis of RR variability in drug-resistant epilepsy patients chronically treated with vagus nerve stimulation. *Autonomic Neuroscience : Basic & Clinical*, 107:52–59, 2003.

[125] Y. Gang and M. Malik. Heart rate variability analysis in general medicine. *Indian Pacing and Electrophysiology Journal*, 3(1):34–40, 2003.

[126] A.H. Garde, B. Laursen, A.H. Jørgensen, and B.R. Jensen. Effects of mental and physical demands on heart rate variablility during computer work. *European Journal of Applied Physiology*, 87:456–461, 2002.

[127] G.J. Gates, S.E. Mateika, and J.H. Mateika. Heart rate variability in non-apneic snorers and controls before and after continuous positive airway pressure. *BioMed Central Pulmonary Medicine*, 5(1):9, 2005.

[128] G. Di Gennaro, P. Quarato, and F. Sebastiano. Ictal heart rate increase precedes eeg discharge in drug-resistant mesial temporal lobe seizures. *Clinical Neurophysiology*, 115:1169–1177, 2004.

[129] C. Gharib, G. Gauquelin, J.M. Pequignot, G. Geelen, C.A. Bizollon, and A. Guell. Early hormonal effects of head-down tilt (−10 degrees) in humans. *Aviation, Space, and Environmental Medicine*, 59:624–629, 1988.

[130] M. Giordano, D. Manzella, G. Paolisso, A. Caliendo, M. Varricchio, and C. Giordano. Differences in heart rate variability parameters during the post-dialytic period in type II diabetic and non-diabetic ESRD patients. *Nephrology Dialysis Transplantation*, 16(3):566–573, 2001.

[131] J. Gisolf, R.V. Immink, J.J. van Lieshout, W.J. Stok, and J.M. Karemaker. Orthostatic blood pressure control before and after spaceflight, determined by time-domain baroreflex method. *Journal of Applied Physiology*, 98:1682–1690, 2005.

[132] L. Glass. Introduction to controversial topics in nonlinear science: Is the normal heart rate chaotic? *Chaos*, 19:028501, 2009.

[133] L. Glass and M.C. Mackey. *From clocks to chaos: The rhythms of life*. Princeton University Press, NJ, USA, 1988.

[134] J. Gleick. *Chaos: Making a new science*. Viking Penguin, New York, USA, 1987.

[135] A.L. Goldberger, L.A. Amaral, J.M. Hausdorff, P.C. Ivanov, C.K. Peng, and H.E. Stanley. Fractal dynamics in physiology: alterations with disease and aging. 19(suppl 1):2466–2472, 2002.

[136] A.L. Goldberger, J.E. Mietus, D.R. Rigney, M.L. Wood, and S.M. Fortney. Effects of head-down bed rest on complex heart rate variability: response to LBNP testing. *Journal of Applied Physiology*, 77:2863–2869, 1994.

[137] A.L. Goldberger, D.R. Rigney, J. Mietus, E.M. Antman, and S. Greenwald. Nonlinear dynamics in sudden cardiac death syndrome: heart rate oscillations and bifurcations. *Experientia*, 44:983–987, 1988.

[138] A.L. Goldberger, D.R. Rigney, and B.J. West. Chaos and fractals in human physiology. *Scientific American*, 262:43–49, 1990.

[139] R. González-Camarena, S. Carrasco-Sosa, R. Román-Ramos, M.J. Gaitán-González, V. Medina-Bañuelos, and J. Azpiroz-Leehan. Effect of static and dynamic exercise on heart rate and blood pressure variabilities. *Medicine and Science in Sports and Exercise*, 32:1719–728, 2000.

[140] G.I. Gorodeski. Impact of menopause on the epidemiology and risk factors of coronary heart disease in women. *Experimental Gerontology*, 29:357–375, 1994.

[141] K. Goto, M. Mirmiran, R. Adams, R. Longford, R. Baldwin, M. Boeddiker M, and R. Ariagno. More awakenings and heart rate variability during supine sleep in preterm infants. *Pediatrics*, 103:603–609, 1999.

[142] T. Goto, H. Fukushima, G. Sasaki, N. Matsuo, and T. Takahashi. Evaluation of autonomic nervous system function with spectral analysis of heart rate variability in a case of tetanus. *Brain and Development*, 23(8):791–795, 2001.

[143] P. Grassberger and I. Procaccia. Measuring the strangeness of strange attractors. *Physica D: Nonlinear Phenomena*, 9(1-2):189–208, 1983.

[144] J.E. Greenleaf. Physiology of fluid and electrolyte responses during inactivity: Water immersion and bed rest. *Medicine and Science in Sports and Exercise*, 16:20–25, 1984.

[145] M.P. Griffin, D.E. Lake, E.A. Bissonette, F.E.Jr. Harrel, T.M. O'Shea, and J.R. Moorman. Heart rate characteristics: novel physiomarkers to predict neonatal infection and death. *Pediatrics*, 116(5):1070–1074, 2005.

[146] P. Grossman and E.W. Taylor. Toward understanding respiratory sinus arrhythmia: Relations to cardiac vagal tone, evolution and biobehavioral functions. *Biological Psychology*, 74:263–285, 2007.

[147] G. Gulli, V.E. Claydon, V.L. Cooper, and R. Hainsworth. R-r interval-blood pressure interaction in subjects with different tolerances to orthostatic stress. *Experimental Physiology*, 90(3):367–375, 2005.

[148] S. Guzzetti, E. Piccaluga, R. Casati, S. Cerutti, F. Lombardi, M. Pagani, and A. Malliani. Sympathetic predominance an essential hypertension: a study employing spectral analysis of heart rate variability. *Journal of Hypertension*, 6(9):711–717, 1988.

[149] I. Hagerman, M. Berglund, M. Lorin, J. Nowak, and C. Sylven. Chaos-related deterministic regulation of heart rate variability in time- and frequency domains: effects of autonomic blockade and exercise. *Cardiovascular Research*, 31:410–418, 1996.

[150] S. Hales. Statical essays: containing haemostaticks. An account of some hydraulick and hydrostatical experiments made on the blood and blood vessels of animals. 1733.

[151] O. Hallioglu, C. Okuyaz, E. Mert, and K. Makharoblidze. Effects of antiepileptic drug therapy on heart rate variability in children with epilepsy. *Epilepsy Research*, 79:49–54, 2008.

[152] A.R. Hargens and D.E. Watenpaugh. Cardiovascular adaptation to spaceflight. *Medicine and Science in Sports and Exercise*, 28:977–982, 1996.

[153] T. Harnod, C.C.H. Yang, Y.L. Hsin, K.R. Shieh, P.J. Wang, and T.B. Kuo. Heart rate variability in children with refractory generalized epilepsy. *Seizure*, 17(4):297–301, 2008.

[154] J. Hartikainen, K. Tahvanainen, and T. Kuusela. Short-term measurement of heart rate variability. In M. Malik Jr., editor, *Clinical Guide to Cardiac Autonomic Tests*, pages 149–176. Kluwer Academic, 1998.

[155] J. Hayano, M. Yamada, Y. Sakakibara, T. Fujinami, K. Yokoyama, Y. Watanabe, and K. Takata. Short-and long-term effects of cigarette smoking on heart rate variability. *The American Journal of Cardiology*, 65(1):84–88, 1990.

[156] B. Healy and J. Peck. Bradycardia induced from stimulation of the left versus right central nucleus of the amygdala. *Epilepsy Research*, 28:101–104, 1997.

[157] M.J. Hilz, O. Devinsky, W. Doyle, A. Mauerer, and M. Dütsch. Decrease of sympathetic cardiovascular modulation after temporal lobe epilepsy surgery. *Brain*, 125:985–995, 2002.

[158] N. Hjortskov, D. Rissen, A.K.K Blangsted, N. Fallentin, U. Lundberg, and K. Søgaard. The effect of mental stress on heart rate variability and blood pressure during computer work. *European Journal of Applied Physiology*, 92:84–89, 2004.

[159] S.H. Hohnloser, T. Klingenheben, M. Zabel, and Y.G. Li. Heart rate variability used as an arrhythmia risk stratifier after myocardial infarction. *Pacing and Clinical Electrophysiology*, 20(10):2594–2601, 2006.

[160] E.H. Hon and S.T. Lee. Electronic evaluation of fetal heart rate: VIII. Patterns preceding fetal death: further observations. *American Journal of Obstetrics and Gynecology*, 87:814, 1963.

[161] J. Hu, J. Gao, and W. Tung. Characterizing heart rate variability by scale-dependent Lyapunov exponent. *Chaos*, 19:028506, 2009.

[162] R.L. Hughson, Y. Yamamoto, A.P. Blaber, A. Maillet, J.O. Fortrat, A. Pavy-Le Traon, J.F. Marini, A. Güell, and C. Gharib. Effect of 28-Day Head-Down Bed Rest with Countermeasures on Heart-Rate-Variability During LBNP. *Aviation, Space, and Environmental Medicine*, 65:293–300, 1994.

[163] H.V. Huikuri, T.H. Makikallio, C.K. Peng, A.L. Goldberger, U. Hintze, and M. Møller. Fractal correlation properties of RR interval dynamics and mortality in patients with depressed left ventricular function after an acute myocardial infarction. *Circulation*, 101(1):47–53, 2000.

[164] H.V. Huikuri, S.M. Pikkujamsa, K.E. Airaksinen, M.J. Ikaheimo, A.O. Rantala, J. Kauma, M. Lilja, and Y.A. Kesaniemi. Sex-related differences in autonomic modulation of heart rate in middle-aged subjects. *Circulation*, 94:122–125, 1996.

[165] S.S.Jr. Hull, A.R. Evans, E. Vanoli, P.B. Adamson, M. Stramba-Badiale, D.E. Albert, R.D. Foreman, and P.J. Schwartz. Heart rate variability before and after myocardial infarction in conscious dogs at high and low risk of sudden death. *Journal of the American College of Cardiology*, 16(4):978–985, 1990.

[166] P.C. Ivanov, L.A.N. Amaral, A.L. Goldberger, S. Havlin, M.G. Rosenblum, Z. Struzik, and H.E. Stanley. Multifractality in human heartbeat dynamics. *Nature*, 399:461–465, 1999.

[167] K.I. Iwasaki, R. Zhang, R. Zuckerman, J.A. Pawelczyk, and B.D. Levine. Effect of head-down-tilt bed rest and hypovolemia on dynamic regulation of heart rate and blood pressure. *American Journal of Physiology. Regulatory, Integrative and Comparative Physiology*, 279:2189–2199, 2000.

[168] J. Brouwer, D.J. Van Veldhuisen, A.J. Man In't Veld, J. Haaksma, W.A. Dijk, K.R. Visser, F. Boomsma, P.H.J.M. Dunselman, K.I. Lie and the Dutch Ibopamine Multicenter Trial Study Group. Prognostic value of heart rate variability during long-term follow-up in patients with mild to moderate heart failure. *Journal of the American College of Cardiology*, 28(5):1183–1189, 1996.

[169] T. Jahnukainen, C.V. Ravenswaaij-Arts, J. Jalonen, and I. Valimaki. Dynamics of vasomotor thermoregulation of the skin in term and preterm neonates. *Early Human Development*, 33:133–143, 1993.

[170] J. Jamsek, A. Stefanovska, and P.V.E. McClintock. Nonlinear cardio-respiratory interactions revealed by time-phase bispectral analysis. *Physics in Medicine and Biology*, 49:4407–4425.

[171] K. Jansen and L. Lagae. Cardiac changes in epilepsy. *Seizure: European Journal of Epilepsy*, page doi:10.1016/j.seizure.2010.07.008, 2010.

[172] J. Janszky, A. Fogarasi, V. Toth, V. Magalovaa, C. Gyimesia, N. Kovacsb, R. Schulza, and A. Ebner. Peri-ictal vegetative symptoms in temporal lobe epilepsy. *Epilepsy and Behavior*, 11:125–129, 2007.

[173] L.B. Johansen, C. Gharib, A.M. Allevard, D. Sigaudo, N.J. Christensen, C. Drummer, and P. Norsk. Haematocrit, plasma volume and noradrenaline in humans during simulated weightlessness for 42 days. *Clinical Physiology*, 17:203–210, 1997.

[174] J.V. Johnson and E.M. Hall. Job strain, work place social support, and cardiovascular disease: a cross-sectional study of a random sample of the swedish working population. *American Journal of Public Health*, 78:1336–1342, 1988.

[175] K. Judd. An improved estimator of dimension and some comments on providing confidence intervals. *Physica D. Nonlinear Phenomena*, 56:216–228, 1992.

[176] A. Just, U. Wittmann, B. Nafz, C.D. Wagner, H. Ehmke, H.R. Kirchheim, and P.B. Persson. The blood pressure buffering capacity of nitric oxide by comparison to the baroreceptor reflex. *American Journal of Physiology. Heart and Circulatory Physiology*, 267(2):H521–H527, 1994.

[177] M. Kallio, K. Suominen, A.M. Bianchi, T. Mäkikallio, T. Haapaniemi, S. Astafiev, K.A. Sotaniemi, V.V. Myllylä., and U. Tolonen. Comparison of heart rate variability analysis methods in patients with Parkinson's disease. *Medical and Biological Engineering and Computing*, 40(4):408–414, 2002.

[178] M.V. Kamath and E.L. Fallen. Correction of the heart rate variability signal for ectopic and missing beats. In M. Malik and A.J. Camn, editors, *Heart Rate Variability*, pages 75–85. Futura, 1995.

[179] D. Kaplan and L. Glass. *Understanding nonlinear dynamics*. Springer, Heidelberg, Germany, 1995.

[180] D.T. Kaplan, M.I. Furman, S.M. Pincus, S.M. Ryan, L.A. Lipsitz, and A.L. Goldberger. Aging and the complexity of cardiovascular dynamics. *Biophysical Journal*, 59:945–949, 1991.

[181] D.T. Kaplan and L. Glass. Coarse-grained embeddings of time series: random walks, gaussian random processes, and deterministic chaos. *Physica D. Nonlinear Phenomena*, 64:431–454, 1993.

[182] P. Katona, A. Frasz, and J. Egbert. Maturation of cardiac control in full-term and preterm infants during sleep. *Early Human Development*, 4:145–149, 1980.

[183] M.J. Katz. Fractals and the analysis of waveforms. *Computers in Biology and Medicine*, 18(3):145–156, 1988.

[184] R.M. Kelsey, J. Blascovich, C.L. Leitten, T.R. Schneider, J. Tomaka, and S. Wiens. Cardiovascular reactivity and adaptation to recurrent psychological stress: The moderating effects of evaluative observation. *Psychophysiology*, 37:748–756, 2000.

[185] K.J. Kemper. The yin and yang of integrative clinical care, education, and research. *EXPLORE: The Journal of Science and Healing*, 3:37–41, 2007.

[186] M.B. Kennel and S. Isabelle. Method to distinguish possible chaos from colored noise and to determine embedding parameters. *Physical review A: General physics*, 46:3111–3118, 1992.

[187] D. Kim, Y. Seo, and L. Salahudin. Decreased long term variations of heart rate variability in subjects with higher self reporting stress scores. In *Proceedings of the* 2^{nd} *International Conference on Pervasive Computing Technologies for Healthcare*, pages 289–292, Tampere, Finland, 2008.

[188] R.I. Kitney, S. Byrne, M.E. Edmonds, P.J. Watkins, and V.C. Roberts. Heart rate variability in the assessment of autonomic diabetic neuropathy. *Automedica*, 4:155–167, 1982.

[189] M. Kivimaki, P. Leino-Arjas, R. Luukkonen, H. Riihimaki, J. Vahtera, and J. Kirjonen. Work stress and risk of cardiovascular mortality: prospective cohort study of industrial employees. *British Medical Journal*, 235:857–861, 2002.

[190] R.E. Klabunde. *Cardiovascular physiology concepts*. Lippincott Williams & Wilkins, 2005.

[191] R. Kleiger, J. Miller, J.T.Jr. Bigger, and A. Moss. Decreased heart rate variability and its association with increased mortality after acute myocardial infarction. *The American Journal of Cardiology*, 59(4):256–262, 1987.

[192] T. Klingenheben, U. Rapp, and S.H. Hohnloser. Circadian variation of heart rate variability in postinfarction patients with and without life-threatening ventricular tachyarrhythmias. *Journal of Cardiovascular Electrophysiology*, 6(5):357–364, 2007.

[193] M. Kobayashi and T. Musha. 1/f fluctutions of heartbeat period. *IEEE Signal Processing*, 29(6):456–457, 1982.

[194] M. Korenberg. Identifying nonlinear difference equation and functional expansion representations: the fast orthogonal algorithm. *Annals of Biomedical Engineering*, 16:123–142, 1988.

[195] M. Kozak, L. Krivan, and B. Semrad. Circadian variations in the occurrence of ventricular tachyarrhythmias in patients with implantable cardioverter defibrillators. *Pacing and Clinical Electrophysiology*, 26:731–735, 2003.

[196] S.G. Kuklin, A.A. Dzizinskii, Y.M. Titov, and A.A.Temnikov. Continuous wavelet analysis: a new method for studying nonstationary oscillations in the cardiac rhythm. *Human Physiology*, 32:116–121, 2006.

[197] T.B.J. Kuo, T. Lin, C.C.H. Yang, C.L. Li, C.F. Chen, and P. Chou. Effect of aging on gender differences in neural control of heart rate. *American Journal of Physiology. Heart and Circulatory Physiology*, 277:2233–2239, 1999.

[198] I. De Rogalski Landrot, F. Roche, V. Pichot, G. Teyssier, J.M. Gaspoz, J.C. Barthelemy, and H. Patural. Autonomic nervous system activity in premature and full-term infants from theoretical term to 7 years. *Autonomic Neuroscience : Basic & Clinical*, 136(1-2):105–109, 2007.

[199] P.A. Lanfranchi and V.K. Somers. Arterial baroreflex function and cardiovascular variability: interactions and implications. *American Journal of Physiology. Regulatory, Integrative and Comparative Physiology*, 283(4):815–826, 2002.

[200] Y. Langan, L. Nashef, and J.W. Sander. Sudden unexpected death in epilepsy: a series of witnessed deaths. *Journal of Neurology, Neurosurgery and Psychiatry*, 68:211–213, 2000.

[201] J.H. Lefebvre, D.A. Goodings, M.V. Kamath, and E.L. Fallen. Predictability of normal heart rhythms and deterministic chaos. *Chaos*, 3:267–277, 1993.

[202] H. Leung, P. Kwan, and C.E. Elger. Finding the missing link between ictal bradyarrythmia, ictal asystole and sudden unexpected death in epilepsy. *Epilepsy and Behavior*, 9:19–30, 2006.

[203] F. Leutmezer, C. Schernthaner, S. Lurger, K. Pötzelberger, and C. Baumgartner. Electrocardiographic changes at the onset of epileptic seizures. *Epilepsia*, 44(3):348–354, 2003.

[204] M.N. Levy, R.M. Berne, and A.J. Pappano. *Cardiovascular physiology*. Mosby Elsevier, 9^{th} edition, 2007.

[205] A.T. Lewicke, E.S. Sazonov, M.J. Corwin, M. Neuman, S. Schuckers, and CHIME Study Group. Sleep versus wake classification from heart rate variability using computational intelligence: consideration of rejection in classification models. *IEEE Transactions on Biomedical Engineering*, 55(1):108–118, 2008.

[206] A.T. Lewicke, E.S. Sazonov, S. Schuckers, and CHIME Study Group. Sleep-wake identification in infants: heart rate variability compared to actigraphy. In *Proceedings of the* 26^{th} *Annual International Conference of the IEEE Engineering in Medicine and Biology Society (EMBS)*, pages 442–445, San Fransisco, USA, 2004.

[207] C. Li, D.K. Tang, D.A. Zheng, G.H. Ding, C.S. Poon, and G.Q. Wu. Comparison on nonlinear indices in analyses of heart rate variability. In *Proceedings of the* 30^{th} *Annual International Conference of the IEEE Engineering in Medicine and Biology Society (EMBS)*, volume 30, pages 2145–2148, Vancouver, Canada, 2008.

[208] L.A. Lipsitz, J. Mietus, G.B. Moody, and A.L. Goldberger. Spectral characteristics of heart rate variability before and during postural tilt. Relations to aging and risk of syncope. *Circulation*, 81(6):1803–1810, 1990.

[209] J.X. Liu, Y.Z. Li, B. Verheyden, Z.H. Cheng, S.G. Chen, Q. Xie, and A.E. Aubert. Cardiovascular control during 60 days head-down bed rest: Chinese herbal medicine as a countermeasure. *Space Medicine & Medical Engineering*, 22:391–398, 2009.

[210] F. Lombardi. Chaos theory, heart rate variability, and arrhythmic mortality. *Circulation*, 101(1):8, 2000.

[211] E. Longin, T. Gerstner, T. Schaible, T. Lenz, and S. Konig. Maturation of the autonomic nervous system: differences in heart rate variability in premature vs. term infants. *Journal of Perinatal Medicine*, 34(4):303–308, 2006.

[212] M. Lossius, J.E. Erikssen, P. Mowinckel, P. Gulbrandsen, and L. Gierstad. Changes in autonomic cardiac control in patients with epilepsy after discontinuation of antiepileptic drugs: a randomized controlled withdrawal study. *European Journal of Neurology*, 14:1022–1028, 2007.

[213] D. Lucini, F. Bertocchi, A. Malliani, and M. Pagani. A controlled study of the autonomic changes produced by habitual cigarette smoking in healthy subjects. *Cardiovascular Research*, 31(4):633–639, 1996.

[214] D. Lucini, G. Norbiato, M. Clerici, and M. Pagani. Hemodynamic and autonomic adjustments to real life stress conditions in humans. *Hypertension*, 39:184–188, 2002.

[215] C. Ludwig. Beitrage zur kenntnis des einflusses der respirationsbewegungen auf den blutlauf im aortensysteme. In *Müller's Archiv für Anatomie, Physiologie and Wissenschaftliche Medicin*, pages 242–302. 1847.

[216] U. Lundberg and M. Frankenhaeuser. Pituitary-adrenal and sympathetic-adrenal correlates of distress and effort. *Journal of Psychosomatic Research*, 24:125–130, 1980.

[217] R. Maestri, G. D. Pinna, A. Accardo, P. Allegroni, R. Balocchi, G. DAddio, M. Ferrario, D. Menicucci, A. Porta, R. Sassi, M. G. Signorini, M.T. La Rovere, and S. Cerutti. Nonlinear indices of heart rate variability in chronic heart failure patients: redundancy and comparative clinical value. *Journal of Cardiovascular Electrophysiology*, 18(4):425–433, 2007.

[218] R. Maestri, G.D. Pinna, A. Porta, R. Balocchi, R. Sassi, M.G. Signorini, M. Dudziak, and G. Raczak. Assessing nonlinear properties of heart rate variability from short-term recordings: are these measurements reliable? *Physiological Measurement*, 28:1067–1077, 2007.

[219] T.H. Mäkikallio, S. Høiber, L. Køber, C. Torp-Pedersen, C.K. Peng, A.L. Goldberger, and H.V. Huikuri. Fractal analysis of heart rate dynamics as a predictor of mortality in patients with depressed left ventricular function after acute myocardial infarction. *The American Journal of Cardiology*, 83(6):836–839, 1999.

[220] M. Malik, R. Xia, O. Odemuyiwa, A. Staunton, J. Poloniecki, and A.J. Camm. Influence of the recognition artefact in automatic analysis of long-term electrocardiograms on time-domain measurement of heart rate variability. *Medical and Biological Engineering and Computing*, 31(5):539–544, 1993.

[221] S.C. Malpas. Neural influences on cardiovascular variability: possibilities and pitfalls. *American Journal of Physiology. Heart and Circulatory Physiology*, 282(1):6–20, 2002.

[222] S.C. Malpas and T.J.B. Maling. Heart rate variability and cardiac autonomic function in diabetes. *Diabetes*, 39:11771181, 1990.

[223] S.C. Malpas, E.A. Whiteside, and T.J.B. Maling. Heart rate variability and cardiac autonomic function in men with chronic alcohol dependence. *British Heart Journal*, 65(2):84–88, 1991.

[224] B.B. Mandelbrot. *The fractal geometry of nature.* Freeman, San Francisco, CA, USA, 1983.

[225] E.J. Marey. Études physiologiques sur les caractères graphiques des battements du Coeur. pages 242–302. Masson, Paris, France, 1863.

[226] M. Marmot and S. Stansfeld. *Stress and the heart: psychosocial pathways to coronary heart disease.* Wiley, London, 2001.

[227] G.J. Martin, N.M. Magid, G. Myers, P.S. Barnett, J.W. Schaad, J.S. Weiss, M. Lesch, and D.H. Singer. Heart rate variability and sudden death secondary to coronary artery disease during ambulatory electrocardiographic monitoring. *The American Journal of Cardiology*, 60(1):86–89, 1987.

[228] R. Massetani, G. Strata, and R. Galli. Alteration of cardiac function in patients with temporal lobe epilepsy: different roles of EEG-ECG monitoring and spectral analysis of RR variability. *Epilepsia*, 38:363–369, 1997.

[229] M.M. Massin, N. Withofs, K. Maeyns, F. Ravet, and P. Gerard. Normal ranges for the variability in heart rate in young infants while sleeping. *Cardiology in the Young*, 11(6):619–625, 2001.

[230] H. Mayer, F. Benninger, L. Urak, B. Plattner, J. Geldner, and M. Feucht. EKG abnormalities in children and adolescents with symptomatic temporal lobe epilepsy. *Neurology*, 63:324–328, 2004.

[231] B.S. McEwen and E.Stellar. Stress and the individual: mechanisms leading to disease. *Archives of Internal Medicine*, 153:2093–2101, 1993.

[232] S. Mehta, D. Super, D. Connuck, A. Salvator, L. Singer, L. Fradley, R.A. Harcar-Sevik, H.L. Kirchner, and E.S. Kaufman. Heart rate variability in healthy newborn infants. *The American Journal of Cardiology*, 89:50–53, 2002.

[233] E. Ben Menachem, A. Hamberger, T. Hedner, E.J. Hammond, B.M. Uthman, J. Slater, T. Treig, H. Stefan, R.E. Ramsay, J.F. Wernicke, and B.J. Wilder. Effects of vagus nerve stimulation on amino acids in the CSF of patients with partial seizures. *Epilepsy Research*, 20:221–227, 1995.

[234] E.S. Mezzacappa, R.M. Kelsey, E.S. Katkin, and R. Sloan. Vagal rebound and recovery from psychological stress. *Psychosomatic Medicine*, 63:650–657, 2001.

[235] T. Mi, Y.Z. Li, Q.C. Fan, S. Zhao, G. Bai, and L.Z. Zhou. Effects of taikong yangxin prescription on heart function in tail suspension rats. *Space Medicine & Medical Engineering*, 21:22–25, 2008.

[236] D.E. Mohrman and L.J. Heller. *Cardiovascular physiology*. Lange Medical Books/McGraw-Hill, 6^{th} edition, 2006.

[237] H. Mølgaard, K.E. Sørensen, and P. Bjerregaard. Attenuated 24-h heart rate variability in apparently healthy subjects, subsequently suffering sudden cardiac death. *Clinical Autonomic Research*, 1(3):233–237, 1991.

[238] G. Morren. *Advanced signal processing applied to in-vivo spectroscopy and heart rate variability*. PhD thesis, K.U.Leuven, 2004.

[239] G. Morren, S. Van Huffel, I. Helon, G. Naulaers, H. Daniëls, H. Devlieger, and P. Casaer. Effects of non-nutritive sucking on heart rate, respiration and oxygenation: a model-based signal processing approach. *Comparative Biochemistry and Physiology. Part A, Physiology*, 132:97–106, 2002.

[240] A. Mortara, M.T. La Rovere, M.G. Signorini, P. Pantaleo, G. Pinna, L. Martinelli, C. Ceconi, S. Cerutti, and L. Tavazzi. Can power spectral analysis of heart rate variability identify a high risk subgroup of congestive heart failure patients with excessive sympathetic activation? A pilot study before and after heart transplantation. *British Medical Journal*, 71(5):422–430, 1994.

[241] A. Mortara and L. Tavazzi. Prognostic implications of autonomic nervous system analysis in chronic heart failure: Role of heart rate variability and baroreflex sensitivity. *Archives of Gerontology and Geriatrics*, 23(3):265–275, 1996.

[242] S. Mukherjee, M. Tripathi, P.S. Chandra, R. Yadav, N. Choudary, R. Sagar, R. Bhore, R.M. Pandey, and K.K. Deepak. Cardiovascular autonomic functions in well-controlled and intractable partial epilepsies. *Epilepsy Research*.

[243] J.E. Muller, P.L. Ludmer, S.N. Willich, G.H. Tofler, G. Aylmer, I. Klangos, and P.H. Stone. Circadian variation in the frequency of sudden cardiac death. *Circulation*, 75:131–138, 1987.

[244] J.E. Muller, J. Morrison, P.H. Stone, R.E. Rude, B. Rosner, R. Roberts, D.L. Pearle, Z.G. Turi, J.F. Schneider, and D.H. Serfas. Nifedipine therapy for patients with threatened and acute myocardial infarction: a randomized, double-blind, placebo-controlled comparison. *Circulation*, 69(4):740–747, 1984.

[245] J.E. Muller, G.H. Tofler, and P.T. Stone. Circadian variation and triggers of onset of acute cardiovascular disease. *Circulation*, 79:733–743, 1989.

[246] H. Mussalo, E. Vanninen, R. Ikäheimo, T. Laitinen, M. Laakso, E. Länsimies, and J. Hartikainen. Heart rate variability and its determinants in patients with severe or mild essential hypertension. *Clinical Physiology*, 21(5):594–604, 2008.

[247] G.A. Myers, G.J. Martin, N.M. Magid, P.S. Barnett, J.W. Schaad, J.S. Weiss, M. Lesch, and D.H. Singer. Power Spectral Analysis of Heart Rate Varability in Sudden Cardiac Death: Comparison to Other Methods. *IEEE Transactions on Biomedical Engineering*, pages 1149–1156, 1986.

[248] M. Myrtek, D. Weber, G. Brügner, and W. Müller. Occupational stress and strain of female students: results of physiological, behavioural, and psychological monitoring. *Biological Psychology*, 42:379–391, 1996.

[249] E. Nagy, H. Orvos, G. Bárdos, and P. Molnar. Gender-related heart rate differences in human neonates. *Pediatric Research*, 47(6):778–780, 2000.

[250] M. Nakagawa, T. Saikawa, and M. Ito. Progressive reduction of heart rate variability with eventual sudden death in two patients. *British Medical Journal*, 71(1):87–88, 1994.

[251] L. Nashef, S. Garner, J.W. Sander, D.R. Fish, and S.D. Shorvon. Circumstances of death in sudden death in epilepsy. *Journal of Neurology, Neurosurgery and Psychiatry*, 64:349–352, 1998.

[252] M. Nei, R.T. Ho, B.W. Abou-Khalil, F.W. Drislane, J. Liporace, A. Romeo, and M.R. Sperling. EEG and EKG in sudden unexplained death in epilepsy. *Epilepsia*, 45(4):336–345, 2004.

[253] M. Nei, R.T. Ho, and R. Sperling. EKG abnormalities during partial seizures in refractory epilepsy. *Epilepsia*, 41(5):542–548, 2000.

[254] D.A. Nelson and C.D. Ray. Respiratory arrest from seizure discharges in limbic system. *Archives of Neurology*, 19:199–207, 1986.

[255] O.N. Niedermaier, M.L. Smith, L.A. Beightol, Z. Zukowska-Grojec, D.S. Goldstein, and D.L. Eckberg. Influence of cigarette smoking on human autonomic function. *Circulation*, 88(2):562–571, 1993.

[256] K.B. Nilsen, T. Sand, L.J. Stovner, R.B Leistad, and R.H. Westgaard. Autonomic and muscular responses and recovery to one-hour laboratory mental stress in healthy subjects. *BioMed Central Musculoskeletal Disorders*, 8:81, 2007.

[257] R.P. Nolan, M.V. Kamath, J.S. Floras, J. Stanley, C. Pang, P. Picton, and Q.R. Young. Heart period variability biofeedback as a behavioral neurocardiac intervention to enhance vagal heart rate control. *American Heart Journal*, 149:1137, 2005.

[258] P. Norsk, M. Damgaard, L. Petersen, M. Gybel, B. Pump, A. Gabrielsen, and N.J. Christensen. Vasorelaxation in space. *Hypertension*, 47:69–73, 2006.

[259] O. Odemuyiwa, M. Malik, T. Farrell, Y. Bashir, J. Poloniecki, and J. Camm. Comparison of the predictive characteristics of heart rate variability index and left ventricular ejection fraction for all-cause mortality, arrhythmic events and sudden death after acute myocardial infarction. *The American Journal of Cardiology*, 68(5):434–439, 1991.

[260] K. Opeskin and S. Berkovic. Risk factors for sudden unexpected death in epilepsy: a controlled prospective study based on coroners cases. *Seizure*, 12:456–464, 2003.

[261] C. Opherc, J. Coromilan, and L.J. Hirsch. Heart rate and EKG changes in 102 seizures: analysis of influencing factors. *Epilepsy Research*, 52:117–127, 2002.

[262] S.M. Oppenheimer, A. Gelb, J.P. Girvin, and V.C. Hachinski. Cardiovascular effects of human insular cortex stimulation. *Neurology*, 42(9):1727–1732, 1992.

[263] S.M. Oppenheimer, J.X. Wilson, C. Guiraudon, and D.F. Cechetto. Insular cortex stimulation produces lethal cardiac arrhythmias: a mechanism of sudden death? *Brain Research*, 550(1):115–121, 1991.

[264] H. Oxenham and N. Sharpe. Cardiovascular aging and heart failure. *European Journal of Heart Failure : Journal of the Working Group on Heart Failure of the European Society of Cardiology*, 5:427–434, 2003.

[265] M. Pagani and D. Lucini. Autonomic dysregulation in essential hypertension: insight from heart rate and arterial pressure variability. *Autonomic Neuroscience*, 90(1-2):76–82, 2001.

[266] M. Pagani, G. Malfatto, S. Pierini, R. Casati, A.M. Masu, M. Poli, S. Guzzetti, F. Lombardi, S. Cerutti, and A. Malliani. Spectral analysis of heart rate variability in the assessment of autonomic diabetic neuropathy. *Journal of the Autonomic Nervous System*, 23(2):143–153, 1988.

[267] M. Pagani and A. Malliani. Interpreting oscillations of muscle sympathetic nerve activity and heart rate variability. *Journal of Hypertension*, 18(12):1709–1719, 2000.

[268] M. Pagani, G. Mazzuero, A. Ferrari, D. Liberati, S. Cerutti, D. Vaitl, L. Tavazzi, and A. Malliani. Sympathovagal interaction during mental stress. A study using spectral analysis of heart rate variability in healthy control subjects and patients with prior myocardial infarction. *Circulation*, 83(suppl 2):43–51, 1991.

[269] J. Pan and W.J. Tompkins. A real time qrs detection algorithm. *IEEE Transactions on Biomedical Engineering*, 32:230–236, 1985.

[270] C. Pater, D. Compagnone, J. Luszick, and C.N. Verboom. Effect of Omacor on HRV parameters in patients with recent uncomplicated myocardial infarction – A randomized, parallel group, double-blind, placebo-controlled trial: study design. *Current Controlled Trials in Cardiovascular Medicine*, 4(1):2, 2003.

[271] A. Patzak, R. Mrowka, S. Springer, T. Eckard, O. Ipsiroglu, T. Erler, and S. Hofmann. Herzfrequenzvariabilitat - methoden, physiologie und application im pädiatrischen schlaflabor. *Wiener Klinische Wochenschrift*, 112:234–250, 2000.

[272] A.M. Pellizzer, P.W. Kamen, M.D. Esler, S. Lim, and H. Krum. Comparative effects of mibefradil and nifedipine gastrointestinal transport system on autonomic function in patients with mild to moderate essential hypertension. *Journal of Hypertension*, 19(2):279–285, 2001.

[273] C.K. Peng, S. Havlin, J.M. Hausdorff, J.E. Mietus, H.E. Stanley, and A.L. Goldberger. Fractal mechanisms and heart rate dynamics. *Journal of Electrocardiology*, 28(Suppl):59–64, 1996.

[274] R. Perini, S. Milesi, N.M. Fisher, D.R. Pendergast, and A. Veicsteinas. Heart rate variability during dynamic exercise in elderly males and females. *European Journal of Applied Physiology*, 82:8–15, 2000.

[275] H. Persson, M. Ericson, and T. Tomson. Carbamazepine affects autonomic cardiac control in patients with newly diagnosed epilepsy. *Epilepsy Research*, 57(1):69–75, 2003.

[276] H. Persson, M. Ericson, and T. Tomson. Heart rate variability in patients with untreated epilepsy. *Seizure*, 16:504–508, 2007.

[277] P.B. Persson, M. Di Rienzo, P. Castiglioni, S. Cerutti, M. Pagani, N. Honzikova, S. Akselrod, and G. Parati. Time versus frequency domain techniques for assessing baroreflex sensitivity. *Journal of Hypertension*, 19(10):1699–1705, 2001.

[278] S.M. Pikkujamsa, T.H. Makikallio, K.E. Airaksinen, and H.V. Huikuri. Determinants and interindividual variation of R-R interval dynamics in healthy middle-aged subjects. *American Journal of Physiology. Heart and Circulatory Physiology*, 280:1400–1406, 2001.

[279] S.M. Pikkujamsa, T.H. Makikallio, L.B. Sourander, I.J. Raiha, P. Puukka, J. Skytta, C.K. Peng, A.L. Goldberger, and H.V. Huikuri. Cardiac interbeat interval dynamics from childhood to senescence: comparison of conventional

and new measures based on fractals and chaos theory. *Circulation*, 100:393–399, 1999.

[280] S.M. Pincus. Approximate entropy as a measure of system complexity. *Proceedings of the National Academy of Sciences of the United States of America*, 88:2297–2301, 1991.

[281] I. Pinhas, E. Toledo, D. Aravot, and S. Akselrod. Bicoherence analysis of new cardiovasculr spectral components observed in heart-transplant patients: statistical approach for bicoherence thresholding. *IEEE Transactions on Biomedical Engineering*, 51:1774–1783.

[282] A. Pipilis, M. Flather, O. Ormerod, and P. Sleight. Heart rate variability in acute myocardial infarction and its association with infarct site and clinical course. *The American Journal of Cardiology*, 67(13):1137–1139, 1991.

[283] C.S. Poon. Cardiac chaos: implications for congestive heart failure. *Congestive Heart Failure*, 5:270–274, 1999.

[284] C.S. Poon. The chaos about heart rate chaos. *Journal of Cardiovascular Electrophysiology*, 11:235–236, 2000.

[285] C.S. Poon and M. Barahona. Titration of chaos with added noise. *Proceedings of the National Academy of Sciences of the United States of America*, 98:7107–7112, 2001.

[286] C.S. Poon and C.K. Merrill. Decrease of cardiac chaos in congestive heart failure. *Nature*, 389:492–495, 1997.

[287] C.A.3^{rd}. Pope, D.J. Eatough, D.R. Gold, Y. Pang, K.R. Nielsen, P. Nath, R.L. Verrier, and R.E. Kanner. Acute exposure to environmental tobacco smoke and heart rate variability. *Environmental Health Perspectives*, 109(7):711–716, 2001.

[288] S.W. Porges. Cardiac vagal tone: a physiological index of stress. *Neuroscience and Biobehavioral Reviews*, 19:225–233, 1995.

[289] S.W. Porges, R.E. Bohrer, M.N. Cheung, F. Drasgow, P.M. McCabe, and G. Keren. New time-series statistic for detecting rhythmic co-occurrence in the frequency domain: The weighted coherence and its application to psychophysiological research. *Psychological Bulletin*, 88(3):580–587, 1980.

[290] S.W. Porges and D.C. Raskin. Respiratory and heart rate components of attention. *Journal of Experimental Psychology*, 81:497–503, 1969.

[291] M. Poyhonen, S. Syvaoja, J. Hartikainen, E. Ruokonen, and J. Takala. The effect of carbon dioxide, respiratory rate and tidal volume on human heart rate variability. *Acta Anaesthesiologica Scandinavia*, 48:93–101, 2004.

[292] H.M. Van Praag. Crossroads of corticopin releasing hormone, corticosteroids and monoamines. about the interface between stress and depression. *Neurotoxicity Research*, 4:531–555, 2002.

[293] M. Quintana, N. Storck, L.E. Lindblad, K. Lindvall, and M. Ericson. Heart rate variability as a means of assessing prognosis after acute myocardial infarction: a 3-year follow-up study. *European Heart Journal*, 18(5):789–797, 1997.

[294] D. Ramaekers, H. Ector, A.E. Aubert, A. Rubens, and F. Van de Werf. Heart rate variability and heart rate in healthy volunteers: is the female autonomic nervous system cardioprotective? *European Heart Journal*, 19:1334–1341, 1998.

[295] D. Ramaekers, H. Ector, J. Vanhaecke, J. Van Cleemput, and F. Werf. Heart rate variability after cardiac transplantation in humans. *Pacing and Clinical Electrophysiology*, 19(12):2112–2199, 1996.

[296] M. Rangari, S. Sinha, D. Kapoor, J.C. Mohan, and S.K. Sarin. Prevalence of autonomic dysfunction in cirrhotic and noncirrhotic portal hypertension. *The American Journal of Gastroenterology*, 97(3):707–713, 2002.

[297] C. Van Ravenswaaij-Arts, J.C.W. Hopman, L.A.A. Kollée, J.P.L. Van Amen, G. Stoelinga, and H.P. Van Geijn. Influences on heart rate variability in spontaneously breathing preterm infants. *Early Human Development*, 27(3):187–205, 1991.

[298] A.L.P. Ribeiro, F. Lombardi, M.R. Sousa, M.V. Lins Barros, A. Porta, V. Costa Val Barros, M.E.D. Gomes, F. Santana Machado, and M. Otávio Costa Rocha. Power-law behavior of heart rate variability in Chagas' disease. *The American Journal of Cardiology*, 89(4):414–418, 2002.

[299] J.S. Richman and R.J. Moorman. Physiological time-series analysis using approximate entropy and sample entropy. *American Journal of Physiology. Heart and Circulatory Physiology*, 278:2039–2049, 2000.

[300] D.R. Rigney, W.C. Ocasio, K.P. Clark, J.Y. Wei, and A.L. Goldberger. Deterministic mechanism for chaos and oscillations in heart rate and blood pressure. *Circulation*, 86:I659, 1992.

[301] J.V. Ringwood and S.C. Malpas. Slow oscillations in blood pressure via a nonlinear feedback model. *American Journal of Physiology. Regulatory, Integrative and Comparative Physiology*, 280(4):1105–1115, 2001.

[302] T. Ritz. Studying noninvasive indices of vagal control: The need for respiratory control and the problem of target specificity. *Biological Psychology*, 80:158–168, 2009.

[303] T. Ritz and B. Dahme. Implementation and interpretation of respiratory sinus arrhythmia measures in psychosomatic medicine: Practice against better evidence? *Psychosomatic Medicine*, 68:617–627, 2006.

[304] H.W. Robbe, L.J. Mulder, H. Ruddel, W.A. Langewitz, J.B. Veldman, and G. Mulder. Assessment of baroreceptor reflex sensitivity by means of spectral analysis. *Hypertension*, 10(5):538–543, 1987.

[305] R. Rocamora, M. Kurthen, L. Lickfett, J. Von Oertzen, and C.E. Elger. Cardiac asystole in epilepsy: clinical and neurophysiological features. *Epilepsia*, 44:179–185, 2003.

[306] M.B. Rocco, J. Barry, S. Campbell, E. Nabel, E.F. Cook, L. Goldman, and A.P. Selwyn. Circadian variation of transient myocardial ischemia in patients with coronary artery disease. *Circulation*, 75:395–400, 1987.

[307] F. Roche, J.M. Gaspoz, I. Court-Fortune, P. Minini, V. Pichot, D. Duverney, F. Costes, J.-R. Lacour, and J.-C. Barthélémy. Screening of obstructive sleep apnea syndrome by heart rate variability analysis. *Circulation*, 100(13):1411–1415, 1999.

[308] E. Ronkainen, H. Ansakorpi, H.V. Huikuri, V.V. Myllylä, J.I. Isojärvi, and J.T. Korpelainen. Suppressed circadian heart rate dynamics in temporal lobe epilepsy. *Journal of Neurology, Neurosurgery and Psychiatry*, 76(10):1382–1386, 2005.

[309] E. Ronkainen, J.T. Korpelainen, E. Heikkinen, V.V. Myllylä, H.V. Huikuiri, and J.I. Isojärvi. Cardiac autonomic control in patients with refractory epilepsy before and during vagus nerve stimulation treatment: a one-year follow-up study. *Epilepsia*, 47:556–562, 2006.

[310] R.W. Roosevelt, D.C. Smith, R.W. Clough ad R.A. Jensen, and R.A. Browning. Increased extracellular concentrations of norepinephrine in cortex and hippocampus following vagus nerve stimulation in the rat. *Brain Research*, 1119:124–132, 2006.

[311] M. Rosenstein, J.J. Collins, and C.J. De Luca. A practical method for calculating largest lyapunov exponents from small data sets. *Physica D. Nonlinear Phenomena*, 65:117–134, 1993.

[312] J. Rossinen, M. Vitasalo, J. Partanen, P. Koskinen, M. Kupari, and M.S. Nieminen. Effects of acute alcohol ingestion on heart rate variability in patients with documented coronary artery disease and stable angina pectoris. *The American Journal of Cardiology*, 79(4):487–491, 1997.

[313] M.T. La Rovere, J.T.Jr. Bigger, F.I. Marcus, A. Mortara, and P.J. Schwartz. Baroreflex sensitivity and heart-rate variability in prediction of total cardiac

mortality after myocardial infarction. ATRAMI (Autonomic Tone and Reflexes After Myocardial Infarction) Investigators. *Lancet*, 351(9101):478–484, 1998.

[314] F.J. Rugg-Gunn, R.J. Simister, M. Squirrell, D.R. Holdright, and J.S. Duncan. Cardiac arrhythmias in focal epilepsy: a prospective long term study. *Lancet*, 364(9452):2212–2219, 2004.

[315] P. Rutecki. Anatomical, physiological,and theoretical basis for the antiepileptic effects of vagus nerve stimulation. *Epilepsia*, 31(supp12):S1–S6, 1990.

[316] J.M. Ryan and L.G. Howes. White coat effect of alcohol. *American Journal of Hypertension*, 13:1135–1138, 2000.

[317] S.M. Ryan, A.L. Goldberger, S.M. Pincus, J. Mietus, and L.A. Lipsitz. Gender- and age-related differences in heart rate: are women more complex than men? *Journal of the American College of Cardiology*, 24(7):1700–1707, 1994.

[318] G. Sammer. Heart period variability and respiratory changes associated with physical and mental load: nonlinear analysis. *Ergonomics*, 41:746–755, 1998.

[319] R. Sassi, M.G. Signorini, and S. Cerutti. Multifractality and heart rate variability. *Chaos*, 19:028507, 2009.

[320] T.N. Sathyaprabha, P. Satishchandra, K. Netravathi, S. Sinha, K. Thennarasu, and T.R. Raju. Cardiac autonomic dysfunctions in chronic refractory epilepsy. *Epilepsy Research*, 72:49–56, 2006.

[321] J.P. Saul, P. Albrecht, R.D. Berger, and R.J. Cohen. Analysis of long term heart rate variability: methods, 1/f scaling and implications. In *Proceedings of the* 14^{th} *Annual International Conference of Computers in Cardiology (CinC)*, volume 14, pages 419–422, Washington, DC, USA, 1987.

[322] L. Saul and L. Bernardi. Heart rate variability after cardiac. In M. Malik and A.J. Camm, editors, *Heart Rate Variability*. Futura, Armonk, NY, USA, 1995.

[323] B.M.A. Sayers. Analysis of heart rate variability. *Ergonomics*, 16(1):17–32, 1973.

[324] C. Schernthaner, G. Lindinger, K. Pötzelberger, K. Zeiler, and C. Baumgartner. Autonomic epilepsy, the influence of epileptic discharges on heart rate and rhythm. *Wiener Klinische Wochenschrift*, 111:392–401, 1999.

[325] R.F. Schmidt and G. Thews. *Human physiology*. Springer-Verlag, 1989.

[326] S. Schuele, A. Bermeo, E. Alexopoulos, E.R. Locatelli, R.C. Burgess, D.S. Dinner, and N. Foldvary-Schaefer. Video-electrographic and clinical features in patients with ictal asystole. *Neurology*, 69:434–441, 2007.

[327] S. Schuele, A. Bermeo, E.R. Locatelli, R.C. Burgess, and H.O. Lüders. Ictal asystole: a benign condition? *Epilepsia*, 49:168–171, 2008.

[328] A. Schumacher. Linear and nonlinear approaches to the analysis of RR interval variability. *Biological Research for Nursing*, 5(3):211–221, 2004.

[329] J.B. Schwartz, W.J. Gibb, and T. Tran. Aging effects on heart rate variation. *The Journal of Gerontology*, 46(3):99–106, 1991.

[330] P.J. Schwartz and S.G. Priori. Sympathetic nervous system and cardiac arrhythmias. In D.P. Pipes and J. Jalife, editors, *Cardiac electrophysiology. From Cell to bedside*, pages 330–343. W.B. Saunders, Philadelphia, USA, 1990.

[331] P.J. Schwartz, M.T. La Rovere, and E. Vanoli. Autonomic nervous system and sudden cardiac death. Experimental basis and clinical observations for post-myocardial infarction risk stratification. *Circulation*, 85:177–191, 1992.

[332] E.M. Scott. *Cardiovascular physiology: an integrative approach*. Manchester University Press, Manchester, England, 1986.

[333] J. Sedy, J. Zicha, J. Kunes, P. Jendelová, and E. Syková. Mechanisms of neurogenic pulmonary edema development. *Physiological Research*, 57(4):499–506, 2008.

[334] H.M. Seong, J.S. Lee, T.M. Shin, W.S. Kim, and Y.R. Yoon. The analysis of mental stress using time-frequency distribution of heart rate variability signal. In *Proceedings of the* 26^{th} *Annual International Conference of the IEEE Engineering in Medicine and Biology Society (EMBS)*, pages 283–285, San Francisco, CA, USA, 2004.

[335] A.B. Setty, B.V. Vaughn, S.R. Quint, K.R. Robertson, and J.A. Messenheimer. Heart period variability during vagal nerve stimulation. *Seizure*, 7:213–217, 1998.

[336] K. Sevre, J.D. Lefrandt, G. Nordby, I. Os, M. Mulder, R.O.B. Gans, M. Rostrup, and A.J. Smit. Autonomic function in hypertensive and normotensive subjects: the importance of gender. *Hypertension*, 37(6):1351–1356, 2001.

[337] L. Sherwood. *Human physiology: from cells to systems*. Brooks/Cole Pub Co, 2008.

[338] M. Shiraishi, T. Kamo, S. Nemoto, M. Narita, M. Kamegai, R.M. Baevsky, and I.I. Funtova. Blood pressure variability during 120-day head-down bed rest in humans. *Biomedicine & Pharmacotherapy*, 57(suppl 1):35–38, 2003.

[339] M.B. Sides, J. Vernikos, V.A. Convertino, J. Stepanek, L.D. Tripp, J. Draeger, A.R. Hargens, C. Kourtidou-Papadeli, A. Pavy-Le Traon, T. Russomano, J.Y. Wong, R.R. Buccello P.H. Lee, V. Nangalia, and M.J. Saary. The bellagio report: Cardiovascular risks of spaceflight: Implications for the future of space travel. *Aviation, Space, and Environmental Medicine*, 76:877–895, 2005.

[340] D. Sigaudo, J. O. Fortrat, A.M. Allevard, A. Maillet, J.M. Cottet-Emard, A. Vouillarmet, R. L. Hughson, G. Gauquelin-Koch, and C. Gharib. Changes in the sympathetic nervous system induced by 42 days of head-down bed rest. *American Journal of Physiology. Heart and Circulatory Physiology*, 274:1875–1884, 1998.

[341] D. Sigaudo, J.O. Fortrat, A. Maillet, A.M. Allevard, A. Pavy-LeTraon, R.L. R.L. Hughson, A. Guell, C. Gharib, and G. Gauquelin-Koch. Comparison of a 4-day confinement and head-down tilt on endocrine response and cardiovascular variability in humans. *European Journal of Applied Physiology and Occupational Physiology*, 73:28–37, 1996.

[342] D. Sigaudo-Roussel, M.A. Custaud, A. Maillet, A. Guell, R. Kaspranski, R.L. Hughson, C. Gharib, and J.O. Fortrat. Heart rate variability after prolonged spaceflights. *European Journal of Applied Physiology*, 86:258–265, 2002.

[343] D. Singh, K. Vinod, and S.C. Saxena. Sampling frequency of the RR interval time series for spectral analysis of heart rate variability. *Journal of Medical Engineering & Technology*, 28(6):263–272, 2004.

[344] P. Sleight and D.L. Eckberg. *Human Baroreflexes in Health and Disease*. Clarendon, Oxford, England, 1992.

[345] R.P. Sloan, P.A. Shapiro, E. Bagiella, S.M. Boni, M. Paik, J.T. Bigger, R.C. Steinman, and J.M. Gorman. Effect of mental stress throughout the day on cardiac autonomic control. *Biological Psychology*, 37:89–99, 1994.

[346] H. Stefíková, E. Sovcíková, and M. Bronis. The circadian rhythm of selected parameters of heart rate variability. *Physiologia Bohemoslovaca*, 35(3):227–232, 1986.

[347] P.K. Stein, J.I. Barzilay, P.H.M. Chaves, P.P. Domitrovich, and J.S. Gottdiener. Heart rate variability and its changes over 5 years in older adults. *Age and Ageing*, 38:212–218, 2009.

[348] P.K. Stein, J.I. Barzilay, P.H.M. Chaves, S.Q. Mistretta, P.P. Domitrovich, J.S. Gottdiener, M.W. Rich, and R.E. Kleiger. Novel measures of heart rate variability predict cardiovascular mortality in older adults independent of traditional cardiovascular risk factors: the cardiovascular health study. *Journal of Cardiovascular Electrophysiology*, 19:1169–1174, 2008.

[349] P.K. Stein and R.E. Kleiger. Insights from the study of heart rate variability. *Annual Review of Medicine*, 50(1):249–261, 1999.

[350] P.K. Stein, R.E. Kleiger, and J.N. Rottman. Differing effects of age on heart rate variability in men and women. *The American Journal of Cardiology*, 80:302–305, 1997.

[351] B. Stemper, O. Devinsky, T. Haendl, G. Welsch, and M.J. Hilz. Effects of vagus nerve stimulation on cardiovascular regulation in patients with epilepsy. *Acta Neurologica Scandinavica*, 117:231–236, 2008.

[352] I. Stevenson and H.S. Ripley. Variations in respirations and respiratory symptoms during changes in emotion. *Psychosomatic Medicine*, 14:476–490, 1952.

[353] N. Takahashi, M. Nakagawa, T. Saikawa, T. Ooie, K. Yufu, S. Shigematsu, M. Hara, H. Sakino, I. Katsuragi, T. Okeda, H. Yoshimatsu, and T. Sakata. Effect of essential hypertension on cardiac autonomic function in type 2 diabetic patients. *Journal of the American College of Cardiology*, 38(1):232–237, 2001.

[354] B. Takase, A. Kurita, M. Noritake, A. Uehata, T. Maruyama, H. Nagayoshi, T. Nishioka, K. Mizuno, and H. Nakamura. Heart rate variability in patients with diabetes mellitus, ischemic heart disease, and congestive heart failure. *Journal of Electrocardiology*, 25(2):79–88, 1992.

[355] Task Force of the European Society of Cardiology and the North American Society of Pacing and Electrophysiology. Heart rate variability: standards of measurement, physiological interpretation and clinical use. *Circulation*, 93:1043–1065, 1996.

[356] S.E. Taylor. Biobehavioral responses to stress in females: tend-and-befriend, not fight-or-flight. *Annual Review of Psychology*, 107:411–429, 2000.

[357] M.C. Teich, S.B. Lowen, B.M. Jost, K. Vibe-Rheymer, and C. Heneghan. Heart rate variability: measures and models. *Arxiv Preprint Physics*, page 0008016, 2000.

[358] The International Paediatric Work Group on Arousals. The scoring of arousals in healthy term infants (between the ages of 1 and 6 months). *Journal of Sleep Research*, 14:37–41, 2005.

[359] S. Tigaran, H. Molgaard, R. Mc Clelland, M. Dam, and A.S. Jaffe. Evidence of cardiac ischemia during seizures in drug refractory epilepsy patients. *Neurology*, 60:492–495, 2003.

[360] P. Tinuper, F. Bisulli, A. Cerullo, R. Carcangiu, C. Marini, G. Pierangeli, and P. Cortelli. Ictal bradycardia in partial epileptic seizures: autonomic investigation in three cases and literature review. *Brain*, 124:2345–2346, 2001.

[361] F. Togo and Y. Yamamoto. Decreased fractal component of human heart rate variability during non-REM sleep. *American Journal of Physiology. Heart and Circulatory Physiology*, 280(1):17–21, 2001.

[362] T. Tomson, M. Ericson, C. Ihrman, and L.E. Lindblad. Heart rate variability in patients with epilepsy. *Epilepsy Research*, 30:77–83, 1998.

[363] T. Tomson, L. Nashef, and P. Ryvlin. Sudden unexpected death in epilepsy: current knowledge and future directions. *Lancet Neurology*, 7:1021–1031, 2008.

[364] G.J. Tortora and S.R. Grabowski. *Introduction to the human body: the essentials of anatomy and physiology.* John Wiley & Sons, 2000.

[365] A. Pavy-Le Traon, M. Heer, M.V. Narici, J. Rittweger, and J. Vernikos. From space to earth: advances in human physiology from 20 years of bed rest studies (1986-2006). *European Journal of Applied Physiology*, 101:143–194, 2007.

[366] A. Pavy-Le Traon, D. Sigaudo, P. Vasseur, A. Maillet, J.O. Fortrat, R.L. Hughson, G. Gauquelin-Koch, and C. Gharib. Cardiovascular responses to orthostatic tests after a 42-day head-down bed-rest. *European Journal of Applied Physiology*, 77:50–59, 1998.

[367] L.C.K. Tripathi. Respiration and heart rate variability: a review with special reference to its application in aerospace medicine. *Indian Journal of Aerospace Medicine*, 48:64–75, 2004.

[368] S.A. Tsementzis, J.S. Gill, E.R. Hitchcock, S.K. Gill, and D.G. Beevers. Diurnal variation of an activivity during the onset of stroke. *Neurosurgery*, 17:901–904, 1985.

[369] M.P. Tulppo, R.L. Hughson, T.H. Makikallio, K.E. Airaksinen, and H.V. Huikuri. Effects of exercise and passive head-up tilt test on fractal and complexity properties of heart rate dynamics. *American Journal of Physiology. Heart and Circulatory Physiology*, 280:1081–1087, 2001.

[370] K. Umetani, D.H. Singer, R. McCraty, and M. Atkinson. Twenty-four hour time domain heart rate variability and heart rate: relations to age and gender over nine decades. *Journal of the American College of Cardiology*, 1:593–601, 1998.

[371] S. Vaishnav, R. Stevenson, B. Marchant, K. Lagi, K. Ranjadayalan, and A.D. Timmis. Relation between heart rate variability early after acute myocardial infarction and long-term mortality. *The American Journal of Cardiology*, 73(9):653–657, 1994.

[372] S. Vandeput, F. Beckers, B. Verheyden, A.E. Aubert, and S. Van Huffel. Application of numerical noise titration during autonomic blockade. In *Proceedings of the* 34^{th} *Annual International Conference of Computers in Cardiology (CinC)*, volume 34, pages 525–528, Durham, NC, USA, 2007.

[373] S. Vandeput, J.X. Liu, Y.Z. Li, Z.H. Chen, S.G. Chen, Q. Xie, S. Van Huffel, and A.E. Aubert. Nonlinear dynamics of cardiovascular control during chinese head-down bed rest. *Space Medicine and Medical Engineering*, Accepted, 2010.

[374] S. Vandeput, M. Milošević, B. Ceulemans, S. Van Huffel, L. Brown, J. Penders, and L. Lagae. Autonomic effects of refractory epilepsy on heart rate variability. Influence of intermittent vagus nerve stimulation. *Developmental Medicine and Child Neurology*, Submitted, 2010.

[375] S. Vandeput, G. Naulaers, H. Daniëls, and S. Van Huffel. Distinction between REM and non-REM Sleep by HRV in Neonatal Population. *Archives of Disease in Childhood*, 93(Suppl 2):pw 277, 2008.

[376] S. Vandeput, G. Naulaers, H. Daniëls, and S. Van Huffel. Heart rate variability during REM and non-REM sleep in preterm neonates with and without abnormal cardiorespiratory events. *Early Human Development*, 85:665–671, 2009.

[377] S. Vandeput, J. Taelman, A. Spaepen, and S. Van Huffel. Distinction between physical and mental stress in a laboratory environment using heart rate variability characteristics. *Journal of NeuroEngineering and Rehabilitation*, Revised, 2010.

[378] S. Vandeput, B. Verheyden, A.E. Aubert, and S. Van Huffel. Circadian variations and influence of age on nonlinear heart rate variability parameters in a large healthy population. *Physiological Measurement*, Revised, 2010.

[379] S. Vandeput, B. Verheyden, A.E. Aubert, and S. Van Huffel. Linear and nonlinear heart rate variability analysis of astronauts before and after spaceflight to the ISS. *International Medical Journal for Experimental and Clinical Research*, Revised, 2010.

[380] B. Verheyden, F. Beckers, K. Couckuyt, J. Liu, and A.E. Aubert. Respiratory modulation of cardiovascular rhythms before and after short-duration human spaceflight. *Acta Physiologica*, 191:297–308, 2007.

[381] B. Verheyden, J.X. Liu, F. Beckers, and A.E. Aubert. Adaptation of heart rate and blood pressure to short and long duration space missions. *Respiratory Physiology & Neurobiology*, 169S:13–16, 2009.

[382] B. Vielle. Mathematical analysis of Mayer waves. *Journal of Mathematical Biology*, 50:595–606, 2005.

[383] A. Vincent, F.I.M. Craik, and J.J. Furedy. Relations among memory performance, mental workload and cardiovascular responses. *International Journal of Psychophysiology : Official Journal of the International Organization of Psychophysiology*, 23:181–198, 1996.

[384] E. Vlemincx, J. Taelman, S. De Peuter, I. Van Diest, and O. Van den Bergh. Sigh rate and respiratory variability during mental load and sustained attention. *Psychophysiology*, In Press, 2010.

[385] A. Voss, S. Schulz, R. Schroeder, M. Baumert, and P. Caminal. Methods derived from nonlinear dynamics for analysing heart rate variability. *Philosophical Transactions of the Royal Society of London. Series A: Mathematical and Physical Sciences*, 367(1887):277–296, 2009.

[386] K. Watanabe, K. Hara, S. Hakamada, T. Negoro, M. Sugiura, A. Matsumoto, and M. Maehara. Seizures with apnea in children. *Pediatrics*, 70:87–90, 1982.

[387] F. Weise, F. Heydenreich, S. Kropf, and D. Krell. Intercorrelation analyses among age, spectral parameters of heart rate variability and respiration in human volunteers. *Biological Rhythm Research*, 21(1):17–24, 1990.

[388] P.D. Welch. The use of Fast Fourier Transform for the estimation of power spectra: A method based on time averaging over short, modified periodograms. *IEEE Transactions on Audio Electroacoustics*, 15:70–73, 1967.

[389] C. Welin, A. Rosengren, H. Wedel, and L. Wilhelmsen. Myocardial infarction in relation to work, family and life events. *Cardiovascular Risk Factors*, 5:30–38, 1995.

[390] N. Wessel, M. Riedl, and J. Kurths. Is the normal heart rate 'chaotic' due to respiration? *Chaos*, 19:028508, 2009.

[391] B.E. Westerhof, J. Gisolf, W.J. Stok, K.H. Wesseling, and J.M. Karemaker. Time-domain cross-correlation baroreflex sensitivity: performance on the eurobavar data set. *Journal of Hypertension*, 22(7):1371–1380, 2004.

[392] W.B. White. Cardiovascular risk and therapeutic intervention for the early morning surge in blood pressure and heart rate. *Blood Pressure Monitoring*, 6:63–72, 2001.

[393] P. Widdess-Walsh, P. Kotagal, L. Jeha, G. Wu, and R. Burgess. Multiple auras: clinical significance and pathophysiology. *Neurology*, 69:755–761, 2007.

[394] O. Wiklund, B. Franklin, and N. Bjerle. Autonomic cardiovascular regulation in patients with obstructive sleep apnoea: a study based on spectral analysis of heart rate variability. *Clinical Physiology*, 20(3):234–241, 2008.

[395] M. Willinger, L.S. James, and C. Catz. Defining the sudden infant death syndrome (SIDS): deliberations of an expert panel convened by the National Institute of Child Health and Human Development. *Pediatric Pathology*, 11:677–684, 1991.

[396] W.P. Wilson and J.C. Evans. Coronary artery disease prediction. *American Journal of Hypertension*, 6:309–313, 1993.

[397] H. Witte, P. Putsche, M. Eiselt, M. Arnold, and K. Schmidt. Nonlinear cardio-respiratory interactions revealed by time-phase bispectral analysis. *Biomedizinische Technik. Biomedical engineering*, 46:42–49.

[398] A. Wolf, J.B. Swift, H.L. Swinney, and J.A. Vastano. Determining Lyapunov exponents from a time series. *Physica D: Nonlinear Phenomena*, 16(3):285–317, 1985.

[399] M.M. Wolf, G.A. Varigos, D. Hunt, and J.G. Sloman. Sinus arrhythmia in acute myocardial infarction. *The Medical journal of Australia*, 2(2):52, 1978.

[400] S. Wolf. The end of the rope: the role of the brain in cardiac death. *Canadian Medical Association Journal*, 97(17):1022–1025, 1967.

[401] B.K. Woodruff, J.W. Britton, S. Tigaran, G.D. Cascino, M.F. Burritt, J.P. McConnell, J. Ravkilde, H. Molgaard, F. Andreasen, M. Dam, and A.S. Jaffe. Cardiac troponin levels following monitored epileptic seizures. *Neurology*, 60:1690–1692, 2003.

[402] G.Q. Wu, N.M. Arzeno, L.L. Shen, D.K. Tang, D.A. Zheng, N.Q. Zhoa, D.L. Echberg, and C.S. Poon. Chaotic signatures of heart rate variability and its power spectrum in health, aging and heart failure. *PloS one*, 4:e4323, 2009.

[403] Y. Yamamoto and R.L. Hughson. Coarse-graining spectral analysis: new method for studying heart rate variability. *Journal of Applied Physiology*, 71:1143–1150, 1991.

[404] Y. Yamamoto and R.L. Hughson. Failure in rejecting a null hypothesis of stochastic human heart rate variability with 1/f spectra. In *AIP Conference Proceedings*, pages 697–700, 1993.

[405] Y. Yamamoto and R.L. Hughson. On the fractal nature of heart rate variability in humans: effects of data length and beta-adrenergic blockade. *American Journal of Physiology*, 266:40–49, 1994.

[406] Y. Yamasaki, M. Kodama, M. Matsuhisa, M. Kishimoto, H. Ozaki, A. Tani, N. Ueda, Y. Ishida, and T. Kamada. Diurnal heart rate variability in healthy subjects: effects of aging and sex difference. *American Journal of Physiology. Heart and Circulatory Physiology*, 271:303–310, 1996.

[407] C.C.H. Yang, T.C. Chao, T.B.J. Kuo, C.S. Yin, and H.I. Chen. Preeclamptic pregnancy is associated with increased sympathetic and decreased parasympathetic control of HR. *American Journal of Physiology. Heart and Circulatory Physiology*, 278(4):1269–1273, 2000.

[408] V.K. Yeregani, E. Sobolewski, J. Kay, V.C. Jampala, and G. Igel. Effect of age on long-term heart rate variability. *Cardiovascular Research*, 35:35–42, 1997.

[409] M. Zak, J.P. Zbilut, and R.E. Meyers. *From instability to intelligence: complexity and predictability in nonlinear dynamics*. Springer, Heidelberg, Germany, 1997.

[410] L. Zapanta, C.S. Poon, D.P. White, C.L. Marcus, and E.S. Katz. Heart rate chaos in obstructive sleep apnea in children. In *Proceedings of the* 26^{th} *Annual International Conference of the IEEE Engineering in Medicine and Biology Society (EMBS)*, volume 26, pages 3889–3892, San Francisco, CA, USA, 2004.

[411] J.F. Zbilut, N. Thomasson, and C.L. Webber. Recurrence quantification analysis as a tool for nonlinear exploration of nonstationary cardiac signals. *Medical Engineering & Physics*, 24(1):53–60, 2002.

[412] P.S. Zeskind and J.L. Gingras. Maternal cigarette-smoking during pregnancy disrupts rhythms in fetal heart rate. *Journal of Pediatric Psychology*, 31(1):5–14, 2006.

[413] J.Q. Zhang, A.V. Holden, O. Monfredi, M.R. Boyett, and H. Zhang. Stochastic vagal modulation of cardiac pacemaking may lead to erroneous identification of cardiac chaos. *Chaos*, 19:028509, 2009.

[414] L.F. Zhang. Vascular adaptation to microgravity: what have we learned? *Journal of Applied Physiology*, 91:2415–2430, 2001.

[415] X. Zhong, H.J. Hilton, G.J. Gates, S. Jelic, Y. Stern, M.N. Bartels, R.E. Demeersman, and R.C. Basner. Increased sympathetic and decreased parasympathetic cardiovascular modulation in normal humans with acute sleep deprivation. *Journal of Applied Physiology*, 98:2024–2032, 2005.

[416] G. Zuanetti, J.M.M. Neilson, R. Latini, E. Santoro, A.P. Maggioni, and D.J. Ewing. Prognostic significance of heart rate variability in post-myocardial infarction patients in the fibrinolytic era: the GISSI-2 results. *Circulation*, 94(3):432–436, 1996.

Publication List

Papers in international journals

1. A.E. Aubert, **S. Vandeput**, F. Beckers, J.X. Liu, B. Verheyden and S. Van Huffel. Complexity of cardiovascular regulation in small animals. Philosophical Transactions of the Royal Society of London. Series A: Mathematical and Physical Sciences, vol. 367, no. 1892, Feb. 2009, pp. 1239-1250.

2. **S. Vandeput**, G. Naulaers, H. Daniëls and S. Van Huffel. Heart rate variability during REM and non-REM sleep in preterm neonates with and without abnormal cardiorespiratory events. Early Human Development, vol. 85, Oct. 2009, pp. 665-671.

3. **S. Vandeput**, J.X. Liu, Y.Z. Li, Z.H. Chen, S.G. Chen, Q. Xie, S. Van Huffel and A.E. Aubert. Nonlinear dynamics of cardiovascular control during Chinese head-down bed rest. Space Medicine and Medical Engineering, accepted Sep. 2010.

Papers submitted to international journals

4. **S. Vandeput**, B. Verheyden, A.E. Aubert and S. Van Huffel. Circadian variations and influence of age on nonlinear heart rate variability parameters in a large healthy population. Physiological Measurement, revised July 2010.

5. **S. Vandeput**, J. Taelman, A. Spaepen and S. Van Huffel. Time-frequency heart rate variability characteristics of young adults during physical, mental and combined stress in laboratory environment. Journal of NeuroEngineering and Rehabilitation, revised Aug. 2010.

6. **S. Vandeput**, B. Verheyden, A.E. Aubert and S. Van Huffel. Linear and nonlinear heart rate variability analysis of astronauts before and after

spaceflight to the ISS. International Medical Journal for Experimental and Clinical Research, revised Sep. 2010.

7. J. Taelman, **S. Vandeput**, E. Vlemincx, A. Spaepen and S. Van Huffel. Instantaneous changes in heart rate regulation due to mental load in simulated office work. European Journal of Applied Physiology, submitted July 2010.

8. K. Jansen, **S. Vandeput**, M. Milošević, B. Ceulemans, S. Van Huffel, L. Brown, J. Penders and L. Lagae. Autonomic effects of refractory epilepsy on heart rate variability. Influence of intermittent vagus nerve stimulation. Developmental Medicine and Child Neurology, submitted Aug. 2010.

9. K. Jansen, **S. Vandeput**, S. Van Huffel and L. Lagae. Heart rate variability in infants with West syndrome. Neurology, submitted Sep. 2010.

Abstracts in international journals

10. **S. Vandeput**, G. Naulaers, H. Daniëls and S. Van Huffel. Distinction between REM and non-REM Sleep by HRV in Neonatal Population. Archives of Disease in Childhood, vol. 93 (Suppl. 2), Nov. 2008, pw. 277.

11. M.A.K.A. Braeken, R.A. Otte, D. Widjaja, **S. Vandeput**, J. Taelman, S. Van Huffel and B.R.H. Van den Bergh. Mental stress and heart rate variability during the first pregnancy trimester. Developmental Psychobiology, in press.

Papers in proceedings of international conferences

12. K. Vanderperren, **S. Vandeput**, J.-B. Poullet, D. Sima and S. Van Huffel. Automatic quantification of magnetic resonance spectroscopic signals: evaluation and comparison of AQSES and QUEST. Proceedings of the 1^{st} Annual Benelux Symposium of the IEEE Engineering in Medicine and Biology Society (EMBS), Brussels, Belgium, Dec. 2006, pp. 251-254.

13. **S. Vandeput**, F. Beckers, B. Verheyden, A.E. Aubert and S. Van Huffel. Application of numerical noise titration during autonomic blockade. Proceedings of the 34^{th} Annual Computers in Cardiology (CinC), Durham, North-Carolina, USA, Oct. 2007, pp. 525-528.

14. **S. Vandeput**, B. Verheyden, A.E. Aubert and S. Van Huffel. Numerical noise titration analysis of heart rate variability in a healthy population. Proceedings of the 5^{th} European Study Group on Cardiovascular Oscillations (ESGCO), Parma, Italy, Apr. 2008, pp. P1B1-P1B4.

15. **S. Vandeput**, B. Verheyden, A.E. Aubert and S. Van Huffel. Day-night variations in nonlinear heart rate variability measures in a large healthy population. Proceedings of the 19^{th} BIOSIGNAL conference, Brno, Czech Republic, June 2008, ID48.

16. **S. Vandeput**, B. Verheyden, A.E. Aubert and S. Van Huffel. Nonlinear heart rate variability in a healthy population: influence of age. Proceedings of the 35^{th} Annual Computers in Cardiology (CinC), Bologna, Italy, Sep. 2008, pp. 53-56.

17. B. Mijović, J. Corthout, **S. Vandeput**, M. Mendez, S. Cerutti and S. Van Huffel. Detection of obstructive sleep apnea by empirical mode decomposition on tachogram. Proceedings of 4^{th} European Congress of the International Federation for Medical and Biomedical Engineering (ECIFMBE), Antwerp, Belgium, Nov. 2008, pp. 247-251.

18. J. Taelman, **S. Vandeput**, A. Spaepen and S. Van Huffel. Influence of mental stress on heart rate and heart rate variability. Proceedings of 4^{th} European Congress of the International Federation for Medical and Biomedical Engineering (ECIFMBE), Antwerp, Belgium, Nov. 2008, pp. 1366-1369.

19. **S. Vandeput**, B. Verheyden, A.E. Aubert and S. Van Huffel. Nonlinear heart rate analysis of astronauts before and after spaceflight by means of Holter recordings. Proceedings of the 30^{th} Annual International Gravitational Physiology Meeting (ISGP), Xi'an, China, May 2009, in press.

20. **S. Vandeput**, B. Verheyden, A.E. Aubert and S. Van Huffel. Modeling the recovery of the sympathetic and parasympathetic modulation in astronauts after short and long duration space missions. Proceedings of the 30^{th} Annual International Gravitational Physiology Meeting (ISGP), Xi'an, China, May 2009, in press.

21. **S. Vandeput**, J. Taelman, A. Spaepen and S. Van Huffel. Heart rate variability as a tool to distinguish periods of physical and mental stress in a laboratory environment. Proceedings of the 6^{th} International Workshop on Biosignal Interpretation (BSI), New Haven, Connecticut, USA, June 2009, pp. 187-190.

22. **S. Vandeput**, K. Jansen, M. Milošević, L. Lagae and S. Van Huffel. Nonlinear cardiovascular oscillations in children with refractory epilepsy before and after the vagus nerve stimulation. Proceedings of the 6^{th} European Study Group on Cardiovascular Oscillations (ESGCO), Berlin, Germany, Apr. 2010, P9:1-4.

23. D. Widjaja, **S. Vandeput**, J. Taelman, M.A.K.A. Braeken, R.A. Otte, B.R.H. Van den Bergh and S. Van Huffel. Accurate R peak detection and

advanced preprocessing of normal ECG for heart rate variability analysis. Proceedings of the 37^{th} Annual Computing in Cardiology (CinC), Belfast, Northern Ireland, Sep. 2010, in press.

24. D. Widjaja, J. Taelman, **S. Vandeput**, M.A.K.A. Braeken, R.A. Otte, B.R.H. Van den Bergh and S. Van Huffel. ECG-derived respiration: comparison and new measures for respiratory variability. Proceedings of the 37^{th} Annual Computing in Cardiology (CinC), Belfast, Northern Ireland, Sep. 2010, in press.

25. J. Taelman, **S. Vandeput**, D. Widjaja, M.A.K.A. Braeken, R.A. Otte, B.R.H. Van den Bergh and S. Van Huffel. Stress during pregnancy: Is the autonomic nervous system influenced by anxiety? Proceedings of the 37^{th} Annual Computing in Cardiology (CinC), Belfast, Northern Ireland, Sep. 2010, in press.

Abstracts in proceedings of (inter)national conferences

26. **S. Vandeput**, G. Naulaers, H. Daniëls and S. Van Huffel. Heart rate variability during active and quiet sleep in preterm neonates. Proceedings of the 7^{th} Annual Belgian Day on Biomedical Engineering, Brussels, Belgium, Nov. 2007, pp. 64.

27. **S. Vandeput**, G. Naulaers, H. Daniëls and S. Van Huffel. Heart rate variability during active and quiet sleep in preterm neonates. Proceedings of the 2^{nd} Annual Benelux Symposium of the IEEE Engineering in Medicine and Biology Society (EMBS), Heeze, the Netherlands, Dec. 2007, pp. 28.

28. **S. Vandeput**, B. Verheyden, A.E. Aubert and S. Van Huffel. Influence of microgravity on linear and nonlinear HRV parameters of astronauts after space missions to the ISS. Proceedings of the 20^{th} European Low Gravity Association (ELGRA) Biennial Symposium and General Assembly *'In the footsteps of Columbus'*, Bonn, Germany, Sep. 2009, pp. 127.

29. **S. Vandeput**, J.X. Liu, Y.Z. Li, Z.H. Chen, S.G. Chen, Q. Xie, S. Van Huffel and A.E. Aubert. The effect of Chinese herbal medicine as a countermeasure to orthostatic intolerance in 60 days head-down bed rest. Proceedings of the joint 31^{th} Annual International Gravitational Physiology (ISGP) Meeting, 11^{th} ESA Life Sciences Symposium, 5^{th} Italian Society for Space Biomedicine and Biotechnology (ISSBB) and 21^{th} European Low Gravity Association (ELGRA) Biennial Symposium *'Life in Space for Life on Earth'*, Trieste, Italy, June 2010, pp. 66.

30. **S. Vandeput**, J.X. Liu, Y.Z. Li, Z.H. Chen, S.G. Chen, Q. Xie, S. Van Huffel and A.E. Aubert. Comparison of nonlinear heart rate

control in head-down bed rest and spaceflight. Proceedings of the joint 31^{th} Annual International Gravitational Physiology (ISGP) Meeting, 11^{th} ESA Life Sciences Symposium, 5^{th} Italian Society for Space Biomedicine and Biotechnology (ISSBB) and 21^{th} European Low Gravity Association (ELGRA) Biennial Symposium *'Life in Space for Life on Earth'*, Trieste, Italy, June 2010, pp. 38-39.

Papers submitted to international conferences

31. M. Milošević, **S. Vandeput**, K. Jansen, L. Lagae and S. Van Huffel. Heart rate variability analysis of children with refractory epilepsy before and after the vagus nerve stimulation. Proceedings of the 4^{th} International Joint Conference on Biomedical Engineering Systems and Technologies (BIOSTEC), Rome, Italy, Jan. 2011.

Curriculum vitae

Steven Vandeput was born in Leuven, Belgium on April 15, 1983. He received the degree of electrotechnical-mechanical engineer with specialization in biomedical techniques, magna cum laude from the Katholieke Universiteit Leuven, Belgium in July 2006. He was laureate Biomedical Society for his thesis 'Automatic quantification of magnetic resonance spectroscopic signals: evaluation and comparison of AQSES and QUEST'.

Since August 2006, he has been working as a researcher, supported by a PhD grant, at the Electrical Engineering Department of the Katholieke Universiteit Leuven under the supervision of Prof. Dr. Ir. Sabine Van Huffel and Prof. Dr. André Aubert. His research interests include biomedical signal processing with a focus on heart rate variability. He was an invited speaker at the Heart Rate Variability seminar series organised by Prof. Dr. Omer Van den Bergh in Leuven (Feb-March 2010) and was invited for a tutorial about heart rate variability at the University of Amsterdam (UvA) in April 2010. In June 2010, he was invited as chair person for the session 'Cardiovascular physiology I' at the ESA conference 'Life in Space for Life on Earth'.

From 2006 on, he was also sports promoter for the SCD division within ESAT and co-organiser of the yearly ESAT sports day.

Arenberg Doctoral School of Science, Engineering & Technology
Faculty of Engineering
Department of Electrical Engineering
Research group SISTA-BIOMED
Kasteelpark Arenberg 10, B - 3001 Leuven

KATHOLIEKE UNIVERSITEIT LEUVEN

ASSOCIATIE K.U.LEUVEN